

A developmental analysis of the mouse mutant
dominant hemimelia (Dh)

Jacob Hecksher-Sørensen

Ph.D.
The University of Edinburgh
2001



The experiments described in this thesis were the unaided work of the author except where acknowledgement is made by reference. No part of this work has previously been accepted for any other degree nor is any part of it being submitted concurrently in candidature for another degree.

Copenhagen 29/8 2001

Abstract

Studies in humans have shown that 1 in 1800 infants are born with limb deficiencies and that 9% of these also suffers from renal abnormalities. Classification of these limb abnormalities revealed that the renal defects commonly associate with limb deficiencies such as micromelia (44%), amelia (18%) and radial/tibial (preaxial) deficiencies (27%). Additionally, experimental evidence has shown that the mesonephros, an important component of the primitive urogenital system, also could be responsible for inducing and maintaining limb development. These observations imply the existence of a developmental link between limb induction and early kidney development. However, this remains controversial since other experiments show that the mesonephros is not required for limb development. The work described in this thesis was prompted by the observation, that the mouse mutants *dominant hemimelia* (*Dh*) and *luxate* (*lx*) disrupt both limb induction and kidney development. Furthermore, both mutants display preaxial abnormalities such as polydactyly, oligodactyly and tibial hemimelia of the hindlimbs. In addition *Dh* also causes asplenia, microgastria, small pancreas, gut atresia.

The studies presented here show that the hindlimbs in *Dh* animals are shifted 2-3 segments anteriorly coinciding with a lumbar-sacral transformation of the axial skeleton. *In situ* hybridisation shows that the anterior boundary of *Hoxc10* in the flank mesenchyme has moved anteriorly in *Dh* embryos while the expression of *Hoxa10* and *Hoxd10* appear to be unaffected. The spinal nerves innervating the hindlimbs also respond to the shift of the limbs. Analysis of the urogenital phenotype shows that the effect *Dh* has on the kidney abnormalities is indirect. It appears that the hydronephrosis observed in *Dh* mice is caused by blockage of the ureter, however, it is possible that this blockage is related to misexpression to *Hoxc10*.

Efforts were therefore made to determine if other traits related to the *Dh* mutation was caused by ectopic *Hoxc10* expression, however, this does not appear to be the case. Nevertheless these studies led to the identification of a novel anatomical structure, the splanchnic mesothelial ridge (SMR). The SMR consists of a thickened mesothelium on the left side of the spleno-pancreatic region, which is required for asymmetric growth. In *Dh* mice the SMR is absent and as a result the spleno-pancreatic region asymmetric growth is impaired. The asplenic phenotype is also related to the absence of the SMR.

Acknowledgements

The work described in this thesis was carried out at the MRC Human Genetics Unit in Edinburgh. During the time I spent at the MRC I met so many nice people and I would like to thank all of you for making those years some of the happiest in my life - after all I stayed in Scotland for more than 6 years despite the weather, which means you must be some of the nicest people around!!!

Especially I would like to thank my supervisor Bob Hill. It has been absolutely brilliant working for you both at a scientific and a personal level. You always supported me no matter how weird my ideas were and you never complained about my frequent trips to Denmark (I am now a silvercard member!!!). I really hope that one day we can go to a baseball game together so you can explain the rules once and for all...cause they are a wee bit tricky. And despite your efforts I am not convinced that American sports are better than soccer! However, I will always remember the Cardinals, Big Mac and I will even admit that Lance Armstrong is an ok cyclist (although he will never compare with Bjarne Riis). Anyway, get back to work boy!!!

Also I would like to thank all the past and present members in Bobs group, Ana, Kate, Carlo, Rob, Alison, Simon, Lorna who did all the transgene injections and finally Laura who taught me almost everything I know.

A big thank you also goes to the crap team James & Lee (the English), Rasmus (the fellow Dane), Ulf (the Swede), Cec (the Creative), Natalie (the English/Spanish), Colin (the Scot), Bibi & Angela (the Italians) and Annemiek (the Dutch). Despite the food!! and the smell!!!! Lunchtime is still one of the best memories.

During the course of the project many people provided me with materials and technical assistance. In particular I would like to thank Mario Capecchi for sending us the *Hoxc10*^{-/-} mice and also Kay Higgins in his lab for her help in shipping the mice from the States to Edinburgh (not an easy task!!), Peter Currie for the *zPax3*-3'UTR construct and Robb Krumlauf for the *Hoxb9* enhancers.

Finally, I would like to thank all my friends outside science!! That includes all my friends in Scotland and Denmark my family and most of all, my girlfriend Camilla.

Table of contents

Abstract	1
Acknowledgements	2
Table of contents	3
Abbreviations	6
Chapter 1: Introduction	7
1.1 Scientific aims	7
1.2 The <i>dominant hemimelia (Dh)</i> mutation	8
Phenotypic characteristics	8
Candidate genes	9
The Genetics of <i>Dh</i>	12
1.3 Limb development	13
Induction of the limb buds	13
<i>Hox</i> genes specify the positions of the limbs	14
Setting up the <i>Hox</i> code	17
Patterning of the limb buds	17
Anterior-posterior asymmetry in the limb	19
Establishing anterior-posterior asymmetry in the limb	20
Fore and hindlimb identity	21
Innervation of the limbs	21
Human applications	22
1.4 Development of the spleno-pancreatic region	24
Left-right asymmetry is determined genetically	24
Establishing left-right asymmetry	25
A genetic pathway for left-right asymmetry	28
Asymmetric organ development	30
Anterior-posterior patterning of the endoderm	31
Pancreas development	33
Spleen development	34
Stomach development	35
Chapter 2: The limb and kidney phenotype	37
2.1 The <i>Dh</i> mutation shifts the hindlimbs anteriorly	37
Homeotic transformation of the axial skeleton in <i>Dh</i>	37
The hindlimbs shifts anteriorly in <i>Dh</i> embryos	39
The expression of <i>Hoxc10</i> is shifted anteriorly in <i>Dh</i> embryos.	43
Gene expression in the <i>Dh</i> hindlimbs	45
Abnormal innervation of the hindlimbs in <i>Dh</i> embryos	45
2.2 The <i>Dh</i> mutation affects kidney development indirectly	48
Severe swelling of the kidneys in <i>Dh/Dh</i> embryos	48
Misexpression of <i>Hoxc10</i> in <i>Dh</i> embryos	50
<i>Wt1</i> expression in wildtype and <i>Dh</i> embryos	54
The ureter is blocked in <i>Dh/Dh</i> .	56
2.3 Transgenic misexpression of <i>Hoxc10</i>	58
The <i>pHEX</i> construct	58
The <i>pHEXc10</i> construct	61
Stable transgenic lines	67
The transgenic insertion causes obesity in line A214	67
2.4 <i>Hoxc10</i> knockout mice	69
2.5 Discussion	69
Is <i>Dh</i> acting through <i>Hoxc10</i> ?	69
Can the shift in <i>Hoxc10</i> expression account for all abnormalities in the hindlimbs?	70
The nerves have maintained some of their original identity	73
The hydronephrosis is due abnormal development of the mesonephros	74
Is there a correlation between the limb and kidney abnormalities in <i>Dh</i> ?	76
2.6 Conclusion	76

Chapter 3: Confocal microscopy of gene expression	78
3.1 Introduction	78
3.2 Verification of the method	79
Neural tube expression	79
<i>Hoxb9</i> is expressed around the growing nerves	82
Studying gene interactions	85
3.3 Discussion	87
3.4 Conclusion	88
Chapter 4: The gut phenotype	89
4.1 Introduction	89
4.2 The SMR mediates a physical requirement for left-right asymmetry	89
The Splanchnic Mesothelial Ridge (SMR)	89
BrdU labelling	91
Development of the SMR and the pancreas	93
The SMR is absent in <i>Dh</i>	93
4.3 The mesenchyme surrounding the pancreas is compartmentalised	95
Left-right markers are expressed in the mesothelium before the SMR thickens	95
Early Spleen development	97
The spleen is not induced in <i>Dh</i>	100
The SMR in other asplenic mutants	103
4.4 Screening for novel genes in the SMR	105
Multiplex PCR	105
Morphogens and growth factors expressed in the developing gut	109
4.5 Genetic interactions and the late pancreas phenotype	113
Genetic interactions	113
Figure 5.11 mature pancreasThe mature pancreas is normal in <i>Dh</i> embryos	116
The mature pancreas is normal in <i>Dh</i> embryos	117
4.6 Stomach development in <i>Dh</i>	117
The asymmetry is lost in <i>Dh/Dh</i> embryos	117
<i>Dh/Dh</i> Stomachs are smaller at E13.5	119
Figure 4.14The anterior stomach and pyloric sphincter is absent in <i>Dh/Dh</i> embryos	122
The anterior stomach and pyloric sphincter is absent in <i>Dh/Dh</i> embryos	123
Figure 5.15 the anterior stomach is missing in <i>Dh</i> The gut ends blind at the midgut-hindgut junction in <i>Dh/Dh</i> embryos	124
The gut ends blind at the midgut-hindgut junction in <i>Dh/Dh</i> embryos	125
4.7 Discussion	127
The SMR mediates a physical requirement for left right asymmetry	127
The SMR is a novel embryonic structure	129
Additional roles of the SMR	130
Regionalisation within the spleno-pancreatic region	132
Genetic interactions underlying spleen development	132
Left right asymmetry in <i>Dh/Dh</i> embryos	136
Other gut abnormalities in <i>Dh</i> embryos	137
4.8 Conclusion	138
Chapter 5: Discussion	140
5.1 Introduction	140
5.2 The <i>Inhβb</i> gene	140
<i>Inhβb</i> is misexpressed in <i>Dh</i> embryos	141
5.3 The <i>Gli2</i> gene	143
The <i>Shh</i> pathway is involved in many aspects of <i>Dh</i> abnormalities	143
<i>Gli2</i> is expressed normally in <i>Dh</i>	143
5.4 The Human sequence	145
The human sequence failed to reveal new candidates for <i>Dh</i>	145
5.5 Conclusion	145
5.6 Speculations	146

Chapter 6: Materials and methods	147
6.1 General techniques	147
#1: Preparation of electro-competent cells	147
#2: Electroporation of plasmid DNA	147
#3: Heat shock transformation of plasmid DNA	147
#4: Preparation of plasmid DNA using QIAGEN plasmid mini Kit	147
#5: Preparation of plasmid DNA using QIAGEN plasmid maxi Kit	148
#6: PCR (conventional)	148
#7: PCR (high fidelity)	148
#8: PCR (Advantage®-GC Genomic PCR)	148
#9: Restriction digest	149
#10: DNA purification (Phenol-Chloroform)	149
#11: DNA purification (Gel extraction)	149
#12: Ligation	149
#13: ABI sequencing	150
6.2 Cloning of the transgenic constructs	150
#14: Cloning of the <i>pHEX</i> construct	150
#15: Cloning of <i>pGZb9-NE</i> and <i>pHEXc10-NE</i>	151
#16: Purification of expression constructs for transgene injections	151
#17: Injection of the <i>pHEXc10-NE</i> transgene into 1-cell embryos	152
6.3 Expression analysis	152
#18: Preparation of DNA for in vitro transcription.	152
#19: <i>In vitro</i> transcription	152
#20: conventional <i>In situ</i> (wholemount)	152
#21: Double labelling <i>In situ</i> (wholemount)	153
6.4 Expression analysis (fluorescence)	154
#22: Agarose embedding	154
#23: Vibratome cutting	154
#24: Fast Red <i>In situ</i> (wholemount)	154
#25: Immunohistochemistry (whole mount)	154
#26: Combined <i>In situ</i> /Immunohistochemistry (whole mount)	155
#27: Phalloidin (wholemount)	155
#28: Confocal microscopy	156
6.5 Histological analysis	156
#29: Wax embedding	156
#30: Microtome cutting	156
#31: Fast Red <i>In situ</i> (sections)	156
#32: Immunohistochemistry (sections)	157
#33: BrdU (sections)	157
#34: Phalloidin and Yo-Pro1 (sections)	158
#35: Histology (sections)	158
6.6 Bone Staining	158
#36: Bonestain	158
6.7 Multiplex PCR	159
#37: Isolation of mRNA	159
#38: Preparation of cDNA	159
#39: MPX-PCR	159
6.8 Mouse Stocks	160
#40: Mouse strains	160
#41: Obtaining mutant embryos	160
#42: Preparation of DNA from mutant embryos	160
#43: Genotyping mutant embryos	160
References	162
Appendix	181

Appendix I: Sequencing of the pHEX construct

Appendix II: MPX-PCR - annotated gels

Appendix III: Degenerate PCR's

Appendix IV: Primer sequences

Appendix V: Data sheets for *In situ* probes and Antibodies

Appendix VI: Confocal Paper

Appendix VII: *Bapx1* Paper

Abbreviations

Abbreviations

SMR	Splanchnic Mesothelial Ridge
AER	Apical Ectodermal Ridge
ZPA	Zone of Polarising Activity
PZ	Progress Zone
Fgf	Fibroblast Growth Factor
TGF	Transforming Growth Factor
BMP	Bone Morphogenetic Proteins
AP	Alkaline Phosphatase
CLSM	Confocal Laser Scanning Microscopy
UTR	Untranslated region
PCR	Polymerase Chain Reaction
WISH	Whole Mount <i>In Situ</i> Hybridisation
FISH	Fluorescent <i>In Situ</i> Hybridisation
ISH	<i>In Situ</i> Hybridisation
BSA	Bovine Serum Albumin
DIG	Digoxigenin
FLU	Fluorescein
RA	Retinoic Acid
FSH	Follicle Stimulating Hormone

Genes and mutations

<i>Shh</i>	<i>Sonic Hedgehog</i> (mammalian homologue of the <i>Drosophila</i> gene <i>hedgehog</i>)
<i>Wnt</i>	(mammalian homologues of the <i>Drosophila</i> gene <i>wingless</i>)
<i>Gli</i>	(mammalian homologues of the <i>Drosophila</i> gene <i>cubitus interruptus</i>)
<i>Hox</i>	(Homeobox containing protein)
<i>Dh</i>	<i>Dominant hemimelia</i>
<i>Ssq</i>	<i>Sasquatch</i>
<i>Xt</i>	<i>Extra toes</i>
<i>Lx</i>	<i>Luxate</i>

Embryonic axes

Anterior	Head end
Rostral	Head end
Posterior	Tail end
Caudal	Tail end
Dorsal	Back
Ventral	Front
Proximal	Near end
Distal	Far end

Translations

Polydactyly	Too many digits
Oligodactyly	Too few digits
Hemimelia	Partial loss of bone
Preaxial	Head end (anterior)

Chapter 1: Introduction

1.1 Scientific aims

It is generally accepted that the molecular mechanisms underlying organogenesis are very specific and highly conserved through evolution. For this reason a lot can be learned about the genetic cues required for correct development by studying situations in which a particular pathway has been disrupted. The project described in this thesis is concerned with the abnormalities inflicted by the mouse mutation *dominant hemimelia* (*Dh*). During embryogenesis *Dh* disrupts the molecular programmes required for proper development of many organs and as a result these organs undergoes abnormal development.

One aspect of the *Dh* mutation is that it affects the anterior mesenchyme of the hindlimbs and as a result mice carrying the mutation display preaxial polydactyly or oligodactyly. Previous studies have shown that the anterior mesenchyme is abnormal throughout limb development in mutant animals, suggesting that *Dh* affects induction of the hindlimbs. However, the *Dh* mutation also affects kidney development and there is evidence that early stages of kidney development are associated with limb induction. The aim of this project was therefore to investigate if the early limb defects observed in *Dh* mice are associated with abnormalities in the developing urogenital system.

Data obtained during the course of the project suggested that both limb and kidney defects might be due to misexpression of the *Hoxc10* gene. To see if other abnormalities observed in *Dh* could be attributed ectopic expression of *Hoxc10* the phenotypic analysis was extended to other organs affected by the *Dh* mutation. These results showed that the effects *Dh* has on the stomach, spleen and pancreas are unrelated to *Hoxc10* expression. Nevertheless they do provide new insights into the development of these organs.

1.2 The *dominant hemimelia (Dh)* mutation

The dominant *hemimelia mutation (Dh)* belongs to the luxoid-polydactylous group of mouse mutations. Characterised by a twisting of the fore and hindlimbs associated with reduction or loss of certain long bones as well as oligodactyly or polydactyly. Other members of this group include *luxoid (lu)*, *luxate (lx)*, *extra toes (Xt)*, *Sasquatch (Ssq)*, *hemimelic extra toes (Hx)* and *Strong's luxoid (lst)*.

Dh arose spontaneously in a crossbred stock carrying a translocation at the Institute of Animal Genetics in Edinburgh. It was discovered in 1954 by T. C. Carter and described by Searle in 1964. The following description of how the mutation was discovered is taken from Searle, 1964.

Dh was discovered in 1954 by Dr T. C. Carter at the Institute of Animal Genetics, Edinburgh. The original male was at first thought to be heterozygous for *lx*. However, some outcross offspring lacked the hallux and had tibial hemimelia with luxation of the hindlegs. Since such severe abnormalities are unknown in *lx/+* mice it was realised that this must be a new luxoid mutation which was named *dominant hemimelia (Dh)* by Dr Carter.

Phenotypic characteristics

The limb abnormalities in *Dh* are confined to the hindlimbs. Heterozygotes show preaxial polydactyly or oligodactyly, tibial hemimelia and sometimes absence of the tibia. Homozygotes always display oligodactyly with loss of up to three digits and complete absence of the tibia (Searle, 1964). The effect *Dh* has on hindlimb development can be traced to the time of induction where the mutation affects the anterior mesenchyme of the limb bud (Hecksher-Sørensen, 1998; Lettice et al., 1999a). It has also been reported that *Dh* homozygotes show abnormal cell death in the forelimbs but without affecting the limb phenotype (Rooze, 1977). Other abnormalities in *Dh* animals include reduction in the number of ribs, sternbrae and presacral vertebrae and the stomach is smaller. These defects are present in both heterozygotes and homozygotes but tends to be more severe in homozygous animals which also display urogenital abnormalities (Holmes and Barton, 1993; Suto et al., 1996; Morin et al., 1999). Additionally, all *Dh* animals are asplenic. However, it appears that the effect *Dh* has on spleen development is non cell-autonomous. Thus

chimeric mice consisting of >90% *Dh/Dh* cells are capable of forming a rudimentary spleen (Suto et al., 1995). Only heterozygous animals reproduce, since homozygotes usually die at birth. *Dh/+* mice display enlarged lymph nodes and elevated levels of lymphocytes, granulocytes and thrombocytes, presumably due to the lack of a functional spleen (Machado and Lozzio, 1976). Also the absent spleen significantly lowers the number of Mast cells in the lymph nodes (Wlodarski et al., 1982) and reduces the rate of T-cell maturation (Fletcher et al., 1977). The earliest effects of *Dh* can be traced back to embryonic day 9.5 (E9.5) where the splanchnic epithelium is defective or absent (Green, 1967). Due to this observation it was suggested that the pleiotropic defects in *Dh* arise because the defective splanchnic epithelium prevents induction of the spleen and disrupts induction of the hindlimbs. However, as is now known developmentally important genes are often expressed in many different tissues during embryogenesis. Thus an alternative explanation for the pleiotropic phenotype is that the gene disrupted by *Dh*, has several roles during development.

Candidate genes

The gene disrupted by the *Dh* mutation is unidentified, but recombination studies have defined a critical region mapping to position 63 on mouse chromosome 1 (Holmes, 1986; Martin et al., 1990; Higgins et al., 1992; Hughes et al., 1997). At present only two genes, *Gli2* and *Inh β b* have been identified within the critical region (figure 1.1).

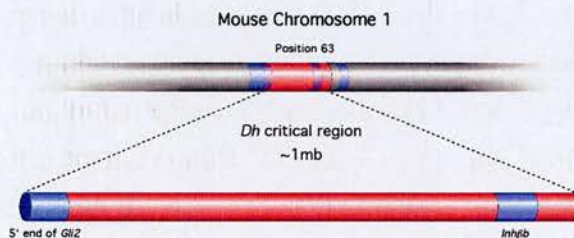


Figure 1.1: The *Dh* critical region. The *Dh* critical region has been mapped to mouse chromosome 1, position 63. The critical region is estimated to be 1Mb and at present *Gli2* and *Inh β b* are the only genes mapping within the region.

Gli2 is a zinc finger transcription factor belonging to the Gli family, which also includes *Gli1* and *Gli3*. The *Gli* genes are mammalian homologues of the *Drosophila* gene *Cubitus interruptus* (*Ci*), which acts as a mediator of *Hedgehog* (*Hh*) signalling and as a repressor of *Hh* expression (Methot and Basler, 2001). This genetic relationship is also true in mammals where the *Gli* genes play an important role in regulating expression of the *Hedgehog* homologue *Shh* (reviewed in Ruiz i Altaba, 1999). However, the regulation of *Shh* in mammals is more complicated and it appears that the *Gli* genes can act as activators of *Shh* expression as well as

repressors (Sasaki et al., 1999; Ding et al., 1998). The *Gli3* gene has been identified as the gene responsible for the luxoid mutation *Xt* (Hui and Joyner, 1993). In *Xt* mice *Shh* is expressed ectopically in the anterior mesenchyme of the developing limb buds and because the *Gli3* gene product is inactivated by the *Xt* mutation it suggests a role for *Gli3* as a repressor of *Shh* expression. *Dh*⁺ mice also display ectopic expression of *Shh* in the anterior mesenchyme of the hindlimbs in a manner very similar to that observed in *Xt* mice (Hecksher-Sørensen, 1998; Lettice et al., 1999a). The polydactylous phenotype in particular makes *Gli2* a good candidate gene for the *Dh* mutation, assuming that *Gli2* also acts as a repressor of *Shh* in the anterior limb mesenchyme. However, sequencing of the *Gli2* gene has failed to reveal any mutations within the gene (Hughes et al., 1997) and *in situ* analysis has not revealed any dramatic changes in the expression of *Gli2*. Nevertheless, *Gli2* can not be ruled out as a candidate for *Dh*, because in humans the *GLI2* gene gives rise to several different isoforms (Tanimura et al., 1998) and it remains a possibility that the *Dh* mutation is affecting a differentially spliced exon, either at the sequence level or by interfering with splicing events.

Inhβb is a secreted protein and belongs to the TGFβ superfamily of signalling molecules. Members of this family are highly conserved through evolution and TGFβ signalling is required in reproduction and numerous developmental processes in all higher eucaryotes (reviewed in Kingsley, 1994; Massague and Chen, 2000). In the mouse, at E12.5, *Inhβb* is expressed in a number of tissues including the eye, oesophagus, stomach endoderm, brain and spinal cord (Feijen et al., 1994). Like other TGFβ molecules *Inhβb* functions as a homodimer or a heterodimer and the activity of these dimers is determined by the pairing of subunits (figure 1.2).

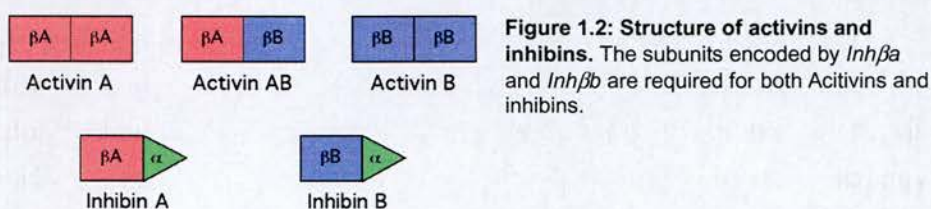


Figure 1.2: Structure of activins and inhibins. The subunits encoded by *Inhβa* and *Inhβb* are required for both Activins and inhibins.

Thus *Inhβb* encodes a subunit required for both the activin and inhibin molecules, which owe their names to the effect they have on the release of follicle stimulating hormone (FSH). Activins (activin-βAβA, -βAβB and -βBβB), which act as activators of FSH, consists of subunits encoded by *Inhβa* and *Inhβb* whereas the inhibins (inhibin-βAα and -βBα), which acts as inhibitors on FSH, contains a subunit encoded by the *Inhα* gene in combination with either *Inhβa* or *Inhβb*. In

Xenopus activin is a potent inducer of mesoderm formation (Smith et al., 1990). Furthermore, disruption of activin signalling reduces the amount of mesoderm (Hemmati-Brivanlou and Melton, 1992) and promotes the formation of neural tissue (Hemmati-Brivanlou et al., 1994; Hemmati-Brivanlou and Melton, 1994), suggesting that *Inhβb* plays an important role in specifying germ layer identity in *Xenopus*. However, in mice lacking functional *Inhβb* the mesoderm develops normally and the only defect is failure to close the eyelids (Schrewe et al., 1994; Vassalli et al., 1994). The phenotype observed in the absence of *Inhβa* is more severe and the mice die within 24 hours of birth but also in this case the mesoderm develops normally (Matzuk et al., 1995b). Furthermore, the production of double knockouts and targeted deletion of the activin antagonist Follistatin and *ActRIIc* has also failed to demonstrate any role for activin in germ layer specification in the mouse (Matzuk et al., 1995b; Matzuk et al., 1995c; Matzuk et al., 1995a). Although the studies carried out in mouse suggest that *Inhβb* has a minor role in development there are several lines of evidence, which makes it a good candidate gene for *Dh*. Activin binds with high affinity to the activin receptors encoded by *ActRIIa* and *ActRIIb* (Mathews and Vale, 1991; Mathews et al., 1992) and mice lacking *ActRIIb* display several abnormalities, including axial defects, laterality defects and reduction of the spleen (Oh and Li, 1997), a phenotype very similar to that observed in *Dh*. Also since the *Dh* mutation is dominant it is likely to involve misexpression and it is known from both frogs and chick, that misexpression of activin has severe consequences on development. In mouse, when *Inhβb* is substituted into the *Inhβa* locus it rescues the abnormalities observed in *Inhβa*-null mice (Brown et al., 2000). However, it also results in a number of novel phenotypes, demonstrating that minor changes in dosage and bioactivity within the activin family affects development. Furthermore, sharing of receptors and the recent discovery of genes such as BAMBI (Bmp and Activin Membrane Bound Inhibitor; Onichtchouk et al., 1999) has confirmed that functional overlap exists between members of the TGFβ family. TGFβ molecules are involved in almost every aspect of development and it is therefore not difficult to envisage a situation where misexpression of *Inhβb* disrupts organogenesis by interfering with other TGFβ signalling pathways. However, *in situ* analysis has failed to demonstrate ectopic expression of *Inhβb* and sequencing of the gene has not revealed any mutations within the open reading frame.

In humans *Gli2* and *Inhβb* also map close to each other on chromosome 2 suggesting that the chromosomal location of the genes is conserved through evolution. However, the recently published sequence of the human genome (Lander

et al., 2001; Venter et al., 2001) failed to identify any novel genes within the critical region, suggesting that *Gli2* and *Inh β b* are the only candidates for the *Dh* mutation.

The Genetics of *Dh*

Attempts to identify the gene responsible for the *Dh* mutation genetically have also been carried out (Hughes et al., unpublished data). Mice heterozygous for the *Dh* mutation were crossed to several different lines heterozygous for chromosomal deletions encompassing the critical region, but the results are difficult to interpret. Firstly, mice carrying only the deletions do not display any of the characteristics associated with the *Dh* mutation demonstrating that the mutation is dominant. In contrast, when the deletions are combined with the *Dh* mutation it results in an enhanced phenotype of the hindlimbs. However, this is also the case, when *Dh* is crossed to mice carrying a targeted deletion of the *Gli2* suggesting that the limb phenotype observed with the deletion is due to the loss of *Gli2* (Hui, pers. com.). In addition the *Dh/Gli2* trans-heterozygous mice also display polydactyly of the forelimbs, a phenotype not observed in either *Dh/+* or *Gli2/+* mutants on their own. However, the limb phenotype in *Dh* is complex and genetic analysis of *Dh* in combination with other limb mutants has revealed that the mutation interacts with several mutations during limb development (Hecksher-Sørensen et al., unpublished data). When crossed to other luxoid mutations such as *lx*, *Xt* and *Ssq* to produce compound heterozygotes it results in an enhanced limb phenotype of both fore and hindlimbs and apart from *Xt* none of these mutations affects forelimb development when heterozygous. Hence it appears that *Dh* affects the developing fore and hindlimbs in a manner, which makes them more sensitive to other defects and that could be the reason why *Dh* displays an enhanced phenotype in combination with *Gli2* deletion. This theory is further strengthened by the fact that the visceral abnormalities in *Dh* are unaffected when the *Dh* is crossed to the chromosomal deletions.

Despite several attempts to determine the gene responsible the *Dh* mutation, it should be stressed that no conclusive results have been obtained and at the moment both *Gli2* and *Inh β b* are good candidates for causing the complex phenotype associated with the *Dh* mutation.

1.3 Limb development

The vertebrate limb has been assigned to many different functions during evolution. But whether appendages are used for flying, swimming, paddling or climbing the same molecular principles are applied during development. Because of its location, on the outside of the developing embryo, the limb has long been a preferred system for studying the molecular mechanisms underlying pattern formation. In recent years tremendous progress has been made in understanding the basics of pattern formation and many genes required in this process, have been isolated (reviewed in Tickle, 1995; Cohn and Tickle, 1996; Johnson and Tabin, 1997).

Induction of the limb buds

When members of the Fgf family are applied to the presumptive lateral flank of chicken embryos they induce formation of ectopic limb buds which can develop into complete limbs (Cohn et al., 1995; Ohuchi et al., 1995; Crossley et al., 1996; Vogel et al., 1996; reviewed in Tanaka and Gann, 1995). This strongly indicates that the endogenous signal for limb induction is mediated by members of the Fgf family.

In stages prior to limb induction, *Fgf8* is expressed in the intermediate mesoderm (IM) adjacent to the limb fields, and in the overlying ectoderm from which the AER later develops (Mahmood et al., 1995; Crossley et al., 1996). *Fgf10* on the other hand is expressed in the limb field mesoderm lying between the IM and the surface ectoderm (Ohuchi et al., 1997). Initially *Fgf10* is expressed in the mesoderm throughout the lateral flank but in the stages immediately prior to limb induction expression becomes restricted to the limb fields and it is believed that Fgf8 signalling from the IM is required to restrict the expression of *Fgf10*. In absence of Fgf10 protein *Fgf8* expression fails to be induced in the presumptive AER and although initial budding occurs subsequent limb development is completely abolished, confirming that the *Fgf10* gene has an essential role during induction of the limbs (Min et al., 1998; Sekine et al., 1999). The role of *Fgf8* in limb development has been more elusive because targeted deletions causes embryonic lethality prior to limb initiation (Sun et al., 1999). Only recently conditional inactivation of *Fgf8* specifically in the AER has allowed researchers to assay the role of *Fgf8* during limb development (Moon and Capecchi, 2000; Lewandoski et al., 2000). These experiments clearly show that *Fgf8* has an important role during limb development, but it remains to be proven whether Fgf8 signalling is required for limb induction because the expression of *Fgf8* in the IM is unaffected by the conditional

inactivation. Nevertheless, it is clear that regulation of *Fgf10* and *Fgf8* is closely linked and that this mutual relationship is essential for the earliest stages of limb development. Indeed, the importance of this relationship is demonstrated in mice lacking the Fgf receptor, *FgfR2*. These mice die at E11 but they also fail to initiate limb development (Xu et al., 1998). *In situ* analysis of mutant embryos revealed that the expression of *Fgf8* in the ectoderm is completely absent while the levels of *Fgf10* transcripts in the underlying mesenchyme are severely down regulated. This is strong evidence that the feedback loop between *Fgf10* and *Fgf8* is acting through the *FgfR2* gene product.

Most recently it has been shown that members of the Wnt family are key regulators of the loop between *Fgf10* and *fgf8* (Kawakami et al., 2001). Application of Wnt2b and Wnt8c to the lateral flank of chick embryos induces ectopic limbs through activation of *Fgf10*. A third gene *Wnt3a* is then required for the induction of *Fgf8* expression in the surface ectoderm. Interestingly, the expression of *Wnt2b* and *Wnt8c* corresponds to the presumptive limb fields of the fore and hindlimbs, respectively and has therefore been proposed that it is the activity of these genes, which restricts the expression of *Fgf10* to the limb regions (figure 1.3). However, it remains unclear whether Fgf8 signalling from the intermediate mesoderm is required for induction of *Wnt2b* and *Wnt8c*.

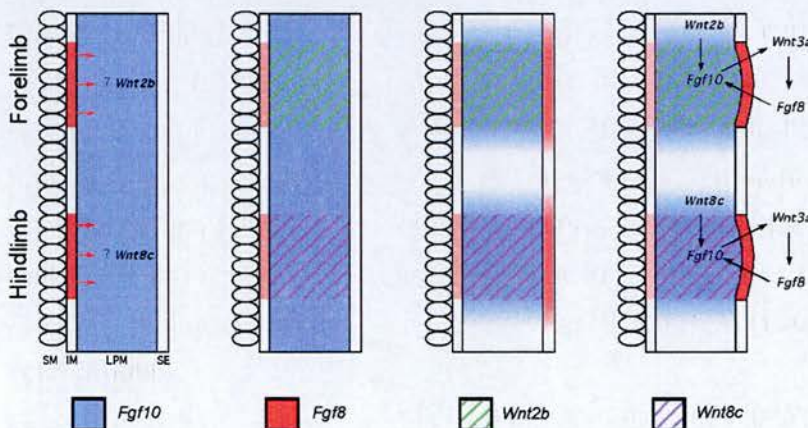


Figure 1.3: Limb induction. Modified from Kawakami et al., 2001. *Wnt2b* (green) and *Wnt8c* (purple) might be required to restrict the expression of *Fgf10* (blue) in forelimb and hindlimb regions respectively. Once restricted *Fgf10* signalling induces *Fgf8* expression (red) in the surface ectoderm (SE) through *Wnt3a*. At present it is unknown whether *Fgf8* signalling from the intermediate mesoderm (IM) is required for the induction of *Wnt2b* and *Wnt8c* expression. (LPM) lateral plate mesoderm and (SM) somites.

Hox genes specify the positions of the limbs

Although members of the Fgf and Wnt families have the ability to induce ectopic limbs throughout the potential limb region, vertebrates only have four appendages, which develop in pairs opposite each other with respect to the midline. Recent studies have demonstrated that a Wnt mediated feed back loop between *Fgf10* and

Fgf8 is required for induction of the limbs (Kawakami et al., 2001). Hence the anterior posterior positions of the limbs are determined by the expression boundaries of *Wnt2c* and *Wnt8b*, but what factors positions the expression of the *Wnt* genes?

The *Hox* genes are grouped in four paralogous clusters *Hoxa*, *Hoxb*, *Hoxc* and *Hoxd*, each consisting of several genes numbered 1-13 (figure 1.4; reviewed in Gruss and Kessel, 1991; Krumlauf, 1994).

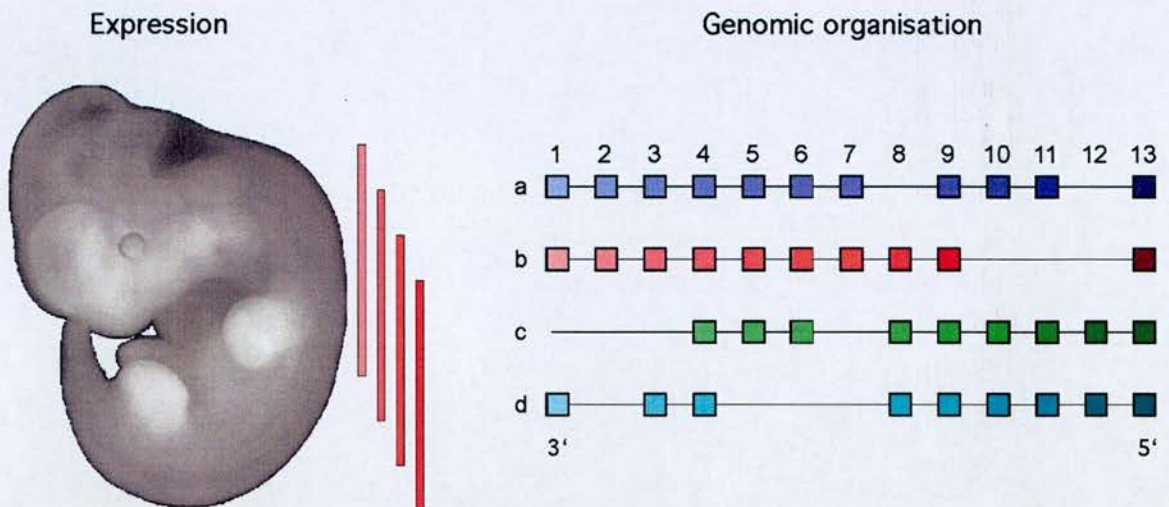


Figure 1.4: Expression and genomic organisation of the *Hox* genes. The *Hox* genes are grouped into four clusters a (blue), b (red), c (green) and d (cyan). Each cluster contain genes numbered from 1 to 13, the lowest being positioned at the 3' end. During development the *Hox* genes are expressed in a collinear manner, which preserves the genomic localisation. Thus genes located at the 3' end of the cluster are expressed more anteriorly while genes at the 5' end are expressed more posteriorly. This expression provides a so-called *Hox* code that specifies segmental identity along the anterior-posterior axis. The expression pattern for the *Hoxb* genes are illustrated as bars next to the embryo; the light red represent 3' genes and dark red represents 5' genes.

Genes positioned at the 3' of each cluster (lowest numbers) are expressed earlier and more anteriorly than genes at the 5' end. This expression pattern provides a so called *Hox* code which specifies segmental identity along the anterior-posterior axis of the developing embryo. In recent years genetic alterations changing the expression patterns of individual *Hox* genes through targeted deletions or misexpression have provided substantial evidence that the *Hox* code is required for segmental identity (Kessel and Gruss, 1991; Small and Potter, 1993; Charite et al., 1994; Suemori and Noguchi, 2000). However, an interesting aspect of the axial specification mediated by *Hox* genes is the segmental variation between different species of vertebrates. In mouse the transition between cervical and thoracic vertebrae is between vertebrae 7 and 8, in chick it is between vertebrae 13 and 14 (figure 1.5).

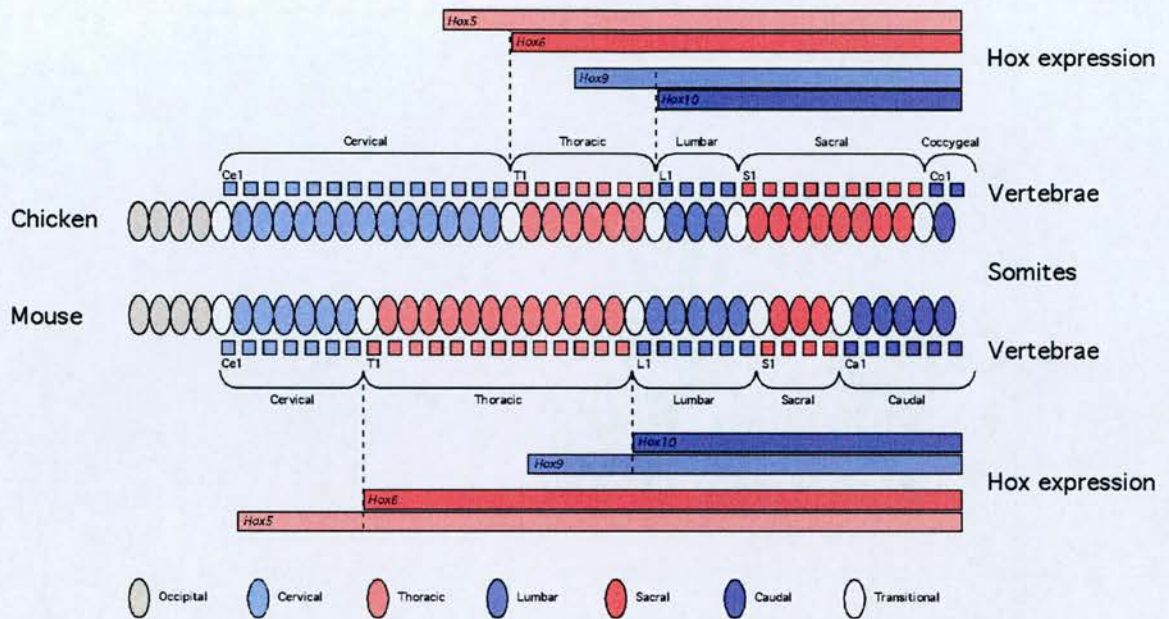


Figure 1.5: Alignment of chicken and mouse vertebrae. The *Hox* genes specifying segmental identity in the two species are conserved despite the different numbers of vertebrae. The boundary between *Hox-9* and *Hox-10* paralogous signifies the thoracic-lumbar transition. The boundary between *Hox-5* and *Hox-6* paralogous determines the cervical-thoracic boundary and correlates with the position of the forelimb. (Modified from Burke et al., 1995).

In both species, the boundary between the *Hox5* paralogues and *Hox6* paralogues defines the transition between cervical and thoracic vertebrae (Burke et al., 1995). Similarly the transition between thoracic and lumbar vertebrae is defined by the boundary between the *Hox9* and *Hox10* paralogues. These results indicate, that although the limbs arise from different somite levels in different vertebrates, their position are always consistent with respect to the level of *Hox* gene expression along the anterior-posterior axis. In fish, amphibians, birds and mammals, the forelimb buds are induced at the anterior boundary of *Hoxc6* expression, the position of the first thoracic vertebrae (Burke et al., 1995; Molven et al., 1995). In mice where both alleles of the *Hoxb5* gene has been deleted, the position of the forelimb is shifted anteriorly (Rancourt et al., 1995). This is strong evidence that *Hox* genes play an important role in positioning the limbs and could be responsible for activation of *Wnt* and *Fgf* expression in the anterior and posterior regions of the potential limb field.

It is clear that the *Hox* code play an important role in determining the anterior-posterior position of the limbs. However, when beads soaked in Fgf are grafted to the lateral flank of chicken embryos it results in respecification of the *Hox* code in the flank mesoderm (Cohn et al., 1997). Hence it appears that the *Hox* code, despite its significant importance in determining segmental identity, also display some plasticity which allows the developing limb buds to shift the relative boundaries of *Hox* gene expression in the flank mesoderm. But, at present the purpose of this plasticity has not been determined.

Setting up the *Hox* code

In *Drosophila* the *polycomb* group and the *trithorax* group genes are required to maintain expression of the *homeotic* genes (reviewed in Orlando and Paro, 1995). Several murine homologues of these genes have been isolated and in accordance with their role in *Drosophila*, patterning of the axial skeleton is disrupted when they are mutated (Yu et al., 1995; Alkema et al., 1995; Akasaka et al., 2001). However, as in *Drosophila* it is thought that the *polycomb* genes only are required to maintain the expression boundaries of the *Hox* genes, not to establish the initial *Hox* code.

Members of the *Cdx* gene family also have a role in regulating the expression of *Hox* genes and mice carrying homozygous deletion of *Cdx1* and *Cdx2* display homeotic transformations of the axial skeleton and altered expression of *Hox* genes (Subramanian et al., 1995; Chawengsaksophak et al., 1997). Additionally, the *Cdx* genes are expressed in overlapping domains in the primitive streak region (Meyer and Gruss, 1993; Gamer and Wright, 1993; Beck et al., 1995), which means that the spatial and temporal expression of the *Cdx* genes is consistent with a role in specifying *Hox* gene expression boundaries. When teratogenic doses of retinoic acid (RA) are administered to pregnant mice it induces severe homeotic transformations and respecification of the *Hox* code (Kessel and Gruss, 1991) as does genetic inactivation of RA receptors, in particular the *RAR γ* gene (Lohnes et al., 1993). However, it has recently been demonstrated that the effect of RA on *Hox* gene expression is mediated through the *Cdx* genes (Houle et al., 2000). Hence there are several lines of evidence implicating the *Cdx* genes as key-regulators in setting up the expression boundaries of the *Hox* genes.

Recent studies have shown that members of the TGF β superfamily might be involved in patterning of the axial skeleton. Thus mice carrying targeted deletions of the *Bmp11* gene display axial abnormalities (McPherron et al., 1999). Similar abnormalities were observed in *ActRIIb*^{-/-} mice (Oh and Li, 1997) and it has therefore been proposed that *Bmp11* is signalling through the *ActivinIIb* receptor. At present *Bmp11* is the only secreted molecule to affect axial patterning and it remains to be shown if it is acting through the *Cdx* genes. Nevertheless it is an indication that secreted molecules might play an important role in establishing the expression boundaries of the *Hox* genes.

Patterning of the limb buds

The vertebrate limb develops along three distinct axes proximal-distal, dorsal-ventral and anterior-posterior (figure 1.6a). Grafting experiments in chicken has identified

three regions in the early limb bud, important for correct limb development, the Apical Ectodermal Ridge (AER), the Progress Zone (PZ) and the Zone of Polarising Activity (ZPA; figure 1.6b). The AER is a rim of epithelial cells, located at the dorsal-ventral boundary at the distal end of the limb bud. Interactions between the AER and the underlying PZ are required for elongation of the developing limb. The mesenchymal cells in the PZ are undifferentiated and proliferate rapidly. If the AER is removed, proliferation in the PZ stops and the cells start to differentiate, resulting in truncation of the manipulated limb (Saunders, 1948; Iten, 1982; Rowe et al., 1982) and as a result the expression of several genes in the PZ is lost.

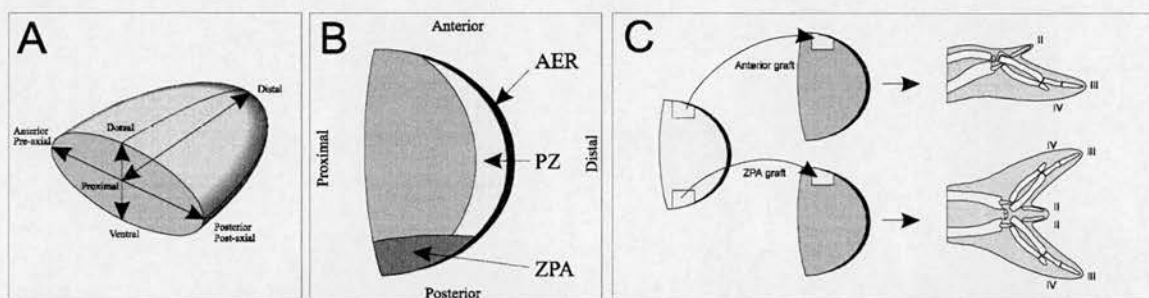


Figure 1.6: Vertebrate limb development. Illustration of the three main axes in the developing limb: proximal-distal, dorsal-ventral and anterior-posterior (A). Important structures in the vertebrate limb bud. The AER is positioned at the dorsal-ventral border at the distal tip of the limb. The PZ is the mesenchyme directly underlying the AER. The ZPA is located in the posterior part of the limb (B). When tissue from the ZPA is grafted to an anterior position in a host limb bud, it reorganises anterior-posterior polarity and induces mirror image duplications. In control experiments where anterior tissue is grafted to an anterior position, wing development occurs normally (C).

It has been shown that most properties of the AER are conveyed by members of the Fgf family, and several Fgf's are capable of rescuing both gene expression and outgrowth, in limb buds where the AER has been removed (Niswander et al., 1993; Vogel and Tickle, 1993; Crossley et al., 1996; Ohuchi et al., 1997). An important function of Fgf signalling from the AER is therefore to stimulate proliferation in the underlying mesenchyme and to maintain the undifferentiated state of the PZ. *Fgf8* and *Fgf4* are both expressed in the AER (Niswander and Martin, 1992; Ohuchi et al., 1994; Crossley and Martin, 1995; Mahmood et al., 1995) and are believed to be the endogenous mediators of AER function. Recent experiments in mouse have demonstrated that *Fgf8* is the major regulator of limb growth. Hence conditional inactivation of *Fgf8* expression in the limb results in truncation and abnormal patterning of the limb (Moon and Capecchi, 2000; Lewandoski et al., 2000) while similar experiments with *Fgf4* has no effect on limb development (Moon et al., 2000; Sun et al., 2000). Interestingly, inactivation of *Fgf8* immediately leads to an up-regulation of *Fgf4* expression, which presumably rescues limb development to some extent and demonstrates the functional redundancy between the two genes.

Anterior-posterior asymmetry in the limb

When posterior limb bud tissue is grafted to an anterior location in a host limb bud, the number of digits in the resulting limb is increased. Moreover, the duplicated digits resemble a mirror image of the normal digit pattern (figure 1.6c; Saunders and Gasseling, 1968; Tickle et al., 1975). Because of its ability to reorganise anterior-posterior polarity of the limb bud, this region has been termed Zone of Polarising Activity (ZPA). On basis of ZPA grafts, it was proposed, that cells in the ZPA secrete a morphogen which specifies the identity of cells along the anterior-posterior limb axis (Wolpert, 1969).

Expression of *Shh* colocalises with ZPA activity in the chicken limb and application of Shh protein or grafting of *Shh* expressing cells to anterior limb bud tissue induce mirror image duplication identical to those produced by ZPA grafting (Riddle et al., 1993; Chang et al., 1994). Also, *Shh* expression is activated following application of Retinoic acid, an agent known to induce ZPA activity, when applied to anterior limb mesenchyme (Riddle et al., 1993). The properties and expression pattern of *Shh* immediately made it a good candidate for being the morphogen produced by the ZPA. However, it has recently been shown that the Shh signal is very short-ranged (Yang et al., 1997). A membrane anchored Shh molecule was engineered by fusing the functional domain of *Shh* to a membrane protein. When cells expressing this chimeric protein were grafted to anterior limb bud tissue they induced mirror image duplications similar to those induced by cells expressing normal *Shh*. Additionally it has been demonstrated that application of Shh does not induce *Shh* expression in host cells. Mirror image duplications induced by ZPA grafts or application of Shh are dose dependent i.e. the number of ectopic digits depends on the number of grafted cells (Tickle, 1981; Yang et al., 1997). If the Shh signal does not directly specify anterior-posterior cell identity, there must be other downstream signals, which are activated by Shh in a dose dependent fashion. Members of the bone morphogenetic protein (BMP) family are good candidates as mediators of the Shh signal, and their response to Shh application has recently been shown to be dose dependent (Yang et al., 1997).

Members of the TGF β superfamily *Bmp2*, *Bmp4* and *Bmp7* are all expressed in the AER and mesenchyme during limb development (Lyons et al., 1990; Jones et al., 1991; Lyons et al., 1995; reviewed in Hogan, 1996), but *Bmp2* in particular has been associated with a role in pattern formation. In chicken wing buds *Bmp2* is expressed in a broader domain than *Shh* in posterior mesenchyme (Francis et al., 1994) and can be induced ectopically by application of Shh (Laufer et al., 1994). Additionally application of BMP2 expressing cells results in duplication of one digit and

activation of *Hoxd-11* and *Hoxd-13* in the anterior mesenchyme and *Fgf4* expression in the AER. However, no *Shh* expression was detected suggesting that *Bmp2* have weak polarising activity and acts downstream of *Shh* (Duprez et al., 1996).

Establishing anterior-posterior asymmetry in the limb

There is evidence that the *Hox* genes also determine anterior-posterior identity within the limb. In particular *Hoxb8* has been implicated with positioning the ZPA in the forelimb. In the lateral flank and neural tube the anterior boundary of *Hoxb8* expression correlates to the ZPA region in the forelimb. In mice where the boundary of *Hoxb8* is shifted anteriorly so it covers the entire forelimb, an ectopic ZPA forms at the anterior border resulting in mirror image duplications (Charite et al., 1994). RA plays an important role in setting up the anterior-posterior *Hox* code along the body axis (Kessel and Gruss, 1991). When beads soaked in RA are grafted to anterior limb bud tissue it induces ectopic ZPA activity, but also it activates *Hoxb8* expression (Lu et al., 1997). RA induces *Hoxb8* expression directly, without protein synthesis, suggesting that the ability of RA to induce *Shh* expression is mediated by *Hoxb8*. These results provide strong evidence that *Hoxb8* is required for positioning of the ZPA in the forelimb. Also they demonstrate that the axial expression of *Hox* genes might play an important role in patterning the developing limbs. Thus other *Hox* genes might be required for activating expression of ZPA repressors such as *Alx4* and *Gli3* in the anterior part of the developing limb (Masuya et al., 1995; Qu et al., 1997; Qu et al., 1998; Takahashi et al., 1998).

Hox genes are also required for correct patterning of the limb later in development. Genes located 5' in the *Hoxd* cluster, *Hoxd9* through *Hoxd13* are initially expressed in nested domains, centred around the ZPA (Dolle et al., 1989; Nelson et al., 1996; reviewed in Izpisua-Belmonte and Duboule, 1992). The region closest to the ZPA expresses all five *Hoxd* genes, but as the distance from the ZPA is increased the number of genes expressed is reduced. When ZPA tissue or *Shh* is applied to anterior limb bud tissue, it results in a mirror image duplication of the entire *Hoxd* expression domain (Izpisua-Belmonte et al., 1991; Nohno et al., 1991; Riddle et al., 1993). Similarly ectopic *Hox* expression in the anterior mesenchyme is induced in several polydactylous mutants (Masuya et al., 1995; Qu et al., 1997; Hecksher-Sørensen, 1998; Lettice et al., 1999a; Sharpe et al., 1999). It therefore appears that the *Hoxd* genes respond to *Shh* signalling. However, the opposite has also been shown and misexpression of *Hoxd12* in the developing limb bud results in polydactyly and tibial hemimelia (Knezevic et al., 1997).

Fore and hindlimb identity

Tbx5 and *Tbx4* are expressed in the forelimb and hindlimb respectively and they are required for determining limb identity (Ohuchi et al., 1998; Isaac et al., 1998; Gibson-Brown et al., 1998; Rodriguez-Esteban et al., 1999). When ectopic limbs are induced in the lateral flank of chick embryos they express both *Tbx5* and *Tbx4* and when allowed to develop it results in a chimeric limb displaying both wing and leg identity (Ohuchi et al., 1998; Isaac et al., 1998). The expression of other genes such as the *Hoxc9*, *Hoxc10*, *Hoxc11* and *Pitx1* are restricted to the hindlimbs (Nelson et al., 1996; Szeto et al., 1996; Lamonerie et al., 1996). Misexpression of *Pitx1* in the developing forelimb induces the expression of other hindlimb specific genes such as *Tbx4*, *Hoxc10* and *Hoxc11* suggesting that *Pitx1* is acting early in the pathway determining hindlimb identity (Logan et al., 1999). At present it is unclear what factors that are responsible for activating differential gene expression between fore and hindlimb buds, but with the recent finding that *Wnt2b* and *Wnt8c* are expressed in the fore and hindlimb region (Kawakami et al., 2001) it will be interesting to see if they have a role in this process. However, since the *Hox* code is thought to position *Wnt* expression along the anterior-posterior axis, it is presumably also involved in determining fore and hindlimb identity, albeit directly or indirectly.

Innervation of the limbs

Evolutionary studies of *Hox* gene expression have shown that transposition in the axial skeleton are reflected by corresponding changes in the expression of *Hox* genes in the paraxial mesoderm (Burke et al., 1995). Likewise it has been demonstrated that the segmental arrangement in the spinal nerves also can be correlated with shifts in the expression domains of *Hox* genes (Gaunt et al., 1999). Hence the expression of *Hoxa7*, in both mouse and chick corresponds to the position of brachial plexus although in chick this landmark is shifted seven segments posteriorly relative to mouse. The vertebrate limb is partly derived from somites (musculature), from lateral plate mesoderm (skeletal elements) and from the neural tube (nerves). Also, it is known that the regulation of *Hox* gene expression in the lateral plate mesoderm is independent of that in the somites and neural tube. So for transposition of the limbs to occur, a coordinated shift in *Hox* gene expression must take place in both the lateral plate mesoderm and in the neural tube. However, recent experiments suggest that the limb itself is responsible for coordinating the surrounding tissue.

Grafting experiments in chicken has revealed that ectopically induced limb are innervated correctly (Ohuchi and Noji, 1999). Additionally it appears that ectopic

limbs signal to the lateral flank and respecify the identity of the mesoderm and as a result the expression of *Hox9* paralogues is altered following implantation of Fgf soaked beads (Cohn et al., 1997). Because ectopic limbs do not affect *Hox* expression in the neural tube these results suggest that nerve innervation of the limbs is coordinated by the limbs themselves. When dorsal somitic tissue transplanted between different axial levels it retains original *Hox* expression. In contrast, the ventral somitic tissue contains cells which migrate into the lateral mesoderm of the host and adopt the *Hox* expression corresponding to the lateral plate and participate in the morphology appropriate to the host level (Nowicki and Burke, 2000). In another experiment it was shown that ectopic expression of *Hoxc6* in the lateral flank mesoderm has severe effects on nerve migration (Burke and Tabin, 1996). Hence it appears that the lateral mesoderm not only has the capacity to instruct entering cells to change their identity, it is also required to ensure proper migration of the peripheral nervous system. Furthermore it seems like *Hox* genes play an important role in the process. A possible scenario is therefore that the induction of an ectopic limb respecifies the identity and *Hox* profile of the lateral flank mesoderm, which then in turn signals to the migrating nerves instructing them to innervate the limb. In mice that are double homozygous for deletions in *Hoxa10* and *Hoxd10* the nerves innervating the hindlimbs are defective and as a result both the tibial and proneal nerves are truncated (Wahba et al., 2001). It is unclear whether this defect is due to lack of *Hoxa10* and *Hoxd10* protein in the nerve cells or in surrounding mesoderm. Nevertheless this observation confirms that *Hoxa10* and *Hoxd10* play an important role in ensuring proper innervation of the hindlimbs.


Human applications

Limb abnormalities similar to those observed in *Dh* also occur in humans and tibial hemimelia affects approximately 1 in 15,000 humans (table 1.1). An extensive investigation carried out in Hungary showed, that 1 in 1800 infants are born with limb deficiencies and that 9% of these also suffer from renal abnormalities (Evans et al., 1992). Classification of the limb defects has revealed that the renal defects most commonly associate with limb defects such as micromelia (44.4%), amelia (17.6%) and radial/tibial deficiencies (27.4%).

In *Dh* and *lx* mice tibial hemimelia also associates with abnormalities in the renal system. This strong correlation between limb and kidney abnormalities evokes an old debate proposing that the mesonephros is required for limb induction. The mesonephros is an important component of the urogenital system and following

surgical removal, limb development is severely impaired suggesting that the mesonephros could be responsible for inducing and maintaining limb development (Geduspan and Solursh, 1992). The presence of *Fgf8* expression in the intermediate mesoderm/mesonephros in the limb

Table 1.1: Tibial hemimelia in humans

Association between limb defects and kidney abnormalities				
<i>Type of limb defect</i>	Number of individuals with limb abnormalities	Cases also suffering from urinary defects	Percentage	Tibial hemimelia in humans
Amelia	17	3	17.6%	
Rudimentary limb	9	4	44.4%	
Terminal transverse	240	5	2.1%	
Rradial/tibial	113	31	27.4%	
Ulnar/fibular	127	2	1.6%	
Intercalary	38	6	15.8%	
Central axis	94	8	8.5%	
Digital amputations	163	1	0.6%	
Other (not classified as above)	10	3	30.0%	
Mixed	28	9	32.1%	
Unclassified	29	3	10.3%	
Total	868	75	8.6%	

Preaxial (similar to *Dh*)
Postaxial

regions has further strengthened this argument (Crossley et al., 1996). However, this remains controversial since recent experiments suggest that the mesonephros is not required for limb development. In these experiments the mesonephros was removed prior to limb induction by apoptotic ablation and still the limbs developed normally (Fernandez-Teran et al., 1997). Despite the controversy, the mesoderm contributing to early limb development is positioned adjacent to the mesonephros. Hence abnormalities in this mesenchyme might affect the development of both the limb and the kidney.

1.4 Development of the spleno-pancreatic region

The spleno-pancreatic region comprises the pancreas, duodenum and the posterior part of the stomach, which are derived from the endoderm and the spleen that is derived from the mesoderm (figure 1.7). In adult life these organs are easily distinguished from each other and their physiological functions are very different and highly specialised. However, during embryogenesis the development of all four organs is closely linked to each other.

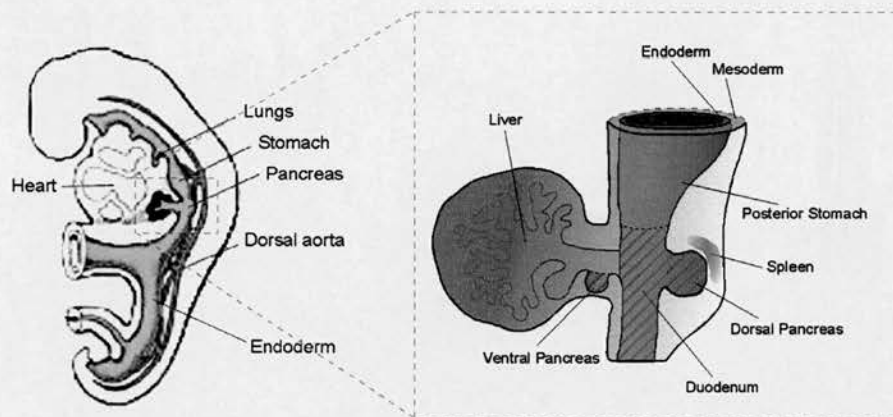


Figure 1.7: The spleno-pancreatic region. The spleno-pancreatic region develops from the endoderm (yellow) and at E10.5 it consists of the dorsal and ventral pancreatic buds, the stomach, the duodenum and the presumptive splenic mesenchyme.

Left-right asymmetry is determined genetically

During early stages of development the spleno-pancreatic region is positioned between the forelimb buds in alignment with the embryonic midline. Later in embryogenesis the region undergoes asymmetric development and as a result the stomach, spleen and pancreas end up in an asymmetric position at the left side of the visceral cavity. However, asymmetric development along the left-right axis is not restricted to the spleno-pancreatic region. Other organs such as the heart, liver, lungs and the loops of the gut tube also develop asymmetrically within the embryo and the position of each organ within the embryo is always the same. In recent years there has been a tremendous increase in our understanding of how these left-right differences are determined in vertebrates (reviewed in Harvey, 1998; Capdevila et al., 2000; Capdevila and Belmonte, 2000). As a result several genes have been found to perturb left-right asymmetry when mutated while other genes are expressed in an

asymmetric manner prior to any morphological differences. There are still many questions, which need to be answered, however, it is clear that the left-right asymmetry is determined genetically.

The normal disposition of the visceral organs is called *situs solitus* whereas *situs inversus* refers to the complete reversal of organ positioning (figure 1.8). Other lateral abnormalities include *right* and *left isomerism*, also called asplenia syndrome and polysplenia syndrome respectively, where the characteristics of one side have been duplicated along the midline, resulting in loss of asymmetry. *Heterotaxia* refers to situations where both normal and inverted morphology of asymmetric organs is observed within the same individual. Whereas *situs inversus* has little or no effect on the survival of the individual, *isomerism* and *heterotaxia* are often associated with severe visceral defects. Particularly the heart appears to be sensitive to alterations in left-right development (Bowers et al., 1996; Yost, 1998).

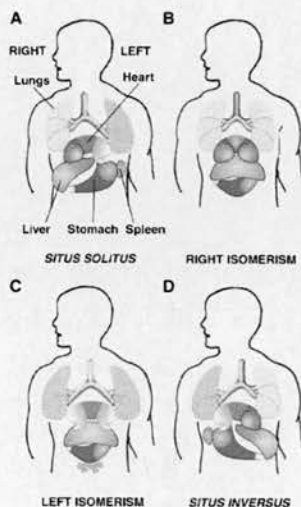


Figure 1.8: Asymmetric disposition of visceral organs in humans. The normal disposition of organs in humans is called *Situs Solitus* (A). The right lung has three lobes, whereas the left lung has two. In addition the apex of the heart points to the left side, the liver is on the right side and the stomach, spleen and pancreas (not shown) are on the left side. Right isomerism, also called asplenia syndrome, the heart and the lungs are double right. The liver and stomach are located at the midline and the spleen is absent (B). Left isomerism, also called polysplenia syndrome, the heart and lungs are double left. The liver and the stomach are usually found at the midline and there is always more than one spleen (C). *Situs inversus* refers to the complete mirror image reversal of asymmetry (D). Since laterality defects are highly variable, this figure depicts simplified cases. The terms *situs inversus*, left and right isomerism can also be used to describe laterality defects for individual organs, although this is usually referred to as *heterotaxia*. (Modified from Capdevila et al., 2000).

Establishing left-right asymmetry

During gastrulation the node progresses from the rostral end of the developing embryo towards the caudal end and in this process it defines the anterior-posterior axis. At the same time the node also signals to the lateral mesoderm and activates the molecular pathway for left-right determination. Asymmetric gene expression in the lateral plate mesoderm anterior to the node therefore represents the first visible evidence of left-right differences (figure 1.9). In recent years many genes have been identified which are expressed in an asymmetric manner, but the interpretation of gene function has been complicated by the fact, that left-right determination varies between species (reviewed in Yost, 1999). Thus several genes, found to be

asymmetrically expressed in chicken, are expressed symmetrically in mouse. This was surprising because in other organs, such as the limb, the basic mechanisms for pattern formation have turned out to be highly conserved between species. However, there are also similarities in the left-right pathway between chick and mouse and it has been possible to establish a hierarchy of the events, which eventually leads to asymmetric disposition of the visceral organs.

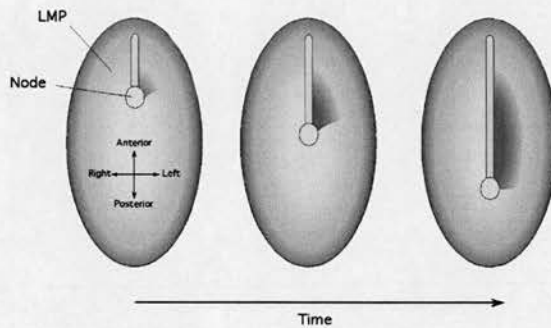


Figure 1.9: Establishing left-right asymmetry. During gastrulation the node progress from anterior to posterior. As it moves it signals to the lateral plate mesoderm (LPM) and induces left specific gene expression (blue). This figure illustrates asymmetric gene expression in a chicken embryo.

Before gastrulation the developing embryo is symmetric. The biggest challenge in unravelling the mechanism for left-right asymmetry has therefore been to determine how the initial symmetry breaks down. Although, the identification of asymmetrically expressed genes indicated that the node was involved in establishing asymmetry they did not answer how. A clue to this enigma came from the observation that males suffering from the condition immotile cilia syndrome (ICS) often showed combined sterility and lateral abnormalities (Afzelius, 1995). Cilia are a flexible prolongation of the cell membrane, present in specialised cell types such as sperm and some epithelial cells. In ICS patients the cilia are immotile and that affects several cell types including sperm cells which are live but immobile (Afzelius, 1976; Afzelius, 1995). Using electron microscopy, studies in mouse revealed that cells in the node are mono-ciliated which means they have a single motile cilia located in central position in the cell surface (Sulik et al., 1994). In a series of elegant studies, using fluorescent particles, it was demonstrated that the motion of cilia in node creates a so-called “nodal flow” towards the left (Nonaka et al., 1998). A model has therefore been proposed, which suggest that the vortical movement of the cilia results in a leftward flow of embryonic fluids in the node (figure 1.10). A yet unidentified signalling molecule, secreted into the nodal fluids, will drift towards the left side and activate the left determining pathway (reviewed in Vogan and Tabin, 1999; Supp et al., 2000). In accordance with the model, several mouse mutations causing laterality defects, have absent or immotile cilia and display randomised nodal flow, followed by ectopic expression of asymmetric genes (Nonaka et al., 1998; Okada et al., 1999;

Takeda et al., 1999). Furthermore, the genes affected by these mutations *Kif3a*, *Kif3b*, *Lrd* and *Polaris* all encode structural molecules required for cilia assembly (Marszalek et al., 1999; Takeda et al., 1999; Nonaka et al., 1998; Supp et al., 1997; Supp et al., 1999; Taulman et al., 2001).

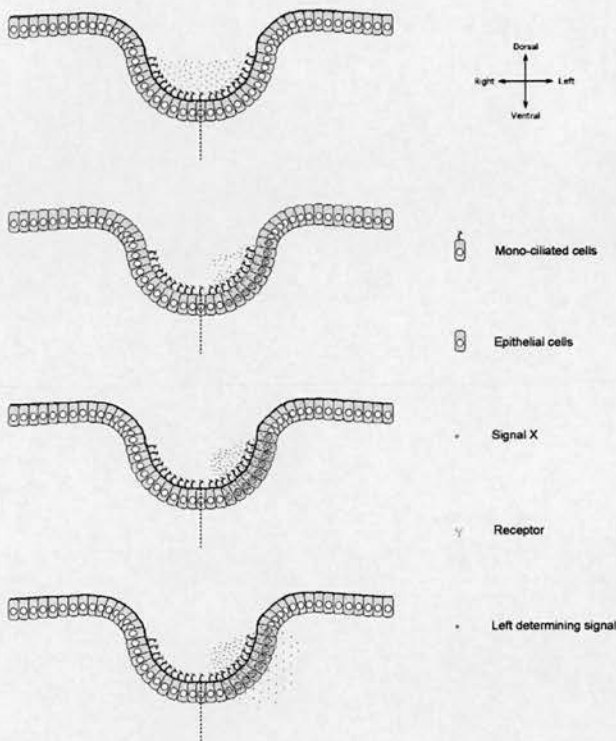


Figure 1.10: The nodal-flow activates asymmetric gene expression. In mouse, cells in the node are monociliated and movement of the cilia creates a leftward flow across the node. As signalling molecules (red) in the node fluids are concentrated on the left side of the node. Here they bind to receptors (pink) and activate the transcription of a left determining gene (blue). When secreted, the left determining gene activates the left specific signalling cascade in the lateral plate mesoderm.

Mice carrying homozygous copies of the *inv* (*inversion of embryo turning*) mutation consistently display complete *situs inversus* (Yokoyama et al., 1993). However, in contrast to the other laterality mutants, the nodal flow appears to be normal in *inv* mice (Okada et al., 1999). This observation is incompatible with the idea that the nodal flow is the sole requirement for establishing left-right asymmetry and has therefore sparked a debate as to whether other factors are required or if other pathways are acting in parallel. Also it has been suggested that *inv* is acting downstream of initial left-right specification. Unfortunately, the molecular nature of the *inv* gene product, a novel cytoplasmic protein called inversin (Mochizuki et al., 1998; Morgan et al., 1998) offers little insight into its function. At present too little is known about the function of the *inv* mutation to suggest a precise role in left-right determination. Another, less convincing argument against the nodal flow model is that the presence of mono-ciliated cells in the node have not been reported in species other than mouse.

A genetic pathway for left-right asymmetry

In chicken embryos the first genes to be activated in an asymmetric manner is the TGF β molecule *Inh β b*, which is expressed on the right side of the node (Levin et al., 1997). The evidence for *Inh β b* having an important role in defining left-right asymmetry in chick was further strengthened by demonstrating that obstruction of activin signalling with Follistatin soaked beads disrupts left-right determination. Activation of asymmetric activin signalling induces the expression of its own receptor *ActRIIa* and *Fgf8* on the right side (Levin et al., 1995; Stern et al., 1995; Boettger et al., 1999), while restricting the otherwise symmetric expression of *Shh* to the left side (Levin et al., 1995; Pagan-Westphal and Tabin, 1998). On the left side of the node Shh signalling initiates a signalling cascade that, mediated by the *Cerberus*-related gene *Caronte* (Rodriguez Esteban et al., 1999; Yokouchi et al., 1999; Zhu et al., 1999), leads to the activation of *nodal* expression in the lateral plate mesoderm.

Caronte belongs to the *Cerberus*/*Dan* family and it is believed that these genes function by binding to ligands of the TGF β family in particular Bmp signalling molecules, thus preventing them from binding to their receptors (Hsu et al., 1998). It therefore appears that activation of *nodal* by *Caronte* is mediated by antagonism of Bmp signalling. In concordance with this idea other inhibitors of Bmp signalling, such as *Noggin*, are also capable of inducing *nodal* expression when applied to the right lateral plate mesoderm (Yokouchi et al., 1999). An interesting aspect of *nodal* is that it shows asymmetric expression in all vertebrate animals examined so far (Levin et al., 1995; Collignon et al., 1996; Lowe et al., 1996; Levin et al., 1997; Lohr et al., 1997; Sampath et al., 1997; Rebagliati et al., 1998). Moreover, misexpression of *nodal* on the right side of the embryo is enough to randomise *situs* determination in multiple organ systems (Levin et al., 1997; Sampath et al., 1997), suggesting that *nodal* has a central role in coordinating left-right asymmetry in vertebrates. Members of the *lefty* family also appear to be a conserved part of the left-right determining pathway (Meno et al., 1996; Meno et al., 1997; Bisgrove et al., 1999; Meno et al., 1999; Thisse and Thisse, 1999; Cheng et al., 2000). *lefty1* is expressed in the left side of the node and prospective floorplate and is required to restrict the expression of *nodal* to the left side of the embryo (Meno et al., 1998). In absence of *lefty1* signalling, *nodal* is expressed on both sides of the midline. It has therefore been proposed that *lefty1* acts as a midline barrier, preventing activation of left sided genes like *nodal*, on the right side of the embryo. Another *lefty* gene, *lefty2*, is also asymmetrically expressed in the left lateral mesoderm in a manner similar to that of *nodal* (Meno et al., 1997). Like *lefty1*, *lefty2* is thought to act as an antagonist of *nodal* signalling although both genes are co-expressed in many cells. It has been

suggested that direct competition between *nodal* and *lefty* proteins for common receptor sites, provides a mechanism for fine-tuning the effect of *nodal* signalling (reviewed in Schier and Shen, 2000). Although the later part of the pathway seems highly conserved between vertebrates there are several significant differences during the early stages of left-right specification (figure 1.11).

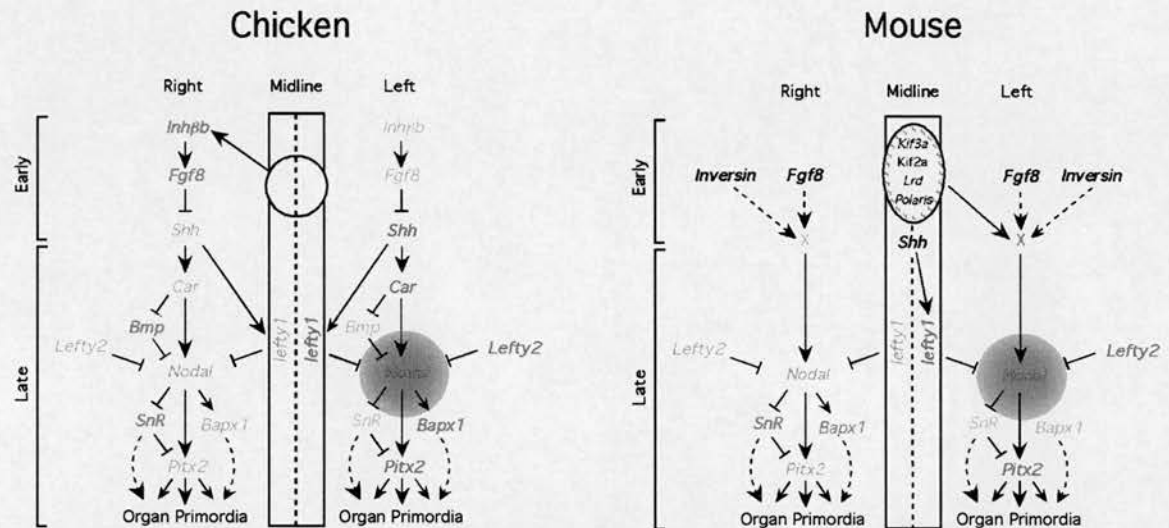


Figure 1.11: Genetic pathway for left-right asymmetry in chicken and mouse. A large number of genes, which play an important role in left-right asymmetry, have been identified. Genes that are expressed are shown in red while genes that are off are shown in grey. The early stages of the pathway differ between mouse and chick and genes such as *Fgf8* and *Shh* that show asymmetric expression in chick are expressed symmetrically in mouse. In contrast the presence of monociliated node cells has only been found in mouse. However, the late pathway, which centres around *Nodal* (blue) appears to be more or less conserved between all vertebrate species. Hence the genes required for regulation of nodal expression are conserved as is most of the genes downstream of *Nodal*. Interestingly *Bapx1* is expressed on the left side in chicken and on the right side in mouse.

As mentioned above the presence of mono-ciliated cells in the node has only been observed in mouse. Another difference is that *Fgf8* and *Shh*, are both asymmetrically expressed in chicken, whereas in mouse they are expressed symmetrically. However, it appears that both genes do have a role in left-right determination in mouse despite the lack of asymmetric expression. Hence, it has recently been shown that both *Shh* and *Fgf8* disrupts laterality in mouse when mutated (Tsukui et al., 1999; Meyers and Martin, 1999). In the absence of *Shh* protein, *lefty1* fails to be expressed suggesting that *Shh* is required for activation of *lefty1* expression along the midline and presumably the laterality defects are due to the absence of *lefty1*. Finally, in chicken *Inhbb* is the first gene to be asymmetrically expressed. There is little doubt that activin signalling has an important function in determining left-right signalling in chick since both misexpression and blocking of the signal with TGF β antagonists, perturbs the expression of downstream genes (Levin et al., 1997). In contrast targeted mutation of *Inhbb* in mouse has no effect on laterality (Matzuk et al., 1995b). The

only indication that might indicate that activin signalling is important in left-right specification in mouse is that targeted deletion of the *ActRIIb* causes laterality defects (Oh and Li, 1997). However, *ActRIIb* probably acts as receptor for many TGF β molecules and since the entire left-right pathway is mediated by members of this family (*Inh β b*, *nodal*, *lefty1*, *lefty2* and *Bmp's*), it is unlikely that the *ActRIIb*^{-/-} phenotype reflects a role for *Inh β b* in mouse.

Asymmetric organ development

The expression of many asymmetric genes is transient and disappears before any morphological differences are visible. So an interesting question has therefore been how asymmetric gene expression is relayed and translated by the organ primordia? The bicoid like homeobox gene *Pitx2* was recently cloned and turned out to be good candidate for mediating early asymmetry to the organ primordia (Meno et al., 1998; Piedra et al., 1998; Logan et al., 1998; Yoshioka et al., 1998). *Pitx2* is expressed in the left lateral mesoderm and unlike other left specific genes it continues to be expressed at subsequent stages in the left side of several organ primordia, including the heart, gut and stomach. Ectopic expression of *Pitx2* can cause laterality defects in a variety of vertebrates (Logan et al., 1998; Ryan et al., 1998; Campione et al., 1999; Essner et al., 2000) and *Pitx2* deficient mice display some laterality defects. These defects include right pulmonary isomerism and right isomerism of the lungs, but surprisingly the heart and gut develops normally (Gage et al., 1999; Kitamura et al., 1999; Lin et al., 1999; Lu et al., 1999). Also the expression of *Pitx2* in mice exhibiting laterality defects reflects the altered organ orientation. Thus homozygous *iv/iv* mice show randomised organ situs and *Pitx2* expression while *inv/inv* mice show reversed expression of *Pitx2* (Piedra et al., 1998; Ryan et al., 1998; Campione et al., 1999). Finally, ectopic *nodal* signalling in the right lateral mesoderm can induce expression of *Pitx2* in both chicken and frog embryos (Logan et al., 1998; Ryan et al., 1998; Campione et al., 1999). Together these results are consistent with the idea that *Pitx2* act downstream in the left right determining pathway and it has the capacity to direct organ orientation.

However, *Pitx2* is not the only gene involved in asymmetric organ development. Other transcription factors such as the zinc finger gene *SnR* and the homeobox gene *Bapx1*¹ are also likely to be involved in various aspects of asymmetric organ development. In both mouse and chicken *SnR* is expressed in the

¹ *Bapx1* is also known as *Nkx3.2* and is usually referred to under that name in papers concerned with left right asymmetry. However, this project involves a phenotypic analysis of *Bapx1* mutant mice and to emphasise that these genes are the same *Nkx3.2* will be referred to as *Bapx1* throughout this thesis.

right lateral mesodermal plate (Isaac, 1997; Sefton, 1998). Ectopic *nodal* signalling in the right lateral mesoderm repress *SnR* expression while inactivation of *SnR* activity with antisense oligos results in randomisation of left-right development, accompanied by ectopic expression of *Pitx2* (Patel, 1999). It has therefore been suggested that *nodal* activates *Pitx2* in the left lateral mesoderm through repression of *SnR*. In chicken and *Xenopus* *Bapx1* is expressed in the left lateral mesodermal plate and appears to be downstream of nodal signalling, whereas in mouse *Bapx1* is expressed in the right lateral plate mesoderm (Schneider, 1999). However, the potential involvement of *Bapx1* in directing left-right development has not yet been characterised. It should be noted that *Bapx1* deficient mice are asplenic (Lettice et al., 1999b; Tribioli and Lufkin, 1999; Akazawa et al., 2000), but since the gene is expressed in the splenic mesenchyme (Tribioli et al., 1997) and other asymmetric organs are positioned correctly, it is unlikely that this phenotype reflects the asplenia syndrome.

The exact mechanism by which left sided expression of *Pitx2* and other genes are interpreted by organ primordia such as the spleno-pancreatic region and conveyed into asymmetric development is unclear. In some mouse mutants with laterality defects the visceral isomerism is restricted to particular organs (Meno et al., 1998; Gage et al., 1999) suggesting that each organ responds individually to left-right signalling. This would require combined integration of anterior-posterior and left-right signalling, which in turn is mediated into local physical differences i.e. changes in cell shape or proliferation. However, as yet no such mechanism has been described.

Anterior-posterior patterning of the endoderm

Although left-right signalling provides some sort of positional information to the visceral organs, it is not involved in specifying organ identity. During development the endoderm gives rise to the intestinal tract and various other organs including the thyroid, parathyroids, thymus, ultimobranchial body, respiratory system, stomach, liver, gallbladder, pancreas and cecum. All these organs arise by branching off the endodermal tube and it appears that the level of branching and identity of individual organs primarily is specified by anterior-posterior patterning (reviewed in Wells and Melton, 1999; Grapin-Botton and Melton, 2000).

At present very little is known about the general molecular mechanisms determining anterior-posterior patterning of the gut tube. Several genes have been shown to be expressed in a region specific manner, which might reflect organ

specification (figure 1.12), but it remains to be confirmed. Because of their role in anterior-posterior patterning in other tissues the *Hox* genes are logical candidates for patterning of the endoderm. Most of the vertebrate *Hox* genes are expressed in the splanchnic mesoderm surrounding the endoderm where they are found in a overlapping and extended pattern (Grapin-Botton and Melton, 2000), but only a few are expressed in the endoderm at levels that are detectable with *in situ* hybridisation. Furthermore there is no evidence that *Hox* mutations causes transformations that affects either organ position or identity, although it should be noted that abnormal gut development has been observed in some *Hox* mutants (Manley and Capecchi, 1995; Boulet and Capecchi, 1996; Aubin et al., 1997; Warot et al., 1997).

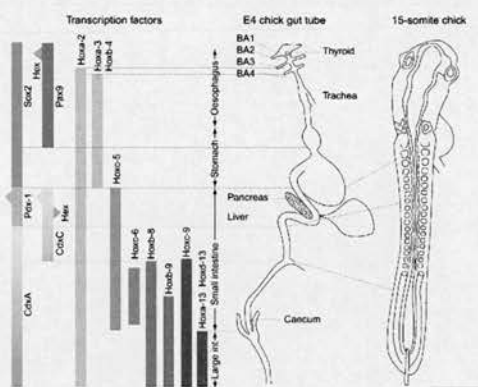


Figure 1.12: Anterior-posterior patterning of the gut tube. Several transcription factors, mostly homeobox genes, are expressed in a regionalised manner in the developing gut tube. It is believed that the overlapping expression patterns provide regional identity, which determines the position and identity of individual organs. These expression domains are based on studies in chicken but the mouse homologues show similar expression patterns. (Modified from Grapin-Botton and Melton, 2000)

However, it is possible that the endoderm is patterned by signals emanating from the mesoderm. This is the case in *Drosophila* where signals from the mesoderm controls expression of the *Hox* gene *labial* in the endoderm (Reuter et al., 1990; Szuts and Bienz, 2000). Also in chicken embryos misexpression of *Shh* can induce ectopic expression of *Hox* and *Bmp* genes in the gut mesoderm (Roberts et al., 1995). *Shh* is normally expressed in the endoderm and might well be regulating gene expression in the mesoderm, however, since it is expressed throughout the gut tube it is unlikely that *Shh* regulates regionalised expression patterns.

In *Amphioxus* another homeobox gene complex, the so-called *ParaHox* cluster has been identified (Brooke et al., 1998), containing homologues of the mammalian homeobox genes *Pdx1* and *Cdx*. The *ParaHox* cluster appears to be conserved in human and mouse and both *Pdx1* and *Cdx* genes show distinct expression boundaries within the endoderm. In particular the *Cdx* genes might play an important role in anterior-posterior patterning of the endoderm, because they have been shown to be regulators of *Hox* genes (Charite et al., 1998).

Pancreas development

The mammalian pancreas is a mixed endodermally derived organ with an important role in the regulation of blood glucose levels and secretion of digestive enzymes into the gut. These two functions are mediated by the exocrine cells that secrete digestive enzymes into the intestine and endocrine cells that secrete hormones into the bloodstream. The exocrine cells are the dominating cell type, which make up almost 98% of the mature pancreas. The endocrine cells are organised in clusters called Islets of Langerhans, which are dispersed throughout the exocrine tissue. These Islets are arranged in a strict manner; the core of the Islets consists of insulin producing β -cells surrounded by glucagon producing α -cells. Somatostatin producing δ -cells and pancreatic polypeptide (PP) producing PP-cells are also predominantly located in the periphery of the Islets. The major function of insulin and glucagon is to regulate glucose levels in the blood and inability to do this leads to the medical condition *diabetes mellitus*. It has been estimated that diabetes affects at least 30 million people world-wide and for this reason pancreas development has received considerable attention in recent years (reviewed in Slack, 1995; Edlund, 1998; Edlund, 1999; Wells and Melton, 1999; Grapin-Botton and Melton, 2000).

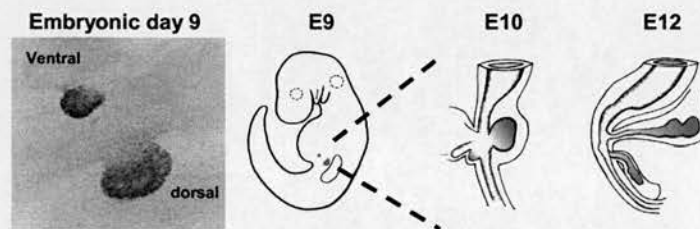


Figure 1.13: Pancreas development. Pancreas development is initiated around E9 when *Pdx1* expression is activated in the dorsal and ventral buds. During subsequent development the endoderm grows into the surrounding mesenchyme. At E12 the two buds fuse and become one. This figure was kindly provided by Dr. Ulf Ahlgren.

Pancreas development is initiated at E9 when the homeobox gene *Pdx1* becomes expressed in the evaginating endoderm destined to become the dorsal and ventral pancreatic buds (Ahlgren et al., 1996). Recombination studies have shown that mesenchymal-epithelial interactions are essential for pancreas development, thus the pancreatic endoderm can only grow and differentiate in the presence of mesenchyme (Golosow and Grobstein, 1962; Wessels and Cohen, 1967). During early stages of pancreas development this mesenchyme has to be of pancreatic origin, but at later stages heterologous mesoderm from the lungs or other tissues is sufficient to maintain growth and differentiation. In chicken *Shh* is involved in patterning of the hindgut (Roberts et al., 1995) and in mouse *Shh* and another member of the

hedgehog family *Indian hedgehog (Ihh)* is expressed uniformly throughout the endoderm except in the pancreatic buds (Bitgood and McMahon, 1995). One important feature of the pancreatic mesoderm is therefore that it is not exposed to Shh signalling and does not express *Shh*-response genes such as *Patched* (Apelqvist et al., 1997). That this is an important aspect of pancreas development has been demonstrated by showing that misexpression of *Shh* in the pancreatic endoderm induces *Patched* in the pancreatic mesoderm and impairs pancreatic development (Apelqvist et al., 1997). Furthermore, genetic disruption of hedgehog signalling in the gut tube leads to a three fold increase in the size of the pancreas (Hebrok et al., 2000) while local inactivation of Shh signalling in *Pdx1* positive endoderm can induce ectopic pancreas development (Kim and Melton, 1998). Hence, it appears that *Shh* has an essential role in specifying pancreatic cell fate. Another gene expressed specifically in the dorsal pancreatic mesoderm is the LIM homeo domain gene *Isl1* (Karlsson et al., 1990; Ahlgren et al., 1997). In mice lacking functional *Isl1* the dorsal pancreatic mesoderm is absent and as a result the dorsal pancreas fails to develop (Ahlgren et al., 1997). Together these results imply that gene expression in the endoderm and mesoderm must be coordinated to ensure proper pancreas development. As described above the *Hox* genes might play a significant role in determining organ identity positional information along the anterior-posterior axis. However, it is also believed that surrounding structures such as the aorta, notochord and heart might provide signals important for endodermal patterning. At E8.5 the endoderm destined to become the dorsal pancreas is in physical contact with the notochord and it has been shown that the notochord provides a permissive signal to the endoderm required for pancreas development (Kim et al., 1997). In absence of notochord signalling *Shh* is not repressed in the dorsal endoderm and pancreas development is abolished. However, application of *Inh β b* and *Fgf2* to the endoderm leads to repression of *Shh* expression and permits expression of pancreatic markers such as *Pdx1* and *insulin* (Hebrok et al., 1998). Although the notochord has an important role in patterning the dorsal part of the endoderm is never in contact with the ventral endoderm. Suggesting that the exclusion of *Shh* and *Ihh* from the endoderm destined to form the ventral pancreas is achieved through a different mechanism.

Spleen development

The spleen is a mesodermally derived organ that plays a role in hematopoiesis, the generation of some immune responses and in the removal of and processing of spent

red blood cells. It is located on the left side of the vertebrate body close to the stomach and pancreas, however, very little is known about the early stages of spleen development. For a long period *Dh* provided the only mouse model for asplenia, but recently several genes have been identified which affect spleen development when disrupted. *Hox11*, *Bapx1* and *Capsulin* all results in complete asplenia when deleted (Roberts et al., 1994; Dear et al., 1995; Lettice et al., 1999b; Tribioli and Lufkin, 1999; Akazawa et al., 2000; Lu et al., 2000) whereas *Wt1*, *Nkx2.3* and *ActRIIb* reduce the size of the spleen when mutated (Oh and Li, 1997; Herzer et al., 1999; Koehler et al., 2000; Pabst et al., 1999). Another gene, *Nkx2.5* is expressed in the spleen primordia in *Xenopus*, but as yet it has not been implicated with spleen development in mouse (Patterson et al., 2000). Although it clear that these genes play an important role in spleen morphogenesis, a genetic hierarchy determining the order of events and individual relationship between the genes, has not yet been established. Histological analyses of frog, chicken, lungfish and mammalian embryos indicate that the splenic rudiment is first recognisable as a single condensation of mesenchyme along the left side of the mesogastrium dorsal to the stomach (Thiel and Downey, 1921; Manning and Horton, 1969; Saito, 1984; Vellguth et al., 1985; Yassine et al., 1989). This places the origin of spleen development within or adjacent to the dorsal pancreatic mesenchyme, suggesting that a spatial relationship might exist between the two organs. Evidence for such a relationship has been further strengthened by several transgenic experiments on pancreas development. Under normal circumstances *Shh* expression is excluded from the pancreatic endoderm and as a result the splenic mesenchyme is not exposed to Shh signalling. In transgenic mice expressing *Shh* in the dorsal pancreatic endoderm the spleen fails to form indicating that the exclusion of *Shh* expression from the dorsal pancreas is an essential requirement for spleen induction (Apelqvist et al., 1997). In *p48* deficient mice the exocrine cells of the pancreas is lacking and in absence of exocrine cells the endocrine cells migrate into the spleen (Krapp et al., 1998). Although these results indicate a developmental association between the pancreas and the spleen, it is known that the pancreas is not required for spleen development. In mice lacking *Pdx1* or *Hlxb9*, where the dorsal pancreas fails to form, the spleen develops normally (Jonsson et al., 1994; Ahlgren et al., 1996; Li et al., 1999; Harrison et al., 1999).

Stomach development

On basis of morphological differences the vertebrate stomach can be divided into two distinct compartments. The anterior stomach or the forestomach is lined with a

mucous layer while the posterior stomach or the glandular stomach is lined with a columnar epithelium that resembles the villi in the gut (figure 1.14). At E9.5 the presumptive stomach can be seen as a swelling of the endodermal tube at the level of the forelimbs. However, the first morphological differences between the anterior and posterior stomach are not detectable until stage E12.5. Although the stomach is the most prominent organ in the spleno-pancreatic region very little is known about the molecular cues underlying its development. Only a few genes have been reported to have a role in stomach development and most of the evidence is based on descriptive analyses. Thus *Bapx1* and *Barx1* are reported to be expressed in the splanchnic mesenchyme surrounding the stomach endoderm at E9.5 and E10.5 (Tribioli and Lufkin, 1997; Tissier-Seta et al., 1995).

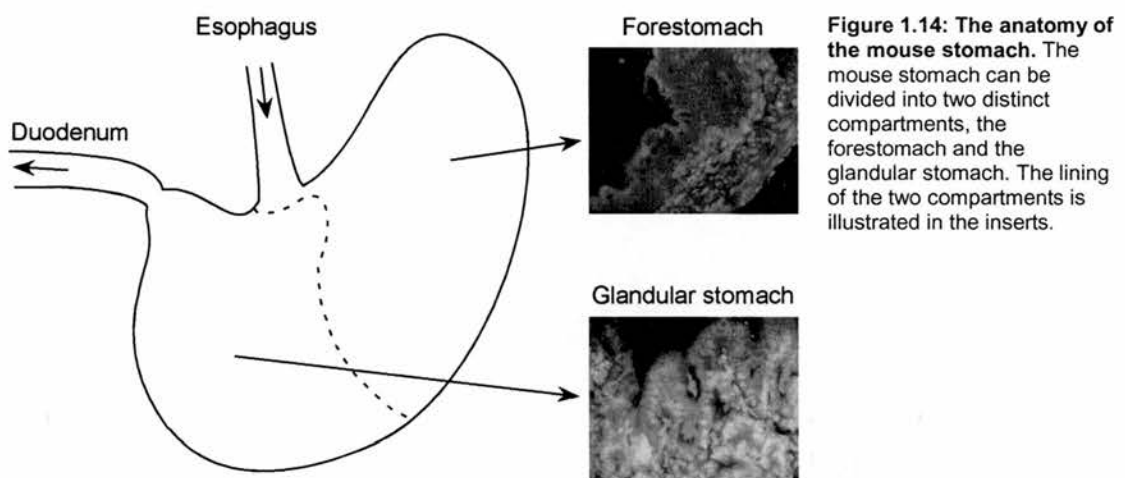


Figure 1.14: The anatomy of the mouse stomach. The mouse stomach can be divided into two distinct compartments, the fore-stomach and the glandular stomach. The lining of the two compartments is illustrated in the inserts.

During early stages of stomach development *Shh* is expressed throughout the endoderm. However, at later stages its expression becomes restricted to the anterior stomach. Interestingly, the restriction of *Shh* expression coincides with an expansion of *Pdx1* expression in the posterior part of the stomach endoderm. Hence the negative feedback loop between *Shh* and *Pdx1*, which is seen in the pancreas, is also present in the stomach. In mice lacking both activin receptors, *ActRIIa* and *ActRIIb*, the posterior stomach is transformed into anterior stomach (Kim et al., 2000), suggesting that members of the TGF β family are involved in specifying stomach identity. Also, consistent with the idea that *Shh* is required for anterior identity the expression domain of *Shh* is extended into the posterior in these mice.

Chapter 2: The limb and kidney phenotype

The *Dh* mutation belongs to the hemimelia-luxate group of mutations, which causes polydactyly, long bone abnormalities and luxation of the hindlimbs. Mice carrying the *Dh* mutation are specifically affected at the preaxial side of the hindlimbs with polydactyly or oligodactyly in the handplate and hemimelia or amelia of the tibia and previous studies have shown that the *Dh* mutation affects hindlimb development from very early stages (Hecksher-Sørensen, 1998; Lettice et al., 1999a). In addition to limb abnormalities *Dh* also affects the axial skeleton and the kidneys. The axial abnormalities include a reduction in the number of ribs, sternebrae and presacral vertebrae (Holmes and Barton, 1993; Suto et al., 1996; Morin et al., 1999) while the kidneys are hydronephrotic. However, in contrast to the limb defects it is largely unknown how *Dh* affects the development of these organs. Studies in humans have revealed a significant relationship between preaxial limb defects and kidney abnormalities (Evans et al., 1992) and combined with experimental studies (Geduspan and Solursh, 1992) there is evidence to suggest the existence of a developmental association between early kidney development and limb induction. Also it is possible that these defects are related to the reduction of lumbar vertebrae. The studies described in this chapter were therefore carried out to investigate if the posterior abnormalities observed in *Dh* are related to each other and to determine if *Dh* might be used as a model system for studying the association between limb and kidney abnormalities.

2.1 The *Dh* mutation shifts the hindlimbs anteriorly

Homeotic transformation of the axial skeleton in *Dh*

E16.5 embryos were dissected out and stained with alizarin red and alcian blue to visualise chondrogenesis in the developing skeleton (figure 2.1). In wildtype embryos the number of lumbar vertebrae is predominantly six and in this experiment all *+/+* embryos examined showed this phenotype (figure 2.1a). However, in both *Dh/+* (figure 2.1b) and *Dh/Dh* (figure 2.1c) there was a reduction in the number of lumbar vertebrae from 6 to 5. This phenotype was consistent and appeared in all *Dh/+* and *Dh/Dh* embryos examined. In contrast the number of cervical, thoracic and sacral vertebrae is

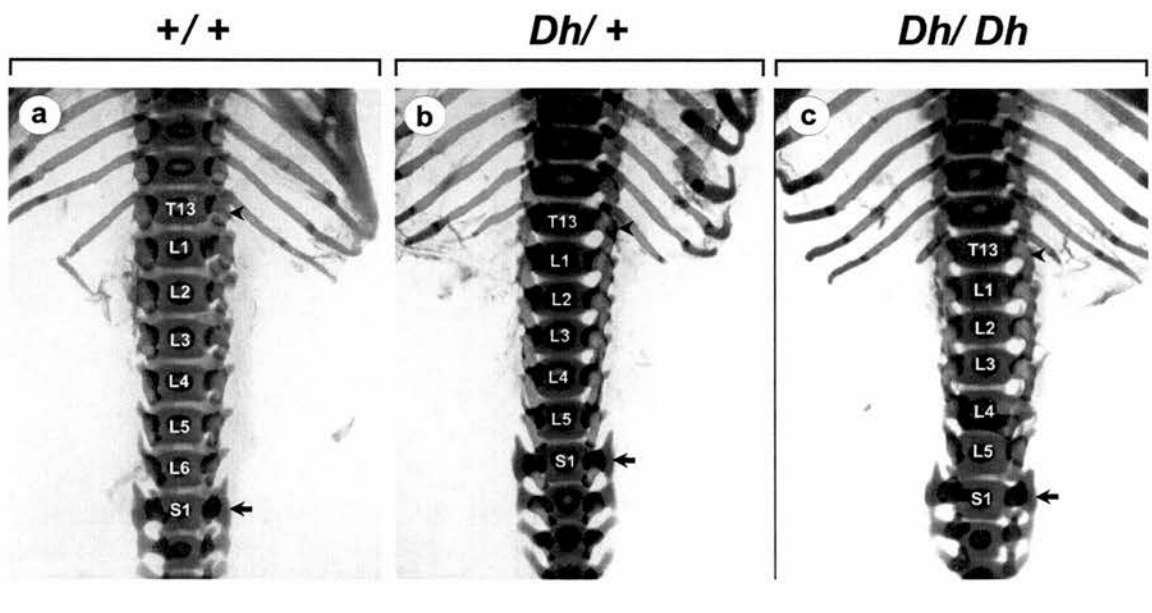


Figure 2.1: Homeotic transformations of the axial skeleton in *Dh*. Alizarin red and alcian blue-stained skeletons of E16.5 embryos. The black arrowhead points to the last thoracic vertebra (T13). The thoracic vertebrae can be distinguished from the lumbar vertebrae because of the associated ribs. The black arrow points to the first sacral vertebra (S1) which is can be recognized because of the characteristic lateral protrusions. **(a)** In *+/+* embryos the predominant phenotype is 6 Lumbar vertebrae labelled L1-L6. In *Dh/+* embryos **(b)** and *Dh/Dh* embryos **(c)** the number of Lumbar vertebrae is reduced to 5.

unaffected by the *Dh* mutation (data not shown). These results agree with previous reports on skeletal abnormalities in *Dh* mice (Holmes and Barton, 1993; Suto et al., 1996; Morin et al., 1999) confirming that the *Dh* mutation causes a reduction in the number of lumbar vertebrae. However, this phenotype is not a unique characteristic associated with *Dh*. An identical phenotype has been reported for mice carrying mutations in genes encoding members of the *Hox* complex (Zakany et al., 1996; Gerard et al., 1997). In these experiments the last lumbar vertebra (L6) undergoes a homeotic transformation and becomes the first sacral vertebra (S1). The mutations also affect all vertebrae posterior of S1 causing them to undergo an anterior transformation and as a result the total number of sacral vertebrae is maintained. These mutations therefore represent an exact phenocopy of the skeletal abnormalities observed in *Dh* animals, strongly implying that the vertebral defects are caused by a homeotic transformation. However, it is also possible that the reduction in the number of lumbar vertebrae is caused by a segmental deletion.

The hindlimbs shifts anteriorly in *Dh* embryos

It is known that *Hox* genes play an important role in specifying segmental identity along the anterior posterior axis (Krumlauf, 1994). In addition, targeted mutagenesis or misexpression of individual *Hox* genes has implied that the *Hox* code is required for correctly positioning the limbs. Thus, *Hoxb5* is necessary for positioning the forelimbs (Rancourt et al., 1995) while *Hox11* paralogues can shift the position of the hindlimbs (Zakany et al., 1996; Gerard et al., 1997). Due to the characteristic expression pattern of the *Hox* genes it is thought that the anterior boundary of expression is the factor that determines segmental identity. The *Hox10* paralogues are believed to determine the lumbar/sacral transition and in an evolutionary study comparing the expression boundaries between different species it was shown that the anterior expression boundary of these genes always coincide with the anterior limit of the hindlimbs (Burke et al., 1995).

Analysis of the skeletal abnormalities in *Dh* mice showed that the last lumbar vertebra (L6) is transformed into the first sacral vertebra (S1) and by definition such a transformation reflects an anterior shift in the position of the hindlimbs. In addition *Dh* affects limb development very early -presumably prior to induction (Hecksher-Sørensen, 1998; Lettice et al., 1999a). Since the *Hox* code is responsible for determining axial identity and positioning the limbs, it is possible that *Dh* is affecting the expression of *Hox* genes.

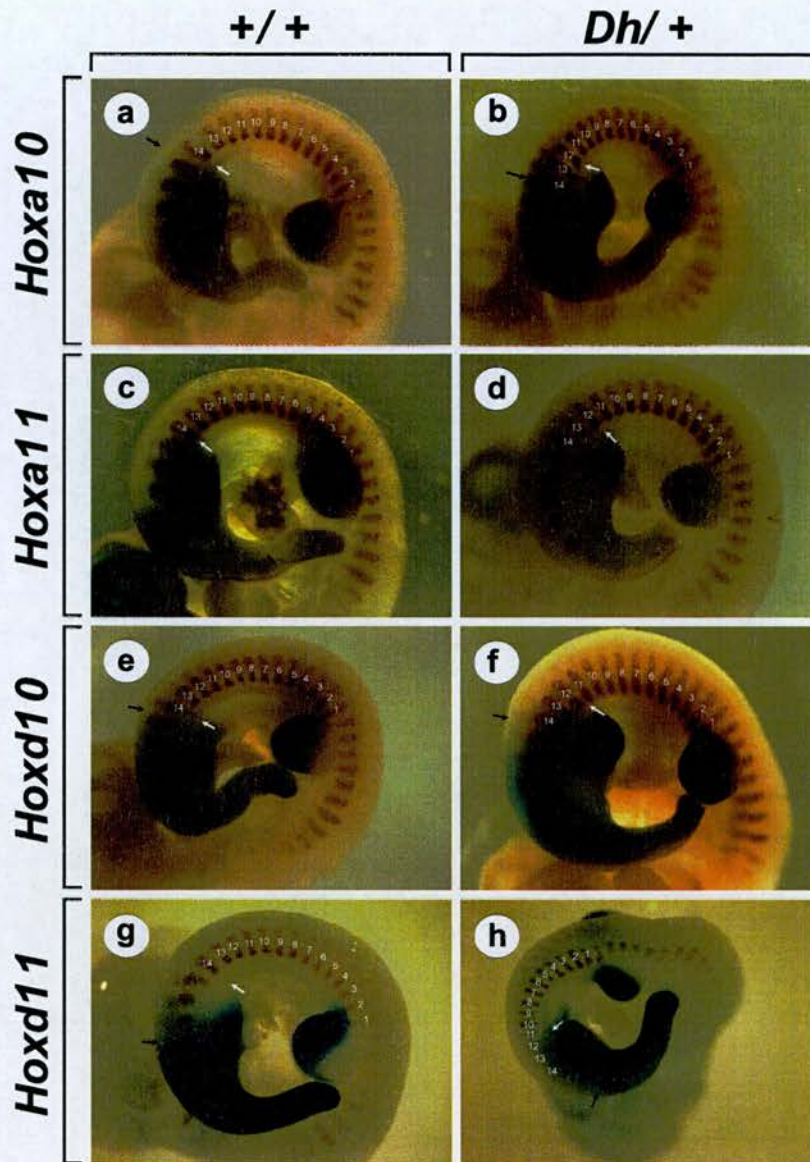


Figure 2.2: The developing hindlimbs have shifted anteriorly in *Dh*/+. Double in situ showing expression of *Hox* genes (blue) and *Myogenin* (brown). (a) Expression of *Hoxa10* at E10.5 in a +/+ embryo. The anterior limit of the developing hindlimb (white arrow) is positioned 14 segments rostral to the posterior limit of the forelimb bud. *Hoxa10* is expressed in the limb buds and weakly in the lateral flank. The anterior expression of *Hoxa10* in the flank (black arrow) corresponds to the anterior limit of the hindlimb bud. (b) Expression of *Hoxa10* at E10.5 in a *Dh*/+ embryo. The anterior limit of the developing hindlimb (white arrow) is positioned 12 segments rostral to the posterior limit of the forelimb bud. The anterior expression of *Hoxa10* (black arrow) is very weak but corresponds roughly to segment 14. (c) Expression of *Hoxa11* at E10.5 in a +/+ embryo. The anterior limit of the developing hindlimb (white arrow) is positioned 14 segments rostral to the posterior limit of the forelimb bud. *Hoxa11* is expressed in the limb buds and very weakly in the lateral flank. (d) Expression of *Hoxa11* at E10.5 in a *Dh*/+ embryo. The anterior limit of the developing hindlimb (white arrow) is positioned 12 segments rostral to the posterior limit of the forelimb bud. (e) Expression of *Hoxd10* at E10.5 in a +/+ embryo. The anterior limit of the developing hindlimb (white arrow) is positioned 14 segments rostral to the posterior limit of the forelimb bud. *Hoxd10* is expressed in the limb buds and in the lateral flank. The anterior expression of *Hoxa10* in the flank (black arrow) corresponds to the anterior limit of the hindlimb bud. (f) Expression of *Hoxd10* at E10.5 in a *Dh*/+ embryo. The anterior limit of the developing hindlimb (white arrow) is positioned 12 segments rostral to the posterior limit of the forelimb bud. The anterior expression of *Hoxd10* (black arrow) corresponds to segment 14. (g) Expression of *Hoxd11* at E10.5 in a +/+ embryo. The anterior limit of the developing hindlimb (white arrow) is positioned 14 segments rostral to the posterior limit of the forelimb bud. *Hoxd11* is expressed in the limb buds and in the lateral flank. The anterior expression of *Hoxd11* in the flank (black arrow) is several segments posterior of the anterior limit of the hindlimb bud. (h) Expression of *Hoxd11* at E10.5 in a *Dh*/+ embryo. The anterior limit of the developing hindlimb (white arrow) is positioned 12 segments rostral to the posterior limit of the forelimb bud. The anterior expression of *Hoxd11* in the flank (black arrow) is several segments posterior of the anterior limit of the hindlimb bud.

Alteration in the *Hox* code might also explain the early effect *Dh* has on limb development, because the *Hox* genes are acting upstream of limb induction. E10.5 embryos were therefore examined for the expression of various *Hox* genes (figure 2.2). The analysis primarily focused on the *Hox10* and *Hox11* paralogues because their expression boundaries coincide with the position of the hindlimbs. Additionally all embryos were simultaneously stained for *Myogenin* expression (Hecksher-Sørensen et al., 1998). *Myogenin* is expressed in the developing myotome (Sassoon et al., 1989) in a segmental pattern, which makes it possible to precisely determine the relative position of the hindlimbs along the anterior posterior axis.

In *+/+* embryos the anterior boundary of the hindlimbs is always positioned 14 somites caudal to the posterior limit of the forelimbs (figure 2.2a,c,e,g; white arrow). However, in *Dh/+* mice only 12 somites separates the fore and hindlimbs confirming that the position of the hindlimbs is shifted two somites anteriorly (figure 2.2b,d,f,h).

In *+/+* embryos the anterior boundary of *Hoxa10* expression can be detected just posterior to segment 14 and it therefore corresponds well with the anterior limit of the hindlimb buds (figure 2.2a; black arrow). In addition the gene is expressed in mesenchyme of the developing fore and hindlimb buds. In *Dh/+* the anterior boundary of *Hoxa10* expression still corresponds to somite 14 despite the shift of the hindlimbs (figure 2.2b). It therefore seems unlikely that misexpression of *Hoxa10* should be responsible for the limb shift and homeotic transformation. For *Hoxa11* expression could be detected in the developing fore and hindlimb in both *+/+* and *Dh/+* embryos (figure 2.2c,d). However, in the posterior part of the embryos transcription levels of *Hoxa11* were too low to confidently determine the anterior boundary of expression. The expression of *Hoxd10* is very similar to that observed for *Hoxa10*. In *+/+* embryos the anterior boundary of *Hoxd10* expression can be detected at somite 14 (figure 2.2e; see also figure 2.3a,b) and in the mesenchyme of both fore and hindlimbs. However, as observed with *Hoxa10* the hindlimb buds shifts independently of *Hoxd10* expression in *Dh/+* (figure 2.2f; see also figure 2.3c,d). Thus, the anterior boundary of *Hoxd10* expression can still be detected at somite 14 while the anterior limit of the hindlimbs correlates to segment 12 and it is therefore unlikely that the limb shift is caused by misexpression of *Hoxd10*. Also for *Hoxd11* the anterior boundary of expression is unaffected by the *Dh* mutation. In *+/+* embryos *Hoxd11* expression can be detected in the posterior mesenchyme in both the fore and hindlimb buds, while the anterior boundary of lateral plate expression correlates to somite 17, within the posterior half of the hindlimb buds (figure 2.2g).

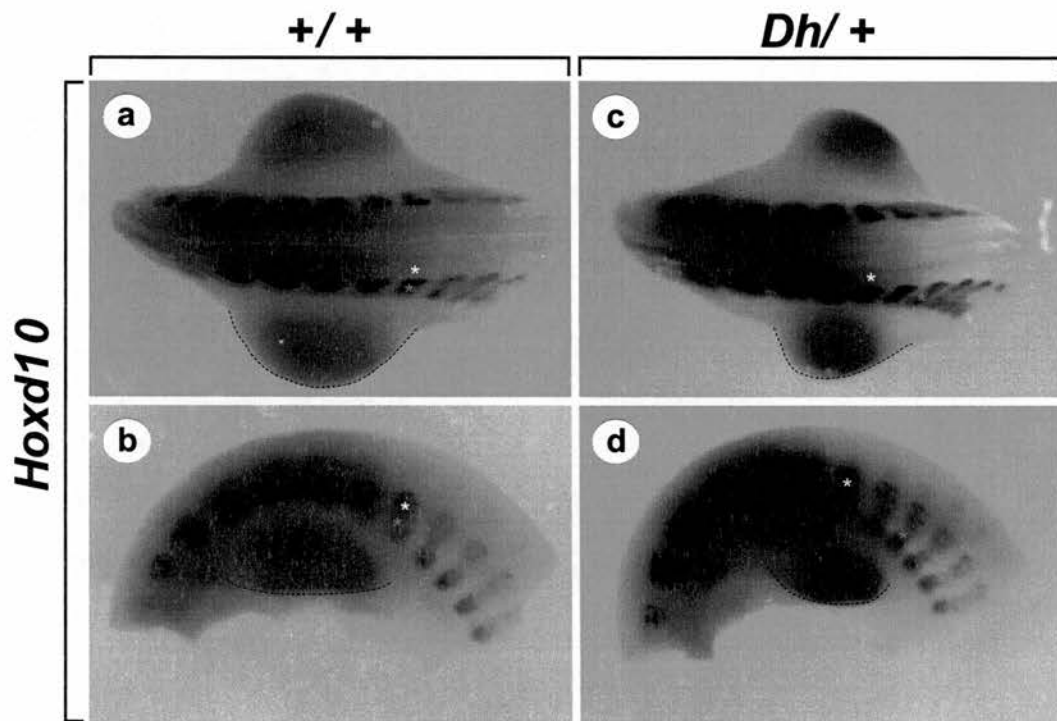


Figure 2.3: *Hoxd10* expression in *+/+* and *Dh/+*. Double *in situ* staining of *Hoxd10* expression (blue) and *Myogenin* (brown). (a) Dorsal view of the developing hindlimbs in an E10.5 *+/+* embryo. The anterior expression of *Hoxd10* (white asterisk) corresponds with the anterior position of the hindlimb bud (red asterisk). (b) Lateral view of the developing hindlimbs in an E10.5 *+/+* embryo. The anterior expression of *Hoxd10* (white asterisk) corresponds with the anterior position of the hindlimb bud (red asterisk). (c) Dorsal view of the developing hindlimbs in an E10.5 *Dh/+* embryo. The anterior position of the hindlimb bud (red asterisk) is positioned two segments caudal to the anterior boundary of *Hoxd10* expression (white asterisk). (d) Lateral view of the developing hindlimbs in an E10.5 *Dh/+* embryo. The anterior position of the hindlimb bud (red asterisk) is positioned two segments caudal to the anterior boundary of *Hoxd10* expression (white asterisk). The extend of the hindlimb buds are outlined by a dashed line.

The *Dh/+* embryo is slightly younger than E10.5 and as a result no *Myogenin* expression can be detected around the hindlimb buds. It is therefore difficult to exactly determine the anterior boundary of *Hoxd11* expression, but it appears to correlate with the posterior limit of the hindlimb buds, suggesting that the limb is moving independently of *Hoxd11* expression.

The data shown in figure 2.2 demonstrates that the developing hindlimb buds are shifted two somites anteriorly in *Dh/+* embryos while the expression pattern of several *Hox* genes is unaffected by the mutation. To further illustrate this point figure 2.3 show a close up of *Hoxd10* expression in developing hindlimb buds at E10.5. The anterior boundary of *Hoxd10* expression and the anterior limit of the hindlimbs are illustrated by a white and red asterix respectively. A dorsal view of *+/+* hindlimbs clearly shows that the anterior expression of *Hoxd10* in the neural tube coincide with the anterior limit of the hindlimb bud (figure 2.3a). This is also the case when the same region is viewed from the side (figure 2.3b). However, in *Dh/+* embryos the anterior boundary of *Hoxd10* expression no longer coincides with the anterior limit of the developing hindlimbs. Instead the hindlimb buds are positioned two somites rostral to the anterior boundary of *Hoxd10* expression (figure 2.3c). This phenotype is even more obvious when the same region is viewed from the side (figure 2.3d). The conclusion is therefore that the shift of the hindlimbs in *Dh/+* must occur independently of *Hoxd10* expression.

Unfortunately, the above analysis did not include a description of homozygous embryos, due to shortage of *Dh/Dh* mice (see material and methods #40).

The expression of *Hoxc10* is shifted anteriorly in *Dh* embryos.

Hoxc10 was the last member of the *Hox10* paralogues to be analysed (*Hoxb10* does not exist). The expression of *Hoxc10* can be divided into two domains. A Neural tube domain (black arrow) and a lateral flank domain (white arrow). At E10.5 the anterior boundary of *Hoxc10* expression in both domains correlates to segment 12 (figure 2.4a). As previously described the anterior limit of the hindlimb buds is positioned at segment 14. Hence the expression domain of *Hoxc10* extends two segments anterior to the rostral limits of the hindlimb buds. Slightly later in development at E11.0 the anterior boundary of *Hoxc10* expression still correlates to segment 12 in both the neural tube and in the flank mesoderm (figure 2.4b). That way the anterior extent of *Hoxc10* expression is defined by a sharp boundary running perpendicular to the anterior-posterior axis at segment 12.

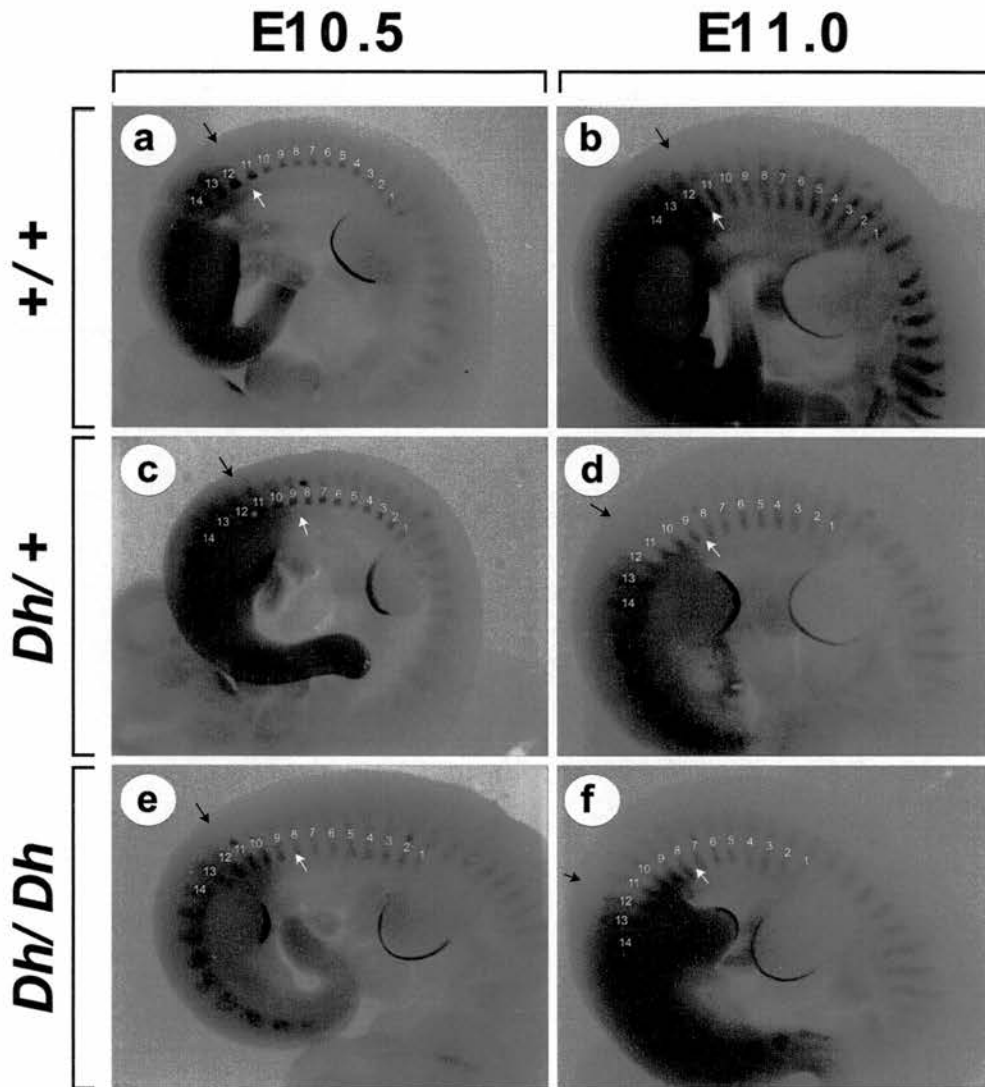


Figure 2.4: *Hoxc10* expression in the lateral flank has shifted anteriorly in *Dh* embryos. Triple *in situ* showing expression of *Hoxc10* (blue), *Fgf8* and *Myogenin* (brown). At E10.5 (a) and E11.0 (b) the wild type expression of *Hoxc10* corresponds to somite 12 in both the neural tube (black arrow) and in the lateral flank (white arrow). That way the anterior boundary of expression forms a sharp line perpendicular to the anterior-posterior axis. In *Dh/+* embryos *Hoxc10* expression in the lateral flank is shifted anteriorly to somite 9 while the neural tube expression is unaffected (c and d; white arrow). The same is true in homozygous embryos (e and f). Hence *Hoxc10* expression in the lateral flank shifts anterior together with the hindlimbs.

In *Dh/+* embryos the neural tube expression of *Hoxc10* correlates to segment 12 and is therefore unaffected by the mutation (figure 2.4c). However, in the lateral flank mesoderm the expression domain has shifted three segments anteriorly and extends up to segment 9. The same is true at E11.0 where the anterior limits of the two expression domains no longer forms a mutual boundary running perpendicular to the body axis. In *Dh/Dh* embryos the expression of *Hoxc10* is also shifted (figure 2.4e). The anterior boundary of *Hoxc10* expression in the flank mesoderm correlates to segment 8 and the extend of the shift is therefore even more pronounced than in heterozygous embryos. The neural tube expression correlates to segment 12 and is therefore unaffected by the mutation. At E11.0 the flank expression can still be detected in the mesoderm posterior to segment 8 (figure 2.4f). It is clear that the expression domain in the flank mesoderm has been displaced anteriorly compared to the expression domain in the neural tube. It is therefore evident that *Hoxc10* expression in the lateral flank mesoderm is shifted anteriorly in mice carrying the *Dh* mutation. Also the shift in homozygous embryos appears to be slightly more severe than in heterozygous embryos.

Gene expression in the *Dh* hindlimbs

The observation that the hindlimbs are shifted anteriorly relative to the expression pattern of *Hoxa10*, *Hoxd10* and *Hoxd11* raised a number of questions regarding cell identity within the hindlimb mesenchyme. For this purpose a number of genes including *Fgf8*, *Fgf10*, *Alx4* and *Gremlin* were analysed (data not shown). However, the expression of these genes confirmed previous studies (Lettice et al., 1999a) showing that the extent of the hindlimb field is reduced in *Dh* at the time of induction and that the mutation specifically affects the anterior mesenchyme.

When ectopic limbs are induced in the flank of chicken embryos they are chimeric and display dual fore and hindlimb identity (Ohuchi et al., 1998). The possibility that the anterior shift in *Dh* mice had caused hindlimbs to become chimeric was also tested. However, the expression of both fore and hindlimb specific genes *Tbx4* and *Tbx5* was found to be normal in mutant limbs (data not shown), suggesting that hindlimb identity is maintained despite the shift.

Abnormal innervation of the hindlimbs in *Dh* embryos

The analysis of *Hox* gene expression in *Dh* embryos clearly shows that the expression of *Hoxc10* is shifted anteriorly while the expression of several other *Hox* genes were unaffected by the mutation. In addition it appeared that only *Hoxc10*

expression in the lateral flank was affected. In the neural tube the anterior boundary of expression was the same in mutant and wildtype. However, it has been shown that *Hox* genes have an important role in determining nerve identity (Rijli et al., 1995; Carpenter et al., 1997; de la Cruz et al., 1999). This raises an interesting problem, because in the neural tube of *Dh* embryos nerve identity is determined according to what looks like a wildtype pattern, while the limb buds they should innervate has shifted anteriorly. It is therefore possible that the nerves innervating the developing hindlimbs in *Dh* embryos display a dual behaviour – a combination of wildtype and mutant identity.

To investigate this further E11.5 embryos were stained as whole mounts with antibodies against Neuro-filament 160 (NF160). The five trajectories of motor neurons, which contribute to innervation of the developing forelimb, have been labelled F1-F5 (red) and the five that contribute to innervation of the hindlimb have been labelled H1-H5 (blue). In +/+ embryos there are 12 intervening nerves between the forelimb and the hindlimb (figure 2.5a; white numbers). In the region around the hindlimb it is apparent that there is a strict definition of nerve identity and a clear distinction can be seen between the nerves migrating into the flank (figure 2.5b; white arrows) and those that will innervate the hindlimb (blue arrows). Hence, the nerves migrating into the flank are sending out lateral projections which can be seen as bright spots near the middle of the nerve whereas the nerves innervating the limb has no projections. The H1 nerve has dual identity (blue and white arrow) and during subsequent development it splits so the anterior half will innervate the flank while the posterior will innervate the limb. However, at E11.5 this dual identity has already been determined and lateral projections can be seen in the anterior half (red arrow) while the posterior half resembles the limb nerves. In *Dh/Dh* the number of nerves between the fore and hindlimb has been reduced to from 12 to 10 (figure 2.5c; white numbers). Again, demonstrating the anterior shift of the hindlimbs. However, closer examination of the hindlimb region reveals severe abnormalities in the organisation of the nerves. It is no longer possible to make a clear distinction between the nerves innervating the limb and the nerves innervating the flank and the nerves 10, H1 and H2 all appear to have dual identity (mixed blue and white arrows). Thus, they are sending out lateral projections characteristic for the nerves innervating the lateral flank, but at the same time they are sending projections into the limb. Small lateral projections can also be seen from the anterior half of H3 (red arrow) although the vast majority of axons in this nerve are migrating into the limb.

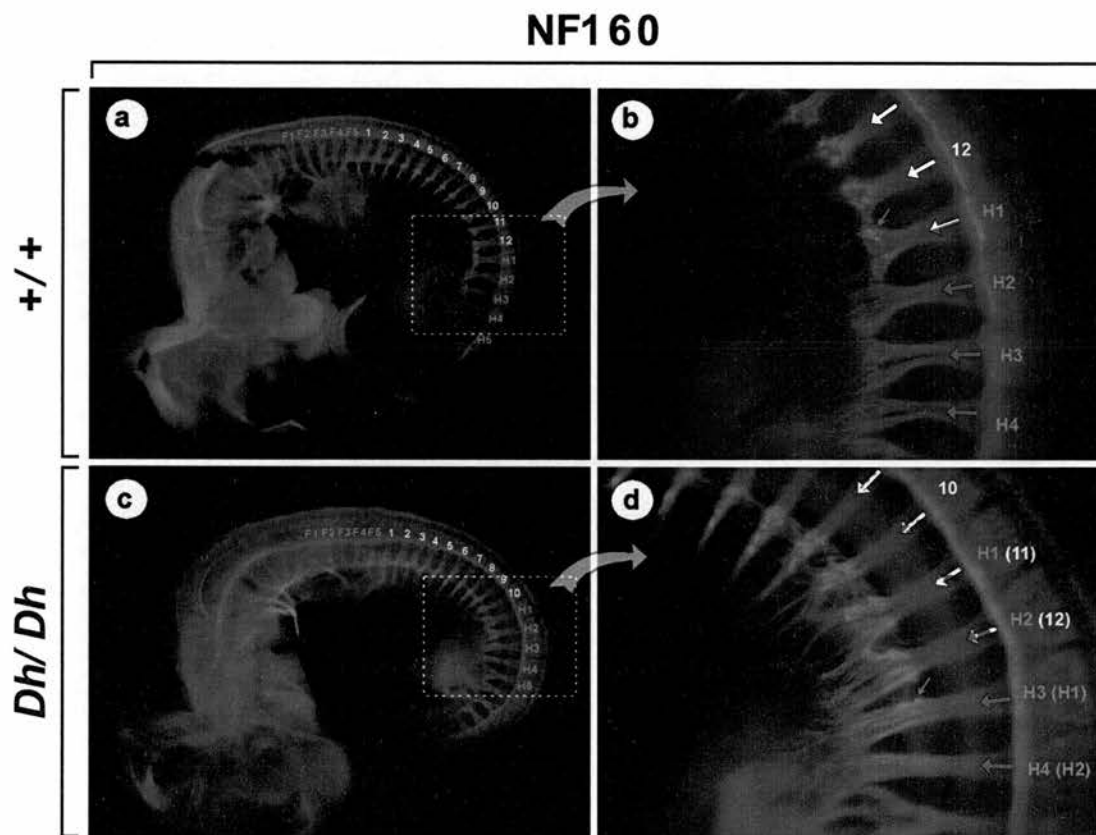


Figure 2.5: Abnormal innervation of the developing hindlimbs in *Dh* embryos. Immunohistochemistry showing Neuro-Filament (NF160) staining at E11.5 in *+/+* and *Dh/Dh*. The nerves innervating the developing forelimb are labelled F1-F5 (red) and the nerves innervating the developing hindlimb are labelled H1-H5 (blue). **(a)** NF160 staining in a *+/+* embryo. The forelimbs and the hindlimbs are separated by 12 nerves (white). **(b)** Close up of the region highlighted in (a). The nerves are well organised and a clear distinction is seen between the nerves migrating into the limb bud (blue arrows) and the nerves migrating into the flank (white arrows). The anterior half of the H1 nerve will migrate into the flank and it is sending out lateral projections (red arrow). **(c)** In *Dh/Dh* the forelimb and the hindlimb are separated by 10 nerves (white). **(d)** Close up of the region highlighted in (c). The nerves are unorganised and it is difficult to distinguish between the nerves migrating into the limb bud (blue arrows) and the nerves migrating into the flank (white arrows). Nerve labels corresponding wild type patterning are shown in brackets. The H3 (H1) nerve is sending out lateral projections (red arrow).

However, due to the displacement of the hindlimb the number, reflecting the identity of the individual nerves, has also been shifted anteriorly. For comparison the individual nerves in the mutant have also been labelled according to wild type patterning (in brackets). In wildtype embryos the H1 nerve will split and innervate both the flank and the limb and it is therefore the most posterior nerve to send out lateral projections. Using wildtype labelling the H3 nerve in *Dh* would be H1 and indeed H3 (H1) is the most posterior nerve to send out lateral projections. This strongly suggests that nerve identity in *Dh* is determined in a wildtype manner and in accordance with this the nerves anterior to H3 (H1) all send out lateral projections just as they would in a wildtype situation.

2.2 The *Dh* mutation affects kidney development indirectly

Studies in humans have demonstrated a strong relationship between preaxial limb abnormalities and kidney defects (Evans et al., 1992). In line with this observation it has been suggested that the mesonephros are required for limb induction (Geduspan and Solursh, 1992), thus providing a developmental link between the two organs. However, this remains controversial since more recent experiments have shown that the mesonephros are not required for limb induction (Fernandez-Teran et al., 1997). Mice carrying the *Dh* mutation display both limb and kidney abnormalities and might therefore represent a model system for studying the association between the two organs. Furthermore, since *Dh* affects limb induction, an analysis of early kidney development, might provide an answer to the controversy surrounding the role of the mesonephros during limb induction.

Severe swelling of the kidneys in *Dh/Dh* embryos

The kidneys of E18.5 *Dh/Dh* is clearly abnormal (figure 2.6f). In all homozygous embryos both kidneys are hydronephric and almost twice the size of normal kidneys (figure 2.6a). However, the swelling is not confined to the kidneys. Also the ureter is swollen and in many cases the bladder (data not shown). Sagittal sections through a normal kidney at E18.5 show how the medulla is surrounded by a horseshoe shaped cavity, which is where the collecting ducts empties into the ureter (figure 2.6a; red arrow). In a *Dh/Dh* kidney this cavity is swollen and filled with fluids (figure 2.6f; red arrow).

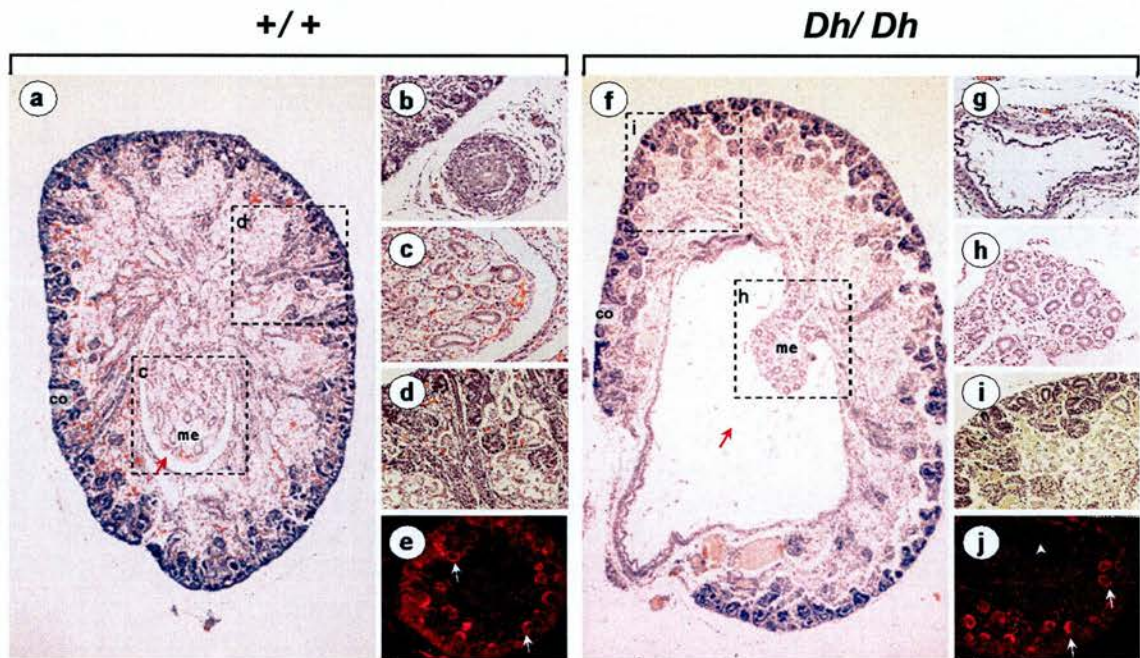


Figure 2.6: Histological comparison between +/+ and *Dh/Dh* kidneys. At E18.5 *Dh/Dh* kidneys (f) are severely swollen compared to +/+ (a). In the +/+ the main collecting duct forms a horseshoe around the medulla (red arrow). In *Dh/Dh* fluids build up in the collecting duct forcing it to swell (red arrow). The highlighted areas refer to the pictures taken at higher magnification. (b,g) Comparison of the ureter in +/+ (b) and *Dh/Dh* (c). The swelling of *Dh/Dh* kidneys extends beyond the kidney itself and into the ureter. (c,h) Comparison of the medulla in +/+ (c) and *Dh/Dh* (h). Morphologically the medulla of *Dh/Dh* embryos is normal. (d,i) Comparison of the cortex in +/+ (d) and *Dh/Dh* (i). Morphologically the cortex of *Dh/Dh* kidney is normal. (e,j) *Wt1* expression at E14.5 in +/+ (e) and *Dh/Dh* (j). Initial swelling can already be seen in *Dh/Dh* (white arrowhead). The characteristic expression pattern of *Wt1* expression in the developing podocytes can be seen in both +/+ and *Dh/Dh* (white arrows). (co) cortex and (me) medulla.

At a higher magnification it is possible to see that the morphology of individual structures within the kidney appear relatively normal. Hence the cortex looks very similar in +/+ and *Dh/Dh* animals and the characteristic circular shaped structure of the podocytes are present in both genotypes (figure 2.6d and figure 2.6i respectively). The medulla is slightly distorted in mutant kidneys (figure 2.6h), presumably because of increased pressure exerted by the fluids accumulating in the ureter. Nevertheless the gross morphology is similar to that observed for +/+ medullas (figure 2.6c).

The swelling of the mutant kidneys extends distal to the kidney into the ureter. The function of the ureter is to drain fluids from the kidney to the bladder and it can be seen as an epithelial structure connecting the two organs. In +/+ embryos it is difficult to define the lumen within the ureter (figure 2.6b). However, in *Dh/Dh* kidneys the ureter is very swollen and the lumen is filled with fluids (figure 2.6g).

These results suggest that the swelling observed in the *Dh* kidneys is caused by a mechanical defect rather than abnormal development of the kidneys. To test this the expression of *Wt1* was examined in +/+ and *Dh/Dh* kidneys. *Wt1* has two roles in kidney development. Initially *Wt1* is expressed in the metanephric mesenchyme (Armstrong et al., 1993). This expression is essential for kidney development and mice lacking functional *Wt1* fail to induce the kidneys (Kreidberg et al., 1993). However, *Wt1* also has a later role in which the gene is expressed in the developing podocytes of the glomeruli (Armstrong et al., 1993). In +/+ embryos at E14.5 this late expression can be seen as horseshoe shaped structures at the cortex of the developing kidney (figure 2.6e; white arrows). A similar expression pattern can be observed in homozygous embryos suggesting that podocyte development is normal in mutant mice (figure 2.6j; white arrows). In addition these results show that swelling of the mutant kidneys can be detected already from E14.5 (white arrowhead). However, since no defects can be detected in kidney ultra structure these results strengthens the idea that kidney defect is secondary in *Dh* mice.

Misexpression of *Hoxc10* in *Dh* embryos

In the previous chapter it was described how the shift of the hindlimbs is likely to be associated with misexpression of *Hoxc10*. To determine whether misexpression of *Hoxc10* could also be responsible for the kidney abnormalities wildtype and *Dh/Dh* embryos were analysed. E10.5 embryos were stained for *Hoxc10* expression and sectioned transversely through the region of the hindlimbs. Each embryo was stained as a whole mount and subsequently sectioned into 100µm sections. Figure 2.7 shows pictures of consecutive sections with the most anterior being at the top. However,

because the hindlimbs are shifted in *Dh* the pictures are aligned from the position of the cloaca (figure 2.7f,l; red arrows). In agreement with previous experiments (Lettice et al., 1999) these results show that the hindlimb buds are more narrow in *Dh* embryos. In the +/+ embryos the developing hindlimbs span at least 5 sections (figure 2.7b-f; 500µm) while in the mutant they only span 4 sections (figure 2.7g-j; 400µm). In addition the mutant limb buds appear thicker and more triangular.

Hoxc10 is expressed throughout most of the posterior tissues in both wildtype and mutant embryo. However, there are some differences in the expression pattern. In the midgut of wildtype embryos *Hoxc10* expression can be detected in the mesoderm surrounding the gut tube and it appears that there is a distinct boundary of expressing and non-expressing cells (figure 2.7a,b; black arrows: see also figure 2.4a; red arrow). In contrast no *Hoxc10* expression could be detected in the gut mesoderm of *Dh/Dh* embryos. However, there is some evidence that the whole midgut region is severely degenerated or entirely missing in *Dh/Dh* embryos and that might explain the absence of *Hoxc10* expression (discussed in chapter 4). Another difference is that in wildtype the mesonephric duct is positioned within the *Hoxc10* expressing mesenchyme (black arrowhead), while in *Dh/Dh* the same duct is positioned outside the *Hoxc10* expressing mesenchyme (a close up of this can be seen in figure 2.8a,b). At the level of the hindlimb bud the mesonephric duct can be seen very close to the *Hoxc10* expressing mesenchyme (figure 2.7i). However, towards the posterior end of the embryo it becomes more obvious that the duct is no longer within the *Hoxc10* expression domain (figure 2.7j,k,l). At the moment it is unclear whether *Hoxc10* is actually misexpressed or not. At the level of the stomach *Dh* affects the mesenchyme around the endoderm, but whether this effect extends more dorsal and lateral to the mesenchyme surrounding the mesonephros is unknown. However, it is possible that abnormal growth or migration of the mesenchyme surrounding the mesonephros displaces the mesonephric duct so it ends up outside the *Hoxc10* expression domain. Nevertheless it is an interesting phenotype because the posterior part of the mesonephric ducts later develops into the ureter, which is abnormal in *Dh/Dh* mice.

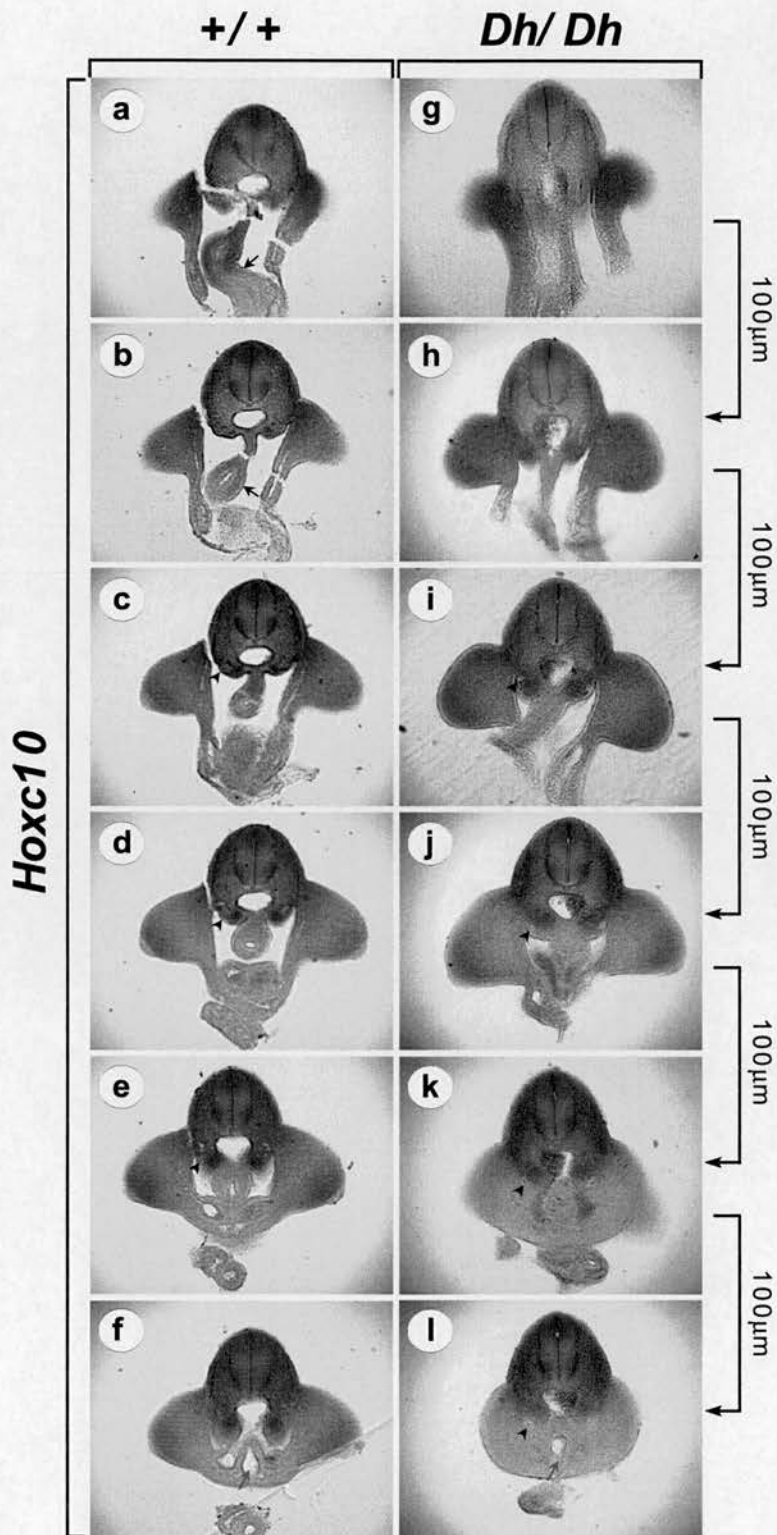


Figure 2.7: *Hoxc10* expression in *+/+* and *Dh/Dh* at E10.5: Embryos stained for *Hoxc10* expression were cut transversely at the level of the developing hind limbs. 100µm thick consecutive sections going from anterior to posterior in *+/+* (a,b,c,d,e,f) and *Dh/Dh* (g,h,i,j,k,l). The two panels have been aligned so they most posterior picture shows the cloaca (f,g; red arrow). In *+/+* embryos *Hoxc10* is expressed in the developing hindgut (a,b; black arrow). In *Dh/Dh* embryos no *Hoxc10* expression could be detected in the hindgut. In *+/+* embryos the mesonephric duct is positioned within the domain of *Hoxc10* expression (c,d,e; black arrowhead). In *Dh/Dh* embryos the mesonephric duct is positioned outside the domain of *Hoxc10* expression (i,j,k; black arrowhead).

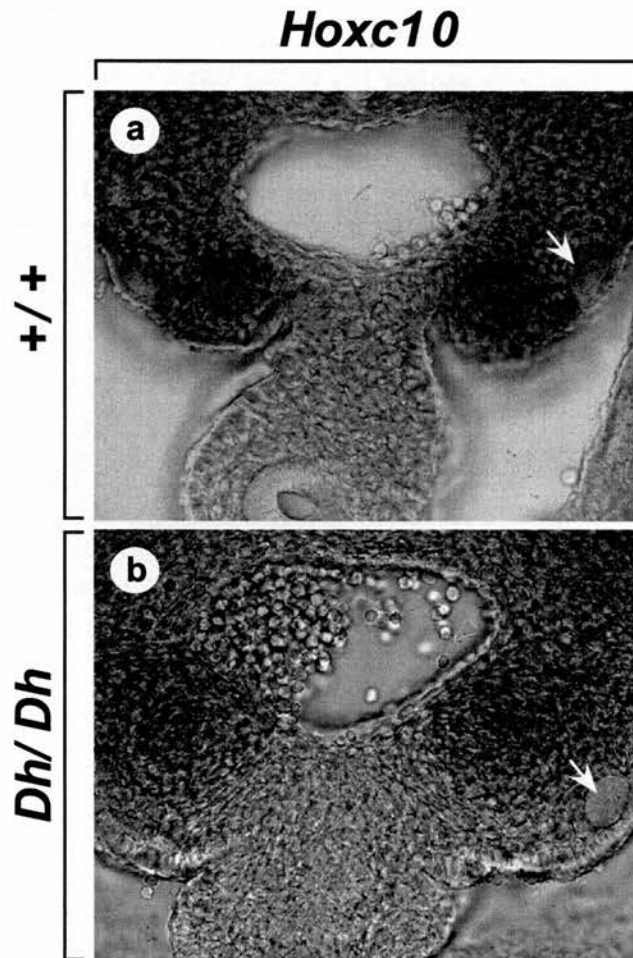


Figure 2.8: The mesonephric duct is outside the *Hoxc10* expression domain in *Dh/Dh*: High power images of the sections shown in figure 3.2 g and i. **(a)** In *+/+* embryos the mesonephric ducts is positioned within the *Hoxc10* expression domain (arrow). **(b)** In *Dh/Dh* embryos the mesonephric ducts is positioned outside the *Hoxc10* expression domain (arrow).

***Wt1* expression in wildtype and *Dh* embryos**

The expression of *Hoxc10* at E10.5 shows that the mesonephric duct is positioned outside the *Hoxc10* expression domain in *Dh* embryos, but there is no genetic evidence that *Hox* genes are directly involved in positioning the kidneys.

Nevertheless, it is not difficult to envisage a situation where the absence of *Hoxc10* expression in the mesonephric duct could have an effect on cell identity and therefore on early kidney development. It is known the metanephric mesenchyme stimulates the growth of the uteric bud and that the place of budding determines the position of the kidney. *Wt1* has an important role during these early stages of kidney development and in mice lacking the gene, the uteric bud fails to grow out of the mesonephric duct and kidney development is abolished (Kreidberg et al., 1993). However, recombination studies have shown that the inability to induce budding is purely mesenchymal. Hence budding of the ureteric bud can be induced if the mesonephric duct from *Wt1*^{-/-} embryos is recombined with wildtype mesenchyme. (Donovan et al., 1999). In order to see if the *Dh* mutation has any effect on the earliest stages of kidney development wildtype and mutant embryos were analysed for *Wt1* expression.

As for *Hoxc10* expression the *Wt1* stained embryos were cut into 100µm consecutive sections. Pictures of the individual sections have been aligned so the most anterior sections are at the top and most posterior at the bottom. Assuming that the relative position of the cloaca is identical in wildtype and mutant, the sections containing the cloaca were used to align the rest (figure 2.9g,n; red arrows).

The condensing metanephric mesenchyme is outlined by a dashed line and can be seen within the *Wt1* expression domain in both wildtype (figure 2.9c,d,e) and *Dh/Dh* (figure 2.9h,i,j,k,l). In the +/+ embryo, however, the condensing mesenchyme is very defined and there is a close correlation between these cells and *Wt1* expression, which makes it easy to identify the boundary of the metanephric mesenchyme. *Wt1* is also expressed in the mesenchyme anterior and posterior of the condensing metanephros, but the expression pattern is different. Anteriorly *Wt1* is expressed in the gonadal ridge and in the mesonephric mesenchyme (figure 2.9a,b) and posteriorly the gene is expressed in the loose mesenchyme dorsal to the mesonephric duct (figure 2.9f,g).

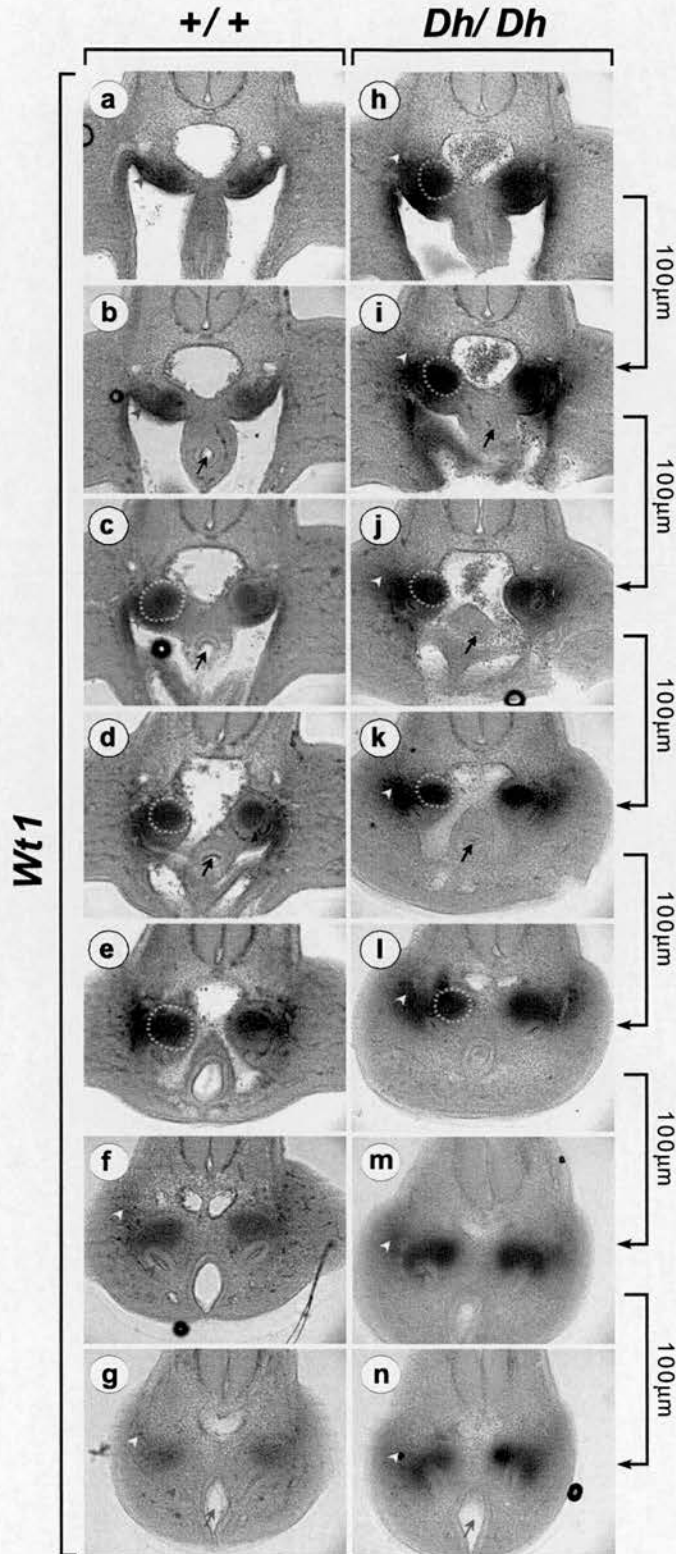


Figure 2.9: *Wt1* expression in *+/+* and *Dh/Dh* at E11.0: Embryos stained for *Wt1* expression were cut transversely at the level of the developing hind limbs. 100µm thick consecutive sections going from anterior to posterior in *+/+* embryo (a,b,c,d,e,f,g) and *Dh/Dh* (h,i,j,k,l,m,n). The two panels have been aligned so they most posterior picture shows the cloaca (g,h; red arrow). The mesonephric duct and ureter are indicated with a red arrowhead. The condensing mesenchyme defining the presumptive kidney is outlined by a dashed line. The developing hindgut is indicated by a black arrow. Diffuse expression of *Wt1* in the lateral flank mesenchyme (white arrowhead).

In *Dh/Dh* the expression of *Wt1* appear to be more diffuse. In the posterior part of the embryo (figure 2.9m,n) *Wt1* is expressed in the loose mesenchyme dorsal to the mesonephric duct in a pattern, which is similar to that observed in wildtype. However, anteriorly the expression of *Wt1* does not change, and it is as if the metanephric condensation extends further anterior in the mutant compared to wildtype (figure 2.9h,i). Also in the lateral flank the expression of *Wt1* appear to be more diffuse than in wildtype (white arrowhead) and in some places the expression domain almost extends into the limb bud mesenchyme (figure 2.9j).

When looking at *Hoxc10* expression the mesonephric ducts was positioned outside the *Hoxc10* expression domain in *Dh/Dh*. This is not the case when looking at *Wt1* (red arrowhead). In both *+/+* and in *Dh/Dh* the position of the mesonephric duct is very similar with respect to the *Wt1* expression domain. Anterior and adjacent to the metanephric condensation the mesonephric duct expresses *Wt1* and is positioned within the *Wt1* expressing mesenchyme (figure 2.9a-e and h-l). However, posterior to the metanephric condensation the mesonephric duct stops expressing *Wt1* and gradually extends outside the *Wt1* expressing mesenchyme (figure 2.9f-g and m-n). One difference between wildtype and mutant, which is very circumstantial, but perhaps worth mentioning is that the mesonephric duct is much easier to see in *Dh/Dh*. This was also the case when looking at *Hoxc10* expression and it might be an indication that the duct is enlarged in *Dh/Dh* embryos.

From the pictures in figure 2.9 it is also obvious that the hindgut is severely affected in *Dh/Dh*. In wildtype the gut tube is clearly visible and the gut lumen can be seen within the endodermal cells (figure 2.9b,c,d; black arrow). Although less pronounced, endodermal cells are present in *Dh/Dh*, but the gut lumen has almost disappeared (figure 2.9i,j,k). This phenotype will be discussed in more detail in Chapter 4.

The ureter is blocked in *Dh/Dh*.

Histological analysis of *Dh/Dh* kidneys suggested that the kidney defect is a secondary effect resulting from abnormal development and subsequent blockage of the ureter. To investigate this further, wildtype and mutant kidneys were analysed for the presence of Calbindin protein (red) and Laminin protein (green). *Calbindin* is expressed in the collecting ducts of the developing kidney (Davies, 1994) while *Laminin* is expressed in the developing epithelial cells during kidney organogenesis (Ekblom et al., 1990).

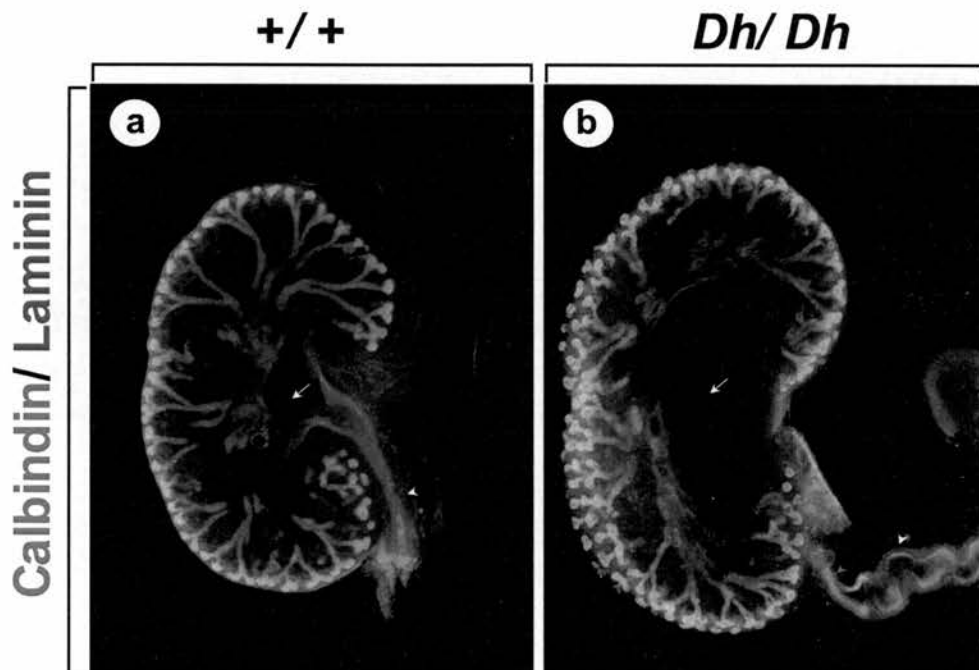


Figure 2.10: Severe malformations of the ureter in *Dh*. Double immunohistochemistry detecting the proteins Calbindin (red) and Laminin (green) at E16.5. Calbindin is found in the collecting ducts of the kidney while Laminin is found in epithelial cells. The collecting ducts connects the glomeruli at the cortex with the ureter in the middle of the kidney (white arrow). The ureter (white arrowhead) then connects the kidney to the bladder. **(a)** In *+/+* embryos the size of the medulla is normal and the ureter is a straight tube. **(b)** In *Dh/Dh* the medulla is enlarged and the ureter is bend. The swelling of the ureter coincide with the first bend (blue arrowhead).

A sagittal section through the middle of an E16.5 wildtype kidney (figure 2.10a) shows how the glomeruli are located at the cortex (red and green). The collecting ducts connect the glomeruli at the cortex with the ureter in the medulla (white arrow). The ureter then leaves the kidney as a straight tube (white arrowhead) and more posteriorly it connects to the bladder. In *Dh/Dh* the overall morphology of the kidney is normal (figure 2.10b). The glomeruli are positioned at the cortex and connected to the ureter by the collecting tubes. However, due to swelling the lumen at the medulla is very enlarged thus pushing the collecting duct towards the cortex. The swelling extends outside the into the ureter, in fact it is in the ureter that the most dramatic phenotype is seen. The ureter which normally forms a straight tube is completely bent in *Dh* animals resembling a corkscrew (white arrowhead). Also, when leaving the kidney the ureter itself is severely swollen, but the posterior extend of the swelling coincides with where the bending begins (blue arrowhead). Thus the swelling of the kidneys appears to be caused by a physical blockage of the ureter somewhere between the kidney and the bladder.

2.3 Transgenic misexpression of *Hoxc10*

Hox genes play a key role in determining segmental identity along the anterior-posterior axis (for review see Krumlauf, 1994) and it has been shown experimentally that they are required for correct positioning of the limbs (Rancourt et al., 1995; Gerard et al., 1997; Zakany et al., 1997). Additionally there is evolutionary evidence that the anterior expression boundary of the *Hox10* paralogues always correlates to the lumbar-sacral transition (Burke et al., 1995). Hence it is possible that the posterior phenotype observed in *Dh* is a direct consequence of the shift in *Hoxc10* expression. However, at present there are no functional studies confirming that *Hoxc10* has a role in positioning the hindlimbs or in kidney development. To determine whether *Hoxc10* has a role in the development of the organs it was decided to ectopically express the gene.

The *pHEX* construct

The aim was to design a vector, which would allow ectopic expression of *Hoxc10* in the lateral flank mesoderm anterior to the hindlimbs. The hypothesis being that an anterior shift of *Hoxc10* expression might induce a rostral shift of the hindlimbs similar to that observed in *Dh* embryos. However, in addition to misexpressing *Hoxc10* the aim was also to make a universal expression vector that could be used to

express various genes under different enhancers. The *pCI* vector from Promega was chosen as a starting point (figure 2.11a) because it contains a chimeric intron and a SV40 Polyadenylation signal. Both these elements are required for RNA stability and increase of the steady-state RNA levels within cells (for a detailed description of the various cloning steps see materials and methods #14).

The first step was to clone the 3'UTR of the zebrafish *Pax3* (*zPax3*-3'UTR; red) into the *pCI* vector to give the *pPAX3.1* plasmid (figure 2.11b; *pCI*). An important aspect of the final construct is that expression of the inserted gene can be detected by RNA *in situ* hybridisation. Fusion of the inserted gene to a reporter sequence with no homology to any mouse genes allows expression from the vector to be detected in a specific manner. A BLAST search to the mouse EST database using the *zPax3*-3'UTR failed to pick out any genes suggesting that the sequence has no homology to any known mouse genes. A plasmid containing the *zPax3*-3'UTR was kindly provided by Dr. Peter Currie.

To allow integration of the expression vector into the mouse genome it is imperative that the vector can be released from the bacterial components of the plasmid. To facilitate this *SacII* and *SfiI* restriction sites were introduced on both sides of the vector (figure 2.11b; *pPAX3.1* and *pPAX3.2*). Both enzymes are rare-cutters and that should lower the chances that they cut within other components of the vector. In addition to *SacII* and *SfiI* the 5' oligo also contained restriction sites for *NgoMI*, *KasI* and *NarI*. The purpose of these sites was to insert a second multiple cloning site (MCS2; purple) 5' of the intron that will allow cloning of tissue specific enhancers.

The next steps were carried out with the specific aim of *Hoxc10* misexpression in mind. As described below the enhancer for driving *Hoxc10* expression in the lateral flank mesoderm is flanked by *HindIII* sites. It was therefore necessary to introduce a *HindIII* site in MCS2 (figure 2.11b; *pPAX3.3* and *pPAX3.4*). However, in addition restriction sites for *SpeI*, *BamHI* and *SmaI* were added to MCS1 while *EcoRV* and *BclI* was added to MCS2. This was done to facilitate subsequent cloning of genes (MCS1) and enhancers (MCS2).

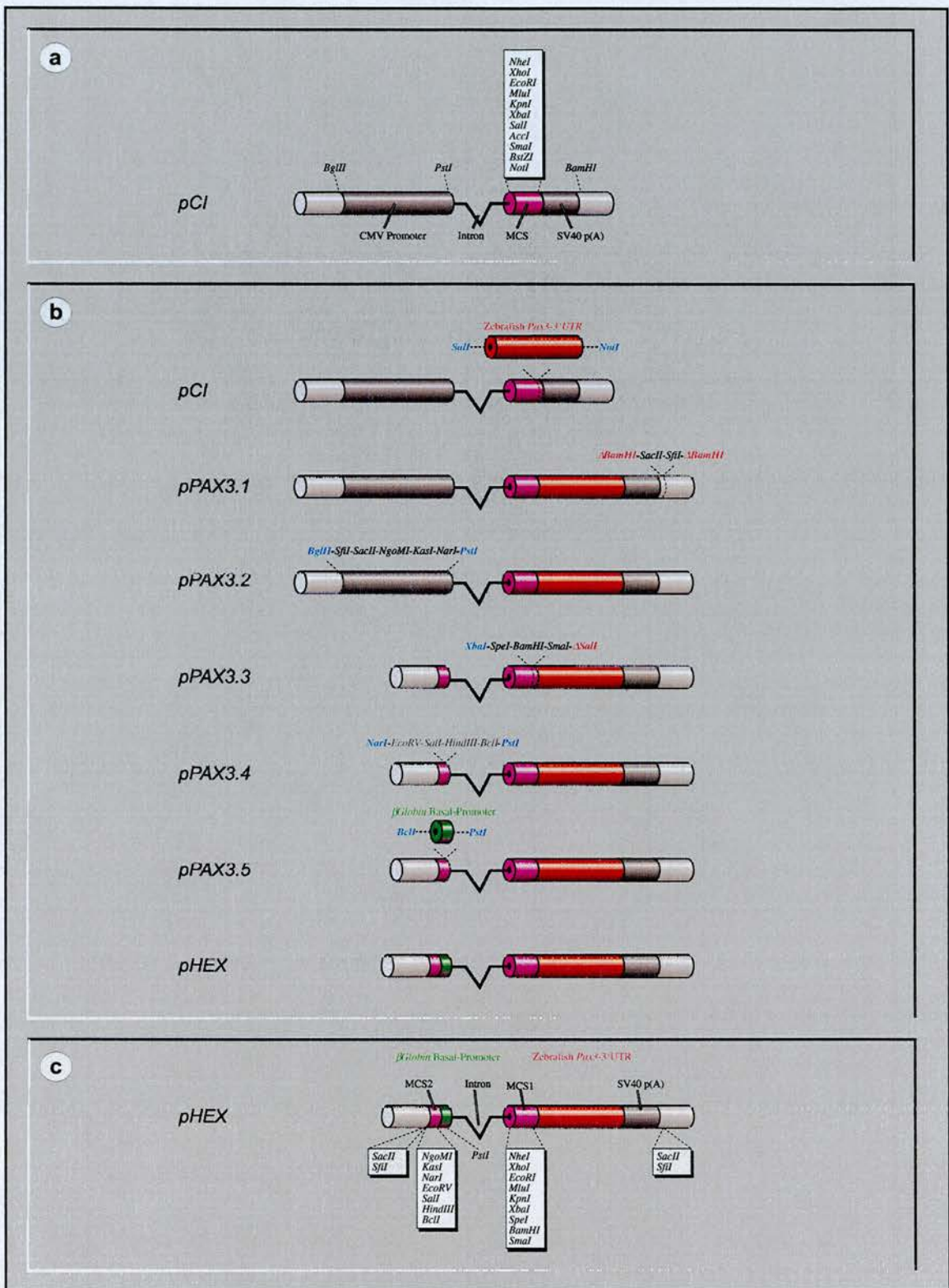


Figure 2.11: Cloning of the *pHEX* construct. (a) Schematic illustration of the Promega *pCI* vector showing relevant restriction sites (top) and other important features (bottom). (b) Diagram showing the various cloning steps carried out in order to obtain the *pHEX* construct. The restriction enzymes used to cut individual constructs are typed in bold. Blue indicates that the restriction site is maintained while red indicates that the sites has been deleted (Δ). (c) The *pHEX* construct has been engineered so it contains two multiple cloning sites (purple). MCS1 and MCS2 are positioned in a manner which allows the integration of a gene and an enhancer respectively. Hence, MSC2 is positioned in front of the β -Globin Basal-Promoter (green) while MSC1 is positioned between the intron and the Zebrafish *Pax3-3'* UTR (red). To release the expression vector from the rest of the construct the whole region is flanked by *SfiI* and *SacII* sites.

The final step was the insertion of the β -Globin Basal-Promoter (green) between MCS2 and the intron (figure 2.11; *pPAX3.5*). The β -Globin Basal-Promoter is required for transcription and has the advantage of being very small (65bp). An oligo identical to the published sequence of the β -Globin Basal-Promoter (Yee and Rigby, 1993) was inserted between MCS2 and the intron.

The resulting construct, Hox gene EXpression vector (*pHEX*; figure 2.11c), is a universal expression construct containing two multiple cloning site (MCS1 and MCS2) for cloning of genes and tissue specific enhancers respectively. MCS2 is positioned 5' of the β -Globin Basal-Promoter bringing the two elements in close proximity to each other. MSC1 is positioned 3' of the intron and directly in front of the *zPax3*-3'UTR. Any gene cloned into MCS1 will therefore form a fusion product with *zPax3*-3'UTR allowing expression to be detected using *in situ* probes specific for this region. The entire region is flanked by *SfiI* and *SacII* sites allowing the expression vector to be released from the bacterial components.

The *pHEXc10* construct

Ectopic expression of *Hoxc10* required that the full-length cDNA was cloned into the *pHEX* vector. The full-length sequence of the murine *Hoxc10* is available on PUBMED (Accession X63507), so primers including both start and stop codon were designed. In addition the primers also contained restriction sites for *MluI* and *SpeI*. The full-length *Hoxc10* gene was amplified from an EST (IMAGE no. 1024271) and cloned into the corresponding sites in *pHEX* to give the *pHEXc10* construct (figure 2.12a). To avoid errors introduced during the PCR, a high-fidelity polymerase, *PfuI*, was used to amplify the *Hoxc10* gene. The promoter region and the *Hoxc10* gene were sequenced to verify that no errors had been introduced during the cloning procedure (figure 2.12b). The primers used for sequencing are shown in black and arrows indicate the direction of sequencing. It was found that the gene integrated was indeed the full length *Hoxc10* and that the sequence matched the published data (see appendix I for sequence alignment). The sequence of the β -Globin Basal-Promoter also corresponded to previously published data suggesting that *pHEXc10* is the correct construct.

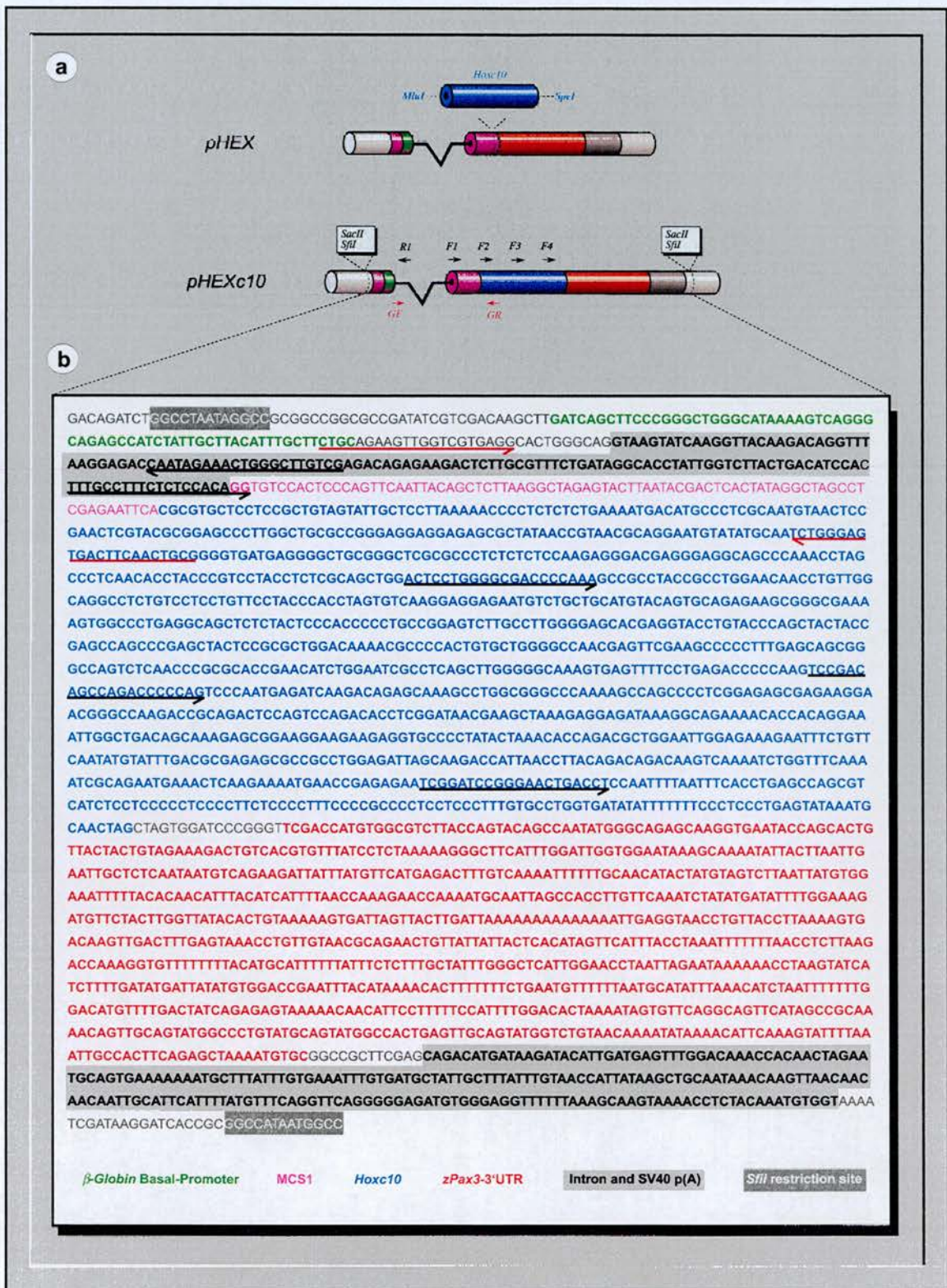


Figure 2.12: The *pHEXc10* construct. (a) To make the *pHEXc10* construct the murine *Hoxc10* gene was cloned into the *MluI*-*SpeI* sites of *pHEX*. The *Hoxc10* gene and the upstream promoter region was sequenced using the primers R1, F1, F2, F3 and F4. The primers GF and GR (red) were used for genotyping. (b) Sequence of the *pHEXc10* construct. The primers used for sequencing and genotyping are shown as arrows with the arrowhead indicating the orientation of the primer. The true sequence of *pHEXc10* matched the expected sequence and alignments of the two are shown in appendix I.

Tissue specific enhancers

The aim of this experiment is to drive the expression of *Hoxc10* ectopically in the lateral flank in the hope that an ectopic boundary will shift the position of the hindlimbs. An enhancer element driving expression in such a manner has been isolated from the *Hoxb9* gene and characterised in Prof. Krumlauf's lab (Sharpe et al., manuscript in preparation) and he kindly agreed to send it to us. At E9.5 the *Hoxb9* enhancer drives *LacZ* expression throughout the posterior part of the embryo (figure 2.13; insert). In the neural tube expression extends up to the anterior limit of the forelimb and in the lateral flank expression stops just posterior of the forelimb. The same is true at E10.5. At E12.5 expression in the lateral flank has almost disappeared whereas the neural tube remains positive for *LacZ*. For this reason this enhancer element was called NE (Neural Element). The fact the expression disappears from the lateral flank at E12.5 should not pose a problem for this experiment since the position of the hindlimbs is established at this stage. At the time of hindlimb induction high levels of *LacZ* can be detected in the lateral flank. The *Hoxb9-NE* enhancer was therefore cloned into the *pHEXc10* plasmid to give *pHEXc10-NE* (figure 2.13).

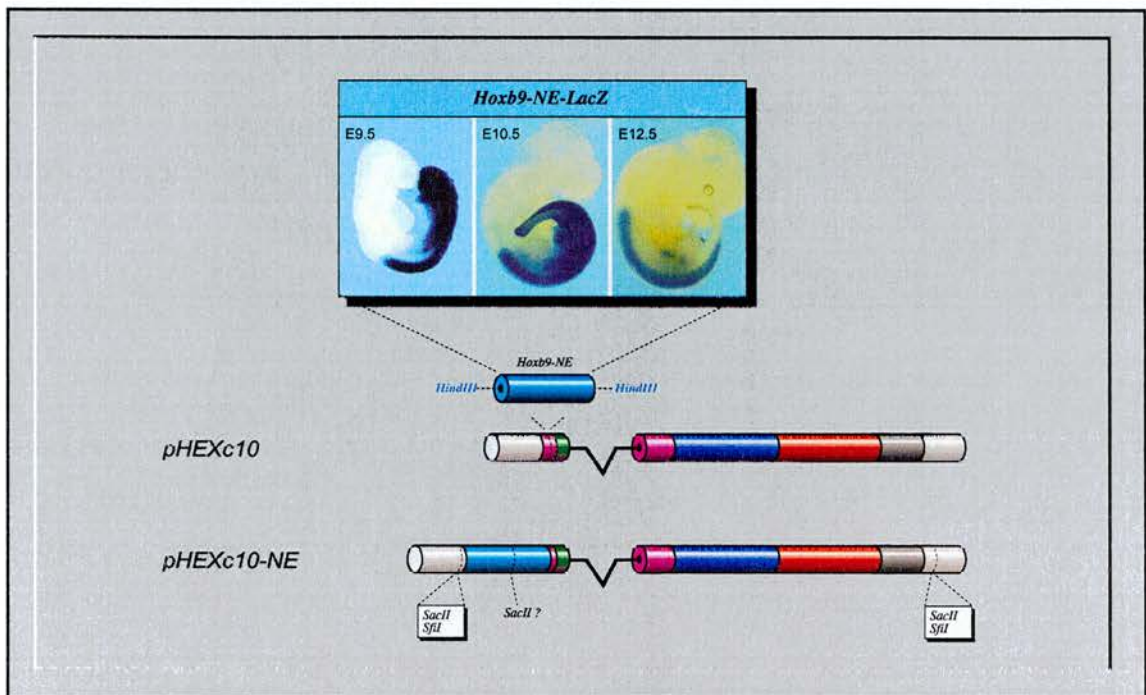


Figure 2.13: The *pHEXc10-NE* constructs. The *pHEXc10-NE* construct was made by cloning the *Hoxb9* Neural Element (NE) into the *pHEXc10* vector. At E9.5 the NE enhancer drives expression Throughout the posterior part of the embryo but later expression becomes restricted to the neural tube (insert). Restriction analysis of NE element showed that *SacII* cuts somewhere within the enhancer and can therefore not be used to release the insert. The pictures showing *LacZ* expression were kindly provided by Dr. James Sharpe.

Transient transgenic mice

When originally described the *Hoxb9*-NE enhancer was driving *LacZ* expression under control of the *Hoxb4* Basal-Promoter. It was therefore necessary to test if the expression pattern was the same in combination with the β -Globin Basal-Promoter. The *Hoxb9*-NE enhancer was therefore cloned into the *p1230* construct, which also utilises the β -Globin Basal-Promoter. The resulting construct *pGZb9-NE*, was injected into fertilised oocytes to produce transient transgenic mice. The embryos were dissected out at E9.0 and stained for LacZ activity. It was found that the NE enhancer can drive expression from the β -Globin Basal-Promoter and that the expression is identical to that of the *Hoxb4* Basal-Promoter (figure 2.14a, b, c, d). Importantly, expression could be detected in the lateral flank mesoderm. The next step was therefore to make transient transgenic mice using the *pHEXc10-NE* construct. However, when the *pHEXc10-NE* was injected very few transgenic embryos were recovered (table 2.1) and they all appeared to be normal. Hence no obvious defects could be detected with respect to the position of the hindlimbs.

Construct	No of Embryos		Percentage
	Total	Transgenic	
<i>pGZb9-NE</i>	13	4	31%
<i>PHEXc10-NE</i>	98	5	5%

The low frequency and normal appearance lead us to believe that the *pHEXc10-NE* might be lethal when injected. Only in rare occasions when the construct integrates into a genomic context that results in silencing of the construct, will the embryos survive. From this it would follow that the transgenic embryos recovered fail to express *Hoxc10* from the construct and that is why the embryos normal. To test this hypothesis it was necessary to examine whether or not the expression could be detected either by *in situ* or by RT-PCR. But because the frequency of transgenic embryos was so low it was difficult to obtain enough embryos and it was therefore decided to make stable transgenic lines. Another added advantage of stable lines is that they would allow homozygous embryos to be analysed. If expression from the construct is very reduced then having two copies might result in a phenotype.

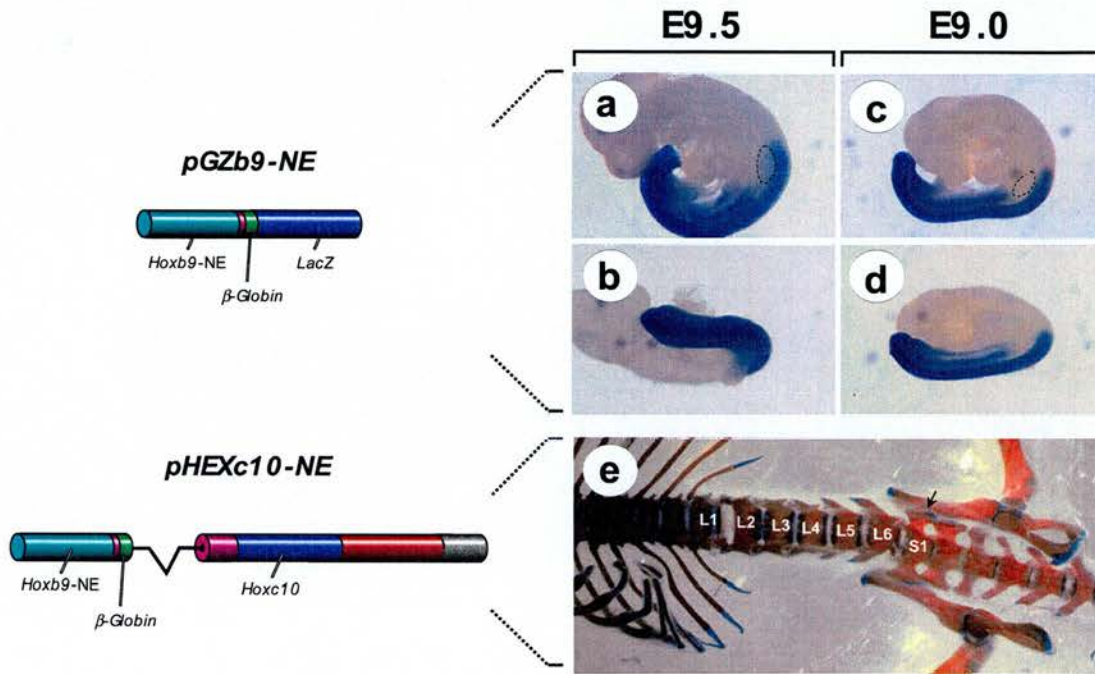


Figure 2.14: Transgenic embryos. The *Hoxb9-NE* enhancer driving expression of *LacZ* in transient transgenic embryos. **(a)** Lateral view of a E9.5 embryo stained for *LacZ* expression. In the neural tube expression extends from the tail to the anterior limit of the forelimb (dashed line). In the flank expression stops posterior of the forelimb bud. **(b)** Frontal view of the embryo in (a). **(c)** Lateral view of a E9.0 embryo stained for *LacZ* expression. In the neural tube expression extends from the tail to the anterior limit of the forelimb (dashed line). In the flank expression stops posterior of the forelimb bud. **(d)** Frontal view of the embryo in (c). **(e)** Bonestain of an adult transgenic mouse from line A214. This line is positive for the *pHEXc10-NE* construct which should be expressing the *Hoxc10* gene under influence of the *Hoxb9-NE* enhancer. The number of lumbar vertebrae is reduced from seven to six. The black arrow points to the characteristic protrusion of the first sacral vertebrae.

Stable transgenic lines

Again the *pHEXc10-NE* construct was injected and five independent founder transgenic lines were established. However, none of them displayed abnormal limb development. *In situ* hybridisation was carried out on transgenic embryos from all five lines using a probe recognising the *zPax3*-3'UTR, but no expression could be detected (data not shown). Even RT-PCR failed to detect any expression of the transgene (data not shown) suggesting that the construct is completely silenced in all five lines.

However, one transgenic mouse from line A214 was smaller than its littermates and appeared to be shaking. When examining the skeleton of this mouse it showed a reduction in the number of lumbar vertebrae from 6-5 (figure 2.14e). But, even in wildtype a low frequency of mice display a reduction in the number of lumbar vertebrae and since this phenotype has only been observed in one transgenic mouse it is unlikely that it is caused by the transgene. This experiment was carried out near the end of the project, which is why no more animals were examined.

The transgenic insertion causes obesity in line A214

The lack of a limb phenotype or any phenotype in the transgenic mice was very disappointing. However, it turned out that mice from line A214 suddenly become very obese when they reach puberty, weighing almost twice as much as their littermates (figure 2.15). An autopsy showed that the extra weight is due to excess storage of fat. Hence the internal organs are all encapsulated in fatty tissue (compare figure 2.15a and b). Using PCR it is possible to confirm that the mice suffering from obesity are positive for the transgene. However, the assay used for genotyping does not allow heterozygotes to be distinguished from homozygotes. To determine if the obese phenotype is restricted to mice homozygous for the transgene a FISH analysis was carried out by Dr. Muriel Lee. DNA was isolated from three transgenic mice from line A214 (shown in figure 2.15a, b, c). Two of these mice were obese (b and c) while one was normal (a). Using the *pHEXc10-NE* transgene as a probe the FISH analysis showed that the normal mouse only carried one copy of the transgene, while both the obese mice carried two copies (figure 2.15d, e). Thus it appears that the obese phenotype correlates with mice that are homozygous for the transgene.

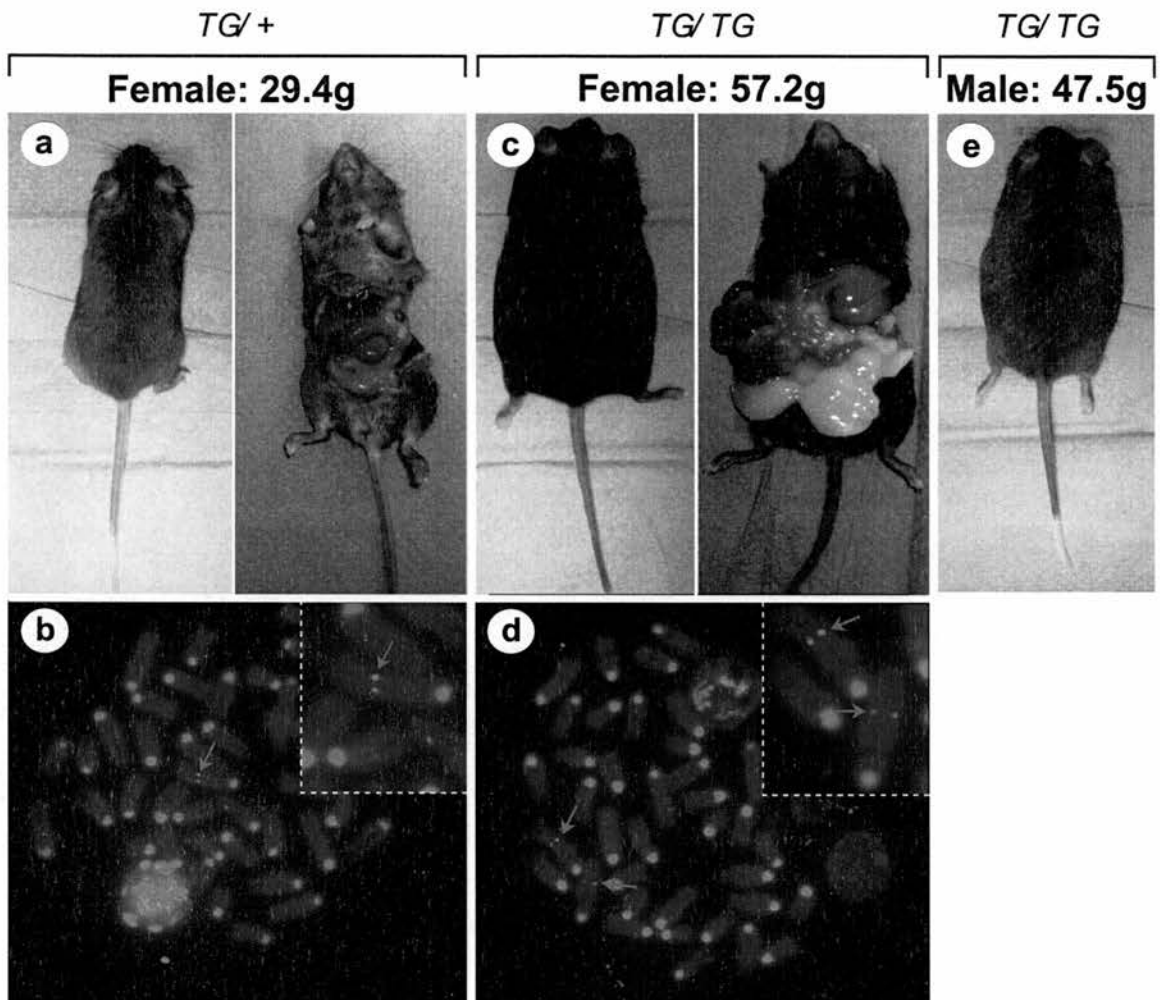


Figure 2.15: Obesity in mice homozygous for transgene insertion. Transgenic mice from the A214 strain. (a) Female transgenic mouse showing normal weight and fat distribution. (b) FISH analysis on a chromosome spread from the mouse shown in (a). One pair of green spots shows that there is only one integration site and that this mouse is heterozygous for the transgene insertion (red arrow). The insert shows a magnification of the transgenic insertion. (c) Female mouse displaying severe obesity. The autopsy demonstrated excessive amounts of fat tissue distributed around all the internal organs. (d) FISH analysis on a chromosome spread from the mouse shown in (c). Two pairs of green spots confirm that this mouse is homozygous (red arrows). (e) The obese phenotype also occurs in male mice and is therefore not sex-specific.

Despite the failure to detect any *Hoxc10* expression during development it is possible that the obese phenotype is due to misexpression of *Hoxc10* at later stages. However, it is more likely that the transgene has disrupted another gene while integrating into the genome. There are two reasons for this. First the obesity phenotype is unique to line A214 and is not seen in the four other lines carrying the transgene. Secondly the obese phenotype is restricted to mice homozygous for the transgene. This implies that the mutation is recessive and not dominant as would be expected if it was due to misexpression of *Hoxc10*.

2.4 *Hoxc10* knockout mice

Another way to demonstrate that the *Dh* mutation is acting through *Hoxc10* is to cross *Dh* to mice carrying homozygous deletions of *Hoxc10*. If the shift of the hindlimbs is a direct consequence of ectopic *Hoxc10* expression then the limb abnormalities associated with *Dh* might be rescued in the absence of *Hoxc10*.

The *Hoxc10* gene has been knocked out in Prof. Mario Capecchis laboratory and although the mutational analysis is unpublished he kindly agreed to send us the mutation. The initial correspondence took place in December 1999. However due to unforeseen problems the mice did not arrive in Edinburgh until December 2000 and at this stage I was finishing up my PhD. So unfortunately the results cannot be presented in this thesis. However, the project has been taken over by Dr. Robert Watson and hopefully it will provide some direct evidence about the function of *Dh*.

2.5 Discussion

Is *Dh* acting through *Hoxc10*?

In mice carrying the *Dh* mutation the developing hindlimbs are shifted two somites anteriorly. This correlates with a lumbar-sacral homeotic transformation of the axial skeleton and an anterior shift of *Hoxc10* expression in the lateral flank mesoderm. Experimental studies have demonstrated that altered expression of *Hox* genes can lead to homeotic transformations of the axial skeleton and shift the position of the limbs (Kessel and Gruss, 1991; Rancourt et al., 1995; Fromental-Ramain et al., 1996; Gerard et al., 1997; Zakany et al., 1997). However, in addition to being shifted, it has

previously been shown that the mutant limb buds also are abnormal from the time of induction (Hecksher-Sørensen, 1998; Lettice et al., 1999a). This early effect on limb development implies that the limb abnormalities in *Dh* embryos might be a direct consequence of the limb shift. Hence, it is possible that the polydactyly and oligodactyly observed at later stages are reflecting the abnormal events taking place earlier in development. Furthermore, the absence of *Hoxc10* expression in the mesonephric duct might be the cause of the kidney phenotype. It is therefore tempting to suggest that all the posterior abnormalities observed in mice carrying the *Dh* mutation are caused by misexpression of the *Hoxc10* gene. That way the shift of the hindlimbs, the late limb defects, the axial abnormalities and the kidney defects could all be contributed altered expression of *Hoxc10*. However, there are several questions that need to be answered. For example it is not known whether *Hoxc10* has the capacity to shift the position of hindlimbs. Also it is unclear whether the entire spectrum of limb abnormalities in *Dh* animals can be accounted for just by shifting the hindlimbs. A number of experiments were designed in order to answer some of these questions (*Hoxc10* misexpression and *Hoxc10*^{-/-} rescue), but at the moment none of them have produced any conclusive evidence. However, there are other lines of evidence, which might help understand the nature of the *Dh* mutation. But, while some of them seem to favour the idea that *Dh* could be acting through *Hoxc10* others suggest that the effect *Dh* has on development is more complex and that the mutation is acting at several stages independently of each other.

Can the shift in *Hoxc10* expression account for all abnormalities in the hindlimbs?

There are several examples in the literature demonstrating that alterations in the expression of *Hox* genes can lead to either anterior or posterior transposition of the sacrum. Thus, administration of Retinoic Acid (RA) to pregnant mice (Kessel and Gruss, 1991), deletion of *Actr11b* (Oh and Li, 1997) and *Bmp11* (McPherron et al., 1999) all lead to a posterior shift of the hindlimbs and an increase in the number of lumbar vertebrae. Nevertheless, the hindlimbs in these mice develop completely normal. A possible explanation for this might be that the limb shift appears to be part of a general homeotic transformation, which affects the entire axial skeleton and in agreement with this the expression patterns of several *Hox* genes are affected. That way all *Hox10* paralogues, which act in concert to determine the lumbar-sacral transition (Burke et al., 1995), are shifting together and maintain the appropriate *Hox* identity along the anterior posterior axis. These examples might therefore not be true

reflections of the *Dh* phenotype, because in mice carrying the *Dh* mutation only the expression of *Hoxc10* is shifted anteriorly. Other *Hox* genes such as *Hoxa10*, *Hoxd10* and *Hoxd11* are unaffected and as a result the hindlimbs are positioned outside their appropriate *Hox* domains. Presumably this is an important aspect of the *Dh* phenotype because in addition to defining the axial positions of the limb buds the *Hox* code might also be required for determining cell identity within the limb bud. Thus it has been shown that *Hoxb8* might be required for determining ZPA activity within the forelimb (Charite et al., 1994). So shifting the hindlimbs without shifting the expression domains of the majority of *Hox* genes could help to explain the severe limb abnormalities observed later in development.

Lumbar-sacral transpositions have also been observed in mice carrying targeted mutations only affecting a particular *Hox* gene (Fromental-Ramain et al., 1996; Gerard et al., 1997; Zakany et al., 1997) and therefore might be more similar to *Dh*. In two of these mutants the hindlimbs develop normally, but in one experiment the axial abnormalities coincide with preaxial polydactyly of the hindlimbs. When *Hoxd11* is expressed under the control of a conserved enhancer element from zebrafish the anterior boundary of expression is shifted anteriorly (Gerard et al., 1997). This later manifest itself as a reduction in the number of lumbar vertebrae from 6-5 and extra digits on the anterior side of the hindlimb. Hence the early events and the late limb phenotype are almost identical to those seen in *Dh*/. However, even in these transgenic mice it is not completely clear whether the extra digits are a direct consequence of the limb shift. In addition to shifting the anterior boundary of expression in the body, the fish enhancer also drives expression of *Hoxd11* in the anterior mesenchyme of the hindlimbs. *Hoxd11* is normally excluded from this region and it cannot be ruled out that it is the expression in the limb mesenchyme, which causes the digit duplication. In concordance with this, misexpression of *Hoxd12* in the anterior limb mesenchyme can induce *Shh* expression and digit duplications (Knezevic et al., 1997).

Another possibility is that the *Dh* phenotype is more complex and that the mutation affects limb development at several stages independently of each other. There are various observations in support of this theory. For example, there is indirect evidence that *Dh* has a role during limb development independent of the shift. In most descriptions of the *Dh* phenotype it is reported that the mutation only affects the hindlimbs (Searle, 1964; Green, 1967). However, under special circumstances mice carrying the *Dh* mutation also display forelimb abnormalities. Hence it has been reported that *Dh* homozygotes show abnormal cell death in the forelimbs but without affecting the limb phenotype (Rooze, 1977). When the *Dh*

mutation is combined with other limb mutations such as *Xt*, *Ssq* and *lx* to produce double heterozygotes the compound mutants display preaxial polydactyly in the forelimbs. None of these mutations (except *Xt*) affect the forelimbs as single heterozygotes, suggesting that they are interacting with *Dh* during forelimb development. Consequently, *Dh* must have a subtle role in forelimb development, which has been undetected because of the normal looking phenotype. Also, the phenotypic effects of the *Dh* mutation depend on genetic background. At the MRC Human Genetics Unit the *Dh* mutation is kept on a C57BL6 background and this gradually leads to an increase in severity of the *Dh* phenotype until the heterozygous mice become infertile due to genital abnormalities (materials and methods #40). On rare occasions, when the phenotype became very severe, sporadic cases of preaxial polydactyly in the forelimbs could be observed in homozygous animals (personal observation). No attempts were made to analyse this further because the heterozygous sterility would result in loss of the colony. Nevertheless, in context with the other experiments it confirms that the *Dh* mutation does affect forelimb development. Assuming the mechanism for anterior-posterior patterning is conserved between the fore and hindlimbs, this implies that *Dh* does have second effect during limb development independent of the shift. Because the forelimbs are not shifted in *Dh* mice.

In chickens ectopic limbs can be induced in the lateral flank between the fore and hindlimb (Cohn et al., 1995). The polarity of these limbs is reversed but otherwise they develop normally. That would suggest that the ectopic limbs have the capacity to recruit and organise the surrounding tissue. This idea is further strengthened by the observation that induction of ectopic limbs leads to respecification of the *Hox9* paralogues in the lateral flank mesoderm (Cohn et al., 1997). If limbs can be induced anywhere between the fore and hindlimbs with no effect on subsequent development it is not immediately obvious why an anterior shift of the hindlimbs in *Dh* should result in polydactyly or oligodactyly. However, one possibility, which could explain the severity of the late limb phenotype, is that the shift causes the hindlimbs to have dual fore and hindlimb identity. In chicken it has been demonstrated that ectopically induced limbs display dual identity so the anterior part of the limb has wing identity and produce feathers while the posterior part of the limb has leg identity and produce scales (Ohuchi et al., 1998). This dual identity is reflected early in limb development by the expression of the forelimb specific gene *Tbx5* in the anterior part of the limb bud and the hindlimb specific gene *Tbx4* in the posterior part. The expression of *Tbx5* and *Tbx4* was examined in *Dh* but found to be

normal (data not shown) indicating that the shift of the hindlimbs has no effect on the identity.

In fact the limb induction experiments raises several questions concerning the limb shift observed in *Dh* animals. For example, if the limb has the capacity to reorganise the expression boundaries of *Hox* genes in the lateral flank why is *Hoxd10* and *Hoxa10* not shifted with the limb? Also if the limb can alter *Hox* gene expression, is the shift of *Hoxc10* expression in the flank then induced by the shifted limb? If so, could the limbs be shifting independently of *Hox* genes? Attempts were made to answer some of these questions by looking at *Hox* gene expression prior to limb induction (E9.5). However, at this stage the myotomal expression of *Myogenin* can only be detected a few segments posterior to the forelimb and does therefore not overlap with the *Hox* expression. Without this marker the shift can not be measured with confidence since the somites are not visible after the *in situ* process. These results have therefore not been included in the analysis. Also, it was believed that the experiments manipulating *Hoxc10* expression would provide answers to some of these questions.

The nerves have maintained some of their original identity

When looking at the nerves innervating the hindlimbs in *Dh* it is immediately clear that the migrating nerves are unorganised in the mutant embryos. As a consequence of the limb shift the hindlimbs are innervated by nerves that would normally innervate the flank. However, it appears that these nerves display dual identity. In wildtype embryos the lumbar nerves projects lateral processes and can therefore easily be distinguished from the sacral nerves in which these projections are missing. In *Dh* embryos the nerves innervating the hindlimbs send out lateral projections indicating that they behave in a manner characteristic for lumbar nerves. It has recently been shown that *Hoxa10* and *Hoxd10* are required for normal innervation of the hindlimbs in mouse (Wahba et al., 2001) and on basis their own results and other experiments the authors suggest that *Hoxc10* play an insignificant role in determining nerve identity. Additionally it has been demonstrated that ectopic limbs induced in the lateral flank of chicken embryos can attract nerves to ensure that they are innervated correctly (Ohuchi and Noji, 1999). Together these results might help explaining the *Dh* phenotype. *Hoxc10* can shift the position of the limbs but has no role in specifying nerve identity. Therefore the identity of the nerves is specified according to the expression of *Hoxa10* and *Hoxd10*, which are expressed normally in *Dh*. At the same time the developing limb buds have the capacity to attract nerves

and as a result the lumbar nerves are migrating into the developing limb bud, but because they maintain lumbar identity they also send out lateral projections.

It is possible that the primary effect of the *Dh* mutation is misregulation of *Hoxc10* expression, and the homeotic transformation of the lumbar vertebrae and the shift of the developing hindlimbs would be a direct consequence of this. However, other phenotypes such as the abnormal innervation of the hindlimbs are probably an indirect effect, which arises because the shifted hindlimbs are attracting the wrong nerves. The nerve phenotype therefore demonstrates an important aspect of the *Dh* mutation, namely that the misexpression of one *Hox* gene can have severe effects on subsequent development because it shifts the position of an organ into a different *Hox* environment. In this situation the phenotype of the hindlimbs is subsequently enhanced because they are shifted out of register with the general *Hox* code and as a result the lumbar nerves try to innervate the limbs. Therefore it cannot be ruled out that it is the shift of the hindlimbs that gives rise to polydactyly and oligodactyly in *Dh* mice. On the other hand there are several lines of evidence to suggest that the *Dh* mutation also have a direct effect during limb development and it is equally possible that the late limb phenotype develops independently of the shift. However, the final outcome of the limb phenotype in *Dh* is probably much more complex than the data described in this chapter suggests, and perhaps it is a combination of the shift and other effects occurring during limb development.

The hydronephrosis is due abnormal development of the mesonephros

The pleiotropic phenotype of the *Dh* mutation affects both the hindlimbs and the kidneys. In the hindlimbs the mutation specifically affects the anterior tissue resulting in loss of preaxial structures (Hecksher-Sørensen, 1998; Lettice et al., 1999a). It has been found that in humans born with preaxial abnormalities 30% also suffer from deficiencies in the urogenital system (Evans et al., 1992). This strong association between preaxial limb abnormalities and kidney defects implies the existence of a developmental link between the two organs. As described above it appears that the limb shift observed in *Dh* can be accounted for by the shift in *Hoxc10* expression. Whether, the late limb phenotype also can be attributed to *Hoxc10* is not clear. However, if there is a link between the limb phenotype and the kidney phenotype in *Dh*, then *Hoxc10* would be a good candidate.

It has previously been reported that mice homozygous for the *Dh* mutation are born with hydronephrotic kidneys while heterozygotes occasionally develop hydronephrosis later in life (Higgins, unpublished data). The results presented here

supports this observation and all homozygous animals analysed displayed hydronephric kidneys. When sectioned the mutant kidneys appear very abnormal because of the large swelling around the medulla. However, following closer examination looking at the individual structures within the kidney it appears that the mutant kidneys are relatively normal. This conclusion is even more apparent at earlier stages. At E14.5 when the swelling is less pronounced. At this stage the expression of genetic markers such as *Wt1* is normal. These results therefore suggest that the kidneys develop normally in *Dh/Dh*, and the abnormal appearance is due to a build up of fluids within the kidney. In concordance with this conclusion the swelling is not restricted to the kidney but extends into the ureter and coincide with what looks like a physical blockage. This has recently been confirmed by Dr. Robert Watson, who showed that fluids are unable to pass from the kidney to the bladder in *Dh/Dh*. Thus it appears that the kidney phenotype in *Dh* is secondary. The primary effect is abnormal development of the ureter, resulting in a physical blockage somewhere between the kidney and the bladder.

Interestingly, the ureter develops from the posterior part of the mesonephric duct and *in situ* analyses have shown that *Hoxc10* is expressed in the mesonephric duct in wild type embryos but excluded in mutant embryos. However, it is unclear whether this phenotype is due to misregulation of *Hoxc10* or whether the mesonephric duct has been misplaced outside the *Hoxc10* expression domain. Presumably it's the later since the dorsal mesenchyme is known to be affected in *Dh* mice (this is based on data presented in chapter 4). Either way, this can probably be ignored, because the important finding is that the mesonephric duct is developing outside its normal context and this might account for abnormal appearance observed later in development. Nevertheless, apart from being expressed in the correct place (Hostikka and Capecchi, 1998), there is no direct evidence linking *Hoxc10* to a role in renal development. However, other *Hox* genes have been associated with hydronephrosis and blockage of the ureter similar to the abnormalities observed in *Dh*. Mice carrying targeted mutations in both *Hoxa13* and *Hoxd13* display severe hydronephrosis of the ureter and kidneys (Warot et al., 1997) and although, the function of *Hoxc10* is unknown, these results confirm that *Hox* genes are involved in the development of the ureter.

Throughout this chapter it has been emphasised that the *Dh* phenotype is mediated by *Hoxc10*. However, it should be stressed that all changes in *Hoxc10* expression are secondary, presumably caused by misexpression of *Gli2* or *Inh β b*, the candidate genes for *Dh*. It is therefore possible that the kidney phenotype is unrelated to *Hoxc10*; instead the abnormalities could be induced directly by *Inh β b*. The

evidence for this is based on experiments examining the role of *Gata2* in development. Mice carrying a targeted deletion of the *Gata2* gene die mid-gestation due to haematopoietic failure (Tsai et al., 1994). Introduction of a YAC containing the *Gata2* gene allows the *Gata2*^{-/-} embryos to complete gestation, however, the newborn pups die soon after birth from urogenital abnormalities (Zhou et al., 1998). Analysis of the mice revealed hydronephrosis and blockage of the ureter almost identical to the phenotype observed in *Dh*. Interestingly, in *Xenopus* *Gata2* is regulated by activin (Walmsley et al., 1994) and in mouse there is evidence that *Gata1* and *Gata4* are transactivators of *Inhβb* (Feng et al., 2000), suggesting a direct link between the *Gata* genes and *Inhβb*.

Is there a correlation between the limb and kidney abnormalities in *Dh*?

It has been shown that the *Dh* mutation affects both limb and kidney development at early stages. But this does not explain why defects in these organs occur simultaneously at such a high frequency. However, it seems like “an early effect” and proximity is the best way to explain this developmental link. From the *Wt1 in situs* it is clear the hindlimbs and the mesonephros are positioned very close to each other. Hence, the mesenchyme contributing to the two organs is lying adjacent to each other during early stages of development. Any mutation affecting the identity of this mesenchyme might therefore affect development of both organs. At the moment the best explanation as to how *Dh* affects both limb and kidney development is therefore, that the mutation affects various tissues in the posterior part of the embryo, either directly through *Gli2* or *Inhβb* or indirectly through a gene like *Hoxc10*. This happens early in development presumably prior to E9.5 and alters the identity of the mesenchyme required for normal development of the limb and ureter. The hindgut phenotype, which will be discussed in chapter 4, is another aspect of the *Dh* mutation pointing in this direction.

2.6 Conclusion

Mice carrying the *Dh* mutation display a number of abnormalities in the posterior part of the body including an anterior shift of the hindlimb buds, homeotic transformations of the lumbar vertebrae and abnormal innervation of the hindlimbs. These abnormalities coincide with an anterior shift of *Hoxc10* expression. Attempts have been made to demonstrate that the *Dh* phenotype is mediated through *Hoxc10* but at present no conclusive evidence have been obtained.

Hydronephrosis of the kidneys observed in mice carrying *Dh* mutation is a secondary effect caused by abnormal development of the ureter. During early stages of kidney development the mesonephric duct is located outside the expression domain of *Hoxc10*. This is presumably due to a physical displacement caused by changes in the mesenchyme surrounding the mesonephric duct. As a consequence the mesonephric duct undergoes abnormal development, resulting in blockage of the ureter. This blockage eventually leads to a build up of fluids around the medulla in the kidneys.

An important aim of this project was to investigate the proposed relationship between limb and kidney defects (Evans et al., 1992). The results presented in this chapter strongly imply that misexpression of *Hoxc10* is responsible for both phenotypes. However, this is only applicable to *Dh* and does explain why combined preaxial limb abnormalities and kidney defects occur at such a high frequency in humans. Neither does it indicate whether or not the mesonephros is required for induction of the limbs. But, the fact that *Hoxc10* is expressed in the mesenchyme, which at early stages represents the presumptive limb mesenchyme and surrounds the mesonephric ducts, suggests that other genes expressed in this mesenchyme might affect the development of both organs if mutated.

Chapter 3: Confocal microscopy of gene expression

3.1 Introduction

Large-scale projects such as mutagenesis screens and genome sequencing are providing developmental biologists with increasing numbers of genes involved in embryogenesis. In order to understand the roles of these genes it is informative to examine their expression, as the spatial and temporal distribution often reveals important clues about the function of a gene. Whole mount *in situ* hybridisation gives a good general idea of which parts of the embryo a gene is expressed in. When more exact information is required, a common approach is to perform *in situ* hybridisation on thin serial sections, allowing the expressing tissues to be examined in detail. However, the spatial relationships of tissues within the embryo are often lost when examining individual sections. To overcome this problem methods have been developed which can reconstruct the 3D shape of expression patterns from a series of sections (Baldock et al., 1997). The resultant reconstructions aid in understanding an expression pattern, but the complete procedure (cutting, staining, digitising and processing hundreds of sections) is time-consuming, and consequently not ideally suited to the analysis of large numbers of genes. As the number of genes to be examined increases, new techniques are needed for capturing this data, which are simple enough and fast enough that researchers can perform them as part of a routine analysis. Ultimately, 3D reconstruction will be a useful format to store entire expression patterns, as they can be transmitted over the Internet for examination by other researchers. Creating a 3D reconstruction using thin sections is laborious not only due to the large number of sections to deal with, but also due to the difficulty of realigning the sections correctly to recreate the original shapes of the embryo. One way to avoid both of these problems, is to use non-invasive imaging techniques which perform virtual sectioning of the tissue and produce inherently registered data, for example, the use of magnetic resonance imaging (MRI) for capturing the 3D pattern of reporter-gene expression within *Xenopus* embryos (Louie et al., 2000). An alternative and more widely accessible technique is confocal laser scanning microscopy (CLSM). While routinely used for observing the distributions of proteins by fluorescence immunohistochemistry (Mohun et al., 2000), CLSM has not been used to map gene expression patterns in mouse.

A method was developed together with Dr. James Sharpe and published in Mechanism of Development (Hecksher-Sørensen and Sharpe, 2001; see Appendix VI), for creating 3D reconstructions of gene expression patterns, which is faster and easier than thin-section methods. It relies on the combination of four widely used techniques: Whole mount *in situ* hybridisation using Fast Red as a substrate for the alkaline phosphatase, thick vibratome sections, confocal laser scanning microscopy, and software for reconstructing confocal data. We have found that both resolution and morphology are superior to standard wax sections. However, in addition to 3D reconstructions, this technique is very useful for high-resolution analysis of gene expression at the single-cell level in 2D. Initially this was seen as a secondary advantage, but it later turned out to be extremely useful for studying the gut phenotype in *Dh* (chapter 4).

Much effort was put into demonstrating that the method works and this resulted in large amounts of data that was not published. Neither does it fit into the other experimental chapters. I therefore present a short chapter showing some of these results. 3D models of some of the data can be accessed at genex.hgu.mrc.ac.uk.

3.2 Verification of the method

Neural tube expression

It turned out that many of the genes examined in the spleno-pancreatic region (chapter 4) also are expressed in the developing neural tube. The neural tube is extremely compartmentalised making it a nice tissue for studying gene expression. Often genes that are expressed in the developing neural tube will show very defined boundaries, ie. a gene is expressed in one subset of cells with no expression in the neighbouring cells.

The *Shh* pathway is believed to have an important role in setting up this compartmentalisation (Ericson et al., 1995). The expression of *Shh* and other members of the *Shh* pathway were examined at E9.5. As previously reported *Shh* was found in the dorsal notochord and the ventral floorplate of the neural tube (Roelink et al., 1994); figure 3.1a). *Patched*, the receptor of *Shh*, is normally activated in cells adjacent to *Shh*

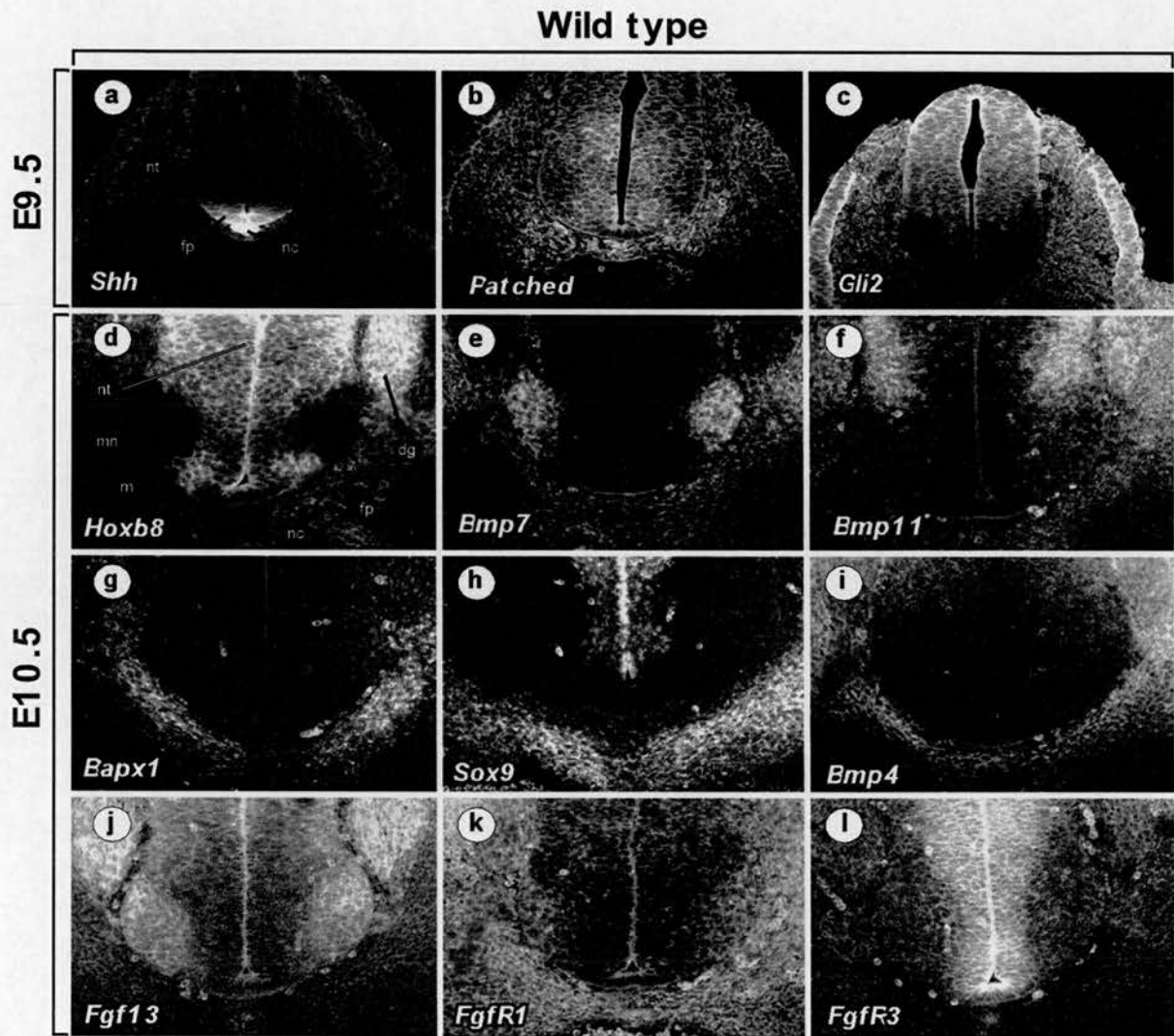


Figure 3.1: Gene expression in the developing neural tube. (a) Expression of *Shh* at E9.5. (b) Expression of *Patched* at E9.5. (c) Expression of *Gli2* at E9.5. (d) Expression of *Hoxb8* at E10.5. (e) Expression of *Bmp7* at E10.5. (f) Expression of *Bmp11* at E10.5. (g) Expression of *Bapx1* at E10.5. (h) Expression of *Sox9* at E10.5. (i) Expression of *Bmp4* at E10.5. (j) Expression of *Fgf13* at E10.5. (k) Expression of *FgfR1* at E10.5. (l) Expression of *FgfR3* at E10.5. (nt) neural tube, (fp) floor plate, (nc) notochord, (m) surrounding mesenchyme, (dg) dorsal root ganglia and (mn) motor neurons.

expressing cells (Stone et al., 1996; Goodrich et al., 1996). At E9.5 *Patched* is expressed in the ventral part of the neural tube and in the mesoderm surrounding the notochord, presumably in response to *Shh* signalling. *Gli2* is reported to be a repressor of *Shh* (Aza-Blanc et al., 2000). At E9.5 *Gli2* is expressed in the dorsal part of the neural tube (figure 3.1c). This expression pattern corresponds with previously published data (Goodrich et al., 1996). Whereas the expression of both *Shh* and *Patched* is relatively easy to visualise using *in situ* hybridisation, *Gli2* expression is much more difficult to detect, presumably due to lower levels of expression. However, using the confocal microscope even the low levels displayed by *Gli2* can easily be detected, demonstrating the sensitivity of this method.

At E10.5 *Hoxb8* is expressed at very high levels along most of the developing neural tube and the dorsal root ganglia (figure 3.1d). However, expression is specifically excluded from the ventral region where the developing motor neurons are located. *Bmp7* is also expressed in the developing neural tube but the expression is the exact opposite of that of *Hoxb8* (figure 3.1e). Thus *Bmp7* is expressed in the developing motor neurons and in the mesenchyme surrounding the dorsal root ganglia. *Bmp11* is expressed in the dorsal root ganglia and laterally in the neural tube dorsal to the motor neurons (figure 3.1f). It appears that the expression of *Bmp11* is a dorsal continuation of *Bmp7* although the expression domains of the two genes do not overlap.

A different set of genes was found to be expressed in the mesenchyme surrounding the neural tube. *Bapx1* expression is completely excluded from the developing neural tube and dorsal root ganglia but can be detected in the mesenchyme surrounding the notochord (figure 3.1g). *Sox9* is also expressed in the mesenchyme around the notochord although the expression domain is slightly wider than that of *Bapx1* (figure 3.1h). Also *Sox9* expression could be detected in the medial part of the neural tube dorsal to the floor plate. The expression pattern of *Bmp4* is very similar to that of *Bapx1* except *Bmp4* is also expressed in the dorsal root ganglia (figure 3.1i). In contrast to *Bmp7* and *Bmp11*, *Bmp4* is not expressed in the ventral part of the neural tube.

Finally the expression of some *Fgf*'s and *Fgf receptors* was examined. *Fgf13* was found to be expressed at high levels in the developing motor neurons and in the dorsal root ganglia (figure 3.1j). Low levels of *Fgf13* expression could be detected in the dorsal part of the neural tube while the gene is off in the ventral part and in the surrounding mesoderm. *FgfR1* is expressed throughout the mesenchyme surrounding the neural tube, but can only be detected at low levels in neural tube itself (figure 3.1k). Low expression could also be detected in the developing motor neurons and in

the dorsal part of the neural tube. *Fgfr3* is expressed at high levels in the floor plate and medial part of the neural tube (figure 3.11). Expression is excluded from the motor neurons and surrounding mesoderm.

***Hoxb9* is expressed around the growing nerves**

While examining the expression of genes in the developing neural tube it became clear that *Hoxb9* in addition to being expressed in the neural tube and dorsal root ganglia could also be weakly detected the region of the growing nerves (figure 3.2a). This expression pattern has not previously been reported and therefore prompted a closer examination. Because the Fast Red technique can utilise the advantages associated with confocal microscopy it was possible to acquire high power images of the relationship between *Hoxb9* expression and the migrating nerves. The fact that the technique is non-invasive means that gene expression can be studied in detail in intact tissue. This turned out to be an advantage when looking at fragile structures such as nerves.

Examining the tip of the migrating nerve at higher power (the highlighted area in figure 3.2a) it becomes clear that *Hoxb9* is expressed close to the nerve fibre, but not in the nerves themselves (figure 3.2b). However, at the tip of the nerve, expression is more widespread and it is unclear whether *Hoxb9* expression precedes the migrating nerves or if the main nerve fibre has branched out so individual fibres no longer can be detected. Even at higher magnification (the highlighted area in figure 3.2b) it is still not possible to see whether the nerve has branched and if there are individual nerve fibres between the *Hoxb9* expressing cells (figure 3.2c). Nevertheless, at this resolution individual cells expressing *Hoxb9* can easily be identified at what is assumed to be the distal limit of the growing nerve.

To further investigate the relationship between *Hoxb9* and the extending nerves, E11.5 wild type embryos were stained simultaneously for *Hoxb9* expression and with an anti-neurofilament antibody (Nf-160) that specifically recognises differentiated nerve cells. At E11.5 the embryo is a day older than the embryo shown in figure 3.2a-c and at this stage the nerves have extended into the limb buds. Hence the remaining images in figure 3.2 have been captured in the ventral half of the developing forelimb. At E11.5 *Hoxb9* is still expressed in the cells surrounding the tip of the migrating nerve (figure 3.2d).

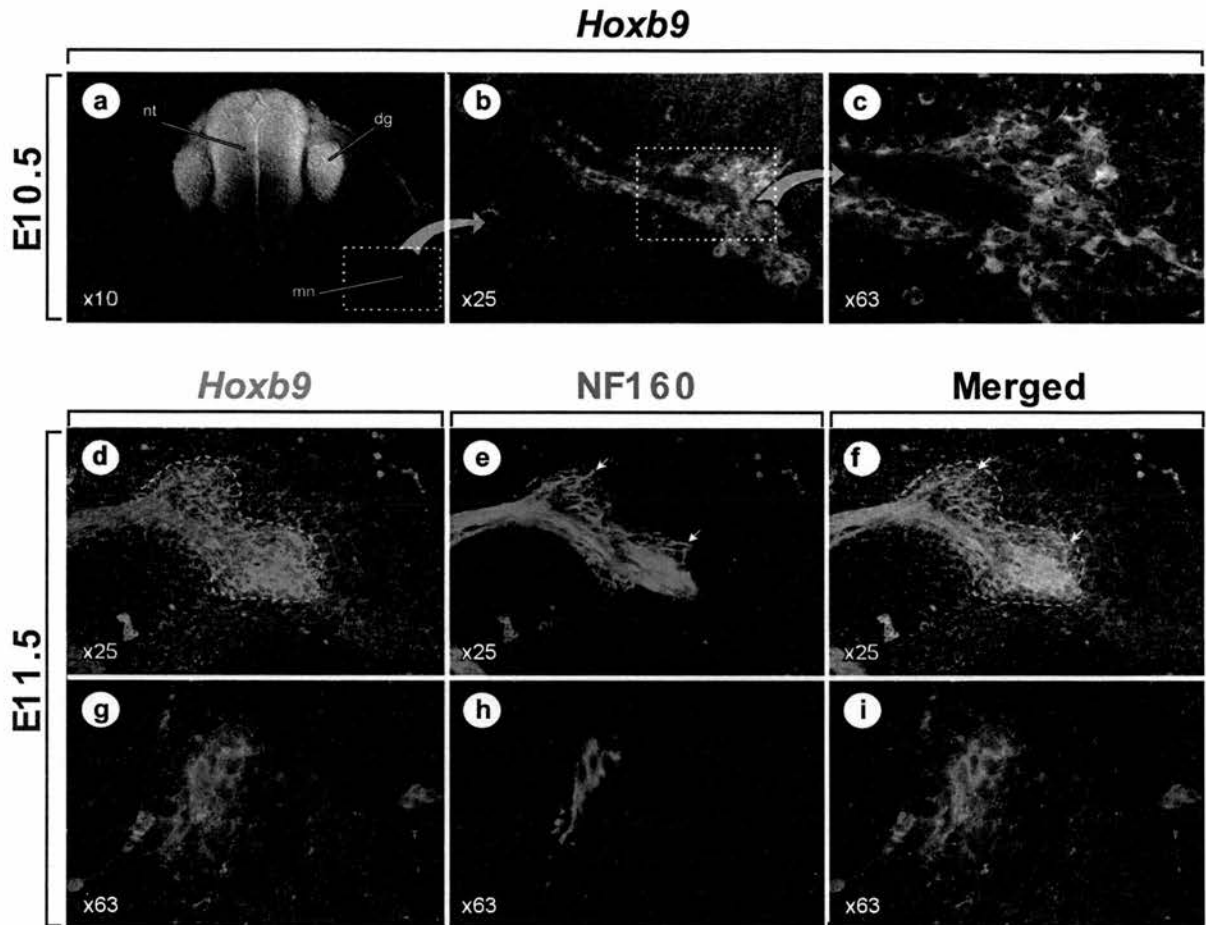


Figure 3.2: *Hoxb9* expression in the mesenchyme surrounding the tip of the migrating neurons. (a) *Hoxb9* expression in the neural tube and dorsal root ganglia at E10.5. Weaker expression can also be seen in association with the motor neuron extending from the dorsal root ganglia. (b) Magnification of the area highlighted in (a). *Hoxb9* is expressed in the mesenchyme surrounding the growing nerve. (c) At even higher magnification individual *Hoxb9* expressing cells can be seen dispersed around the tip of the growing nerve. (d) *Hoxb9* expression in the mesenchyme surrounding the migrating nerve (dashed line). The image is captured in the ventral half of the developing forelimb at E11.5. (e) Antibody staining against NF160 in the same section. Individual nerves can be seen (arrows). (f) Merged image combining *Hoxb9* expression (d) and NF160 protein (e). (g) High power magnification of *Hoxb9* expression in the same nerve. (h) Antibody staining against NF160 in the same section. (i) Merged image combining *Hoxb9* expression (g) and NF160 protein (h). The number in the lower left corner of each image indicates the power of the objective used when capturing the image. (nt) neural tube, (dg) dorsal root ganglia and (mn) migrating nerve.

The extent of *Hoxb9* expression is outlined by a dashed line. The *Hoxb9* expressing cells that could be seen around the extending nerve at E10.5 can no longer be seen. Looking at Nf-160 protein it is clear that the tip of the nerve is branching, and smaller bundles of nerves diverging from the main fibre can be seen (figure 3.2e; arrows). Indeed, when the two images are merged it is obvious that the extent of *Hoxb9* expression coincides with the tip of the migrating nerves (figure 3.2f). The same can be seen at an even higher magnification (figure 3.2g, h, i). Here the extreme end of a nerve fibre is shown and it appears that *Hoxb9* expression is restricted to the cells that are in close proximity to the nerve.

At later stages of development a particular cell type called Schwann cells surround all the peripheral nerves. These eventually lay down the myelin sheath that insulates the myelinated nerve fibres and are of primary interest in understanding myelin disorders. Definitive Schwann cells (as recognised by a number of criteria including expression of specific markers) are first detected in association with the nerves at about E15.5 in the mouse. Lineage analysis has shown that the Schwann cells are of neural crest origin (Frank and Sanes, 1991) and it is believed that these cells migrate with the extending nerves as they project through the trunk of the embryo. Although no markers exist to visualise the cells in place on the nerves before E15.5, primary culture experiments have identified a population of cells, which occupy the nerves from as early as E12.5. These cells are of neural crest origin and are capable of differentiating into definitive Schwann cells under very specific culture conditions (Jessen et al., 1994; Dong et al., 1995) and are referred to as Schwann cell precursors. Schwann cells follow a multistep pathway of differentiation and although a number of the steps can be reproduced and examined in culture (Murphy et al., 1996), very little is known about what happens in vivo between the initial migration of the neural crest cells from the neural tube and the formation of definitive Schwann cells in place on the nerves 5 to 6 days later.

The results shown in figure 3.2 clearly demonstrate that *Hoxb9* expression is closely associated with the tip of the growing nerves, and it is intriguing to speculate that the cells expressing *Hoxb9* are Schwann cell precursors. What the possible roles of *Hoxb9* expression in these cells might be, are still very speculative. Although the *Hoxb9* gene has been knocked out, the phenotypic analysis does not report any nerve defects (Chen and Capecchi, 1997; Medina-Martinez et al., 2000), so at present there are several questions that need to be answered. i) Are these cells of neural crest origin and in the Schwann cell lineage? ii) Are the *Hoxb9* cells migrating together with the growing nerves? If they are, are they guiding the nerves or are they

passively following the same path? iii) Is *Hoxb9* expression dependent on physical contact with the nerves?

To address some of these questions the project is continued by Dr. Paula Murphy at the MRC Human Genetics Unit who has a particular interest in Schwann cell differentiation and hopefully it will reveal new insights into the functions of *Hoxb9*.

Studying gene interactions

Another interesting aspect of using confocal microscopy to visualise gene expression is the possibility of studying gene interaction. In the future the demand for understanding how genes affect each other will undoubtedly increase and in order to get an exact idea of how two genes interact, it will be necessary to study their expression patterns at the single cell level. To demonstrate that the Fast Red technique has the capacity to do this the expression of *Shh* and *Pdx1* was analysed in the developing pancreas at E9.5. It has been shown that turning off *Shh* in the dorsal pancreatic endoderm is essential for pancreas development (Apelqvist et al., 1997). *Pdx1* on the other hand is expressed exclusively in the developing pancreas at E9.5 and it is therefore tempting to suggest that these two genes might be interacting with each other.

At E9.5 strong *Shh* expression was detected in the middle of the endoderm but expression was excluded from the dorsal pancreatic bud (figure 3.3a). The distribution of the PDX1 protein was visualised using antibodies. As expected PDX1 was found in the nuclei of cells in the dorsal pancreatic endoderm (figure 3.3b), but from the merged image it became clear that the relationship between the two genes is not defined by a specific boundary. Thus there are several cells separating the two expression domains, which do not express either gene (figure 3.3c; flanked by arrows). However, since *Shh* is a secreted molecule it has the capacity of acting over a distance and could therefore affect *Pdx1* expression several cell diameters away.

To see if the distance of *Shh* diffusion corresponded roughly to the repression of *Pdx1*, the expression of *Patched* was analysed. In addition to being a mediator of *Shh* signalling *Patched* is also activated in response to *Shh* signalling and can therefore be used as an indicator of *Shh* diffusion (Goodrich et al., 1996). As previously reported (Apelqvist et al., 1997), *Patched* is expressed at high levels in the mesoderm adjacent to the *Shh* expressing endoderm, while no transcripts could be detected in the mesoderm dorsal to the to the pancreatic endoderm (figure 3.3d).

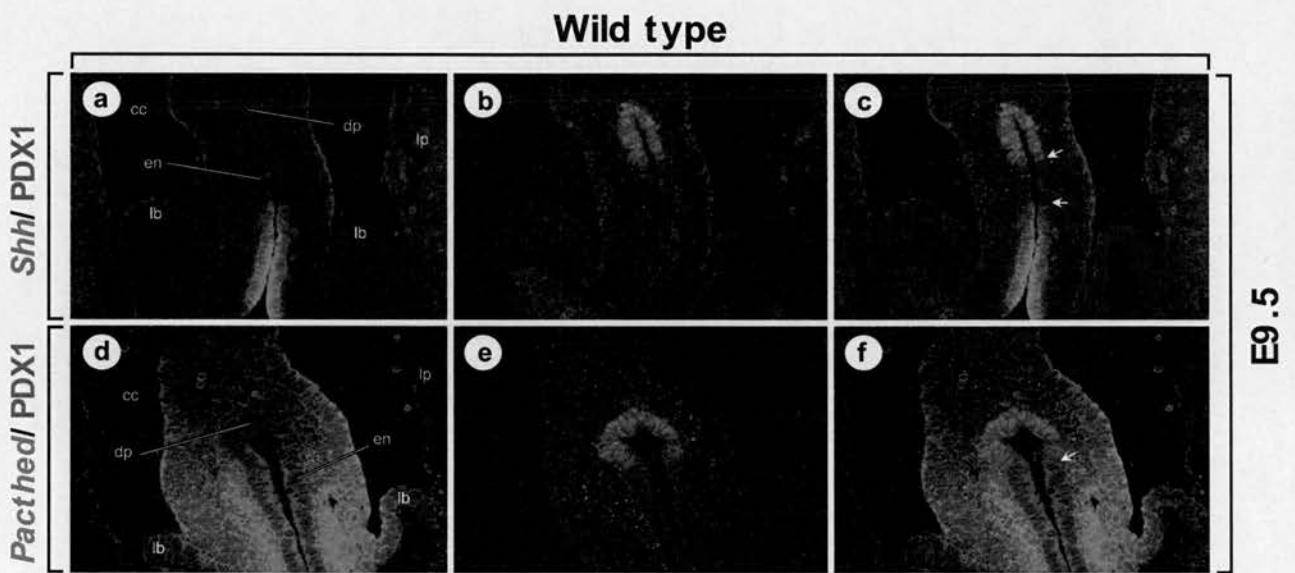


Figure 3.3: *Shh* is down regulated in the pancreatic endoderm. (a) *Shh* expression in the gut endoderm at E9.3. Transverse section at the level of the forelimbs. (b) PDX1 antibody staining of the same section. (c) Merged image combining *Shh* expression (a) and PDX1 protein (b). Cells that does not express either gene are flanked by arrows. (d) *Patched* expression in the mesoderm surrounding the gut endoderm at E9.5. Transverse section at the level of the forelimbs. (e) PDX1 antibody staining of the same section. (f) Merged image combining *Patched* expression (d) and PDX1 protein (e). The mesenchymal extent of *Patched* is marked by an arrow. (dp) dorsal pancreatic bud, (en) endoderm, (lb) liver bud, (cc) coelomic cavity and (lp) lateral plate.

PDX1 was restricted to dorsal pancreas (figure 3.3e). However, in contrast to *Shh* the dorsal boundary of *Patched* expression in the mesoderm correlates well with the ventral limit of PDX1 distribution (figure 3.3f; arrow). This indicates that diffusion of Shh could be responsible for repressing *Pdx1* expression in the endoderm and therefore defining the ventral limit of PDX1 protein. However, the opposite scenario where PDX1 is defining the dorsal limit of *Shh* expression can be ruled out because PDX1 is a transcription factor and will only effect gene expression in cells where the protein is present.

It should be pointed out that these experiments are very preliminary and although the results are indicative they are not conclusive. The two embryos analysed are not exactly stage matched (the patched embryo is slightly older) and gene expression is very dynamic at this stage. It is therefore possible that *Shh* and *Pdx1* at slightly later stages are expressed in cells adjacent to each other.

3.3 Discussion

The expression patterns of the genes shown in figure 3.1 are all distinct. In most cases the expression domains are defined and the boundaries between expressing and non-expressing cells is very distinct. This clearly demonstrates that the resolution of the technique is high, even at the single cell level. However, because the Fast Red technique relies on the embryos being stained as whole mounts, the penetration of probes and antibodies becomes an important factor. The embryos that are pictured in this thesis were generally stage E9.5 or E10.5 and at these stages penetration does not appear to be a significant problem. However, at stages older than E10.5 probes and antibodies cannot penetrate to the centre of the embryo and the results will therefore no longer reflect the real expression pattern i.e. they become weaker towards the middle. But at E11.5 most organs have been defined so one way to overcome the problem of penetration is to dissect out the organs and process them individually.

It immediately became clear that the high resolution offered by the confocal microscope would be ideal for looking at more than one gene product, as has been demonstrated here using a combination of immunohistochemistry and *in situ* hybridisation. Efforts were made to find other fluorescent substrates that would work together with Fast Red allowing double *in situs*, but unfortunately substrates such as ELF (ELF is another fluorescent substrate for alkaline phosphatase) did not work with the confocal. Also, instead of using enzymatic amplification attempts were made to use fluorescently labelled secondary antibodies, but that also failed. The

only way it was possible to visualise two gene products at the same time was to use a combination of immunohistochemistry and *in situ* hybridisation. This requires some optimisation of protocols and it does not circumvent the problem that antibodies against the gene of interest must be available. Nevertheless, it is a step in the right direction and the results in figure 3.2 and figure 3.3 clearly demonstrate that the Fast Red technique has the capacity of analysing two gene products simultaneously at the single cell level. Another interesting aspect of this technique, which remains to be tested, is to look for differences in distribution between RNA and protein products of the same gene.

3.4 Conclusion

The Fast Red method can be used to visualise gene expression in intact tissue at the single cell level. In combination with immunohistochemistry two gene products can be visualised simultaneously making this method ideal for studying gene interaction at a very high resolution.

Chapter 4: The gut phenotype

4.1 Introduction

At E9.5 the endoderm of the stomach and pancreas is positioned in the middle of the embryo between the developing forelimbs. The endoderm is surrounded by mesoderm that is flanked by a layer of mesothelium on both sides. These mesothelial layers flanking the anterior gut were first described by Green in 1967 and termed the Anterior Splanchnic Mesodermal Plate (ASMP). During subsequent development the gut rotates, and at E10.5 the stomach and spleno-pancreatic region is positioned at the left side of the embryo. This rotation coincides with a thickening of the mesothelium on the left side while the mesothelium on the right side becomes thinner. As a result, a ridge like structure can be observed on the left/dorsal side of the gut mesoderm at E10.5, which we have termed the Splanchnic Mesothelial Ridge (SMR). The SMR is a novel embryonic structure and this chapter describes some of the features associated with the SMR.

4.2 The SMR mediates a physical requirement for left-right asymmetry

The Splanchnic Mesothelial Ridge (SMR)

To visualise the extent of the SMR around the spleno-pancreatic region at E10.5, embryos were stained with phalloidin and sectioned transversely at the level of the pancreas (figure 4.1g; represented by plane d in figure 4.1a). Phalloidin stains f-actin and outline the shape of individual cells, making it possible to distinguish the loosely packed mesenchyme from endoderm and mesothelium. The SMR and the pancreatic endoderm are clearly visible and have been colour coded blue and red respectively. The section shows that the SMR encapsulates the mesenchyme surrounding the dorsal pancreas. The SMR runs all the way from the lung buds (anterior) to the duodenum (posterior), but it is thickest at the level of the dorsal pancreatic bud.

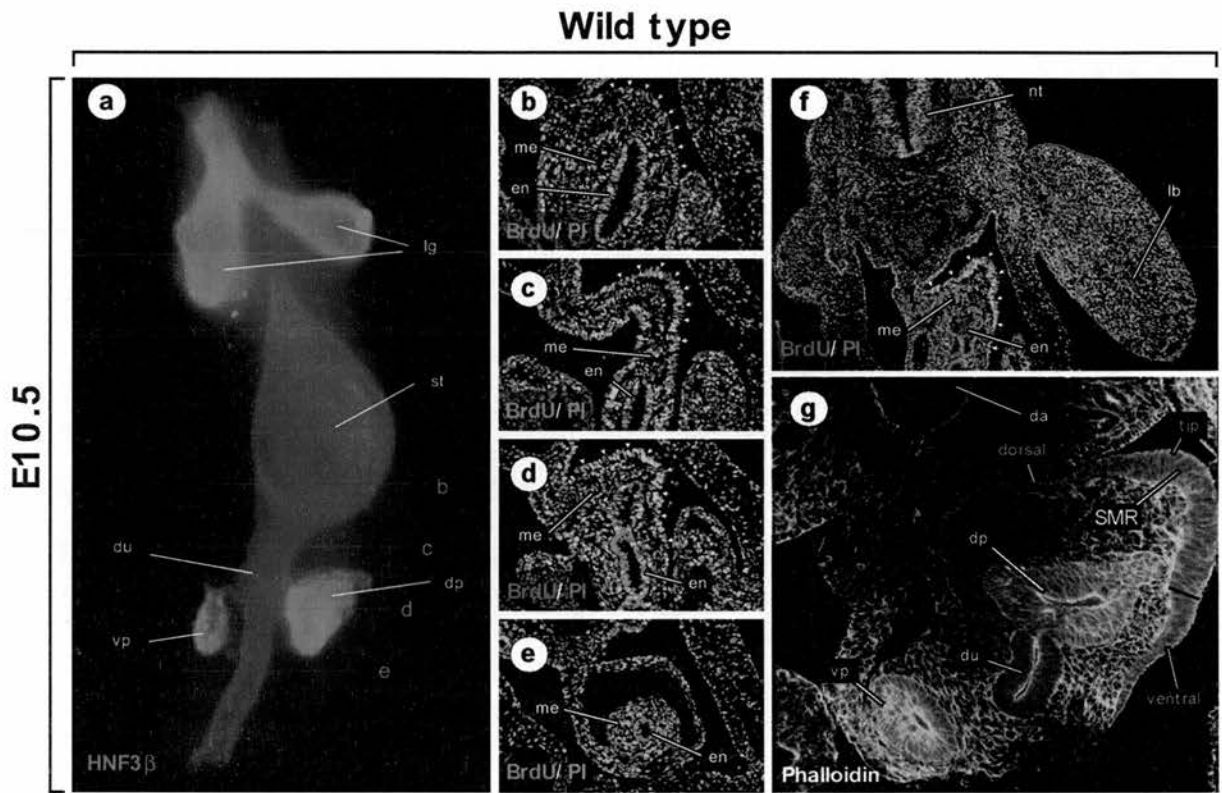


Figure 4.1: The Splanchnic Mesothelial Ridge (SMR) divides rapidly. (a) Endodermal localisation of HNF3 β protein (red) in a wild type embryo at E10.5. (b) Transverse section at the level of the stomach represented by line b in (a). At this level the SMR is relatively thin (white arrows). All nuclei are labelled with Propidium Iodide (PI; red) while only cells in S-phase are labelled with BrdU antibodies (green). The proportion of cells in S-phase is not dramatically different from the underlying mesenchyme. (c) Transverse section at the level of the duodenum represented by line c in (a). At this level the SMR is well defined (white arrows) and the proportion of cells in S-phase is significantly higher than in underlying mesenchyme. (d) Transverse section at the level of the pancreatic buds represented by line d in (a). At this level the SMR is thickest (white arrows) and the proportion of cells in S-phase is much higher than in underlying mesenchyme. (e) Transverse section just posterior of the pancreatic buds represented by line e in (a). At this level the SMR can no longer be detected. (f) Low magnification of a transverse section at the level of the pancreatic buds represented by line d in (a). Compared to other places in the developing embryo the SMR (white arrows) is dividing very rapidly. (g) Phalloidin staining of F-actin at E10.5. The SMR is clearly visible and can be divided into three regions dorsal, tip and ventral. (lg) lungs, (st) stomach, (du) duodenum, (vp) ventral pancreas, (dp) dorsal pancreas, (da) dorsal aorta, (nt) neural tube, (lb) limb bud, (me) mesoderm, (en) endoderm and (SMR) splanchnic mesothelial ridge.

BrdU labelling

Between E9.5 and E10.5 the spleno-pancreatic region undergoes a dramatic leftward expansion coinciding with the formation of the SMR. BrdU is incorporated into dividing cells and was therefore used to investigate if the rotation of the spleno-pancreatic region could be attributed to the SMR. Wild type E10.5 embryos were labelled with BrdU for 30 minutes and transverse sections through different regions of the gut (represented in figure 4.1a) were stained for BrdU uptake (figure 4.1b, c, d, e). The first section is taken through the stomach where the SMR is relatively thin (figure 4.1b). Between the stomach and the pancreas the SMR starts to thicken and here more cells have incorporated BrdU (figure 4.1c). At the level of the pancreas the SMR is still heavily labelled and it appears that the increased division rate is defined by the extend of the SMR (white arrows). Hence, the underlying mesoderm and the mesothelium adjacent to the SMR both have a lower BrdU uptake (figure 4.1d). Posterior to the pancreas the gut mesoderm is no longer flanked by the SMR and the BrdU uptake in the mesoderm is relatively normal (figure 4.1e).

The mitotic index for the SMR is high and between 73-86% of the cells have entered S-phase during the 30 minutes labelling period (table 4.1). This is higher than in the underlying mesenchyme where 57-60% of the cells has incorporated BrdU and the endoderm where approximately 27% of the cells have entered S-phase. In fact the mitotic index of the SMR is comparable to that of the progress zone in the limb and it represents one of the places with the highest BrdU uptake in the entire embryo (figure 4.1f; white arrows).

Structure	PI Labelled cells	BrdU labelled cells	Mitotic index
SMR (embryo 1)	86	63	73.2%
Mesoderm (embryo 1)	44	76	57.9%
SMR (embryo 2)	130	113	86.9%
Mesoderm (embryo 2)	161	91	56.5%
SMR (embryo 3)	126	97	77.0%
Mesoderm (embryo 3)	119	71	59.6%
Endoderm	88	33	27.3%
Progress Zone	143	405	73.9%

The number of labelled cells in the SMR and underlying mesenchyme is based on counts from the same section

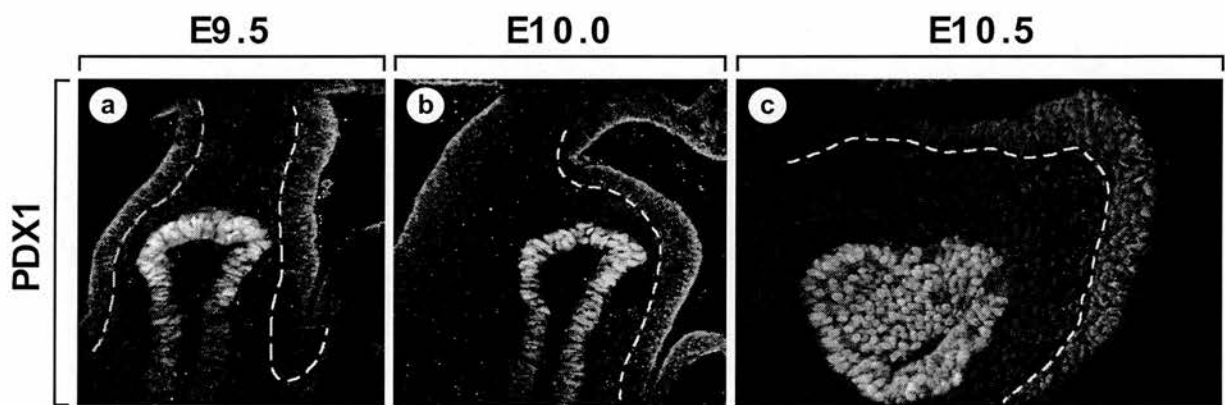


Figure 4.2: Development of the SMR. Immunohistochemistry showing PDX1 protein in the dorsal pancreatic bud at various stages during wild type development. **(a)** At E9.5 there are no obvious differences between left and right in the spleno-pancreatic region. A mesothelial layer can be detected on either side of the dorsal pancreas (dashed lines). **(b)** At E10.0 the dorsal pancreas is starting to grow towards the left. This coincide with a thickening of the left mesothelial layer and a disappearance of the right mesothelium. **(c)** At E10.5 the spleno-pancreatic region has achieved the characteristic triangular shape and the SMR is fully developed.

These results therefore strengthen the idea that the SMR is physically involved in the turning of the gut. Also, they suggest that the asymmetric expansion towards the left primarily is achieved through cell proliferation within the SMR rather than in the underlying mesenchyme.

Development of the SMR and the pancreas

It appears that the SMR has an important role in directing the growth of the spleno-pancreatic region. To investigate the relationship between the SMR and the developing pancreas, embryos were stained with antibodies against the homeobox protein PDX1. At E9.5 the dorsal pancreatic bud is positioned in alignment with the embryonic midline and between the left and right mesothelium (figure 4.2a). As the SMR thickens and the left side expands, the pancreatic endoderm also starts to grow towards the left. At E10.0 the dorsal pancreas remains in close proximity to the SMR (figure 4.2b). Half a day later at E10.5 the SMR is fully developed and has formed a characteristic triangle. The dorsal pancreas can be seen adjacent to the ventral part of the SMR and growing towards the tip (figure 4.2c). Thus the proliferation of the SMR results in a triangular shaped structure in which the dorsal pancreas grows. As the region expands the dorsal pancreatic endoderm grows in close proximity to the ventral part of the SMR as if attracted to it.

The SMR is absent in *Dh*

The SMR is absent in mice carrying the *Dh* mutation and it was this phenotype which initially led to the identification of the SMR. The effect *Dh* has on gut development was initially described by (Green, 1967) who showed that the mesothelium surrounding the splanchnic mesoderm was absent in *Dh* mice at E9.5. To confirm these results E9.5 *Dh* embryos were double stained for the proteins PDX1 and ISL1. Both genes have been shown to have an important role in pancreas development (Ohlsson et al., 1993; Jonsson et al., 1994; Ahlgren et al., 1996; Ahlgren et al., 1997). At E9.5 *Isl1* (green) is expressed in the dorsal mesenchyme and mesothelium while *Pdx1* (red) is expressed in the pancreatic endoderm (figure 4.3a). Both proteins localise to the nuclei and the mesothelial layers on either side can easily be distinguished from the underlying mesenchyme because the ISL1 positive nuclei are aligned. The developing SMR is outlined between the dashed blue and white lines. In *Dh/+* and *Dh/Dh* embryos there is no outer layer of aligned nuclei indicating that the mesothelial layers on both sides are absent in mutant embryos (figure 4.3b, c). The lack of mesothelial ridges is consistent in both *Dh/+* and *Dh/Dh* embryos.

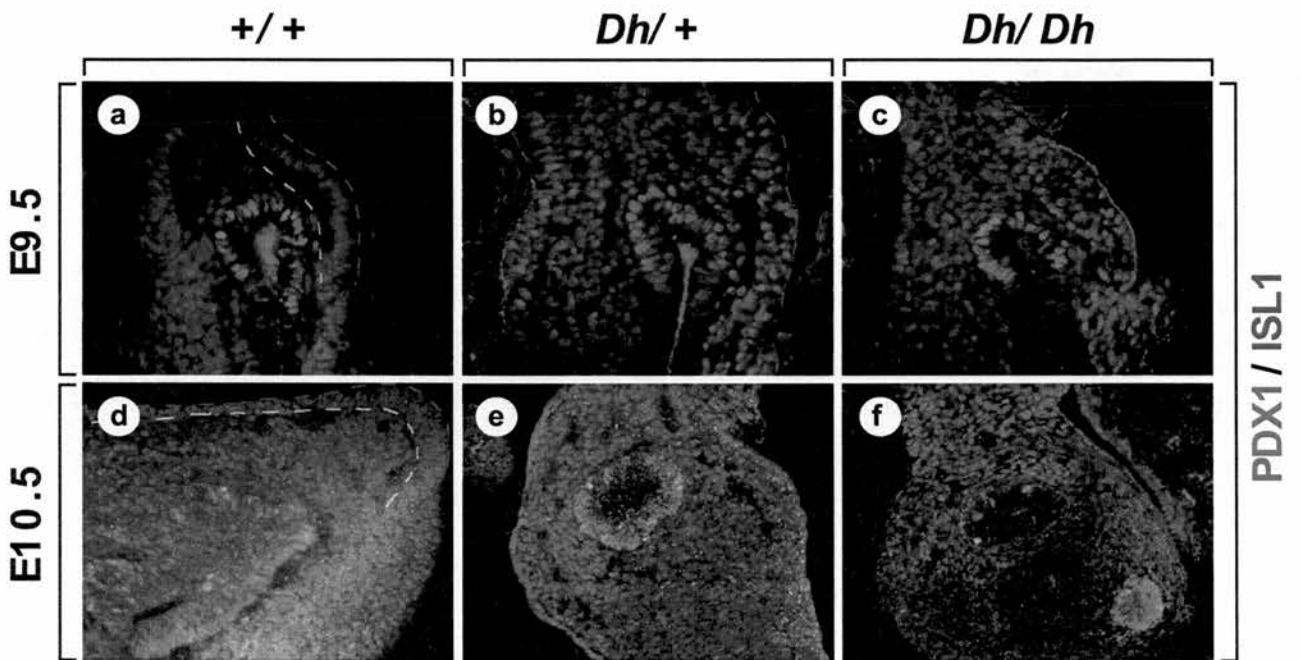


Figure 4.3: Abnormal growth in absence of the SMR. Immunohistochemistry showing the presence of ISL1 protein (green) and PDX1 protein (red). **(a)** In *+/+* embryos the dorsal pancreatic endoderm is positioned in the middle of the spleno-pancreatic region at E9.5. The developing SMR can easily be distinguished because the nuclei are aligned. The outside of the SMR is marked by a blue dashed line and the inside by a white dashed line. **(b)** In *Dh/+* the pancreatic endoderm is positioned in the middle of the spleno-pancreatic region at E9.5, but the SMR is absent (only a blue dashed line). **(c)** In *Dh/Dh* the pancreatic endoderm is positioned in the middle of the spleno-pancreatic region at E9.5, but the SMR is absent (only a blue dashed line). **(d)** At E10.5 in *+/+* embryos the SMR has thickened (dashed lines) and the dorsal pancreatic endoderm is growing towards the left. **(e)** In *Dh/+* the SMR is absent (blue dashed line) and the pancreatic endoderm remains in the middle of the spleno-pancreatic region. **(f)** In *Dh/Dh* the SMR is absent (blue dashed line) and the pancreatic endoderm remains in the middle of the spleno-pancreatic region.

In wild type embryos the SMR develops from the left mesothelial plate and at E10.5 it consists of a thickened layer of mesothelium on the left side of the spleno-pancreatic region (figure 4.3d). The dorsal pancreas (red) develops in close proximity to the ventral part of the SMR. In *Dh* embryos the mesothelium layers that flank the splanchnic mesoderm are absent and as a result the SMR does not develop (figure 4.3e, f). In the absence of the SMR there is no leftward expansion and the spleno-pancreatic region remains symmetrical. Also the dorsal pancreas, which in wild type grows towards the tip of the SMR, lacks directional growth and remains in the middle of the splanchnic mesoderm.

4.3 The mesenchyme surrounding the pancreas is compartmentalised

Left-right markers are expressed in the mesothelium before the SMR thickens

At E9.5 there are no morphological differences between the left and right side of the gut. The dorsal-ventral axis of the endoderm is aligned along the midline of the developing embryo and the flanking mesothelia is equally thick on both sides. It was therefore of interest to investigate if asymmetric gene expression specific to the left mesothelium precedes the morphological differences.

In situ hybridisation with *Pitx2* was carried out on E9.5 embryos (figure 4.4a). At the level of the dorsal pancreatic bud *Pitx2* expression could be detected in the left mesothelium that will become the SMR and at lower levels in the underlying mesenchyme. Another homeobox gene *Barx1* is also expressed in an asymmetric manner (figure 4.4b). *Barx1* is expressed throughout the mesenchyme of stomach (Tissier-Seta et al., 1995), and has not previously been implicated in left-right asymmetry. The asymmetric expression of *Barx1* is specific for the region around the pancreas and more anteriorly the gene is expressed in the mesenchyme and mesothelium on both sides of the endoderm (data not shown). Thus the asymmetric expression of *Barx1* correlates to the part of the mesothelium that will form the thickest part of the SMR. At E10.5 when the SMR has formed, *Barx1* expression remains high in the tip and ventral part of the SMR (figure 4.4e). There is also high expression of *Barx1* in the underlying mesoderm.

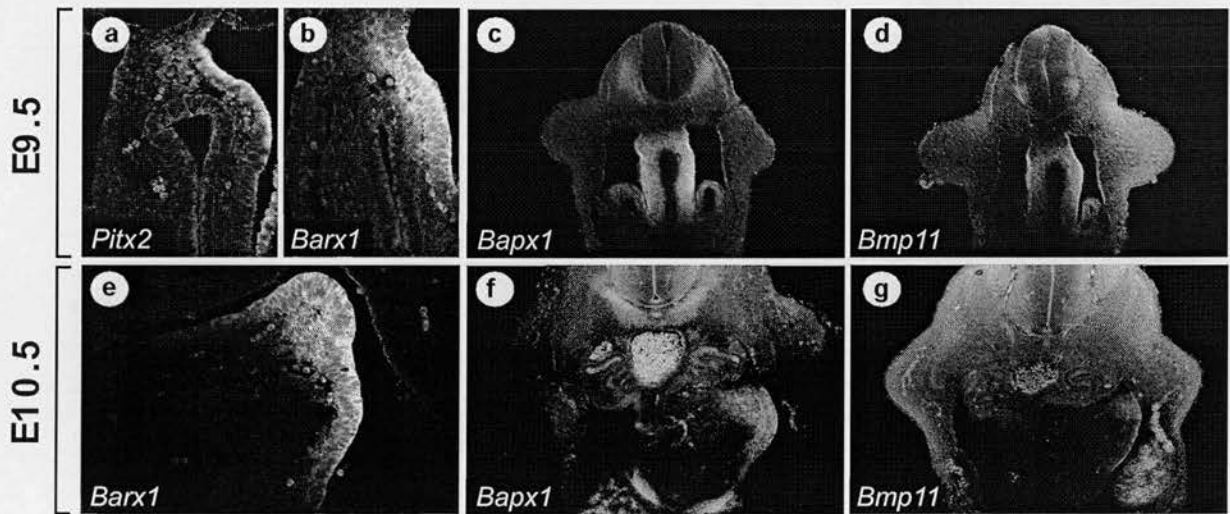


Figure 4.4: Asymmetric gene expression in the spleno-pancreatic region. *In situ* hybridisation showing gene expression in the developing spleno-pancreatic region. (a) At E9.5 *Pitx2* is expressed asymmetrically in the developing SMR and underlying mesenchyme. (b) At E9.5 *Barx1* is expressed asymmetrically in the developing SMR and underlying mesenchyme. (c) At E9.5 *Bapx1* is expressed symmetrically on both sides of the pancreatic endoderm. (d) At E9.5 *Bmp11* is expressed symmetrically on both sides of the pancreatic endoderm. (e) At E10.5 *Barx1* is expressed at high levels in the tip and ventral part of the SMR. (f) At E10.5 *Bapx1* is expressed asymmetrically on the left side in the SMR and in the underlying mesenchyme. (g) At E10.5 *Bmp11* is expressed asymmetrically on the left side in the SMR and in the underlying mesenchyme.

In contrast to setting up asymmetry, other genes seem to respond to the formation of the SMR in that they show symmetric expression at E9.5 and subsequently become restricted to the left side. Both *Bapx1* and *Bmp11* are expressed in the mesothelium and mesoderm on both sides of the pancreatic endoderm at E9.5 (figure 4.4c, d). An expression pattern identical to that reported for *Isl1* (REF). However, at E10.5 the expression of both genes has been switched off on the right side while expression is maintained in the SMR and underlying mesoderm (figure 4.4f, g). Whereas *Bapx1* has been suggested to have a role in left-right patterning and gut development, *Bmp11* has not previously been implicated in either.

Early Spleen development

The embryonic origin of the spleen is more obscure than that of the pancreas, it therefore remained a possibility that the SMR represented the earliest stages of spleen development. *In situ* hybridisation was therefore carried out to visualise the expression pattern of genes that are known to have a role during spleen development. The homeobox gene *Hox11* is the only reported gene that is expressed exclusively in the spleen (Roberts et al., 1994; Dear et al., 1995) and is a good marker for spleen precursor cells. At E10.5 *Hox11* expression is restricted to the mesenchymal cells directly under the dorsal part of the SMR and no transcripts could be detected in the mesenchyme adjacent to the dorsal pancreas (figure 4.5a). However this expression pattern is transient and at later stages *Hox11* expression could be observed throughout the mesenchyme between the dorsal SMR and pancreatic endoderm (data not shown). Thus it appears that the initial induction of *Hox11* expression is closely associated with the SMR. At no stage was *Hox11* expression detected in the SMR itself or in the mesenchyme under the tip of the SMR.

Nkx2.5 has not previously been reported to have a role in spleen development in the mouse, but studies in *Xenopus* have shown that *Nkx2.5* is a very early marker of spleen precursor cells (Patterson et al., 2000). At E10.5 the initial expression of *Nkx2.5* is restricted to the mesenchymal cells directly under the dorsal SMR (figure 4.5b) and is therefore very similar to that of *Hox11*, a strong indication that the spleen specific expression of *Nkx2.5* is conserved between frogs and mice. However, in addition *Nkx2.5* is also expressed in the ventral region left of the dorsal pancreas. The two expression domains are separated by a stripe of non-expressing mesenchymal cells.

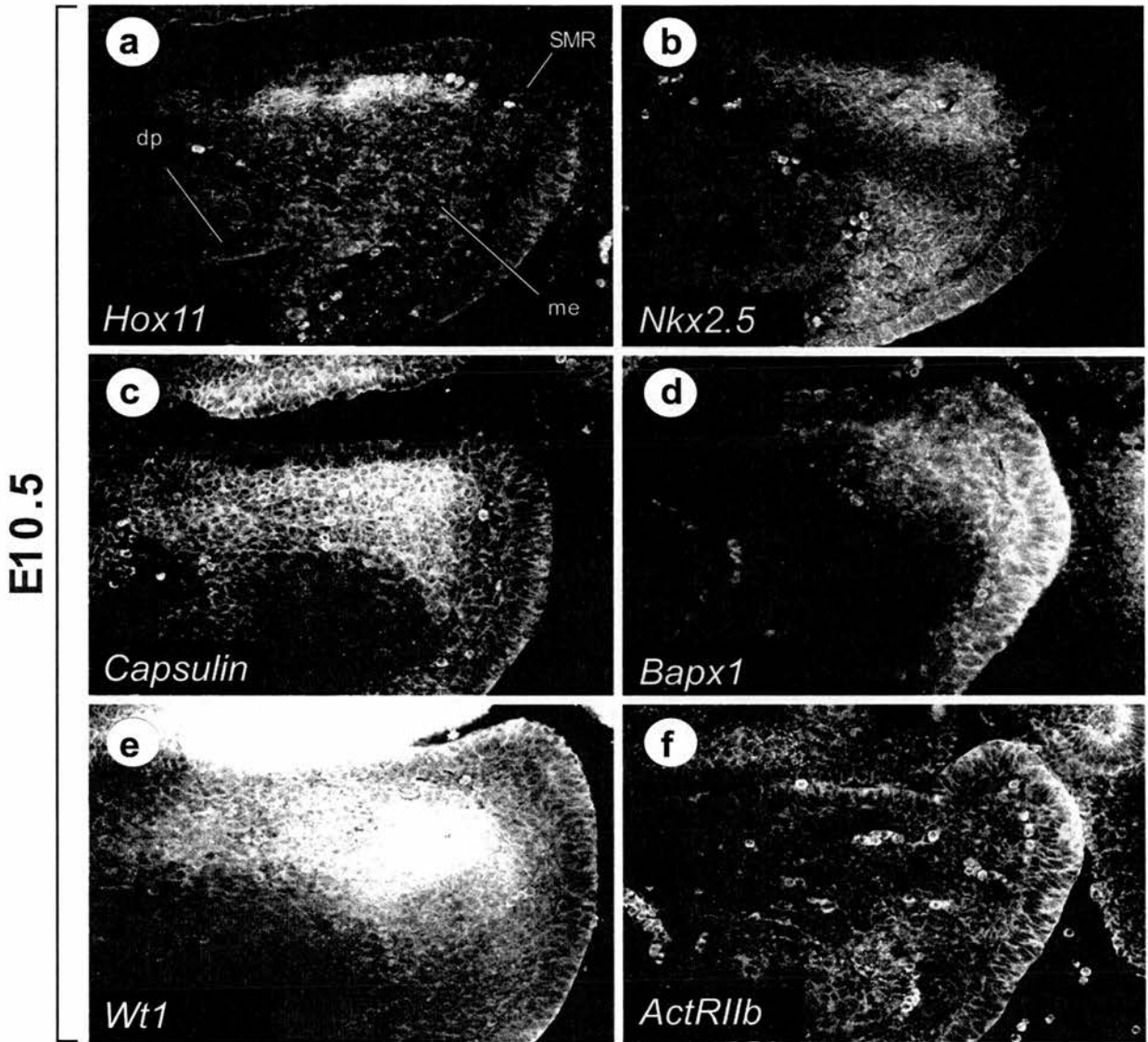


Figure 4.5: The spleen is induced directly under the SMR. *In situ* hybridisation showing gene expression of spleen specific markers in the spleno-pancreatic region at E10.5. (a) *Hox11* expression can first be detected in the mesenchyme directly under the dorsal part of the SMR. (b) *Nkx2.5* expression can first be detected in the mesenchyme directly under the dorsal part of the SMR and in an additional domain in the ventral part of the SMR and underlying mesenchyme. (c) *Capsulin* expression can be detected in the mesenchyme between the dorsal part of the SMR and the pancreatic endoderm. (d) *Bapx1* expression can be detected in the tip and ventral half of the SMR and in the underlying mesenchyme. (e) At E10.75 *Wt1* expression can be detected in the mesenchyme between the dorsal part of the SMR and the pancreatic endoderm. (f) It is possible that *ActR11b* is expressed in the tip of the SMR at E10.5 but the expression levels are low. (SMR) splanchnic mesothelial ridge, (dp) dorsal pancreatic endoderm and (me) mesoderm.

However, the second expression domain never overlaps with the *Hox11* expression domain and is therefore unlikely to exclusively mark spleen precursor cells. At later stages *Nkx2.5* expression becomes more widespread and transcripts can be detected throughout the mesenchyme between the dorsal SMR and the pancreatic mesoderm (data not shown), but expression is always excluded from the dorsal mesothelium and from the mesenchyme under the tip of the SMR.

Capsulin, is also expressed in the mesenchyme under the dorsal SMR (figure 4.5c) and although the expression levels appear to be higher directly under the dorsal SMR, the expression is never restricted to the mesenchymal cells under the ridge as *Hox11* and *Nkx2.5*. *Capsulin* expression can also be detected in the mesenchyme prior to E10.5, thus preceding the expression of *Hox11* and *Nkx2.5* in the spleen precursor cells (data not shown). At later stages an additional expression domain appears left of the dorsal pancreas and in the ventral most part of the SMR (figure 3.10d). This second domain is similar to that observed for *Nkx2.5* and is presumably not reflecting spleen precursor cells. As for the previous two genes the spleen specific expression of *Capsulin* is always excluded from the dorsal SMR and from the mesenchyme directly under the tip of the SMR.

Bapx1 is also expressed in the splenic mesenchyme (figure 4.5d). However, the expression domain is less specific than that of *Hox11*, *Capsulin* and *Nkx2.5*. In addition to the spleen precursor cells *Bapx1* is also expressed in all mesenchymal cells dorsal and left of the pancreatic endoderm. However, the expression of *Bapx1* is very dynamic. At E9.5 the gene is expressed in both mesoderm and mesothelium on either side of the endoderm (figure 3.4c). As the SMR thickens and the spleno-pancreatic region grows towards the left *Bapx1* is turned off on the right side while maintained on the left side in the SMR and the underlying mesenchyme. At E10.25 *Bapx1* is expressed throughout the SMR and in the mesenchyme surrounding the pancreatic endoderm on the left side (data not shown). Slightly later in development at E10.5 (figure 3.5d), expression is also down-regulated in the dorsal part of the SMR. Thus it appears that *Bapx1* expression gradually becomes more left sided as the spleno-pancreatic region develops.

Wt1 is also expressed at high levels in the spleen precursor cells (figure 4.5e), albeit slightly later during spleen development compared to the other splenic markers. The embryo in figure 4.5e is older than the other embryos (E10.75), because of difficulties in detecting *Wt1* expression in the splenic mesenchyme at E10.5 (data not shown). *Wt1* is also expressed at low levels in the dorsal part of the ridge, although the signal is obscured by the very strong staining in the gonadal ridge and mesonephros lying dorsal to the SMR.

ActRIIb has also been reported to have a role in spleen development. However, no expression could be detected in the splenic mesenchyme at E10.5 (figure 4.5f). It is possible that the gene is expressed weakly in the tip of the SMR, but the levels of expression are not conclusive.

These results confirm that spleen develops from the mesenchyme lying between the dorsal pancreatic endoderm and the dorsal part of the SMR. Thus the SMR must represent a novel anatomical structure which is distinct from the spleen. All the genes examined are expressed throughout the dorsal mesenchyme suggesting that a spleen-inducing signal, if it exists, would emanate either from the dorsal SMR or from the pancreatic endoderm. However, in mice lacking the *Pdx1* or *Hlxb9* genes the dorsal pancreas fails to bud and in absence of pancreatic endoderm the spleen develops normally (Jonsson et al., 1994; Ahlgren et al., 1996; Offield et al., 1996; Li et al., 1999). Also the initial expression of *Hox11* and *Nkx2.5* localises to the mesenchyme directly under the SMR rather than to the pancreatic mesenchyme. These results therefore suggest that the spleen is induced in the mesenchymal cells under the SMR, perhaps by a signal from the SMR, and later spreads to the entire mesenchyme between the pancreas and the dorsal SMR. It is also evident that *Hox11* and *Nkx2.5* are the most specific markers of the initial stages of spleen development, because *Bapx1*, *Capsulin* and *Wt1* are never restricted to the cells directly under the ridge. Nevertheless, the expression of *Bapx1* and *Capsulin* precedes that of *Hox11* and *Nkx2.5* suggesting that the two genes are required for defining the identity of the dorsal mesenchyme.

Common for all the genes expressed in the spleen precursor cells, except *Bapx1*, is that they are not expressed in the mesenchyme directly under the tip of the SMR. Interestingly, several other genes such as *Barx1* and *Bmp11* display the opposite expression pattern in that they are expressed in the mesenchyme at the tip, but excluded from the splenic mesenchyme (figure 2e and 3j). In most cases these boundaries are well defined and because they are reflected by several different genes it suggests that the mesenchyme is regionalised. Hence, at E10.5 the mesenchyme under the tip of the SMR is distinct from the splenic mesenchyme.

The spleen is not induced in *Dh*

Hox11 and *Nkx2.5* are specific markers of spleen precursor cells and the close association between their expression and the dorsal SMR, suggests that the mesothelium might have a role in induction and maintenance of spleen determining genes in the underlying mesenchyme.

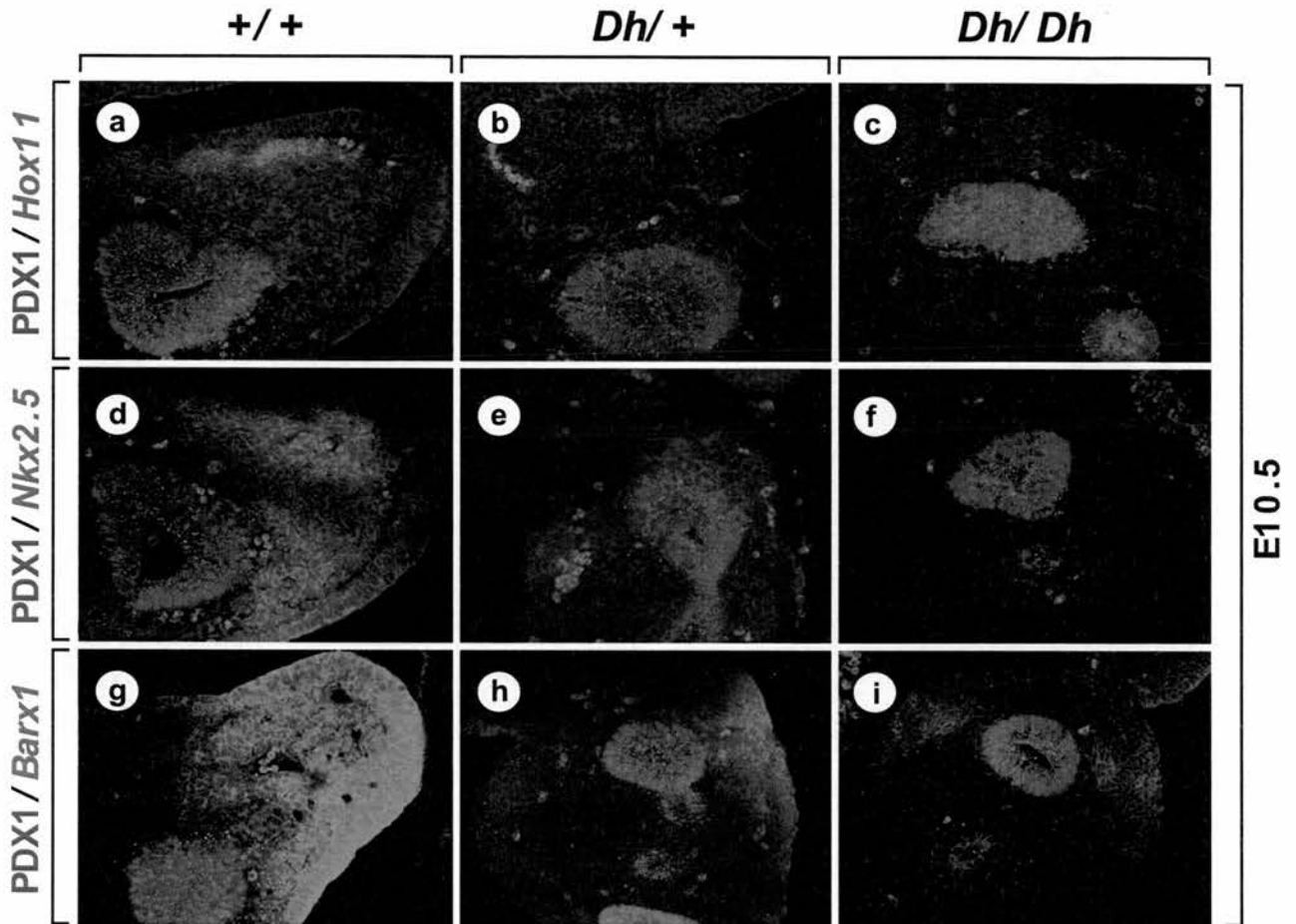


Figure 4.6: The spleen is not induced in *Dh* embryos. Immunohistochemistry showing the presence of PDX1 protein in the pancreatic endoderm (green) and *in situ* hybridisation showing gene expression of spleen markers at E10.5. (a) In +/+ embryos *Hox11* expression (red) is induced in the mesenchyme directly under the SMR. In *Dh/+* (b) and *Dh/Dh* (c) no *Hox11* expression can be detected in the mesenchyme. (d) In +/+ embryos *Nkx2.5* expression (red) is induced in the mesenchyme directly under the SMR and in the ventral part of the SMR. In *Dh/+* (e) and *Dh/Dh* (f) no *Nkx2.5* expression can be detected in the mesenchyme. (g) In +/+ embryos *Barx1* expression (red) at high levels in the SMR and in the underlying mesenchyme. (h) In *Dh/+* embryos *Barx1* expression can be detected in the mesenchyme on the left side. (i) In *Dh/Dh* embryos *Barx1* expression can be detected in the mesenchyme on both sides of the pancreatic endoderm.

In mice carrying the *Dh* mutation the spleen fails to develop, but it is not known at what stage spleen development is arrested. One possibility is that the spleen is never induced. To test this *Dh* embryos were examined for *Hox11* expression. In E10.5 wild type embryos *Hox11* expression (red) could be detected in the splenic mesenchyme directly under the dorsal SMR (figure 4.6a). The endoderm of the dorsal pancreas has been stained with antibodies against PDX1 (green). In both *Dh/+* and *Dh/Dh* embryos no *Hox11* expression could be detected at E10.5 (figure 4.6b, c). The red cells visible in the sections are embryonic blood cells that auto-fluoresce.

We also examined the expression of *Nkx2.5*, which is also expressed in the splenic mesenchyme. Similar to the results obtained with *Hox11* the spleen specific expression of *Nkx2.5* could not be detected in *Dh* embryos at E10.5 (figure 4.6e, f). Thus the two genes marking spleen precursor cells fail to be induced in *Dh* embryos, confirming that this cell type is absent in *Dh* embryos and subsequently results in the asplenic phenotype. However, the ventral expression domain of *Nkx2.5* is also absent in *Dh*, suggesting that the effects of the mutation are not specifically affecting the spleen precursor cells. Because the gene affected by the *Dh* mutation is unknown it cannot be ruled out that *Dh* is affecting the mesoderm as well as the SMR. The lack of spleen precursor cells could also occur if the identity of the mesenchyme has been altered.

To test if the identity of the underlying mesenchyme is preserved in *Dh*, E10.5 embryos were hybridised with *Barx1* (red) and PDX1 (green). In wild type embryos *Barx1* is expressed at high levels in the tip and ventral SMR and in the underlying mesenchyme (figure 4.6h). In *Dh/+* embryos *Barx1* expression can be detected in the mesenchyme left of the dorsal pancreas (figure 4.6i). It is obvious that the number of *Barx1* expressing cells is reduced in *Dh/+* embryos. However, because most of the *Barx1* expressing cells normally are located in the SMR the number must be expected to be lower than in wild type because the ridge is absent in *Dh* embryos.

Similar expression was also detected in *Dh/Dh* embryos although the expression levels were lower than in heterozygous embryos (figure 4.6j). However, in addition to the expression on the left side *Barx1* is also expressed ectopically, as mirror image, on the right side of the spleno-pancreatic region. This duplication of *Barx1* expression suggests that asymmetry is lost in *Dh/Dh* embryos (this will be described in more detail below).

The SMR in other asplenic mutants

At E9.5 the *Bapx1* gene is expressed in the mesothelial layers and in the splanchnic mesoderm (figure 4.4c), but later expression becomes restricted to the SMR and underlying mesoderm (figure 4.5d). To investigate if the gene has a role during the development of the SMR embryos homozygous for deletions in *Bapx1* were examined. At E9.5 no morphological distinction can be found when comparing *Bapx1*^{-/-} to *Bapx1*^{+/+} embryos (data not shown). However, during subsequent development the SMR fails to thicken and at E10.5 the mesothelial layer surrounding the left side of the spleno-pancreatic region consists of a single cell layer (figure 4.7b). The region is still growing towards the left side (figure 4.7d), but the expansion does not result in the characteristic triangular shape observed in wild type embryos, suggesting that the leftward expansion in *Bapx1*^{-/-} embryos lacks the directional growth provided by the SMR (figure 4.7a, c). Also the dorsal pancreas remains in the middle of the embryo indicating that the ridge or *Bapx1* function in the mesoderm is required for directional growth of the dorsal pancreatic endoderm. Later in development mice carrying homozygous deletions in the *Bapx1* gene display gastroduodenal malformations (data not shown; Akazawa et al., 2000). These abnormalities are very similar to those observed in *Dh* embryos and suggest that asymmetric growth of the spleno-pancreatic region is required for correct looping of the gut.

Mice carrying homozygous deletions in the zinc finger gene *Wt1* are partially asplenic with the severity depending on the genetic background (Herzer et al., 1999; Koehler et al., 2000). However, in contrast to *Dh* and *Bapx1*^{-/-} mice, they do not display any gastroduodenal abnormalities. To investigate the morphology of the SMR, *Wt1*^{-/-} mice were analysed for *Capsulin* expression and the presence or absence of WT1 protein. In E10.5 wild type mice, WT1 protein (green) can be detected in the gonadal ridge and mesonephros lying dorsal to the spleno-pancreatic region and *Capsulin* expression (red) was detected in the mesoderm surrounding the dorsal pancreas (figure 4.7e). No WT1 protein could be detected in the splenic mesoderm at this stage supporting the observation that spleen specific expression of *Wt1* is activated at later stages in spleen development. In *Wt1*^{-/-} embryos no WT1 protein could be detected anywhere in the embryo (figure 4.7f). Nevertheless, the mesothelium has thickened as in wild type embryos and morphologically the SMR appears to be normal. Also the dorsal pancreas is growing directly adjacent to the ventral part of the SMR. So despite the phenotypic similarities to *Dh* and *Bapx1*, concerning spleen development, *Wt1* does not affect the SMR or the asymmetric growth of the spleno-pancreatic region.

E10.5

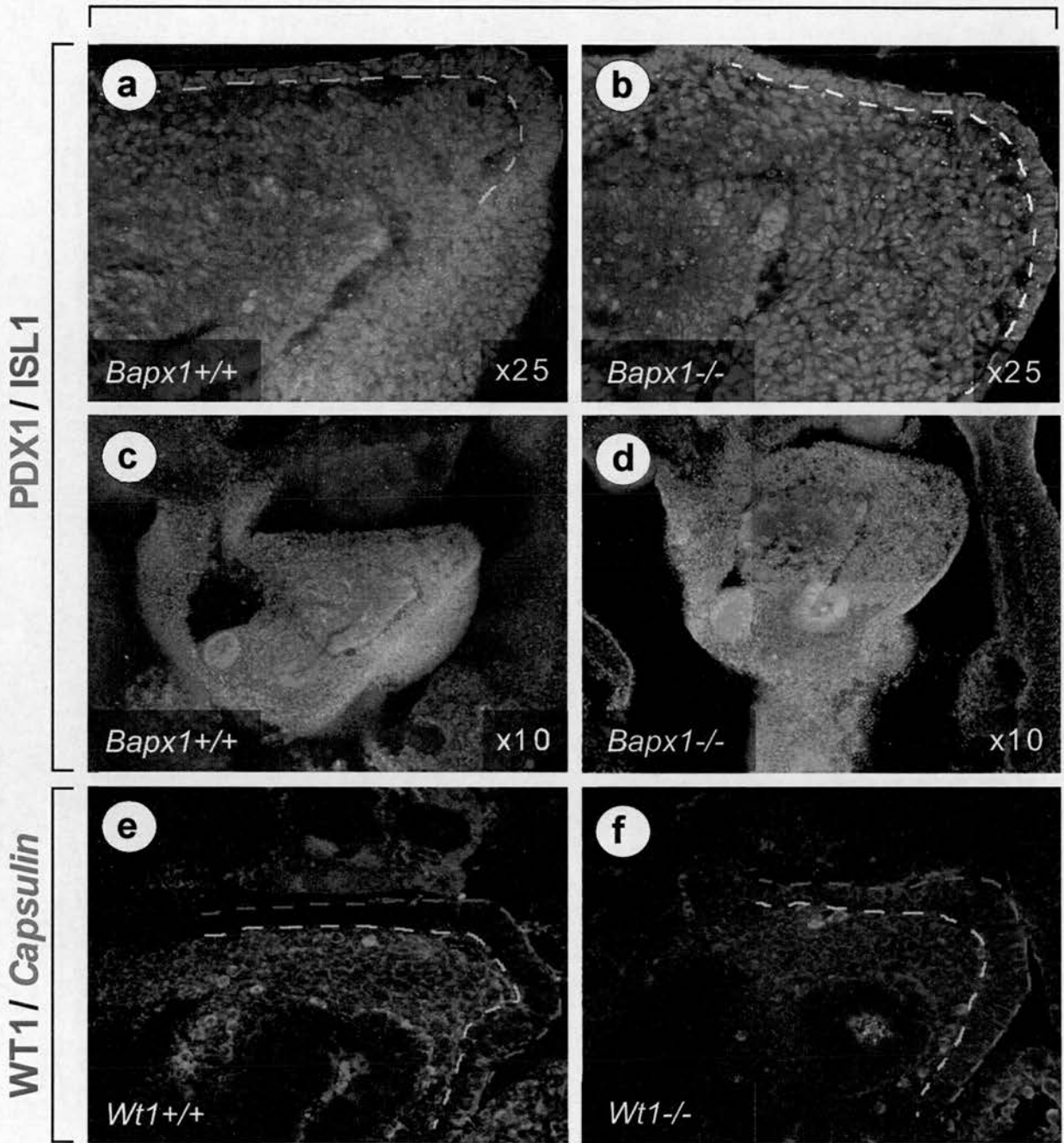


Figure 4.7: Spleno-pancreatic growth in other asplenic mutants. Immunohistochemistry showing the presence of ISL1 protein (green) and PDX1 protein (red). (a) At E10.5 in *Bapx1*^{+/+} embryos the SMR can be seen as a thickened layer of mesothelium (blue and white dashed lines) and the dorsal pancreatic endoderm is growing towards the left. (b) At E10.5 in *Bapx1*^{-/-} the SMR is present (blue and white dashed lines) but it fails to thicken and the dorsal pancreatic endoderm remains in the middle. (c) Low magnification of the spleno-pancreatic region showing the dorsal pancreatic endoderm growing towards the left in *Bapx1*^{+/+} embryos. (d) Low magnification of the spleno-pancreatic region showing the dorsal pancreatic endoderm remaining at the midline in *Bapx1*^{-/-} embryos. (e) A E10.5 *Wt1*^{+/+} embryo stained for WT1 protein and *Capsulin* RNA. The SMR can be seen as a thickened layer of mesothelium (blue and white dashed lines) and the dorsal pancreatic endoderm is growing towards the left. (f) A E10.5 *Wt1*^{-/-} embryo stained for WT1 protein and *Capsulin* RNA. The SMR appears normal (blue and white dashed lines) and the dorsal pancreatic endoderm is growing towards the left.

4.4 Screening for novel genes in the SMR

Multiplex PCR

From the studies described above it is tempting to suggest that the SMR acts as a signalling centre directing growth of the spleno-pancreatic region. However, a gene expressed specifically in the SMR would demonstrate uniqueness of the mesothelium and further strengthen this hypothesis.

Table 4.2: Alphabetic list of genes tested with MPX-PCR.

<i>ActR1</i>	<i>Cerberus</i>	<i>FgfR1a</i>	<i>Hlxb9</i>	<i>Prcd</i>
<i>ActR1la</i>	<i>Chordin</i>	<i>FgfR1b</i>	<i>Hnf3 beta</i>	<i>Prox1</i>
<i>ActR1lb</i>	<i>ChymoTrypsin</i>	<i>FgfR2</i>	<i>Hnf6</i>	<i>Shh</i>
<i>Alk1</i>	<i>Dan</i>	<i>FgfR3</i>	<i>Ihh</i>	<i>Somatotatin</i>
<i>Alk3</i>	<i>Dhh</i>	<i>FgfR4</i>	<i>Inha</i>	<i>TgfB1</i>
<i>Alk4</i>	<i>Fgf1</i>	<i>Fkh6</i>	<i>Inhba</i>	<i>TgfB2</i>
<i>Alk5</i>	<i>Fgf2</i>	<i>Folli-like</i>	<i>Inhbb</i>	<i>TgfB3</i>
<i>Alk6</i>	<i>Fgf3</i>	<i>Folli-rel</i>	<i>Inhbc</i>	<i>TgfB4</i>
<i>Amylase</i>	<i>Fgf4</i>	<i>Follistatin</i>	<i>Inhbe</i>	<i>TgfBR11</i>
<i>Bapx1</i>	<i>Fgf5</i>	<i>Gata4</i>	<i>Insulin</i>	<i>Trypsin</i>
<i>Barx1</i>	<i>Fgf6</i>	<i>Gdf1</i>	<i>Isl1</i>	<i>Wnt11</i>
<i>Bmp2</i>	<i>Fgf7</i>	<i>Gdf3</i>	<i>Isl2</i>	<i>Wnt15</i>
<i>Bmp3b</i>	<i>Fgf8</i>	<i>Gdf5</i>	<i>Jagged1</i>	<i>Wnt16</i>
<i>Bmp4</i>	<i>Fgf9</i>	<i>Gdf6</i>	<i>Jagged2</i>	<i>Wnt2b</i>
<i>Bmp5</i>	<i>Fgf10</i>	<i>Gdf7</i>	<i>Ngn3</i>	<i>Wnt4</i>
<i>Bmp6</i>	<i>Fgf11</i>	<i>Gdf8</i>	<i>Nkx2.2</i>	<i>Wnt5a</i>
<i>Bmp7</i>	<i>Fgf12a</i>	<i>Gdf9</i>	<i>Nkx2.3</i>	<i>Wnt5b</i>
<i>Bmp8a</i>	<i>Fgf12b</i>	<i>Gli1</i>	<i>Nkx2.6</i>	
<i>Bmp8b</i>	<i>Fgf13</i>	<i>Gli2</i>	<i>Nkx6.1</i>	
<i>BmpR11</i>	<i>Fgf14a</i>	<i>Gli3</i>	<i>Noggin</i>	
<i>Bmp10</i>	<i>Fgf14b</i>	<i>Glucagon</i>	<i>Patched1</i>	
<i>Bmp11</i>	<i>Fgf16</i>	<i>Gremlin</i>	<i>Patched2</i>	
<i>Bmp15</i>	<i>Fgf17</i>	<i>Hes1</i>	<i>Pax6</i>	
<i>Cdx2</i>	<i>Fgf18</i>	<i>Hex</i>	<i>Pdx1</i>	

- Positive result (the PCR reaction produced a band at the expected size)
- Negative result (the gene is not expressed or the PCR reaction did not work)

In an attempt to find such a gene, a collaboration was set up with Dr. Jan Jensen at the Hagedorn Research Institute in Denmark. Multiplex-PCR (MPX-PCR) was used to compare the expression levels of a large number of genes in *Dh* and wild type. A gene expressed exclusively in the SMR would give a positive result in wild type and a negative result in *Dh* because the ridge is absent in all mutant embryos. All genes tested are listed in table 4.2.

Table 4.3: Relationship between gel names and genes tested.

Gel Name	Int. Control	Gene assayed (product size)				
✓ Heck01	A ✓ Tubulin (250) B ✓ Tubulin (250) C ✓ TBP (190) D ✓ G6PDH (214)	<i>Insulin</i> (312) <i>Amylase</i> (300) <i>Pdx1</i> (224) <i>Nkx2.2</i> (190)	<i>Glucagon</i> (161) <i>Ch.Trypsin</i> (210) <i>Nkx6.1</i> (284) <i>Nkx2.3</i> (240)	<i>Somatostatin</i> (232) <i>Trypsin</i> (310) <i>Barx1</i> (170) <i>Prox1</i> (250)	<i>Pax8</i> (298,340) <i>Cdx2</i> (160)	
✓ Heck02	A ✓ TBP (190) B ✓ TBP (190) C ✓ TBP (190) D ✓ G6PDH (214)	<i>Isl2</i> (272) <i>Bmp2</i> (150) <i>Fkh6</i> (200) <i>Hnf3 beta</i> (200)	<i>Ngn3</i> (160) <i>Bmp4</i> (210) <i>Gata4</i> (180) <i>Gli1</i> (300)	<i>Hnf6</i> (240) <i>Bmp7</i> (160) <i>Jagged1</i> (270) <i>Gli3</i> (290)	<i>Isl1</i> (255) <i>Noggin</i> (180) <i>Wnt4</i> (240) <i>Jagged2</i> (200)	<i>Hes1</i> (270)
✓ Heck03	A ✓ G6PDH (214) B ✓ TBP (190) C ✓ TBP (190) D ✓ TBP (190)	<i>Inhba</i> (230) <i>Fgf4</i> (160) <i>Fgf5</i> (230) <i>Fgf3</i> (250)	<i>Inhbb</i> (260) <i>Fgf9</i> (230) <i>Fgf12b</i> (160) <i>Fgf14a</i> (200)	<i>Inhbc</i> (170) <i>Fgf7</i> (200) <i>Fgf1</i> (300) <i>Fgf16</i> (170)	<i>Inhbe</i> (200) <i>Fgf18</i> (300) <i>Fgf17</i> (260) <i>Fgf2</i> (150)	<i>Inha</i> (190)
✓ Heck04	A ✓ G6PDH (214) B ✓ TBP (190) C ✓ TBP (190) D ✓ G6PDH (214)	<i>Fgf10</i> (190) <i>Fgf14b</i> (180) <i>FgfR1a</i> (290) <i>FgfR3</i> (176,230)	<i>Fgf6</i> (250) <i>Fgf13</i> (250) <i>FgfR1b</i> (150) <i>FgfR4</i> (190)	<i>Fgf11</i> (150) <i>Fgf8</i> (158,191,350) <i>FgfR2</i> (165)	<i>Fgf12a</i> (200)	
✓ Heck05	A ✓ TBP (190) B ✓ G6PDH (214) C ✓ TBP (190) D ✓ TBP (190)	<i>Bmp2</i> (150) <i>Bmp7</i> (160) <i>Gdf3</i> (180) <i>Gdf9</i> (230)	<i>Bmp4</i> (210) <i>Gdf7</i> (190) <i>Bmp15</i> (150) <i>Gdf6</i> (240)	<i>Bmp10</i> (160) <i>Bmp3b</i> (290) <i>Bmp11</i> (160) <i>Bmp6</i> (250)	<i>Bmp8b</i> (270) <i>Gdf8</i> (240) <i>Bmp5</i> (200) <i>Gdf1</i> (220)	
✓ Heck06	A × Tubulin (250)	<i>Insulin</i> (312)	<i>Somatostatin</i> (232)	<i>Glucagon</i> (161)	<i>Amylase</i> (300)	<i>Ch.Trypsin</i> (210)
✓ Heck07	A ✓ G6PDH (214) B ✓ G6PDH (214) C × G6PDH (214)	<i>TgfB1</i> (200) <i>Alk1</i> (200) <i>Follistatin</i> (180)	<i>TgfB2</i> (160) <i>Alk4</i> (280) <i>Folli-like</i> (240)	<i>TgfB3</i> (280) <i>Alk5</i> (180) <i>Folli-rel</i> (290)	<i>TgfB4</i> (250) <i>Alk3</i> (270) <i>Cerberus</i> (260)	<i>Alk6</i> (160) <i>Gremlin</i> (170)
× Heck08	A ✓ G6PDH (214) B ✓ G6PDH (214) C ✓ G6PDH (214) D ✓ G6PDH (214)	<i>BmpRII</i> (150) <i>Dan</i> (200) <i>Patched1</i> (250) <i>Wnt4</i> (240)	<i>TgfBRII</i> (200) <i>Prcd</i> (240) <i>Patched2</i> (280) <i>Wnt5a</i> (204)	<i>ActRIIa</i> (180) <i>ActRIIb</i> (225,249,297,321) <i>Shh</i> (284) <i>Wnt5b</i> (170)	<i>ActRI</i> (230) <i>lhh</i> (254) <i>Wnt11</i> (160)	<i>Dhh</i> (243) <i>Wnt2b</i> (188)
✓ Heck09	A ✓ G6PDH (214) B ✓ G6PDH (214) C ✓ G6PDH (214) D ✓ G6PDH (214)	<i>Inhbb</i> (260) <i>Fgf5</i> (230) <i>Fgf10</i> (190) <i>FgfR3</i> (176,230)	<i>Inha</i> (190) <i>Fgf17</i> (260) <i>Fgf11</i> (150) <i>FgfR4</i> (190)	<i>Fgf2</i> (150) <i>Fgf13</i> (250)		
✓ Heck10	A ✓ G6PDH (214) B ✓ G6PDH (214) C ✓ G6PDH (214) D ✓ G6PDH (214)	<i>Bmp10</i> (160) <i>Bmp11</i> (160) <i>Fgf4</i> (160) <i>Fgf4</i> (160)	<i>Gdf8</i> (240) <i>Bmp6</i> (250) <i>Inhba</i> (230) <i>Fgf3</i> (250)	<i>Inhbc</i> (170) <i>Fgf14a</i> (200)	<i>Inhbe</i> (200) <i>Fgf16</i> (170)	
✓ Heck11	A ✓ G6PDH (214) B ✓ G6PDH (214) C ✓ G6PDH (214) D ✓ G6PDH (214)	<i>Fgf12a</i> (200) <i>Fgf8</i> (158,191) <i>Bmp2</i> (150) <i>Wnt15</i> (?)	<i>Fgf14b</i> (180) <i>Gdf7</i> (190) <i>Wnt16</i> (?)	<i>Gdf6</i> (240)		
✓ Heck12	A ✓ Tubulin (250) B ✓ G6PDH (214) C ✓ G6PDH (214)	<i>Insulin</i> (312) <i>Gli2-ab</i> (371) <i>Gli2-gd</i> (300)	<i>Barx1</i> (170) <i>Gli2-ab</i> (320) <i>Gli2-gd</i> (350)	<i>Glucagon</i> (161) <i>Gli2-gd</i> (1496)	<i>Fgf17</i> (260)	<i>Fgf18</i> (300)
✓ Heck13	A ✓ TBP (190) B ✓ G6PDH (214)	<i>Nkx2.6</i> (200) <i>Hex</i> (160)	<i>Bapx1</i> (240) <i>Shh</i> (284)	<i>Patched1</i> (250)	<i>Hlxb9</i> (230)	
✓ Heck14	A ✓ G6PDH (214) B ✓ G6PDH (214) C ✓ G6PDH (214)	<i>Fgf1</i> (300) <i>Follistatin</i> (180) <i>Cerberus</i> (260)	<i>Fgf9</i> (230) <i>Folli-like</i> (240) <i>Gremlin</i> (170)	<i>Cdx2</i> (160) <i>Folli-rel</i> (290) <i>Chordin</i> (230)	<i>Noggin</i> (180)	

- ✓ The gel was readable. The internal markers worked.
- × The gel was unreadable. The internal markers failed to work.
- Positive result (the PCR reaction produced a band at the expected size)
- Negative result (the gene is not expressed or the PCR reaction did not work)

The genes that produced a PCR product at the expected size are coloured red, while the genes that did not produce a result are coloured black. A negative result may reflect that the gene analysed is not expressed or that PCR reaction failed to work. The spleno-pancreatic region and stomach were dissected out from wild type and *Dh* embryos. This was done carefully to avoid contamination from surrounding tissues such as the lungs which are known to express *Fgf's* (Bellusci et al., 1997). At E10.5 it is possible to phenotypically distinguish *Dh* embryos from wild type embryos. However, it is not possible to distinguish heterozygous from homozygous mutant embryos, but since the SMR is missing in both genotypes, tissue from all embryos carrying the *Dh* mutation was pooled. As a precaution the wild type tissue was obtained from a wild type cross. The remainder of the embryos (the posterior part of the body minus the internal organs) was also collected and used as a control. At the time the MPX-PCR was carried out it was unknown whether *Dh* had any effect on the differentiation of endocrine and exocrine cells in the mature pancreas and therefore, pancrei from E16.5 embryos were also screened. At this stage the different genotypes (+/+, *Dh*/+ and *Dh*/*Dh*) can readily be distinguished from each other based on the severity of the hindlimb phenotype. Each MPX reaction therefore contained seven samples (E16.5 +/+ pancreas, E16.5 *Dh*/+ pancreas, E16.5 *Dh*/*Dh* pancreas, E10.5 WT spleno-pancreatic region, E10.5 *Dh* spleno-pancreatic region, E10.5 WT posterior body and E10.5 *Dh* posterior body). The genes tested in each MPX reaction and respective gel is shown in table 4.3. Annotated pictures of the original gels are attached in appendix II.

The positive results obtained in the MPX experiment are summarised in table 4.4, however, some of these results have been enhanced digitally. The intensity of the bands within a sample is always preserved, but to get a true indication of the intensity of the bands compared to other genes and to the internal standard one should refer to the original gel pictures in appendix II.

A test for measuring the reliability of the MPX assay is to look for differentially expressed genes. For example there are a number of pancreas specific genes such as insulin and amylase, which are specific to the E16.5 pancreatic samples. Glucagon on the other hand is expressed in both the E16.5 pancreatic samples and in the E10.5 spleno-pancreatic samples. However, glucagon is switched on around E10.5 and therefore glucagon should come up in both the late and early pancreas. *Barx1* is expressed highly in the stomach at E10.5 and from the *in situ* data (Tissier-Seta et al., 1995) the gene should not be expressed in the posterior part of the body. The MPX data seems to support this observation. Finally there are also a number of genes such as *Fgf8* and *Gdf8* that appear to be specific to the posterior

Table 4.4. MPX-PCR results

Gene	Gel No.	Expression								Gene	Gel No.	Expression							
		1	2	3	4	5	6	7	8			1	2	3	4	5	6	7	8
<i>Alk3</i>	Heck07 C									<i>Gata4</i>	Heck02 C								
<i>Alk6</i>	Heck07 C									<i>Gdf1</i>	Heck05 D								
<i>Amylase</i>	Heck01 B									<i>Gdf6</i>	Heck11 C								
<i>Barx1</i>	Heck01 C									<i>Gdf8</i>	Heck10 A								
<i>Bmp2</i>	Heck02 B									<i>Gli1</i>	Heck02 D								
<i>Bmp3b</i>	Heck05 B									<i>Gli2</i>	Heck12 B								
<i>Bmp4</i>	Heck05 A									<i>Gli3</i>	Heck02 D								
<i>Bmp5</i>	Heck05 C									<i>Glucagon</i>	Heck01 A								
<i>Bmp7</i>	Heck05 B									<i>Gremlin</i>	Heck14 C								
<i>Bmp10</i>	Heck10 A									<i>Hes1</i>	Heck02 D								
<i>Bmp11</i>	Heck10 B									<i>Hnf6</i>	Heck02 A								
<i>Cdx2</i>	Heck01 D									<i>Inha</i>	Heck03 A								
<i>Cerberus</i>	Heck14 C									<i>Inhbb</i>	Heck03 A								
<i>Chymotryp.</i>	Heck01 B									<i>Insulin</i>	Heck01 A								
<i>Fgf1</i>	Heck03 C									<i>Isl1</i>	Heck02 A								
<i>Fgf6</i>	Heck04 A									<i>Isl2</i>	Heck02 A								
<i>Fgf7</i>	Heck03 B									<i>Jagged1</i>	Heck02 C								
<i>Fgf8</i>	Heck11 B									<i>Nkx2.2</i>	Heck01 D								
<i>Fgf9</i>	Heck03 B									<i>Nkx2.3</i>	Heck01 D								
<i>Fgf10</i>	Heck09 C									<i>Nkx2.6</i>	Heck13 B								
<i>Fgf11</i>	Heck09 C									<i>Noggin</i>	Heck02 B								
<i>Fgf13</i>	Heck09 c									<i>Patched1</i>	Heck13 C								
<i>Fgf14b</i>	Heck11 A									<i>Pax6</i>	Heck01 C								
<i>Fgf17</i>	Heck03 C									<i>Prox1</i>	Heck01 D								
<i>Fgf18</i>	Heck03 B									<i>Shh</i>	Heck13 C								
<i>FgfR2</i>	Heck04 C									<i>Trypsin</i>	Heck01 B								
<i>FgfR3</i>	Heck09 D									<i>TgfB2</i>	Heck07 C								
<i>FgfR4</i>	Heck09 D									<i>TgfB3</i>	Heck07 C								
<i>Folli-rel</i>	Heck14 B									<i>Wnt15</i>	Heck11 D								
<i>Follistatin</i>	Heck14 B																		

+/- pancreas
 Dh/+ pancreas
 Dh/Dh pancreas
 +/- E10.5 stomach and pancreas
 Dh E10.5 stomach and pancreas
 +/- E10.5 posterior body
 Dh E10.5 posterior body
 Negative control

part of the body. In most cases the genes were tested in two or more independent experiments and there were cases where different results were obtained. *Bmp11* (table 4.3) also appears to be expressed exclusively in the posterior part of the embryo, but in another experiment (Heck05 C) the gene was also expressed in the

spleno-pancreatic region of *Dh* embryos. However, this was a semi quantitative experiment, where the aim was to identify new genes that might be expressed in the SMR.

Initially the hope was that the absent SMR in *Dh* would enable the selection of genes expressed in spleno-pancreatic samples of wild type but not *Dh*. Unfortunately, no genes showed this kind of expression pattern. However, the MPX assay was still useful because it helped identifying genes expressed in the spleno-pancreatic region and the stomach. In particular I was interested in secreted factors, which might be involved in promoting the leftward growth of the region.

Morphogens and growth factors expressed in the developing gut

In the limb the AER secretes a number of growth factors which are necessary to maintain proliferation and gene expression (Niswander et al., 1993; Crossley et al., 1996). To test whether the SMR might have a similar function in the spleno-pancreatic region we looked for expression of Fgf's in the SMR. Using MPX-PCR we detected expression of *Fgf9*, *Fgf10*, *Fgf13* and *Fgf18*. Of these genes *Fgf9* and *Fgf10* was expressed in the region of interest.

Fgf10 has previously been shown to be expressed in the stomach although no gut phenotype has been described in mice where *Fgf10* has been deleted (Sekine et al., 1999). At E9.5 *Fgf10* is expressed at very low levels on both sides of the endoderm (data not shown) in a pattern similar to that of *Bapx1* and *Bmp11*. At E10.5 strong expression was detected in the ventral part of the SMR which lies adjacent to the dorsal pancreatic bud, the tip of the SMR and the mesenchyme underlying the tip (Figure 4.9a). *Fgf9* is also expressed in the SMR at the tip and in the underlying mesenchyme, but in contrast to *Fgf10*, *Fgf9* expression was low in the ventral part of the SMR and high in the dorsal (Figure 4.9b). However, the expression of *Fgf9* is dynamic and varies between embryos of different ages. At slightly later stages expression is up regulated in the mesenchyme at the tip but down regulated in the overlying mesothelium (data not shown). Expression of *FgfR3* could also be detected at the tip of the SMR (figure 4.9c). This is the region where the expression of *Fgf9* and *Fgf10* overlap.

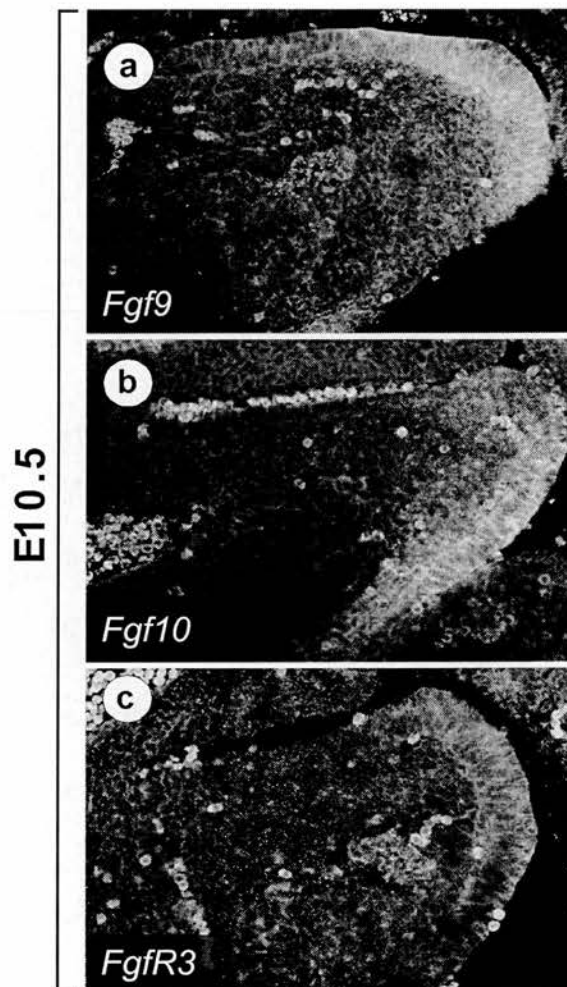


Figure 4.8: Expression of *Fgf*'s and *FgfR*'s in the spleno-pancreatic region. *In situ* hybridisation showing gene expression in the spleno-pancreatic region at E10.5 (a) In wild type embryos *Fgf9* is expressed in the dorsal part of the SMR and in the tip. (b) In wild type embryos *Fgf10* is expressed in the ventral part of the SMR and in the tip. Expression can also be detected in the underlying mesenchyme. (c) In wild type embryos *FgfR3* is expressed in the tip of the SMR.

In addition to Fgf's, the expression pattern of several members of the TGF β superfamily was examined. From the MPX results it appears that *Bmp4* is expressed highly in the spleno-pancreatic region. However, at both E9.5 and E10.5 *Bmp4* is expressed highly in the lateral flank but no transcripts could be detected in the spleno-pancreatic region at either stage (figure 4.10a, b). This is not likely to be a false result from the MPX, because in chicken *Bmp4* is expressed in the midgut and hindgut (Nielsen et al., 2001; Smith et al., 2000) and presumably some of the midgut has been included when dissecting out the stomach and spleno-pancreatic region. At E9.5 *Bmp7* is expressed in the dorsal pancreatic endoderm but not in the surrounding mesoderm or in the splanchnic mesothelium (figure 4.10c). A day later the gene is still expressed in the pancreatic endoderm, but in addition the left mesoderm and the ventral part of the SMR has also started to express *Bmp7* (figure 4.10d). *Bmp11* is also expressed in the spleno-pancreatic region despite the negative result obtained with MPX. At E9.5 the gene is expressed in the mesoderm and splanchnic mesothelium on both sides of the pancreatic endoderm, while the endoderm itself is negative for *Bmp11* expression (figure 4.10e). This expression is very similar to that observed for both *Isl1* and *Bapx1* ((Ahlgren et al., 1997); figure 4.4b and 5.5c). Subsequently *Bmp11* expression is turned off on the right side while expression is maintained in the ventral part of the SMR and in the underlying mesenchyme (figure 4.10f). Two other TGF β signalling molecules *Gdf6* and *Follistatin* both looked promising from the MPX data. However, none of them are expressed in the spleno-pancreatic region (figure 4.10g, h).

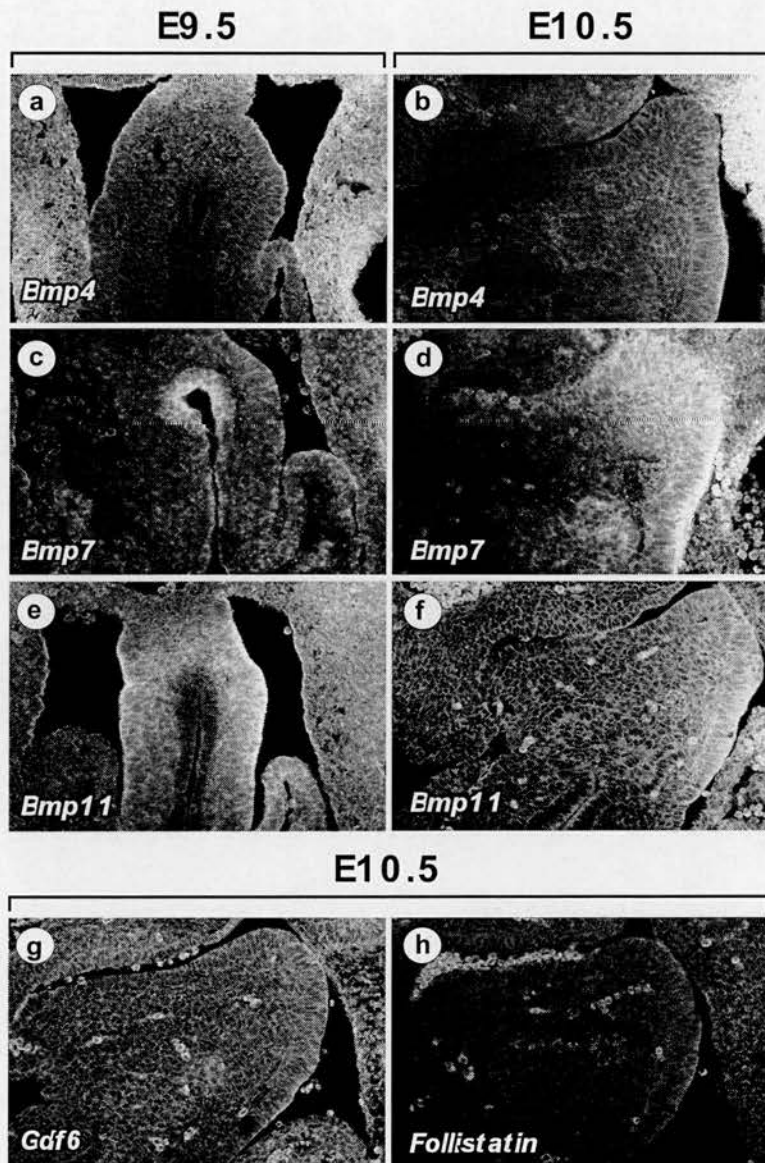


Figure 4.9: Expression of Tgf β 's in the spleno-pancreatic region. *In situ* hybridisation showing wild type expression of TGF β genes in the spleno-pancreatic region at E9.5 and E10.5 *Bmp4* is excluded from the spleno-pancreatic region at both E9.5 (**a**) and E10.5 (**b**). At E9.5 *Bmp7* is expressed in the dorsal pancreatic bud (**c**) and at E10.5 *Bmp7* is expressed in the pancreatic endoderm and in the SMR and underlying mesenchyme (**d**). At E9.5 *Bmp11* is expressed in the mesenchyme surrounding the dorsal pancreatic bud (**e**) and at E10.5 *Bmp11* is expressed in the SMR and underlying mesenchyme (**f**). No expression of *Gdf6* (**g**) or *Follistatin* (**h**) could be detected at E10.5.

4.5 Genetic interactions and the late pancreas phenotype

Genetic interactions

In embryos carrying the *Dh* mutation the spleen fails to be induced and genes expressed in the spleen precursor cells such as *Hox11* and *Nkx2.5* are absent. *Bapx1*^{-/-} embryos are also asplenic and at E12.5 they do not express *Hox11* (Lettice et al., 1999b). However, in order to elucidate the underlying pathway leading to spleen development, other spleen markers were examined in *Dh* and *Bapx1*^{-/-} embryos. In mice lacking functional BAPX1 protein *Nkx2.5* is not expressed in either the splenic mesenchyme or the ventral domain suggesting that the spleen is never induced (figure 4.10l). However, it is difficult to pinpoint the exact cause of asplenia, because *Bapx1* is expressed in both the SMR and the splenic mesenchyme. The gene could therefore have a direct effect in spleen development if required in the splenic mesenchyme. Or the effect could be indirect, if the spleen fails to be induced because the SMR is disrupted. For this reason it was important to examine *Bapx1* expression in *Dh* embryos. Lack of *Bapx1* in the mesenchyme could provide an alternative explanation for asplenia in *Dh* while the presence of *Bapx1* expression would suggest that the mesenchyme is normal in *Dh* and that asplenia is caused by the absent SMR. In *Dh*/+ embryos *Bapx1* is expressed in the mesenchyme dorsal and left of the pancreatic endoderm (figure 4.10b); an expression pattern very similar to that observed in wild type, although the expression levels might be slightly reduced. However, in *Dh* homozygous embryos *Bapx1* expression is severely impaired (figure 4.10c). *Bapx1* transcripts could be detected between the gut tube and the ventral pancreas but not around the dorsal pancreas. Additionally *Bapx1* is expressed at the joint between the liver and the stomach, which will later give rise to the diaphragm. This expression domain is believed to be authentic since it can also be observed in wild type embryos (figure 4.4f).

The bHLH gene *Capsulin* also has an essential role in spleen development and it has been reported that *Hox11* and *Bapx1* expression is absent from the developing spleen in embryos carrying homozygous deletion of the *Capsulin* gene (Lu et al., 2000). Like *Bapx1*, *Capsulin* is not specific for the spleen precursor cells and the expression of both genes precedes that of *Hox11* and *Nkx2.5*. At E10.5 *Capsulin* is expressed in the splenic mesoderm and in another more ventral domain but is always excluded from the mesenchyme directly under the tip of the SMR (figure 4.10d). In *Dh*/+ embryos *Capsulin* expression can be detected throughout the mesenchyme surrounding the

E10.5

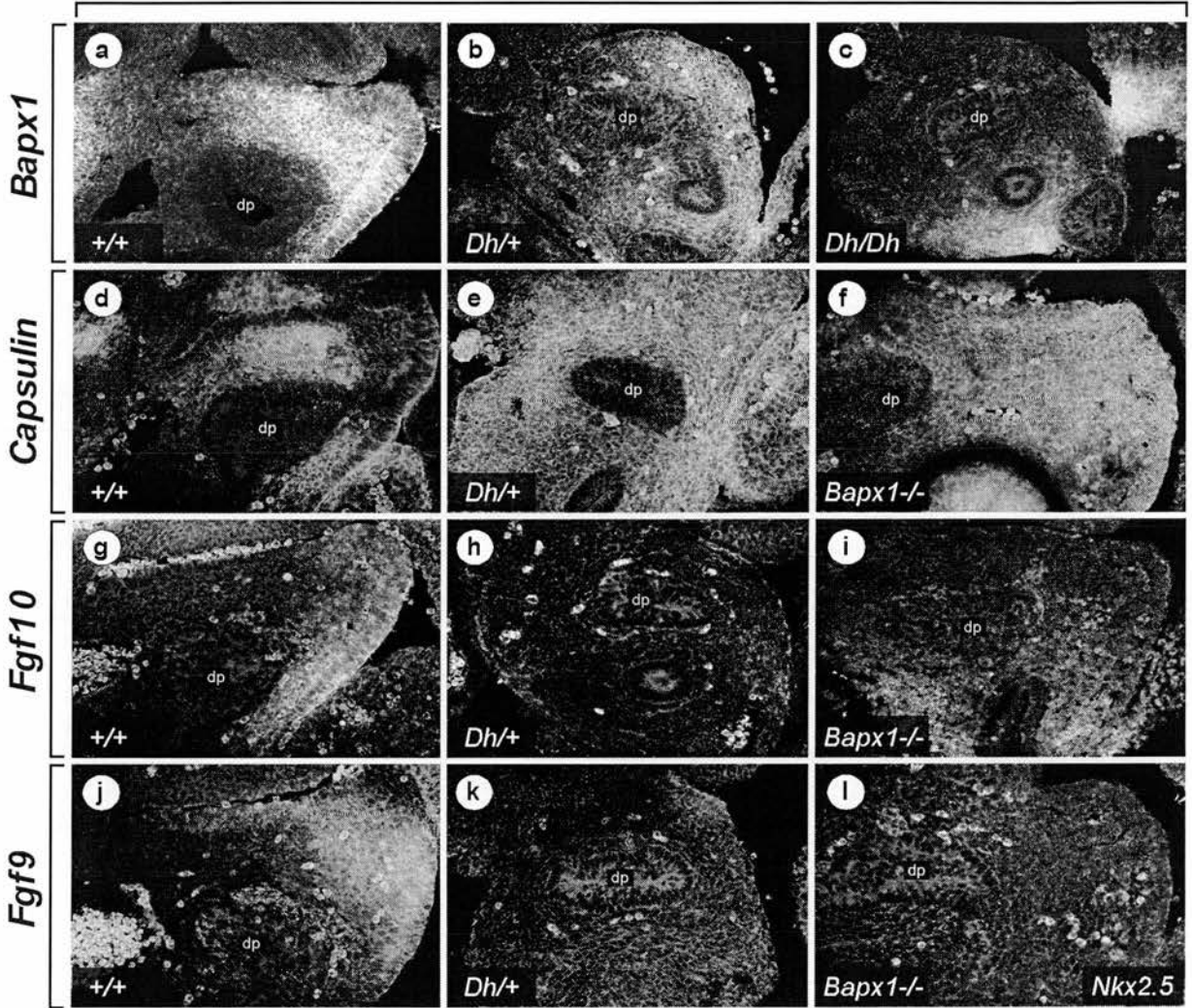


Figure 4.10: Genetic interactions in the spleno-pancreatic region. *In situ* hybridisation showing gene expression in the spleno-pancreatic region at E10.5 (a) *Bapx1* expression in +/+ at E10.5. (b) *Bapx1* expression in *Dh/+* at E10.5. Expression can be detected around the pancreatic endoderm. (c) *Bapx1* expression in *Dh/Dh* at E10.5. No expression can be detected around the dorsal pancreas. (d) *Capsulin* expression in +/+ at E10.5. (e) *Capsulin* expression in *Dh/+* at E10.5. Expression can be detected at high levels throughout the mesoderm. (f) *Capsulin* expression in *Bapx1*^{-/-} at E10.5. Expression can be detected at high levels throughout the mesoderm. (g) *Fgf10* expression in +/+ at E10.5. (h) *Fgf10* expression in *Dh/+* at E10.5. Very little or no expression can be detected in the ventral mesenchyme. (i) *Fgf10* expression in *Bapx1*^{-/-} at E10.5. Expression is no longer defined to the left but can be detected on both sides of the endoderm. (j) *Fgf9* expression in +/+ at E10.5. (k) *Fgf9* expression in *Dh/+* at E10.5. Low expression can be detected in the dorsal-left mesoderm. (l) *Nkx2.5* expression in *Bapx1*^{-/-} at E10.5. No expression can be detected. (dp) dorsal pancreatic endoderm.

pancreatic endoderm (figure 4.10e) and similar expression was observed in *Bapx1*^{-/-} embryos (figure 4.10f) suggesting that the expression of *Capsulin* is unaffected by either mutation. However in both mutants *Capsulin* is expressed in the region corresponding to the mesenchyme underlying the tip of the SMR. Thus in the absence of a functional SMR *Capsulin* becomes expressed in the tip mesenchyme suggesting that the SMR has an active role in regulating gene expression in the underlying mesenchyme.

One way the SMR could regulate gene expression in the underlying mesenchyme is by the secretion of morphogens. I have shown that *Fgf10* and *Fgf9* are expressed in different parts of the SMR and although they themselves might not be regulating *Capsulin* they might reflect the expression patterns of other genes in the SMR. In wild type embryos *Fgf10* is expressed at high levels in the ventral part of the SMR and in low levels at the tip (figure 4.10g). Expression can also be detected in the mesenchyme lying between the ventral SMR and the pancreatic endoderm. In *Dh/+* embryos almost no *Fgf10* expression could be detected in the mesenchyme (figure 4.10h). Perhaps a few cells in the ventral mesenchyme might be expressing *Fgf10* at very low levels. In absence of BAPX1 protein *Fgf10* is expressed in the mesenchyme on both sides of the duodenum but in the mesenchyme around the dorsal pancreas the expression levels are very low (figure 4.10i). Also there is no *Fgf10* expression in the ventral mesothelium confirming that the SMR is defective. In wild type mice there is a close relationship between the dorsal pancreas and the ventral, *Fgf10* expressing, part of the SMR. In both the mutants analysed the dorsal pancreas lacks directional growth and in both mutants the *Fgf10* signalling adjacent to the pancreatic endoderm is severely impaired. It is therefore tempting to suggest that the ventral SMR provides a source of *Fgf* signalling required for directional growth of the dorsal pancreas. In agreement with this studies have shown that over expression of *Fgf10* causes excessive growth of the pancreatic endoderm.

Fgf9 is normally expressed at the tip and in the dorsal part of the SMR and also in the mesenchyme underlying the tip (figure 4.10j). In *Dh/+* embryos *Fgf9* expression can be detected at very low levels in the dorsal mesenchyme (figure 4.10k). This expression pattern is very similar to that observed for *Barx1*, suggesting that these cells represent the tip mesenchyme. Hence the expression of *Fgf9* also indicates that cell identity is preserved in *Dh* heterozygous embryos despite the reduction in expression levels.

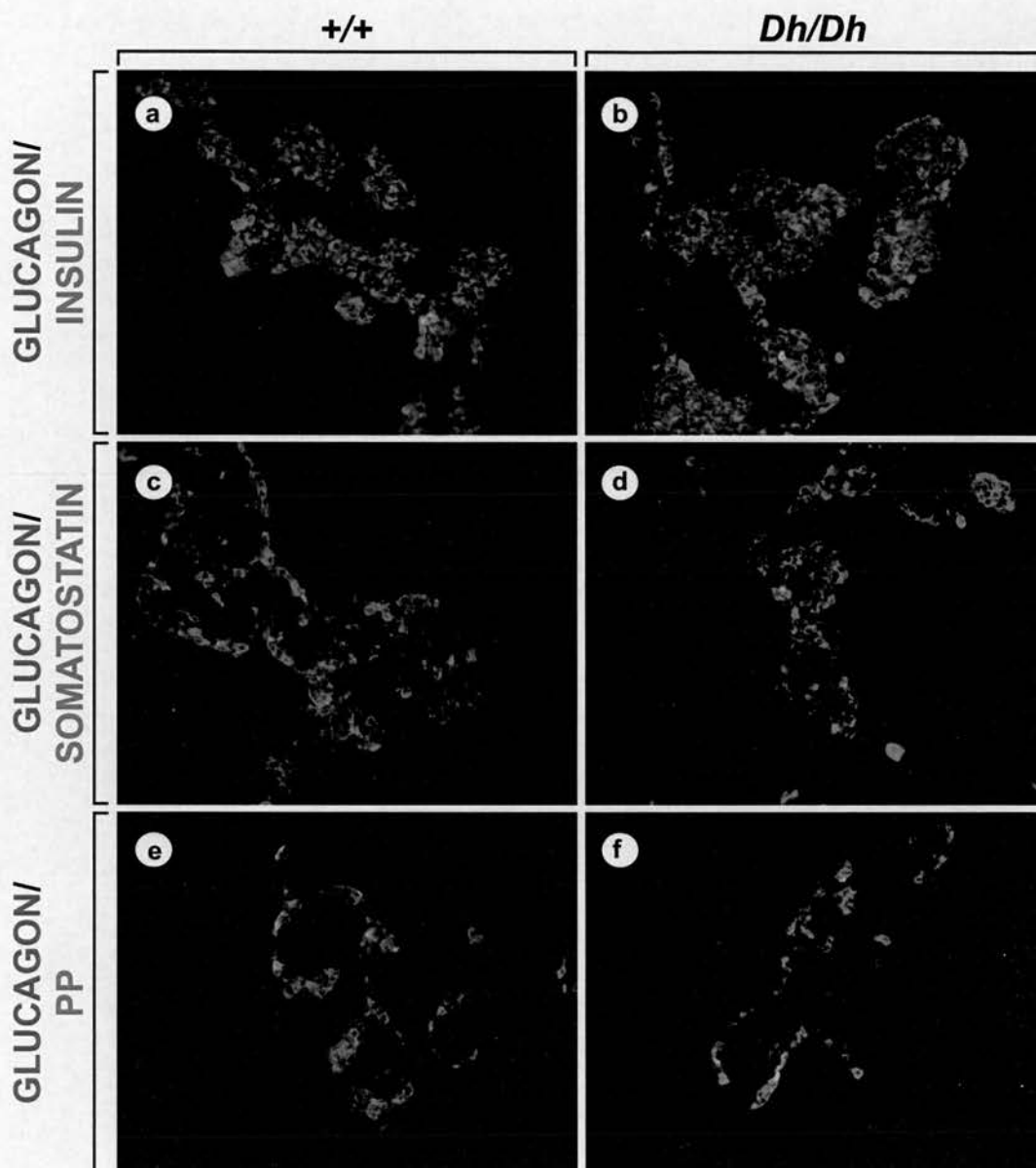


Figure 4.11: The mature pancreas is normal in *Dh* embryos. Immunohisto-chemistry in +/+ and *Dh/Dh* pancreas at E18.5. (a) In +/+ embryos Glucagon is found in the α -cells (green) while Insulin is found in the β -cells (red). (b) In *Dh/Dh* both Glucagon producing cells (green) and Insulin producing cells (red) are present and their distribution appear normal. (c) In +/+ embryos Glucagon is found in the α -cells (green) while Somatostatin is found in the δ -cells (red). (d) In *Dh/Dh* both Glucagon producing cells (green) and Somatostatin producing cells (red) are present and their distribution appear normal. (e) In +/+ embryos Glucagon is found in the α -cells (green) while Pancreatic Polypeptide (PP) is found in the PP-cells (red). (f) In *Dh/Dh* both Glucagon producing cells (green) and PP producing cells (red) are present and their distribution appear normal.

The mature pancreas is normal in *Dh* embryos

The absence of a functional SMR in *Dh* embryos results in abnormal growth of the dorsal pancreas, but whether it has any effect on the function of the pancreas is unknown. Pancreas from E18.5 wild type and mutant foetuses were sectioned and stained with antibodies recognising the four most important endocrine cell types. In the wild type pancreas the insulin producing β -cells (red) are surrounded by glucagon producing α -cells (green; figure 4.11a). In *Dh/Dh* both cell types are present and the islets appear to be organised normally with the insulin producing cells in the middle and the glucagon cells at the periphery (figure 4.11b). Also the somatostatin producing δ -cells (figure 4.11c, d) and the pancreatic polypeptide (PP) producing PP cells (figure 4.11e, f) are normal in *Dh*. Thus it seems that the endocrine portion of the pancreas is normal in *Dh* despite the dramatic effect the mutation has the growth of the dorsal pancreas. No experiments were done to see if the exocrine portion of the pancreas were normal in *Dh*. However in the MPX-PCR assay, a number of exocrine markers (Amylase, Chymotrypsin and Trypsin) tested positive in both *Dh/+* and *Dh/Dh* suggesting that exocrine cells are present in the *Dh* pancreas.

4.6 Stomach development in *Dh*

The asymmetry is lost in *Dh/Dh* embryos

At the level of the stomach *Barx1* is expressed in the mesenchyme on both sides of the endoderm although the expression levels are higher in the left mesenchyme (figure 4.12a, d). At E10.5 the stomach is positioned at the left side of the embryo and it has rotated so the dorsal-ventral axis of the endoderm is no longer aligned with the midline of the embryos. In *Dh/+* the dorsal mesogastrium appears abnormal but the stomach still rotates correctly and the angle between the embryonic midline and the dorsal ventral axis of the endoderm is similar to that observed in wild type (figure 4.12b, e). In *Dh* homozygous embryos however, the stomach is symmetric. At E10.5 the stomach fails to rotate and the endodermal axis remains aligned with the embryonic midline (figure 4.12c, f). The loss of asymmetry in *Dh* homozygous embryos prompted us to examine the expression of *Pitx2*, a downstream gene in the left-right determining pathway (Piedra et al., 1998; Essner et al., 2000). In wild type embryos the *Pitx2* expression, at the level of the stomach, is restricted to the mesoderm and mesothelium left of the endoderm (figure 4.12g). In *Dh/Dh* embryos *Pitx2* is expressed on the left side of the endoderm, but ectopic expression in the

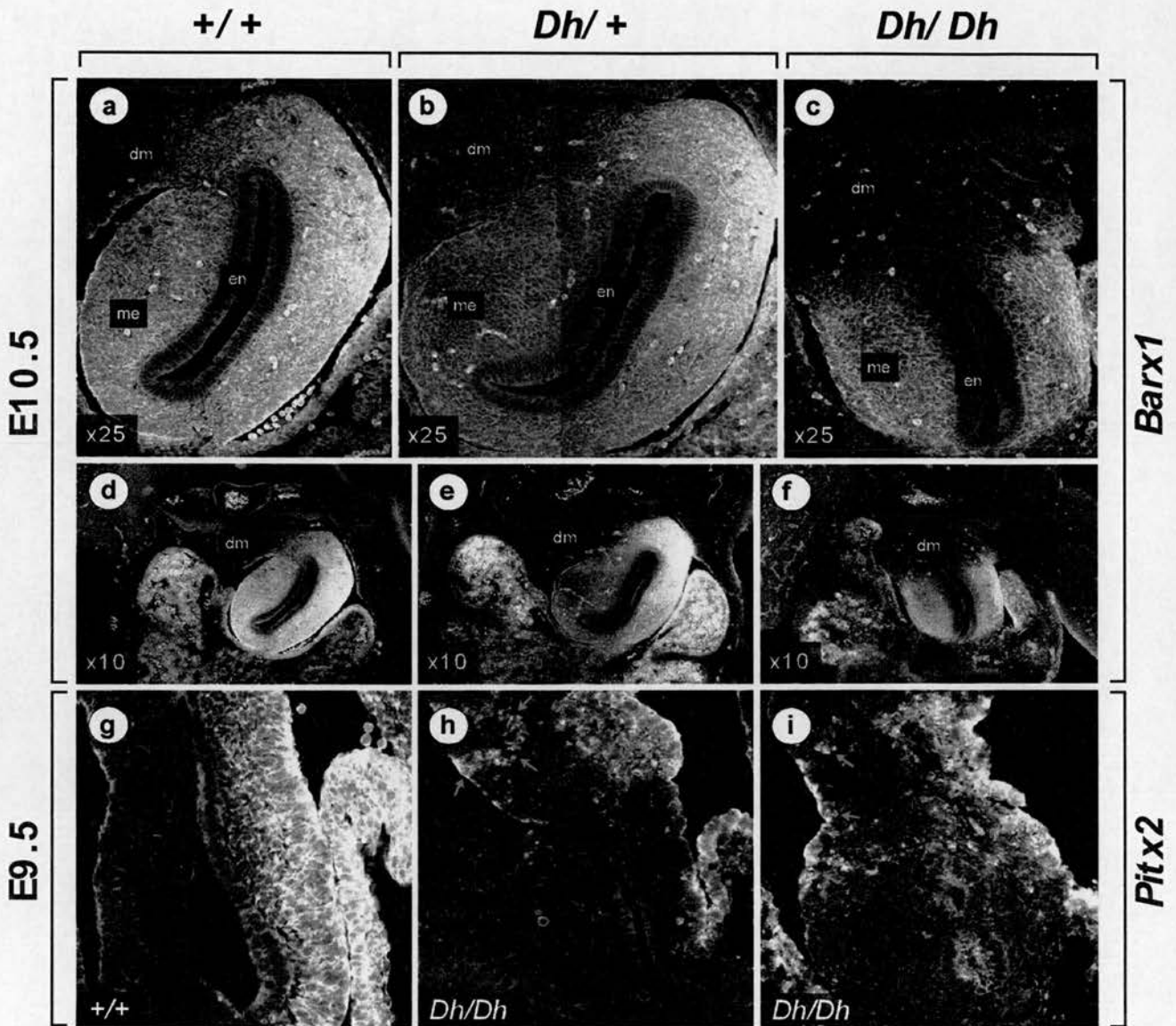


Figure 4.12: Loss of asymmetry in *Dh/Dh* embryos. *In situ* hybridisation showing gene expression in the stomach region at E10.5 (a) *Barx1* expression in *+/+* at E10.5. Expression can be detected in throughout the mesoderm, but not in the endoderm. (b) *Barx1* expression in *Dh/+* at E10.5. Expression can be detected in throughout the mesoderm, but not in the endoderm. The morphology of the dorsal mesogastrium is abnormal. (c) *Barx1* expression in *Dh/Dh* at E10.5. The morphology of the dorsal mesogastrium is very abnormal almost symmetric. Expression can be detected in most of the mesoderm but not in the mesoderm on the dorsal side. (d) Low magnification of (a). In *+/+* embryos the stomach is positioned at the left side. (e) Low magnification of (b). In *Dh/+* embryos the stomach is positioned at the left side although the dorsal mesogastrium is abnormal. (f) Low magnification of (c). In *Dh/Dh* embryos the dorsal mesogastrium is very abnormal and the stomach is positioned in the middle of the embryo. (g) *Pitx2* expression at E9.5 in a *+/+* embryo. Expression can only be detected on the left side of the endoderm. In *Dh/Dh* ectopic expression of *Pitx2* (red arrows) can be detected both at the level of the stomach (h) and at the level of the pancreas (i). (dm) dorsal mesogastrium, (en) endoderm and (me) mesoderm.

right mesoderm could also be detected (figure 4.12h). This strongly suggests that the left-right determining pathway is disrupted in the homozygous embryos and that this is the reason the stomach does not rotate. Ectopic expression of *Pitx2* could also be detected at the level of the pancreas (figure 4.12.i) thus coinciding with the ectopic expression of *Barx1*. However, this loss of asymmetry only appears to affect *Dh* homozygous embryos. In *Dh/+* embryos the stomach rotate to the left and thus far all genes examined show correct asymmetric expression (data not shown).

***Dh/Dh* Stomachs are smaller at E13.5**

At later stages in development the stomachs of *Dh/Dh* continues to be severely abnormal. The results shown in figure 4.13 are whole mount *in situ* looking at the expression of *Hox11* and *Wt1* at E13.5. Both genes are expressed in the spleen (Roberts et al., 1994; Herzer et al., 1999) and these experiments were initially carried out to demonstrate the lack of spleen development in *Dh*. However, in light of the results described above which show that the spleen fails to be induced in *Dh* embryos, it is not surprising that the spleen specific expression of *Hox11* and *Wt1* is absent at E13.5. But in addition to confirming, that all stages of spleen development are completely abrogated in *Dh*, they also show that stomach development in the homozygous mutants is severely impaired.

In *+/+* embryos both *Hox11* and *Wt1* are expressed at high levels in the spleen mesenchyme (figure 4.13a, d). In addition *Wt1* is expressed in the mesothelium of the liver and in the stomach. The stomach can be seen lying on the left surrounded by the liver (dashed line). In *Dh/+* no *Hox11* expression can be detected (figure 4.13b). *Wt1* is still expressed in the stomach and in the lining of the liver but there is no expression where the spleen should be (figure 4.13.e). The stomach is probably slightly smaller in *Dh/+* but it is positioned correctly on the left side. However, in homozygous embryos the size of the stomach is severely reduced compared to both heterozygotes and wild type (figure 4.13c, f). No expression of either *Hox11* or *Wt1* can be detected in the region where the spleen should be developing, but *Wt1* is still expressed in the mesothelium surrounding the liver although the expression levels in the stomach are reduced.

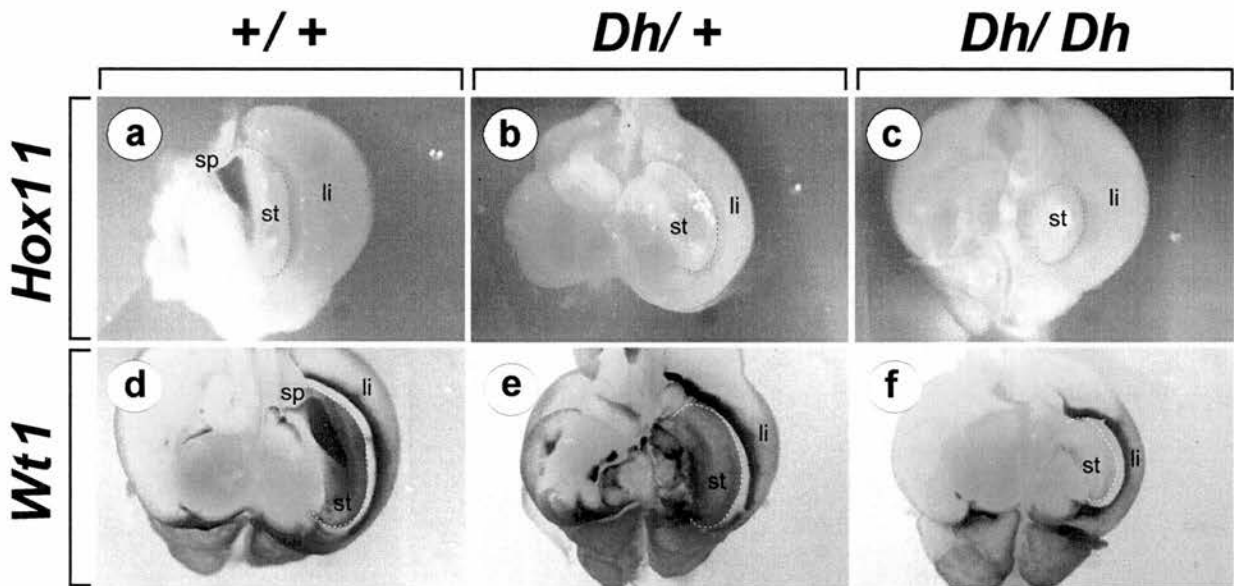


Figure 4.13: The stomach is smaller in *Dh/Dh* embryos. Gene expression of *Hox11* and *Wt1* in the spleen and surrounding tissue at E13.5. **(a)** In wild type embryos *Hox11* is expressed exclusively in the developing spleen and no expression can be detected in either the stomach or the liver. The stomach is outlined by a black dashed line. **(b)** In *Dh/+* the spleen is absent and no *Hox11* expression can be detected. The size of the stomach is comparable to wild type. **(c)** Also in *Dh/Dh* the spleen is absent and no *Hox11* expression can be detected. However, the size of the stomach is severely reduced compared to both *+/+* and *Dh/+*. **(d)** In wild type embryos *Wt1* is expressed at high levels in the spleen, the lining of the liver and the stomach. The stomach is outlined by a white dashed line. **(e)** In *Dh/+* the spleen specific expression of *Wt1* can no longer be detected, but expression can still be detected in the lining of the liver and in the stomach. Again the size of the stomach is similar to that of wild type. **(f)** In *Dh/Dh* the stomach is considerably smaller than in *+/+* and *Dh/+*. Also the stomach specific expression of *Wt1* can no longer be detected. Only the lining of the liver is expression *Wt1* in *Dh* homozygous embryos. **(sp)** spleen, **(st)** stomach and **(li)** liver.

***Dh* causes abnormal looping of the duodenum**

In addition to affecting the size and position of the stomach itself, *Dh* also affects the looping of the duodenum. To analyse this further full length intestinal tracts were dissected out from E18.5 embryos (figure 4.14a, b, c). In *+/+* embryos the oesophagus enters the stomach in the middle on one side and the duodenum leaves the stomach from the posterior end at the same side as the oesophagus enters (figure 4.14d). After leaving the stomach in the same direction as the oesophagus the duodenum loops back towards the stomach creating an almost full circle. The space within the duodenal loop is occupied by the ventral pancreas, which is attached to the duodenum through a thin epithelial membrane. The dorsal pancreas and the spleen can also be seen in close association with the stomach (figure 14.g). The pyloric sphincter, a constriction that marks the boundary between duodenum and the stomach, can also be seen (black arrowheads). In *Dh/+* the duodenum leaves the stomach at the right place, posterior of the oesophagus (figure 4.14e). However, it immediately bends back on itself and fails to make a loop. As a result the ventral pancreas ends up lying on top of the duodenum instead of being splayed out within the duodenal loop (figure 4.14h). Also the stomachs of *Dh/+* animals are slightly smaller than wild type and they appear more muscular. The abnormal looping of the duodenum is also present in *Dh/Dh* and is even more dramatic than in *Dh/+* (figure 4.14f, i). After leaving the stomach the duodenum forms a sharp U-turn and in the absence of a loop the ventral pancreas can be seen lying posterior to the duodenum. The size of the stomach is reduced to less than half the size of a wild type stomach and the constriction associated with the pyloric sphincter seems to be absent.

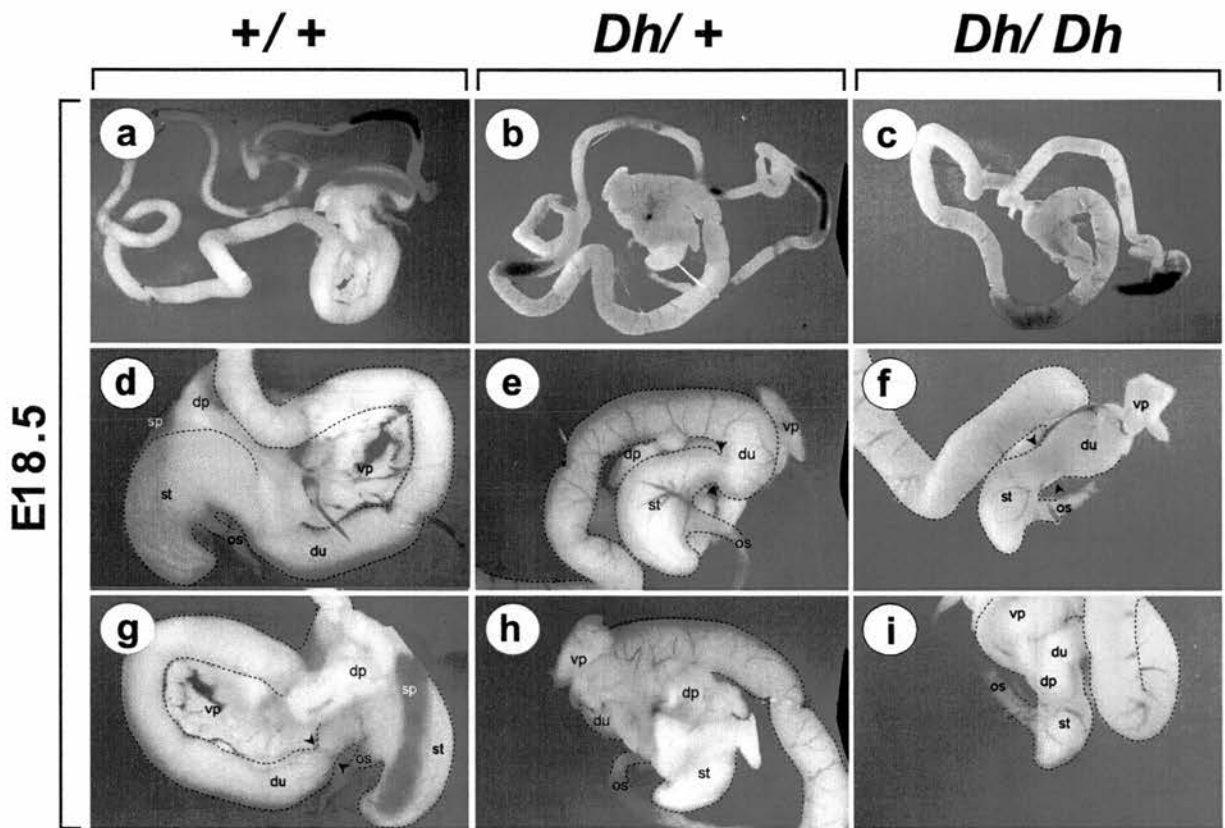


Figure 4.14: Abnormal looping of the duodenum in *Dh* mice. E18.5 full length intestine running from the stomach to the rectum from +/+ (a), *Dh*/+ (b) and *Dh*/*Dh* (c). However, in *Dh* homozygotes the gut ends blind at the level of the cecum. (d) Close up of a +/+ stomach with the oesophagus entering the stomach from the left. After leaving the stomach to the left the duodenum forms a large loop which is occupied by the ventral pancreas. (e) Close up of a *Dh*/+ stomach with the oesophagus entering the stomach from the left side. Instead of forming a large loop the duodenum makes a sharp bend to the right and as a result the ventral pancreas is no longer spread out within the loop. The stomach is slightly smaller than in wild type and it appears more compact. (f) In *Dh*/*Dh* the duodenal phenotype is similar to that observed in *Dh*/+ although it is more severe. Also the stomach is only half the size compared to wild type. (g) The same stomach as in (d) but flipped over so the oesophagus is now entering the stomach from the right side. The spleen and the dorsal pancreas can be seen in close proximity to the stomach. The ventral pancreas is lying within the duodenal loop. (h) The same stomach as in (e) but flipped over. The spleen is completely absent and the inability of the ventral pancreas to attach itself to the inside of the duodenal loop results in a more compact appearance. It is therefore difficult to distinguish between the dorsal and ventral pancreas. (i) The same stomach as in (f) but flipped over. The size of the stomach is severely reduced and as in the heterozygous animals the absence of a duodenal loop causes the ventral pancreas to become more compact. (sp) spleen, (st) stomach, (du) duodenum, (os) oesophagus, (dp) dorsal pancreas and (vp) ventral pancreas. The digestive tract is outlined by a black dashed line. The position of the pyloric sphincter is marked by black arrowheads.

The anterior stomach and pyloric sphincter is absent in *Dh/Dh* embryos

As a result of the reduction in size and the presumed lack of a pyloric sphincter *Dh/Dh* stomachs look almost like a continuation of the duodenum. To see if this is the case or whether positional identities have been preserved within the mutant stomachs, wild type and homozygous stomachs were sectioned and stained with phalloidin (red) and Yo-Pro1 (green; figure 4.15).

In wild type the stomach can be divided into an anterior and a posterior compartment (figure 4.15a). The anterior compartment of the stomach is lined with a mucus membrane (figure 4.15c; white dashed line). The mucus layer is rich in F-actin and stains strongly with phalloidin. In the cells that are located within the mucus layer the DNA localises to the inside of the nuclear membrane and the nuclei can be seen as green circles. Hence there is a distinct histological difference between these nuclei and the nuclei of cells located at the base of the mucus layer. The lining of the posterior compartment is covered with structures resembling the villi of the gut (figure 4.15e). The boundaries between the anterior and posterior compartments of the stomach are well defined. One boundary coincides with the position where the oesophagus enters the stomach (figure 4.15b; white arrow) while the other is positioned midway along the greater curvature of the stomach (figure 4.15d). The pyloric sphincter is also visible as a constriction defining the boundary between the stomach and duodenum (figure 4.15a; blue arrowheads).

As shown previously the *Dh/Dh* stomachs are much smaller than in wild type (figure 4.15f). However, from the section it becomes clear that this reduction has happened at the expense of the anterior compartment, which has been almost completely depleted. Remnants of the mucus layer associated with anterior identity can be seen at the anterior tip of the stomach (white arrow) and as in wild type apoptotic cells are present within this layer suggesting that the remains of the mucus layer has maintained correct identity (figure 4.15h, i). The rest of the stomach however, appears to have posterior identity (figure 4.15j). In wild type one of the anterior-posterior boundaries coincided with the entry point of the oesophagus. This is not the case in *Dh/Dh* where the lining of the stomach display posterior identity on both sides of the oesophagus (figure 4.15g). Hence, in addition to the reduction in size the boundaries determining positional identity has been shifted anteriorly in *Dh/Dh* stomachs, strongly suggesting a posterior transformation of the anterior stomach. Also, the pyloric sphincter is absent in *Dh/Dh* embryos. The boundary between the stomach and the duodenum can still be seen, however, there is no longer a constriction of the stomach before entering the duodenum (figure 4.15f; blue arrowheads).

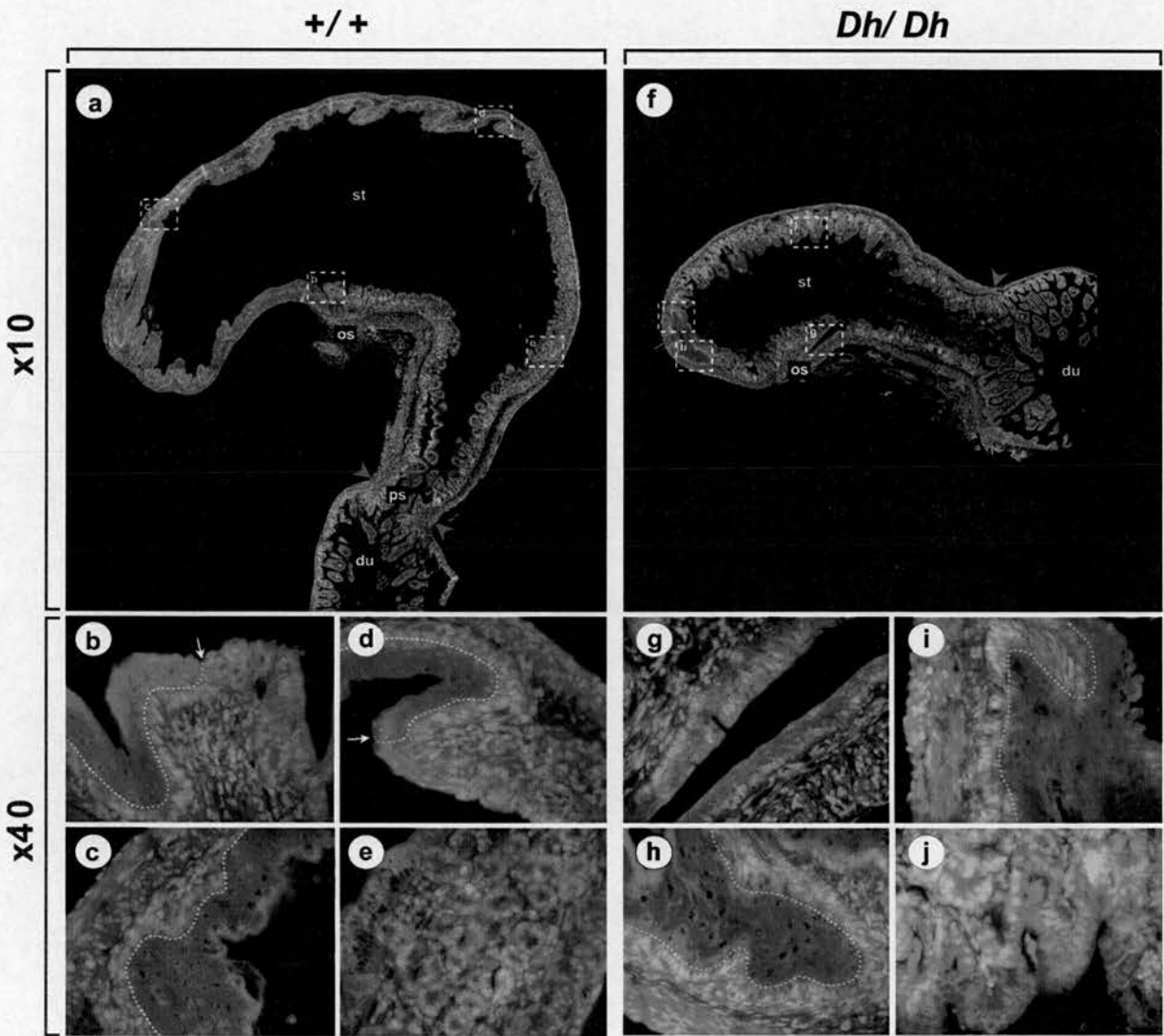


Figure 4.15: The anterior stomach and pyloric sphincter is missing in *Dh/Dh* embryos. Wax sections of E18.5 stomach stained with Phalloidin (red) and Yo-pro1 (green) recognizing F-actin filaments and individual nuclei respectively. (a) Composite picture of an E18.5 *+/+* stomach. The anterior stomach is lined with a mucus membrane while the posterior stomach is covered with villi. The muscle layer is also thicker in the posterior half of the stomach. The pyloric sphincter can be seen as a narrowing of the stomach lumen and a thickening of the muscle layer at the boundary between the stomach and the duodenum (blue arrowheads). (b) High magnification of area b in (a) showing the posterior-anterior boundary (white arrow). This is also the region where the oesophagus enters the stomach. (c) High magnification of area c in (a) showing the mucus membrane lining the anterior part of the stomach. (d) High magnification of area d in (a) showing the anterior-posterior boundary (white arrow). (e) High magnification of area e in (a) showing the morphology of the posterior half of the stomach. (f) Composite picture of an E18.5 *Dh/Dh* stomach. Only a very little part of the stomach is lined with mucus membrane (blue arrow) which is the characteristic of the anterior stomach. The rest of the stomach appear to have posterior identity. Also there is no pyloric sphincter (blue arrowheads) (g) High magnification of area g in (f). This is the region where the oesophagus enters the stomach, but there is no anterior-posterior boundary. (h) High magnification of area h in (f) showing the the posterior-anterior boundary at the tip of the stomach. (i) High magnification of area i in (f) showing the the anterior-posterior boundary. (j) High magnification of area j in (a) showing the morphology of the posterior stomach. (st) stomach lumen, (du) duodenum, (os) oesophagus and (ps) pyloric sphincter. The base of the mucus layer is outlined with a white dashed line.

The gut ends blind at the midgut-hindgut junction in *Dh/Dh* embryos

Most of the phenotypic analysis of *Dh* has concentrated on the effects the mutation has on the spleno-pancreatic region and the stomach. However the mutation also affects hindgut development and a few experiments were carried out to look at this aspect of the phenotype.

The junction between the large intestine and the colon defines the boundary between the midgut and the hindgut (figure 4.16f). The cecum, a small extension of the gut tube, which ends blind, also correlates with this boundary. At E18.5 there are no obvious differences between the large intestine and the colon and the best way to determine the hindgut-midgut boundary is to locate the cecum (figure 4.16a). The large intestine is outlined in black, the cecum in red and the colon in white. When dissecting out the gut from *Dh/Dh* it became clear that colon was absent and as a result the gut ends in a T-shape level of the cecum (figure 4.16b).

To investigate the hindgut phenotype further E10.5 embryos were stained as whole mounts with antibodies against Hnf3 β . Hnf3 β a marker for the definitive endoderm and is expressed throughout the intestinal tract (Ang et al., 1993). In +/+ embryos the endoderm could be seen as a continuous tube running from the developing mouth in the anterior end to the cloaca in the posterior end. In the posterior end the gut forms a loop, which defines the boundary between the hindgut and the midgut (white arrow). In *Dh/Dh* the endoderm of the hindgut is severely impaired and the endodermal tube is much thinner than in wild type (figure 4.16d). In addition a part of the hindgut has degenerated so there is a gap between the hindgut and midgut.

The comparison of *Hoxc10* expression and *Wt1* expression between +/+ and *Dh/Dh* in chapter 3 also showed that the posterior endoderm is affected by the *Dh* mutation. Here it was found that *Hoxc10* is expressed around the endoderm in the posterior part of the gut (figure 3.2a, b; black arrows: see also figure 2.4a; red arrow). However this expression domain is absent in *Dh/Dh* embryos. Also, when looking at *Wt1* expression it was clear that the diameter of the *Dh/Dh* hindgut is much smaller than wild type and that the lumen within the endoderm is absent (figure 3.4; black arrows).

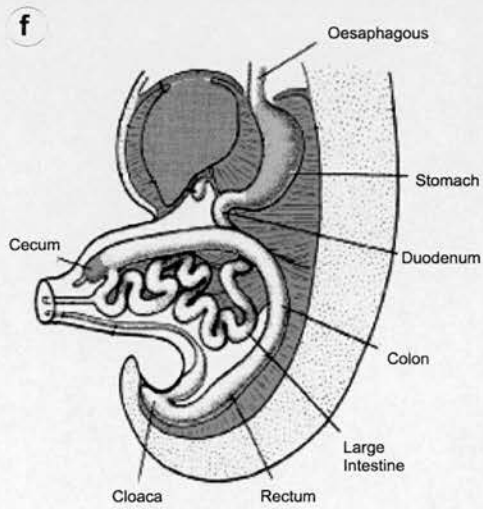
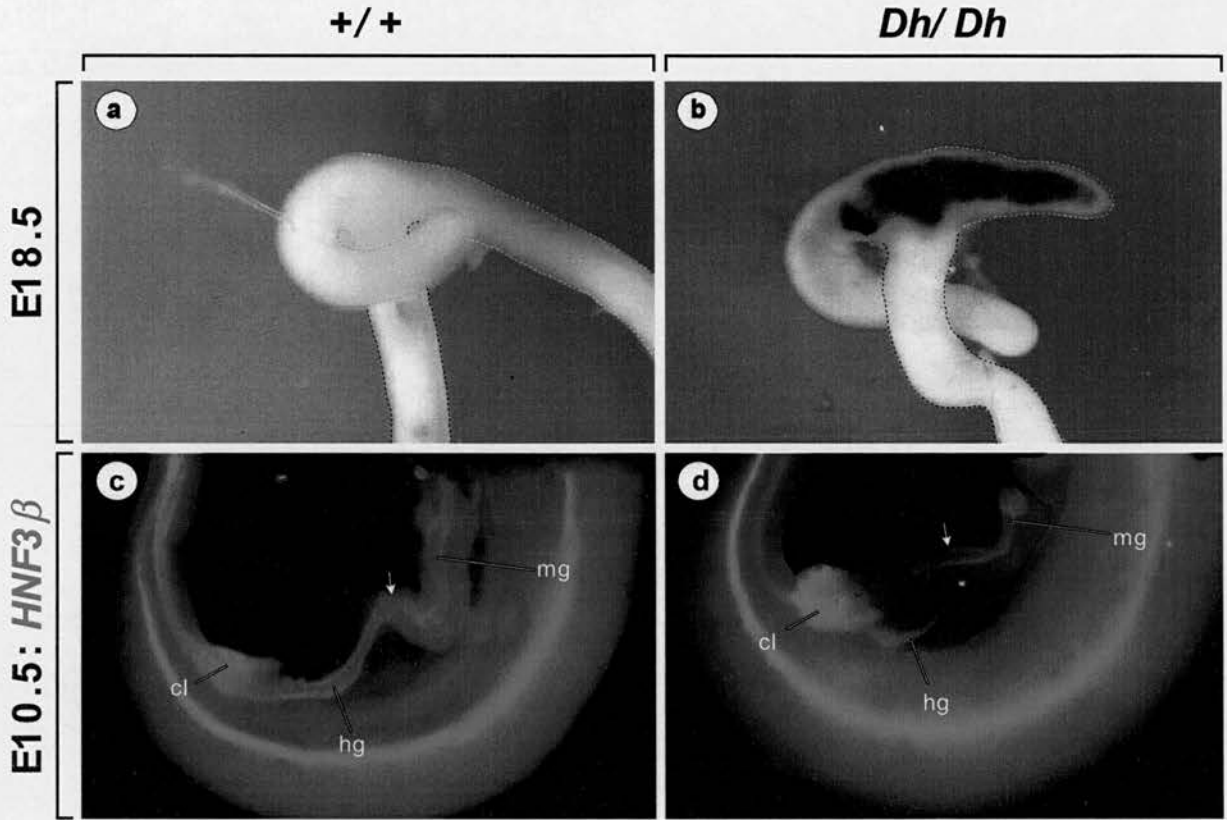


Figure 4.16: Blind ending of the gut in *Dh/Dh* embryos. In mice homozygous for the *Dh* mutation the hindgut is abnormal and the gut ends blind at the level of the cecum. **(a)** Wild type intestine at E18.5. The cecum is outlined in red while the large intestine and the colon are outlined in black and white respectively. **(b)** In *Dh* homozygous animals the cecum is present but the colon has degenerated. As a result the gut end in a T-shape with both arms ending blind. **(c)** E10.5 wild type embryo stained with antibodies against HNF3β. The gut tube forms a loop which defines the boundary between the hindgut and the midgut. The cecum will form at the tip of this loop (white arrow). **(d)** In *Dh/Dh* the endodermal tube of the hindgut is very thin compared to wild type and in addition there is a gap between the hindgut and the midgut. **(f)** schematic illustration showing the digestive system at E11.5. The cecum (red) is positioned at the boundary between the midgut and the hindgut (downloaded from http://www.med.unc.edu/embryo_images). (cl) cloaca, (hg) hindgut and (mg) midgut

4.7 Discussion

During vertebrate development several organs such as the heart, lungs, stomach, spleen and liver are displaced towards one side of the embryo and develop asymmetrically relative to the midline. Recently much effort has been put into understanding how asymmetry is achieved and this has revealed an intricate genetic pathway (for review see Roberts, 2000; Capdevila et al., 2000). In many cases the genes involved in this pathway are expressed in an asymmetric manner prior to any morphological differences and in their absence the asymmetry is either lost or randomised. However, little is known about how these left-right signals are interpreted by cells in the developing organs and subsequently mediated into asymmetric development.

The SMR mediates a physical requirement for left right asymmetry

From studying the *Dh* mutation it has been possible to identify a structure called the Splanchnic Mesothelial Ridge (SMR), which is required for asymmetric growth of the spleno-pancreatic region (figure 4.17). At E9.5 a splanchnic mesothelial plate can be observed on both sides of the endoderm, first described by Green in 1967. However, during subsequent stages of development the mesothelial ridge on the right side disappears while the ridge on the left side thickens and become the SMR. Concurrently as the SMR thickens the spleno-pancreatic region starts to expand, but only on the left side where the SMR is present. BrdU labelling shows that cells in the SMR are dividing rapidly thereby providing a mechanism for the leftward expansion. In mutants where the SMR is absent or defective asymmetry is disrupted and as a result the dorsal pancreas remains at the midline instead of growing towards the left. These results therefore strongly imply that the SMR is mediating a physical requirement for establishing left-right asymmetry in the spleno-pancreatic region. However, apart from the Green's description of the splanchnic mesothelial plate at E9.5 there are no descriptions of the SMR in the literature. Hence we propose that the SMR is a novel embryonic structure, which functions to mediate asymmetric development. This theory is further strengthened by the presence of *Fgf9* and *Fgf10* expression in the SMR.

The *in situ* analysis has shown that asymmetric genes such as *Pitx2* and *Barx1* are expressed at high levels in the SMR before it thickens. It is therefore possible that the SMR is a direct target of the asymmetric pathway. One way to demonstrate this would be to show that the SMR responds to left-right signalling. Mice carrying

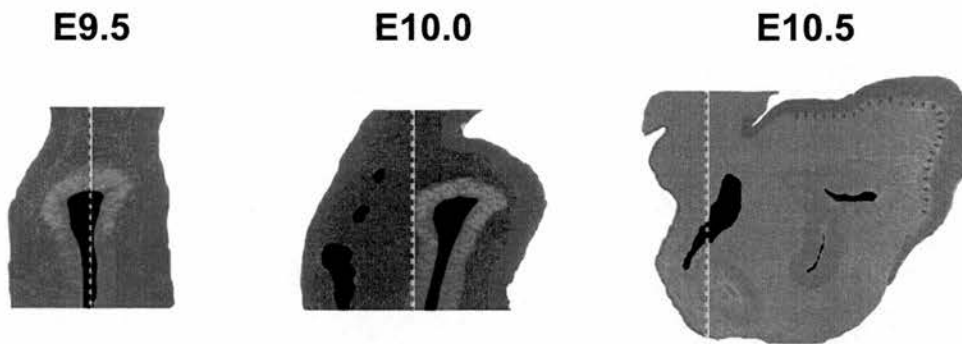


Figure 4.17: The SMR mediates asymmetric growth towards the left. Model showing three stages of SMR development. At E9.5 the right mesothelial plate (blue) and the left mesothelial plate (green) are equally thick and positioned symmetrically on both sides of the pancreatic endoderm (red) and the embryonic midline (white dashed line). However at this stage the left mesothelial ridge is expressing asymmetric genes like *Pitx2* and *Barx1* and is presumably signalling to the underlying mesoderm to promote growth (green arrows). Half a day later at E10.0 the left mesothelial plate is starting to thicken and is signalling more intensely. At the same time the right mesothelial ridge is starting to disappear. As a result the spleno-pancreatic region is expanding towards the left side and the pancreatic endoderm is no longer positioned at the midline. At E10.5 the SMR is fully developed and the right mesothelial ridge no longer visible. Several *Fgf's* are expressed in the SMR to stimulate growth and at this stage almost the entire region is positioned left of the embryonic midline. Growth of the pancreas is also stimulated by signals from the SMR and as a result the pancreatic endoderm is positioned in the pocket formed by the SMR.

homozygous deletion in the gene *situs inversus (inv)* display complete reversal of all asymmetry and consequently the SMR should develop on the right side. Dr Judith Goodship was approached and agreed to send some *inv*^{-/-} embryos for analysis.

The SMR is a novel embryonic structure

Since the SMR has not been described previously it was necessary to analyse it using molecular markers. In particular it was important to establish whether the SMR represented the early stages of spleen development. Using probes to most genes reported to have a function in spleen development it became clear that the SMR is not the spleen, because most of these genes were specifically excluded from the SMR. In fact the only place where the expression patterns of all genes overlapped was in the mesenchyme between the SMR and the dorsal pancreatic endoderm.

Interestingly the initially expression of *Hox11* and *Nkx2.5* is restricted to the mesenchymal cells directly under the SMR, indicating that the SMR might be responsible for inducing the spleen. Furthermore in *Dh* and *Bapx1*^{-/-} mutant mice the SMR is either missing or defective respectively and in both cases the spleen fails to be induced. However, at present these results are not conclusive, because it remains possible that both *Dh* and *Bapx1* affects spleen development directly through the mesenchyme. *Bapx1* is expressed in both the SMR and in the mesenchyme and could therefore be affecting spleen development directly through the mesenchyme or indirectly through the SMR. For *Dh* the gene affected by the mutation is unknown and it is therefore difficult to predict at what level the mutation affects spleen development. The SMR is completely absent but at present it is unknown to what extent the mesenchyme is affected. In *Dh*/+ embryos the mesenchyme appears to be relatively normal and is expressing all markers except *Hox11* and *Nkx2.5*. However, in *Dh/Dh* embryos the expression of some mesenchymal genes such as *Bapx1* is severely reduced or absent and several asymmetrically expressed genes such as *Barx1* and *Pitx2* are expressed symmetrically. These observations suggest that the *Dh* mutation is affecting the mesenchyme and hence the mutation could be affecting spleen development directly.

Attempts have been made to answer this particular question on basis on the following assumption: If the *Dh* mutation affects spleen induction through the SMR and the mesenchyme is normal, then it must be possible to induce *Hox11* and *Nkx2.5* expression in *Dh* cells. Furthermore, if the mesenchyme is normal in *Dh* and only thing missing is an inductive signal that would confirm that the SMR is required for induction of the spleen. There is reason to think that this assumption might be

correct, because in $+/+ \Leftrightarrow Dh/Dh$ chimeras a rudimentary spleen is formed even when *Dh/Dh* cells make up >90% of the embryo (Suto et al., 1995). The authors also demonstrate that *Dh* cells are contributing to spleen development, but this conclusion is only based on Gpi-1 allelism and since the spleen is populated by blood and lymph cells the results must be considered with some degree of caution. Nevertheless, they conclude that *Dh* cells can contribute to spleen development and hence it should be possible to induce *Hox11* and *Nkx2.5* expression in *Dh* cells. However, instead of using a chimeric approach an in vitro culture system was set up with help from Dr. Ulf Ahlgren. The idea was to label *Dh* mesenchyme with DiO and graft them under a wild type SMR. However, at present no conclusive results have been obtained but the project has been taken over by Alison Wright.

Additional roles of the SMR

Another role of the SMR might be to direct the growth of the dorsal pancreas. In wild type embryos the pancreatic endoderm is aligned with the ventral part of the SMR and is growing towards the tip. However, in both *Dh* and *Bapx1*^{-/-} embryos where the SMR is disrupted the dorsal pancreas shows abnormal growth and loss of asymmetry. Interestingly this phenotype coincides with abnormal expression of *Fgf10*. In wild type embryos, *Fgf10* is expressed in the ventral SMR and underlying mesenchyme and is therefore expressed along the left side of the pancreatic endoderm. However, in *Dh* embryos where the SMR is absent, *Fgf10* expression is almost completely lost. At the same time the dorsal pancreas remains aligned with the midline and shows no sign of asymmetric growth. In *Bapx1*^{-/-} embryos where the SMR is defective, *Fgf10* expression is no longer restricted to the left side of the pancreatic endoderm. Instead diffuse expression can be detected on both side of the endoderm and as in *Dh* the pancreas fails to undergo asymmetric growth. It therefore appears that the SMR is providing a defined source of *Fgf10* signalling which is required to promote asymmetric growth of the dorsal pancreas.

Because the absence of an SMR in *Dh* embryos has dramatic consequences on pancreatic growth, it became interesting to analyse if this affected differentiation of the pancreatic cell types. However, antibody staining revealed that the late *Dh* pancreas is relatively normal and that all the endocrine cell types are present. The same is true for the late *Bapx1*^{-/-} pancreas (Ahlgren, unpublished data). It therefore appears that although the SMR is important for pancreatic growth it has little or no effect on differentiation of the pancreatic cell types.

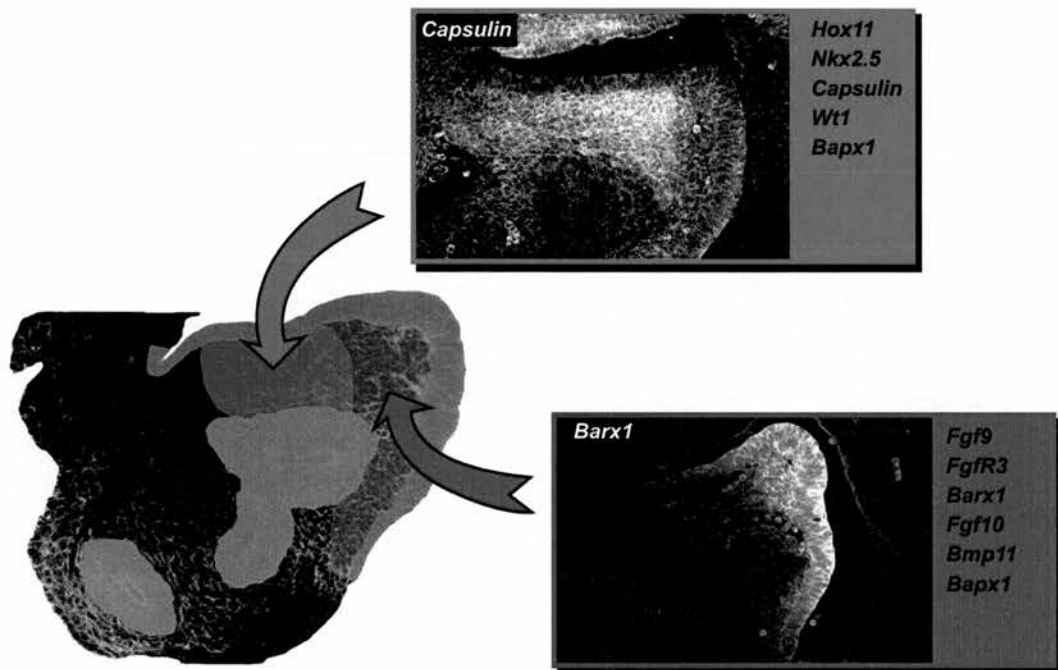


Figure 4.18: Regionalisation within the spleno-pancreatic region. Model showing regionalised gene expression within the spleno-pancreatic region at E10.5. Several genes are expressed in the splenic mesenchyme (red) while other genes are expressed in the tip and ventral part of the region (blue). Most genes expressed in the region are restricted to one of the two domains. The examples shown are *Capsulin* and *Barx1*.

Regionalisation within the spleno-pancreatic region

When analysing the expression patterns of genes in the spleno-pancreatic region it became clear that in many cases the genes fall into specific categories according to their expression pattern (figure 4.18). Hence most gene expressed in the splenic mesoderm are excluded from the mesoderm underlying the tip of the SMR while genes expressed in the ventral part and tip of the SMR are often excluded from the splenic mesoderm. This regionalisation of gene expression strongly indicates the presence of defined boundaries within the mesoderm. Interestingly an important function of the SMR might be to maintain these boundaries. In wild type embryos *Capsulin* expression is completely excluded from the SMR and the mesenchyme at the tip. However, in both *Dh* and *Bapx1*^{-/-} embryos *Capsulin* is expressed throughout the mesenchyme. Thus in the absence of a functional SMR *Capsulin* expression is no longer restricted to the splenic mesenchyme. At present the best explanation for this regionalisation is that factors secreted from the tip of the SMR, repress the expression of *Capsulin* and in absence of these factors *Capsulin* expression is upregulated in the tip mesenchyme.

Genetic interactions underlying spleen development

The expression of splenic markers in asplenic mice might provide important information about the genetic hierarchy underlying the earliest stages of spleen development (table 4.5).

Structure/gene	<i>Dh</i>	<i>Bapx1</i> ^{-/-}	<i>Wt1</i> ^{-/-}	<i>Capsulin</i> ^{-/-}	<i>Hox11</i> ^{-/-}
Functional SMR	x	x	✓	(✓)	(✓)
<i>Hox11</i>	x	x ¹	✓ ²	✓ ³	-
<i>Nkx2.5</i>	x	x	?	?	?
<i>Bapx1</i>	✓	-	?	✓ ³	?
<i>Capsulin</i>	✓	✓	✓	-	?
<i>Wt1</i>	?	?	-	?	✓ ²

✓ Functional SMR or expression detected
 (✓) SMR Assumed to be functional since the gene is not expressed in the mesothelium
 x Defective SMR or no expression detected
 ? No experimental data available
 1 (Lettice et al., 1999b)
 2 (Herzer et al., 1999)
 3 (Lu et al., 2000)

In both *Dh* and *Bapx1*^{-/-} embryos the expression of *Nkx2.5* and *Hox11* (Lettice et al., 1999b) is never induced. However, the *Capsulin* gene is expressed in the splenic mesenchyme of both mutants. *Bapx1* expression in *Dh* embryos is complicated because it varies between *Dh/+* and *Dh/Dh*. In heterozygous embryos *Bapx1* is expressed in what appears to be a normal pattern while in homozygous embryos expression levels are severely reduced. But, because *Bapx1* is expressed in heterozygotes it is clear that the asplenic phenotype is independent of *Bapx1*. Additionally, it has been shown that *Bapx1* and *Hox11* are expressed during early stages of spleen development in *Capsulin*^{-/-} embryos (Lu et al., 2000) and both *Capsulin* and *Hox11* (Herzer et al., 1999) expression can be detected in *Wt1*^{-/-} embryos. Finally, *Wt1* is expressed in the spleen anlage of *Hox11*^{-/-} (Herzer et al., 1999) although the expression levels might be somewhat reduced compared to wild type (Koehler et al., 2000). The assumption, that the SMR is normal in *Capsulin*^{-/-} and *Hox11*^{-/-} embryos, is based on the fact that these genes are not expressed in the SMR and it is therefore unlikely that they should affect it.

With the data available at the moment it is not possible to predict one unifying mechanism for spleen development. There are several observations, which could be explained equally well through different mechanisms. It appears that there are several different genetic pathways, which must converge during development to give rise to the mature spleen. This idea is also put forward by (Lu et al., 2000), but another possibility is that the genes are acting at different stages during development. However, because the descriptive analysis of each mutation is looking at different stages of spleen development it is sometimes difficult to draw direct comparisons between the data. The model in figure 4.19, shows at what stage the different mutations are acting during spleen development. Spleen development is initiated around E10.5 in the mesenchyme between the dorsal pancreas and the SMR (1). A signal secreted from the dorsal part of the SMR (2), activates *Hox11* expression in the underlying mesenchyme (3). Cells expressing *Hox11* differentiate into spleen precursor cells (4). During subsequent development these cells mature (5) and start to proliferate (6).

Starting at the late stages of spleen development, it seems certain that *Wt1* is the last gene to be activated in the spleen pathway. Although *Wt1* expression can be detected in the splenic mesenchyme from E10.5 onwards, a rudimentary spleen is present in *Wt1*^{-/-} embryos (Herzer et al., 1999). Confirming that the mesenchymal cells have the capacity to differentiate into mature spleen cells in the absence of *Wt1*. Also *Wt1* is expressed in the splenic mesenchyme in *Hox11*^{-/-} where mature spleen cells are absent suggesting that *Wt1* expression is not directly associated with the

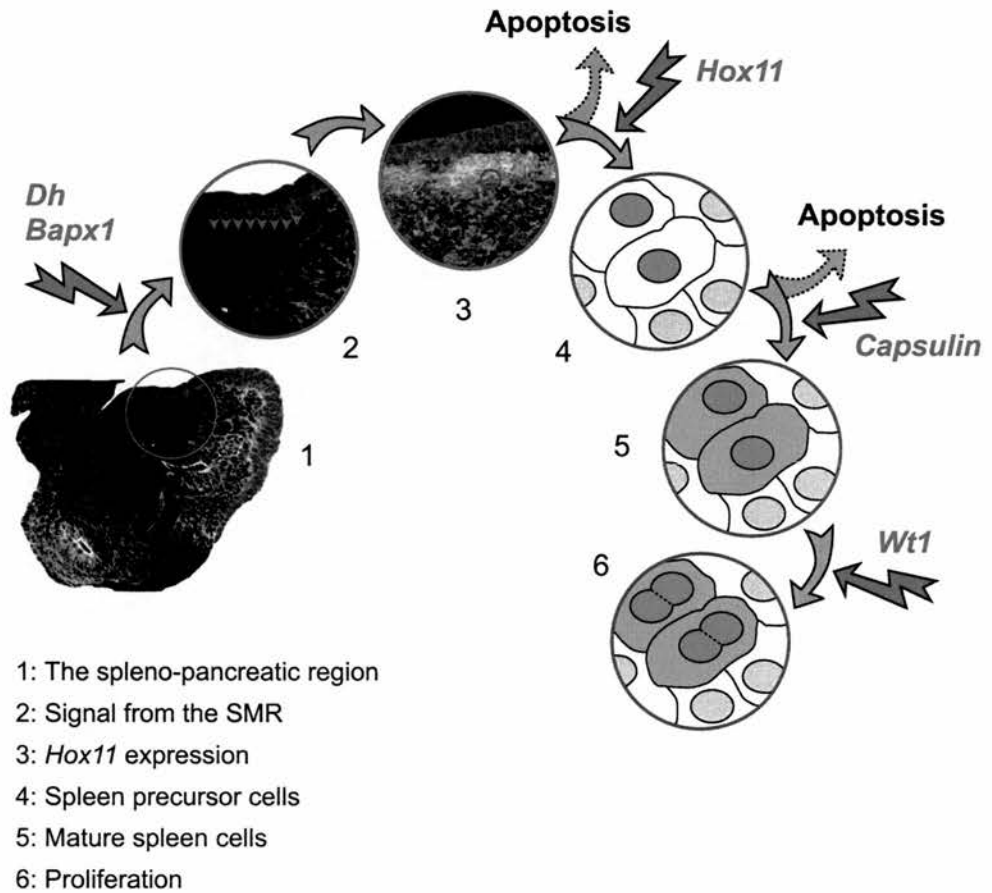


Figure 4.19: Genetic pathway for spleen development. A signal from the SMR induces *Hox11* expression in the mesenchyme directly under the SMR. *Hox11* is expressed in spleen precursor cells and is required for their differentiation. Later in development the spleen precursor cells differentiate and become mature spleen cells and *Capsulin* is required for this process. In the absence of *Capsulin* the cells undergo apoptosis. Finally *Wt1* is required for proliferation of the mature spleen cells. The SMR is highlighted in blue. A step affected by a mutation is indicated with a red arrow and the name of the mutation.

splenic cell fate. A possible role for *Wt1* is therefore that the gene is acting after the mature spleen cells have differentiated perhaps to stimulate proliferation. The role of *Capsulin* is also asserted relative late during spleen development. Hence, the initial stages of spleen development appear to be normal in *Capsulin*^{-/-} embryos and expression of both *Hox11* and *Bapx1* can be detected in the splenic primordia (Lu et al., 2000). However in the absence of *Capsulin* the spleen precursor cells starts to undergo apoptosis around E13.5 and as a result the mature spleen never appear. The expression of *Capsulin* can be detected in the splanchnic mesenchyme from E9.5 and therefore precedes the defects observed in *Capsulin*^{-/-} embryos by several days. Nevertheless, the conclusion from these results therefore suggests that *Capsulin* affects spleen development after the spleen precursors cells have differentiated but before the mature spleen cells appear. *Capsulin* has no effect on early spleen development despite the early expression. The expression of *Hox11* is strictly associated with the splenic mesenchyme through all stages of spleen development (Roberts et al., 1994; Dear et al., 1995). In the absence of *Hox11* the spleen precursor cells undergo apoptosis around E12.5, a day earlier than *Capsulin*. Combined with the expression data presented in this chapter these results confirm that *Hox11* is the earliest and most specific marker of spleen development and is required to direct the splanchnic mesenchyme towards a splenic fate. *Nkx2.5* might also have an important in this process, but although the gene has been knocked out there is no description of the splenic phenotype (Schott et al., 1998; Tanaka et al., 2001). When studying gene expression in the spleno-pancreatic region it became clear that *Hox11* and *Nkx2.5* expression is induced directly under the dorsal part of the SMR. This observation strongly implies that the spleen is induced by a signal from the ridge. An additional step, showing the spleen-inducing signal emanating from the SMR (blue arrows), has therefore been included in the model. Accordingly, *Hox11* and *Nkx2.5* expression are the first visible signs of spleen development, but in absence of the SMR signal all gene expression associated with splenic cell fate associated is abolished. In agreement with the model *Dh* and *Bapx1* are the only mutations affecting the SMR and in both mutants no *Hox11* and *Nkx2.5* expression can be detected (this is based on the assumption that the SMR is normal in *Capsulin*^{-/-} and *Hox11*^{-/-} embryos). *Bapx1* and *Dh* are therefore the earliest acting mutations with respect to the genetic pathway underlying spleen development and they manifest the asplenic phenotype by disrupting the spleen inducing signal from SMR. At the time of spleen induction genes like *Capsulin* and *Bapx1* are not exclusively associated with spleen precursor cells and their expression is unaffected by the absence of a functional SMR.

Left right asymmetry in *Dh/Dh* embryos

At the level of the pancreas the phenotypic abnormalities are very similar between *Dh/+* and *Dh/Dh*. However, at the level of the stomach the homozygous phenotype is much more severe than the heterozygous. In *Dh/+* embryos the stomach develops asymmetrically on the left side of the embryo, and the mature stomach is very similar to wild type, perhaps slightly smaller. In *Dh/Dh* the stomach does not develop asymmetrically and as a result it is positioned closely to the midline. Also the mature stomach is reduced to half the size of a wild type stomach. A histological analysis showed that this reduction happens on expense of the anterior portion of the stomach. The failure of *Dh/Dh* stomachs to turn coincides with mirror-image duplications of asymmetric genes such as *Pitx2* and *Barx1*. The obvious conclusion from these expression patterns is that *Dh* homozygotes display left isomerism where the left side has been duplicated along the anterior-posterior axis. However, the asplenic phenotype associated with *Dh* suggests that the mutation causes right isomerism. One explanation for this paradox is that *Dh* has two effects on spleen development. An early effect, which results in ectopic expression of left specific genes in the right splanchnic mesenchyme and a late effect, which prevents induction of genes, required for spleen development. In *Dh/+* embryos, the stomach develops asymmetrically and no ectopic expression of *Pitx2* and *Barx1* can be detected, suggesting that the loss of asymmetry is specific for homozygous embryos. Hence the effect of the *Dh* mutation is affecting the left-right pathway in a dose dependent manner. Although the laterality defects observed in homozygous mice show complete penetration, the stomachs always display some degree of asymmetry towards the left side. The reason for this is that the mirror-image duplication is not complete. *Pitx2* and *Barx1* are always induced ectopically on the right side but never in the same levels as seen on the left side. Another interesting aspect of the *Dh* mutation is that it only affects laterality in the gut. Hence the looping of the heart and the number of lobes in the lungs are always normal in *Dh* mice. One explanation for this could be that the mutation affects left-right asymmetry relatively late. As the node progresses from anterior to posterior, left right asymmetry is laid down by a cilia mediated flow across the node (Nonaka et al., 1998). Since the node is progressing from anterior to posterior it is possible that a mutation acting relatively late in this process specifically would affect more posterior organs such as the stomach. Another possibility is that left-right asymmetry of a particular organ is controlled by the organ itself. The initial asymmetry is established early during development through a general mechanism such as the nodal flow. However, once the individual organs start to develop the left-right information is maintained and mediated through pathways

specific for each organ. A mutation affecting this specific pathway would therefore only affect the symmetry in that particular organ. In agreement with this hypothesis it has been shown that mice carrying homozygous deletions of the *Pitx2* gene only affects asymmetry in the lungs (Gage et al., 1999).

Other gut abnormalities in *Dh* embryos

When dissecting out the gut from *Dh* foetuses it is immediately clear that the gut displays abnormal looping. Hence the duodenum forms a sharp bend just posterior of the stomach. The analysis of the spleno-pancreatic region clearly demonstrated that in the absence of the SMR there is no leftward expansion and the dorsal pancreatic endoderm remains in alignment with the midline. At E10.5 the duodenum is very closely associated with the spleno-pancreatic region. The retarded growth of this region undoubtedly affects the morphology of the duodenum and therefore it is not surprising that this particular part of the gut is abnormal in *Dh* embryos.

However, a histological analysis of late *Dh/Dh* stomachs revealed that the duodenal abnormalities also included loss of the pyloric sphincter. It has recently been demonstrated in chicken that *Nkx2.5* is a marker for the pyloric sphincter and is required for its development (Smith et al., 2000). The *in situ* analysis of *Nkx2.5* showed that the gene is expressed in the splenic mesenchyme and in the ventral part of the SMR adjacent to the duodenum. In *Dh* embryos both expression domains of *Nkx2.5* are absent. The loss of the pyloric sphincter in *Dh* embryos might therefore be a direct consequence of the lack of *Nkx2.5*.

The last aspect of the *Dh* mutation is the blind ending of the gut. In contrast to the other gut abnormalities described in this chapter the truncation of the gut happens at the level of the cecum and is therefore not related to the absent SMR. It is more likely that the truncated gut is associated with the abnormalities found in the posterior part body. However, this part of the gut phenotype was only discovered towards the end of this project so no efforts were made to pursue it further.

Nevertheless, it raised two important questions concerning the effect *Dh* has on development. First it showed that the posterior phenotype is unlike to be mediated through *Hoxc10* alone. Initially it seemed like misexpression of *Hoxc10* could also be responsible for this part of the phenotype, since no *Hoxc10* expression was found in the gut of mutant embryos (figure 3.2a, b; black arrows). However, recently it was demonstrated that deletion of the entire *Hoxc* cluster has no effect on the gut (Suemori and Noguchi, 2000) so other factors must be involved. The other question was that *Dh* affected the endoderm. At E10.5 the lumen of the hindgut is absent

(figure 3.4; black arrows). Additionally Hnf3 β staining showed that the endoderm of the hindgut is severely abnormal. The problem is that if *Dh* affects the endoderm in the posterior part of the embryo it might also affect the endoderm in the spleno-pancreatic region. This came as a surprise because it was believed that the abnormalities inflicted by the *Dh* mutation were restricted to the SMR and the mesenchyme. Although spleen development can occur in absence of the pancreatic endoderm (Jonsson et al., 1994; Ahlgren et al., 1996; Offield et al., 1996; Li et al., 1999), it has been demonstrated that ectopic expression of *Shh* in the dorsal pancreatic endoderm causes asplenia (Apelqvist et al., 1997). It has also been shown that *Shh* is expressed ectopically in the hindlimbs of *Dh/+* embryos (Hecksher-Sørensen, 1998; Lettice et al., 1999a) and one of the candidate gene for the *Dh* mutation is *Gli2*, a member of the *Shh* pathway. Due to difficulties in obtaining homozygous embryos the expression of *Shh* in the spleno-pancreatic region has not been analysed in *Dh* embryos. However, there is indirect evidence that the *Shh* expression is normal. The expression pattern of *Shh* in the endoderm is the reciprocal of *Pdx1* expression and it is believed that *Shh* represses *pdx1* expression. Also ectopic expression of *Shh* in the pancreatic endoderm has severe effects of the differentiation of pancreatic cell types (Apelqvist et al., 1997). If *Shh* was ectopically expressed in the endoderm it would therefore affect the expression of *Pdx1* and affect differentiation of the pancreatic cell types. However, PDX1 protein is present in the pancreatic endoderm of *Dh* embryos and the late pancreatic phenotype is normal, suggesting the *Dh* mutation is not affecting the endoderm in the midgut and foregut.

4.8 Conclusion

The SMR is a novel embryonic structure required for asymmetric growth. It appears transiently between E9.5 and E11.5 and through rapid proliferation it directs the growth of the spleno-pancreatic region towards the left side of the embryo. In absence of a functional SMR the region fails to undergo asymmetric displacement and as a result the pancreatic buds remain in alignment with the midline. Additionally the SMR might be required for induction of the spleen and for establishing/maintaining regionalised gene expression in the spleno-pancreatic region.

Using a various genetic markers for spleen development and a number of asplenic mutants it has been possible to explore the genetic pathway required for spleen development. It has been demonstrated that *Dh* and *Bapx1* affects spleen development very early by disrupting spleen induction presumably via the SMR. In *Wt1*^{-/-} embryos the SMR is normal and the early stages of spleen development is normal.

Chapter 5: Discussion

5.1 Introduction

Mice carrying the *Dh* mutation suffer from a variety of abnormalities. However, the gene affected by the mutation remains unknown and so far all attempts to positional clone the gene have turned out to be unsuccessful. Nevertheless the critical region has been narrowed down to approximately 1Mb on mouse chromosome 1 (Higgins et al., 1992; Hughes et al., 1997; Lettice, unpublished data). The project described in this thesis has not been directly involved in the attempts to clone *Dh*. However, some results obtained provide additional information concerning the nature of the mutation and in this chapter these results will be discussed in relation to other observations from the literature.

5.2 The *Inh β b* gene

Members of the *Inh β b* pathway are involved in all aspects of the *Dh* phenotype. The *Inh β b* gene is positioned within the *Dh* critical region and there are several observations, which makes *Inh β b* a very good candidate for being the gene affected by the mutation. *Inh β b* encodes a subunit required for activinB and activinB. Activin is a secreted molecule required for many developmental processes and although studies in mouse have demonstrated that the absence of *Inh β b* has little effect on development (Vassalli et al., 1994; Schrewe et al., 1994), it is clear that misexpression of this gene can have severe consequences on subsequent development. In *Xenopus* activin induces mesoderm formation at the expense of other germ layers when misexpressed (Smith et al., 1990) and in Chicken ectopic application of activin disrupts left-right asymmetry (Levin et al., 1995; Stern et al., 1995; Boettger et al., 1999). Also in mouse *Inh β b* disrupts development when it is expressed in the *Inh β a* locus (Brown et al., 2000). Hence, there is little doubt that misexpression of *Inh β b* could disrupt the development of many organs as does *Dh* and because *Dh* is dominant it might well be affecting the regulation of gene expression. In addition to this, members of the *Inh β b* pathway can account for almost every phenotype observed in *Dh*. Mice carrying homozygous deletions of the activin receptor *ActRIIb*, display homeotic abnormalities in the axial skeleton, shifted

position of the hindlimbs, impaired spleen development and left-right anomalies (Oh and Li, 1997; Kim et al., 2000). In addition, when the *ActRIIb* mutation is combined with deletion of *ActRIIa*, the anterior-posterior identity of the stomach endoderm is altered (Kim et al., 2000). In mice carrying a targeted deletion in *Bmp11*, a closely related TGF β molecule, the hindlimbs are shifted posteriorly and the shift correlates with altered expression of *Hox* genes, in particular *Hoxc10* (McPherron et al., 1999). activin has also been linked with the regulation of *Gata2* (Walmsley et al., 1994), which has been associated with kidney abnormalities identical to those observed in *Dh* (Zhou et al., 1998). In fact the only phenotype, which have not been associated with *Inh β b*, is the late limb phenotype. However, there is accumulating evidence that different members of the TGF β family share receptors and are inhibited by the same factors. Hence it has been proposed that *Bmp11* acts through the *ActRIIb* receptor (McPherron et al., 1999). Also, the *BAMBI* gene product will inhibit members of both the Bmp and activin families (Onichtchouk et al., 1999). Several members of the Bmp family are expressed in the developing limb and *Bmp2* in particular has been associated with digit duplication in chicken (Duprez et al., 1996). So one way *Inh β b* could affect patterning of the developing limb in *Dh* is by interfering with endogenous Bmp signalling

***Inh β b* is misexpressed in *Dh* embryos**

When carrying out the multiplex PCR, screening for genes expressed in the SMR, most genes were expressed at the same levels in wild type and mutant embryos. In fact *Inh β b* was the only gene to be differentially expressed (figure 5.1a). In stomachs from wild type embryos *Inh β b* is expressed at very low levels while a distinct band can be detected in stomachs from *Dh* embryos. In contrast the bands representing the internal control (*G6PDH*) display the same intensity in both wild type and mutant embryos. Similarly, the RNA samples isolated from the posterior part of the body also show higher expression of *Inh β b* in *Dh* embryos. It was possible to repeat these results from a new batch of cDNA and therefore it appears that the *Inh β b* gene specifically is upregulated or misexpressed in embryos carrying the *Dh* mutation. Attempts were made to visualise the expression pattern of *Inh β b* in *Dh* stomachs using *in situ* hybridisation. However, it was not possible to detect any transcription either using DIG labelled probes or S³⁵ labelled probes (data not shown), suggesting that expression levels are very low.

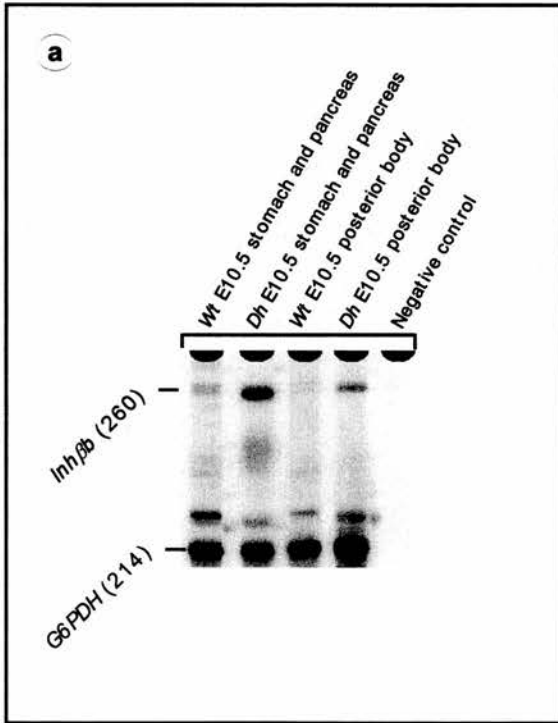


Figure 5.1: RT-PCR showing upregulation of *Inhb* in *Dh* embryos. (a) *Inhb* expression is elevated in both stomach and posterior body of mutant embryo at E10.5. The internal standard *G6PDH* expressed consistently in all tissues.

Attempts were made to sequence the open reading frame of *Inhβb*. *Inhβb* consists of two exons, which were amplified with PCR using +/+ and *Dh/Dh* genomic DNA as template (data not shown). However, as with previous attempts (Hughes, unpublished data) no conclusive differences were found between the *Inhβb* gene from +/+ and the *Dh/Dh*. Suggesting that the coding region of the *Inhβb* gene is normal.

Degenerate primers that would recognise members of the inhibin and Bmp families (appendix III) were used to screen the YAC contig spanning the *Dh* critical region. However, only *Inhβb* was detected, suggesting that this gene is the only detectable member of the two families within the region.

5.3 The *Gli2* gene

The *Shh* pathway is involved in many aspects of *Dh* abnormalities

The *Gli2* gene is one of three mammalian homologues of the *Drosophila* gene *Cubitus Interruptus (Ci)*. The *Gli* genes and *Ci* are all Zinc finger transcription factors and have been shown to have a role in mediating *Hedgehog* signalling (Dominguez et al., 1996; Methot and Basler, 1999; Methot and Basler, 2001). It has previously been demonstrated that the polydactylous phenotype observed in *Dh* coincides with ectopic expression of *Shh* (Hecksher-Sørensen, 1998; Lettice et al., 1999a) an observation that correlates well with the idea that GLI2 is a repressor of *Shh* signalling. Also *Gli3*, which is a homologue of *Gli2*, is responsible for another *Luxoid* mutation *extra-toes (Xt)* (Hui and Joyner, 1993). Like *Dh* the *Xt* mutation causes preaxial polydactyly and ectopic expression of *Shh* (Masuya et al., 1997). The *Gli* genes have not been directly implicated in some of the other abnormalities observed in *Dh* mice such as left-right asymmetry or spleen development. However, since *Shh* plays an important role in both systems it cannot be ruled out that *Gli2* could affect both left-right asymmetry and spleen development through ectopic activation of *Shh* (Levin et al., 1995; Tsukui et al., 1999; Apelqvist et al., 1997).

Gli2* is expressed normally in *Dh

In situ analysis has shown that *Gli2* is expressed normally in *Dh* limb buds at several stages of development, suggesting that the mutation does not affect the regulation of *Gli2* (Hecksher-Sørensen, unpublished data). Another possibility is therefore that *Dh* affects the splicing of *Gli2* transcripts. It has been shown that different isoforms of *Gli2* are present in human cells (Tanimura et al., 1998).

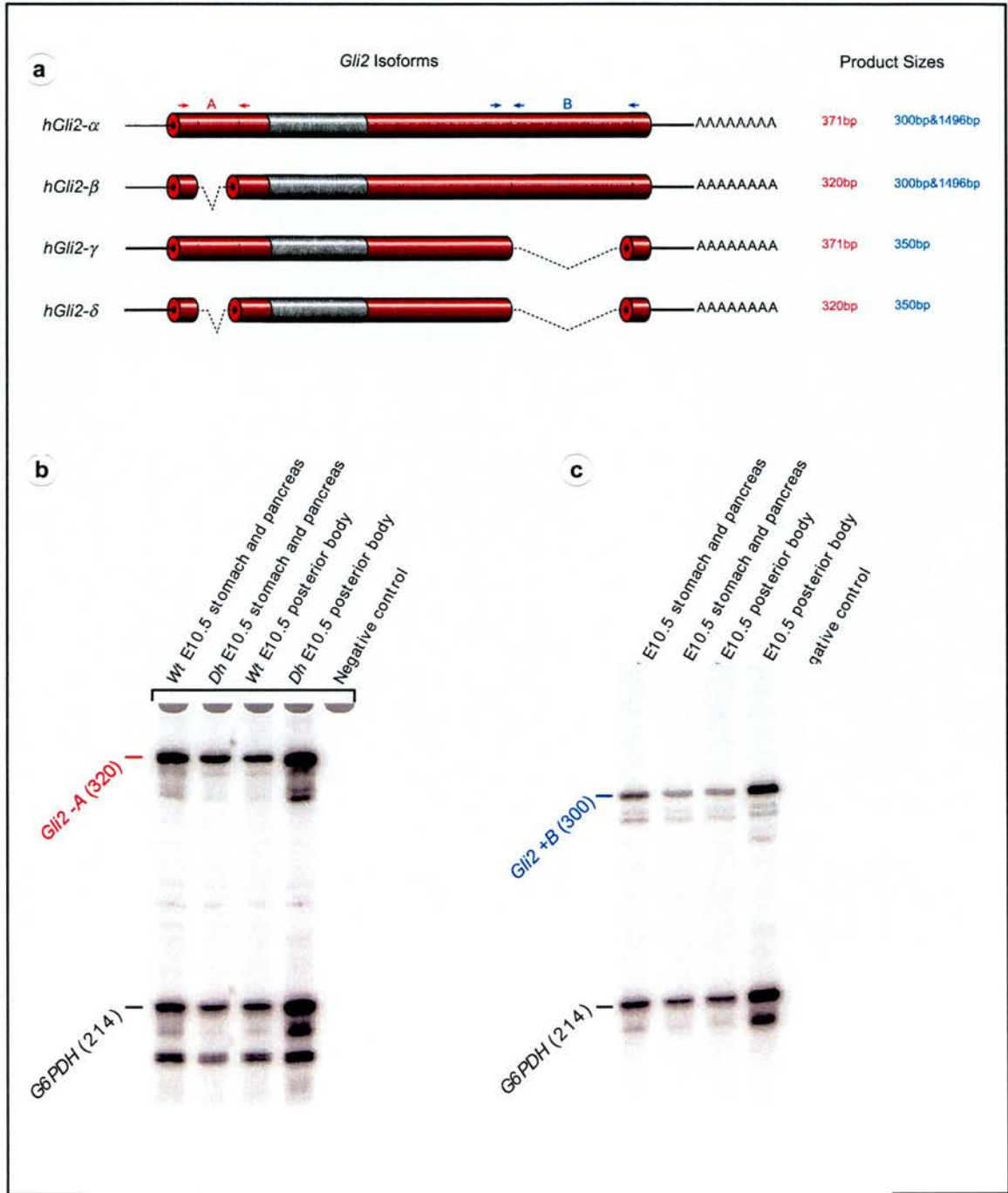


Figure 5.2: RT-PCR showing normal expression of *Gli2* isoforms in *Dh* embryos. (a) MPX-PCR showing *Gli2* expression in *Dh* and wild type. (a) Different splicing produces 4 different isoforms of *Gli2* in humans. Primers were designed so they would distinguish between the different mRNAs. Primer set A produces a 371bp product for the α and γ isoforms and a 350bp fragment for the β and δ isoforms. Primer set B produces two fragments at 300 and 1496bp for the α and β isoforms and one 350bp fragment for the γ and δ isoforms. (b) Primer set A only produces one band at 320bp suggesting that only the β and δ isoforms are present. Primer set B one fragment at 300bp representing the α or β isoforms. However, there are no differences in the expression levels between wild type and *Dh* embryos.

Two exons called A and B gives rise to four different isoforms (*Gli2- α* , *- β* , *- γ* and *- δ*) through alternative splicing (figure 6.2a). When carrying out the MPX-PCR experiment several primers were designed which would distinguish between the various *Gli2* isoforms (Exon A; blue arrows and Exon B; red arrows). The exon A primers only produced one band at 320bp which indicate absence of exon A (figure 6.2b) while the exon B primers produced a band at 300bp indicating presence of exon B (figure 6.2c). Hence, these results show that only the *Gli2- β* isoform is present in the tissues examined. Furthermore, when comparing the intensity of the *Gli2* bands the differences between the samples are also reflected in the internal control (*G6PDH*). It therefore appears that the levels of *Gli2* transcription are the same in wild type and *Dh*.

5.4 The Human sequence

The human sequence failed to reveal new candidates for *Dh*

In humans *Gli2* and *Inh β b* are positioned in close proximity on chromosome 2, suggesting the genomic relationship between the two genes is conserved through evolution. The sequencing of the human genome (Lander et al., 2001; Venter et al., 2001) therefore presented a valuable tool for identification of novel genes within the *Dh* critical region. However, the software available for analysing large genomic sequences has not identified any genes, thus strengthening the argument that *Gli2* and *Inh β b* are the only candidate genes for the *Dh* mutation.

5.5 Conclusion

Misexpression of *Inh β b* and subsequent disruption of TGF β signalling can explain almost every aspect of the *Dh* mutation. Additionally, RT-PCR has demonstrated that *Inh β b* is expressed at higher levels in embryos carrying the *Dh* mutation. Combined these observations make *Inh β b* a very strong candidate for being the gene affected by *Dh*.

5.6 Speculations

In order to carry out a thorough analysis of *Dh* it has been necessary to focus on a few important genes. To focus on one gene like *Hoxc10* has made it easier to get to grips with the complexity of the *Dh* mutation. However, if the primary effect of the *Dh* mutation is misexpression of *Inh β b* then *Dh* is likely to affect a large number of pathways involved in limb induction, renal development, and axial patterning and to fully understand how *Dh* affects all these systems would require the analysis of many more genes. Nevertheless, it is my feeling that this is the true nature of *Dh* is very complex; the shift in *Hoxc10* expression is only part of the phenotype.

Although the final proof that *Inh β b* is the gene affected by *Dh* is still missing, the data presented in this thesis strongly favors *Inh β b* over *Gli2*. And since these two genes appear to be the only genes within the critical region it is almost certain that pleiotropic phenotype inflicted by the *Dh* mutation involves misexpression *Inh β b*. Hopefully this will lead to renewed interest in the role of activins and help address some important questions in developmental biology ie. What is the role of *Inh β b* in left-right signaling (in particular mouse vs. chicken differences)? How is the *Hox* code established? What determines the anterior-posterior position of the hindlimbs?

Chapter 6: Materials and methods

6.1 General techniques

#1: Preparation of electro-competent cells

INV α F' One Shot™ cells (Invitrogen) were plated on non-selective media and grown at 37°C overnight. A single colony was picked and grown in Luria-broth (L-Broth) to 0.5-1.0 at OD₆₀₀. The cells were prepared for electro-transformation by washing twice in cold H₂O and once in 10% glycerol and then stored in aliquots at -70°C in 10% glycerol in H₂O.

#2: Electroporation of plasmid DNA

Electro-competent cells (#1) were mixed with 10-100ng of plasmid DNA and kept on ice for 5 minutes. The mixture of cells and DNA was transferred to a pre-cooled cuvette and placed in an electroporation apparatus (BIO-RAD Gene Pulser™). The apparatus was set to 25 μ F, 2.5 kV and 200 Ω , producing a field strength of 12.5 kV/cm. The cell mixture was then exposed to a 5 second pulse and resuspended in 1ml of L-broth. To allow activation of the ampicillin resistant gene within the plasmid, the cells were incubated for 1 hour at 37°C, before being plated out on a selective media containing 100 μ g/ml Ampicillin. The plates were placed at 37°C overnight to allow growth of colonies.

#3: Heat shock transformation of plasmid DNA

For heat shock transformation, INV α F' One Shot™ cells (Invitrogen) or *CSH26 dam* cells were mixed with plasmid DNA and incubated on ice for 30 minutes. The mixture was then transferred to 42°C for 1 minute and then put on ice for 2 minutes. After resuspending the cells in 500 μ l L-broth they were plated out on selective media and grown at 37°C overnight.

#4: Preparation of plasmid DNA using QIAGEN plasmid mini Kit

Several single colonies were picked and resuspended in 2ml L-broth containing 100 μ g/ml ampicillin and grown overnight at 37°C with shaking. Plasmid DNA from each clone was then prepared from 1.5ml bacterial culture using QIAGEN plasmid mini kit according to manufacture's instructions. Each preparation was tested with

appropriate restriction enzymes to check that the restriction map of the plasmid matched the expected pattern.

#5: Preparation of plasmid DNA using QIAGEN plasmid maxi Kit

Following restriction enzyme verification of the miniprep DNA (#4) one sample matching the expected plasmid were used for large-scale plasmid preparation. 0.5ml bacterial culture was resuspended in 250ml L-broth containing ampicillin and grown overnight at 37°C in a large conical flask, with shaking to allow aeration of the bacteria. Plasmid DNA was prepared using QIAGEN plasmid maxi kit according to manufacture's instructions. The purified DNA was rechecked with appropriate restriction enzymes to ensure the correct plasmid had been isolated.

#6: PCR (conventional)

PCR reactions were set up using 8.5µl dH₂O, 1µl genomic DNA, 0.5 µl AmpliTaq® (Perkin Elmer) and 10 µl 2×buffer [50ng primer^{forw} (Genosys), 50ng primer^{rev} (Genosys) 100µM dNTP's, 5mM MgCl₂ (Perkin Elmer) and 2×PCR buffer (Perkin Elmer)]. The reaction was covered with a drop of mineral oil (SIGMA) to prevent evaporation. The PCR reactions were carried out on a PCR machine (HYBAID OmniGene).

#7: PCR (high fidelity)

For amplification of the full length *Hoxc10* gene from IMAGE clone 1024271 it was important that no errors occurred during the PCR reaction. The *Pfu* DNA polymerase (Stratagene) is reported to have the lowest error rate of any thermostable DNA polymerase studied and was used for this PCR reaction. The experiment was carried out according to manufacture's instructions. Primers and PCR conditions are listed in appendix IV (table A4.1).

#8: PCR (Advantage®-GC Genomic PCR)

The GC context of exon 1 from the *Inhβb* gene is very high, making it difficult to amplify using conventional PCR. The (Clontech) reportedly facilitates amplification of GC rich templates and was therefore used to amplify *Inhβb* exon1 from both +/+ and *Dh/Dh*. The experiment was carried out according to manufacture's instructions. Primers and PCR conditions are listed in appendix IV (table A4.1).

#9: Restriction digest

Restriction digests were carried out using 1-10µg miniprep (#4) or maxiprep (#5) DNA, 1µl restriction enzyme, 1µl buffer and 6µl sterile water. The enzymatic reaction was carried out using the buffer and temperature recommended for any particular enzyme. When more DNA was needed the volumes were increased using the same proportions.

#10: DNA purification (Phenol-Chloroform)

The DNA solution was resuspended to a final volume of 250µl in sterile water and mixed with 250µl phenol:chloroform:isoamyl alcohol (25:24:1). The sample was vortexed for 30 seconds then centrifuged for 5 minutes before the supernatant was transferred to a fresh tube. 250µl chloroform was added to the supernatant, vortexed for 30 seconds and centrifuged for 5 minutes. The supernatant was transferred and the DNA was precipitated by adding 25µl Sodium Acetate and 500µl Ethanol (EtOH). After mixing the sample was stored at -70°C for 30 minutes, centrifuged for 10 minutes and washed in 70% EtOH. Finally, the DNA was resuspended in 10µl sterile water.

#11: DNA purification (Gel extraction)

To purify linearised DNA fragments or PCR products, enzyme digests (#9) or PCR reactions (#6-8) were loaded on a 1% Low Melting Point (LMP) agarose gel. The gel was run in TBE or TAE for approximately 2 hours at 80V. The desired band was excised under UV light and purified using QIAquick gel extraction kit (QIAGEN) according to manufacture's instructions. All optional steps were always included.

#12: Ligation

Depending on the concentration of the DNA approximately 1µl purified vector (#12 or #11) was mixed with 1µl of purified insert or 1µl pre-annealed oligos, 1µl ligation buffer, 1µl T4 ligase [Boehringer Mannheim] and 6 µl sterile water. The ligation was carried out overnight at 16°C and then heated to 70°C for 20 minutes to inactivate the ligase. To remove any salt from the buffer the mixture was placed on a miliporefilter and floated in sterile water for 2 hours.

When oligos were used in the ligation they were first annealed to each other by mixing 5µl of oligo1 (1µg/µl), 5µl of oligo2 (1µg/µl) 2µl ligation buffer (to provide

salt) and 8µl sterile water. The mixture was denatured at 94°C for 5 minutes and then allowed to cool at room temperature.

#13: ABI sequencing

For sequencing 2 µl purified template DNA (#12) was mixed with 8µl Terminator Ready Reaction Mix, 20ng primer and 9µl sterile water. The reaction was covered with a drop of mineral oil and carried out under the following conditions: 94°C for 30 seconds, 50°C for 15 seconds and 60°C for 4 minutes. This program was then repeated 25 times. When completed the PCR reaction, excluding the oil, was added to a tube containing 2µl 3M NaAC pH7.2 and 50µl EtOH. The sample was mixed and stored on ice for 15 minutes, centrifuged for 20 minutes and washed with 70% EtOH. Finally the pellet was dried ready to be loaded on a sequencing machine (ABI 377 Perkin Elmer).

6.2 Cloning of the transgenic constructs

#14: Cloning of the *pHEX* construct

The various cloning steps undertaken to make the *pHEX* construct is shown in figure 2.6. The zebrafish *Pax3*-3'UTR was amplified from genomic zebrafish DNA with primers containing *Sall* and *NotI* restriction sites (#6). The resulting PCR product was purified (#12), digested with *Sall* and *NotI* (#9) and ligated into the corresponding sites (#10) of the mammalian expression vector pCI (Promega). The ligation was transformed into cells (#2) and plated on selective media. Single colonies were picked and the resulting plasmid *pPAX3.1* was prepared (#4) and verified by cutting with *EcoRI* and *NotI* (#6). The enzymes used to verify individual constructs and the results are listed in appendix IV (table A4.5). To make *pPAX3.2* an oligo containing *SacII* and *SfiI* restriction sites was cloned into the *BamHI* site in *pPAX3.1* and at the same time deleting the *BamHI* site. Restriction analysis with *BglI*, *SfiI* and *NheI* showed that the oligo had integrated correctly. Next the CMV promoter was removed by cutting the *pPAX3.2* plasmid with *BglIII* and *PstI* and an oligo containing restriction sites for *SfiI*, *SacII*, *NgoMI*, *KasI* and *NarI* was inserted in its place. Both the *PstI* and the *BglIII* sites were maintained. The expression vector should now be flanked by two *SfiI* sites. The *pPAX3.3* plasmid was therefore confirmed by demonstrating that *SfiI* digestion released a 1.5kb product representative for the expression vector. To make *pPAX3.4* an oligo was ligated into the *XbaI* and *Sall* sites on the *pPAX3.3* vector. The oligo contained restriction sites

for *SpeI*, *BamHI* and *SmaI*. When introduced it deleted the *Sall* site while the *XbaI* site was maintained. The *pPAX3.4* was confirmed by showing that a *SpeI* site had replaced the *Sall* site. Next another oligo containing *EcoRV*, *Sall*, *HindIII* and *BclI* restriction sites was ligated cloned into the *NarI* and *PstI* sites of *pPAX3.4*. Both the *NarI* and the *PstI* restriction sites were preserved. A restriction digest revealing the introduction of a *Sall* site was used to verify that *pPAX3.5* was the right thing. The final step involved cloning of the β *Globin* Basal-Promoter into the *BclI* and *PstI* sites of *pPAX3.5*. However, *BclI* only cuts unmethylated DNA and for this reason the *pPAX3.5* plasmid had to be transformed in to *dam⁻* cells (#3). Having obtained unmethylated *pPAX3.5* DNA was digested sequentially; first with *BclI* at 50°C and then repurified before cutting with *PstI* at 37°C. The β *Globin* Basal-Promoter was obtained as an oligo, matching the published sequence (REF), and ligated into *pPAX3.5*. The resulting plasmid was to be used for Hox EXpression and was therefore termed *pHEX*. The properties of the *pHEX* construct were verified by cutting with *HindIII* and *BamHI* and with *SmaI*.

#15: Cloning of *pGZb9-NE* and *pHEXc10-NE*

The neural element (NE) was released from its original vector *p1662* by digesting with *HindIII* and ligated into the corresponding sites of *pHEX*, to give *pHEX-NE*. Also the NE enhancer was ligated into the *HindIII* site of the *p1230* vector, which contains a *LacZ* gene driven by the β *Globin* Basal-Promoter, to give the *pGZb9-NE* construct. The *Hoxc10* gene was amplified from an EST (IMAGE no. 1024271) using high fidelity PCR (#7). The primers used to amplify the *Hoxc10* gene contained restriction sites for *MluI* and *SpeI* allowing the PCR product to be ligated into the corresponding sites of the *pHEX-NE* vector. The final product, *pHEXc10-NE*, was verified by sequencing (#7) to ensure that no mistakes had occurred during the cloning procedure.

#16: Purification of expression constructs for transgene injections

The expression constructs were released from the plasmid vector using the appropriate enzymes. The *pGZb9-NE* was released with *NotI* and *Sall* while *SfiI* was used to excise the transgene from *pHEXc10-NE*. The digested DNA was loaded on a 0.8% agarose gel and the bands were separated at 80V. The appropriate bands were excised and purified (#12). The purified DNA was passed through a microcon 30 column (Amicon) and washed three times in microinjection buffer [0.1mM EDTA/1mM TRIS pH7.4]. The DNA was eluted according to manufacture's

instructions and diluted 1:10 in transgenic buffer [0.1mM EDTA/10mM TRIS pH7.4]. The concentration of the DNA was determined by running 1µl and 5µl of the dilution alongside known standards.

#17: Injection of the *pHEXc10-NE* transgene into 1-cell embryos

The transgene injection was carried out by Lorna Purdie, as described in (MacKenzie et al., 1997).

6.3 Expression analysis

#18: Preparation of DNA for *in vitro* transcription.

Plasmids containing cloned gene fragments or PCR products amplified from cDNA were used as templates for *in vitro* synthesis of labelled RNA probes. To produce antisense RNA from plasmids the DNA was linearised with appropriate restriction enzymes cutting at the 5' end of the inserted gene fragment (#9). When using PCR to generate template DNA (#6) a T7 promoter was incorporated into the 3' primer. In both cases the DNA was purified through gel extraction (#11). A complete list of plasmids can be found in appendix V (table A5.1) while primers and PCR conditions are listed in appendix IV (table A4.4).

#19: *In vitro* transcription

In vitro transcription and RNA precipitation was carried out using Boehringer RNA labelling kit according to manufacture's instructions. Template DNA (#18) was transcribed using an appropriate RNA-polymerase (T3, T7 or SP6) and nucleotides labelled with either digoxigenin (DIG) or fluorescein (FLU). The success of the transcription reaction was assessed by running an aliquot on a 1% agarose gel at 120V.

#20: conventional *In situ* (wholemout)

To protect the mRNA from degradation, all steps prior to hybridisation was carried out on ice using DEPC treated reagents. Littermates with similar genotypes were pooled and rehydrated in a series of methanol 25%, 50% and 75% in dPBT [dPBS + 0.1% Tween 20 (SIGMA)]. After three washes in dPBT, the embryos were treated with 10µg/ml proteinase K (Boehringer) in dPBT at room temperature. The time of treatment varied according to the size of the embryos. E10.5, E11.5 and E12.5 were

treated for 15, 25 and 35 minutes respectively. The embryos were then fixed for 45 minutes in 4% paraformaldehyde (Sigma). After fixation the embryos were washed twice in hybridisation solution [50% formamide (Sigma), 5xSSC, 2% Blocking powder (Boehringer), 0.1% Triton X-100 (Sigma), 0.5% CHAPS (Sigma), 5mM EDTA, 50µg/ml Heparin (Sigma) and 1mg/ml yeast RNA (Sigma)]. These steps were carried out at room temperature and each time the embryos were allowed to sink in solution. The embryos were then incubated in hybridisation solution at 65°C. After 1hr the solution was changed and the pre-hybridisation continued for another 3-4 hours. 0.2~1µg/ml DIG labelled RNA probe (#19) was denatured at 80°C for 3 minutes, added to the embryos and hybridisation was carried out overnight at 65°C. The post-hybridisation washes consisted of decreasing concentrations of hybridisation solution in 2xSSC (75%, 50% and 25%) each step carried out at room temperature for 10 minutes. This was followed by two 30 minutes washes in 2xSSC, 0.1% CHAPS at 55°C and two 30 minutes washes in 0.2xSSC, 0.1% CHAPS at 55°C. The embryos were washed twice in TNT [100mM TRIS pH7.5, 150mM NaCl and 0.1% Triton X-100] before being transferred to blocking solution [TNT, 2% BSA (BDH) and 15% heat inactivated sheep serum (Sigma)]. After 3-4 hours at 4°C fresh blocking solution, containing antibody against DIG [anti-DIG-AP (Boehringer)], was added to the embryos. The antibody incubation was carried out overnight at 4°C. To remove unbound antibody the embryos were washed in TNT containing 0.1% BSA five times 1 hour then overnight. The embryos were washed twice with NMT (100mM NaCl, 50mM MgCl₂ and 100mM TRIS pH 9.5) for 30 minutes and then three times in NMT for 10 minutes. The signal was visualised in NMT containing 3.5µl/ml BCIP (Boehringer) [50mg/ml in 100% dimethylformamide (BDH)] and 4.5µl/ml NBT (Boehringer) [75mg/ml in 70% dimethylformamide]. When developed to the desired extent, the colour reaction was stopped by rinsing the embryos twice in PBS and fixing them overnight in 4% paraformaldehyde.

#21: Double labelling *In situ* (wholemound)

The method used for double labelling is described in detail in (Hecksher-Sørensen et al., 1998). The pre-treatment step is identical to that used for single labelling (#20). For hybridisation two RNA species are added to the embryos; one labelled with DIG and another labelled with FLU. Following a blocking step, the first signal was detected with an appropriate AP coupled antibody and visualised in NMT containing 3.5µl/m BCIP. The colour reaction was stopped by fixing 1hr in 4%

paraformaldehyde. To inactivate the first antibody the embryos were incubated for 1hr at 65°C. Another blocking step was then carried out before adding the second antibody. The second signal was detected in NMT containing 3.5µl/m BCIP and 4.5µl/ml NBT. The colour reaction was stopped by overnight fixing in 4% paraformaldehyde.

6.4 Expression analysis (fluorescence)

#22: Agarose embedding

After fixing in 4% paraformaldehyde the embryos were incubated in 5% LMP agarose in PBS at 65°C for 2-3 hours. The embryos were then poured into moulds and the agarose was allowed to set at room temperature. While the agarose was setting the embryos could be orientated with a pair of forceps. When set, the agarose block containing the embryo was trimmed with a razor blade and mounted on the vibratome.

#23: Vibratome cutting

The agarose embedded embryos were cut into 70-100µm sections on a vibratome. Each section was lifted from the vibratome waterbath onto a slide. The section was then covered by a thin coverslip, which was glued to the slide at either end – a slight pressure being applied at each end, to ensure that the section lies flat. In order to protect the morphology of the tissue the lifting and mounting was performed very carefully. The mounted sections were stored in PBS to prevent them from drying out.

#24: Fast Red *In situ* (wholemout)

In situ hybridisation was carried out as in (#20) with the following modifications. Prior to staining the embryos were washed twice in 0.1 M TRIS pH 8.2 for 30 minutes and signal was visualised in 2mL 0.1 M TRIS pH 8.2 containing 1 Fast Red tablet (Roche).

#25: Immunohistochemistry (whole mount)

Embryos (#40) were transferred from 100% Methanol to Methanol:DMSO (4:1) for 2 hours and bleached in Methanol:DMSO:H₂O₂ (7:2:1) for 24 hours at 4°C. On occasions fresh embryos were used. In that case the embryos were dissected out in ice cold PBS and washed 2 times for 5 minutes in cold PBT [PBS, 0.2% Triton X-

100]. Fixation was then carried out in Methanol:DMSO (4:1) for 2 hours and bleaching in Methanol:DMSO:H₂O₂ (7:2:1) for 48 hours at 4⁰C. In both cases the bleaching step was followed by rehydration in a series 25%, 50% and 75% of methanol in PBT [PBS + 0.1% Triton X-100 (Sigma)]. After two 30 minutes washes in PBT, the embryos were transferred to blocking solution [2% Skimmed milk powder, 1% DMSO in PBT] and blocked for 6 hours. Primary antibodies (appendix V (table A5.2)) were diluted in fresh blocking solution in appropriate concentrations and added to the embryos, which were then incubated overnight at 4⁰C. To remove unbound antibodies the embryos were washed in PBT for 6 times 1 hour in PBT. For incubation with the secondary antibody the embryos were blocked for 2 hours before being transferred to fresh blocking solution containing appropriate concentration of the secondary antibody. After overnight incubation at 4⁰C unbound antibodies were removed by washing in PBT for 5 times 1 hour. Finally the embryos were embedded and sectioned (#22, #23). For double labelling, two primary and secondary antibodies were added instead of one.

#26: Combined *In situ*/Immunohistochemistry (whole mount)

Primary antibodies were added together with the anti DIG antibodies (#20). The antibody incubation was carried out overnight at 4⁰C. Unbound antibodies were removed by washing in TNT containing 0.1% BSA 8 times 1 hour. The embryos were then blocked for 1 hour in blocking solution [TNT, 2% BSA (BDH) and 15% heat inactivated sheep serum (Sigma)] and incubated overnight with the secondary antibodies. Residual antibodies were removed by washing 5 times 1 hour in TNT containing 0.1% BSA. Finally, the *in situ* signal was then developed as in (#24).

#27: Phalloidin (wholemout)

The phalloidin stain is incompatible with methanol. So for this protocol embryos were dissected out in PBS and washed twice in PBT [0.2% Triton X-100 in PBS]. Fixation was carried out overnight at 4⁰C in 4% paraformaldehyde in PBS. The embryos were then washed three times 30 minutes in PBT before being transferred to blocking solution [2% Bovine Serum Albumin, 2% DMSO in PBT] for 6 hours. Fresh blocking solution containing 20 units of Alexa Fluor™ 594 phalloidin (Molecular Probes) was added to the embryos and incubation was carried out for 48 hours at 4⁰C. To remove unbound phalloidin the embryos were washed for 6 times 1 hour. Finally the embryos were embedded and sectioned (#22, #23).

#28: Confocal microscopy

Expression patterns and protein localisation were visualised with an MRC-600 confocal fitted with an Argon ion laser (488/514nm) and the standard A1, A2 filter set (514nm excitation filter, 540nm green channel, >600nm red channel). Image intensity was controlled by turning the gain up to maximum and keeping the pinhole to the minimal size that still provides a bright image. All scanning was performed using Calman amplification and the slowest scanning speed (3 seconds per frame).

6.5 Histological analysis

#29: Wax embedding

For wax embedding embryos were dehydrated in 100% Ethanol. The embryos were then washed 3 times 30 minutes in Xylene and transferred to molten wax. To ensure proper penetration of the wax the embryos were incubated in molten wax for 3 times 1 hour at 65⁰C before being transferred to moulds. The wax was then allowed to set at room temperature.

#30: Microtome cutting

The wax embedded embryos were cut into 7µm sections on a microtome. The sections were floated out in a 42⁰C waterbath and transferred to microscope slides. To dry the slides were incubated overnight at 65⁰C. The wax was then removed by taking the slides through three 10 minutes washes of Xylene and three 10 minutes washes of ethanol.

#31: Fast Red *In situ* (sections)

To minimise RNA degradation great care was taken to use sterile or DEPC treated reagents. This was also applied to preparation of sections (#29, #30). The slides containing dewaxed sections were transferred to 100% methanol and rehydrated through a series of 100%, 75%, 50% and 25% methanol in PBS. After three washes in dPBT, the embryos were treated with 10µg/ml proteinase K (Boehringer) for 20 minutes in dPBT at room temperature and fixed for 20 minutes in 4% paraformaldehyde (Sigma). After fixation the slides were washed 3 times in PBS and then dehydrated through a series of 25%, 50%, 75%, 100% and 100% methanol in PBS. After air drying 100µl hybridisation mix [50% formamide (Sigma), 5xSSC, 2% Blocking powder (Boehringer), 0.1% Triton X-100 (Sigma), 0.5% CHAPS

(Sigma), 5mM EDTA, 50µg/ml Heparin (Sigma) and 1mg/ml yeast RNA (Sigma)] containing 1:200 RNA probe (#19) were applied to the slides. The slides were covered with a plastic cover slide and hybridisation was carried out at 65⁰C overnight in an OmniSlide rack (Hybaid). To remove unbound probe the slides were washed in 25% formamide in 2 x SSC, 2 x SSC, and 0.2 x SSC. All buffers were prewarmed and the washes were carried out at 65⁰C. Subsequently the slides were washed 3 times 10 minutes in TNT [100mM TRIS pH7.5, 150mM NaCl and 0.1% Triton X-100] before being transferred to blocking solution [TNT, 2% BSA (BDH) and 15% heat inactivated sheep serum (Sigma)]. After 3-4 hours at 4⁰C fresh blocking solution, containing antibody against DIG [anti-DIG-AP (Boehringer)], was added to the slides. The antibody incubation was carried out overnight at 4⁰C. To remove unbound antibody the slides were washed in TNT containing 0.1% BSA five times 1 hour. To visualise the signal the slides were washed twice in 0.1 M TRIS pH 8.2 for 30 minutes then in 2mL 0.1 M TRIS pH 8.2 containing 1 Fast Red tablet (Roche).

#32: Immunohistochemistry (sections)

The sections were rehydrated through a series of 100%, 75%, 50% and 25% methanol in PBS. After two 30 minutes washes in PBT [0.2% Triton X-100 in PBS], the slides were transferred to blocking solution [2% Skimmed milk powder, 1% DMSO in PBT] and blocked for 6 hours. Primary antibodies (appendix V, (table A5.2)) were diluted in fresh blocking solution in appropriate concentrations and added to the slides (approximately 1ml per slide), which were then incubated overnight at 4⁰C. Unbound antibodies were removed by washing the slides 5 times 10 minutes in PBT. Before adding the secondary antibody the slides were blocked for 30 minutes. The slides were incubated for 3 hours with a secondary antibody coupled to a fluorochrome [Alexa Flour 488 or Alexa 594 (molecular probes)] and unbound antibodies were removed by washing 4 times 10 minutes in PBT. Finally the slides were mounted by adding mounting media (Molecular Probes) and a coverslip. To avoid evaporation the slides were sealed with nail polish.

#33: BrdU (sections)

E10.5 embryos were labelled with BrdU by injecting 200µl BrdU (10mg/ml) into a pregnant female. After a 30 minute labelling period the embryos were dissected out and fixed in 4% PFA. The embryos were then imbedded in wax (#29) and cut into sections using the microtome (#30). The sections were rehydrated and trypsinised for 10 minutes at 37⁰C to facilitate penetration of the antibodies. After washing in PBS

the slides were incubated in 1N HCl for 10 minutes to denature the DNA. Incorporation of BrdU into the DNA was detected with antibodies and the remainder of the protocol is similar to that used for protein detection (#32). After visualising the BrdU signal the slides were counterstained with Propidium Iodide (1:5000) and mounted.

#34: Phalloidin and Yo-Pro1 (sections)

Because the phalloidin stain is incompatible with methanol, the sections were rehydrated through a series of 100%, 75%, 50% and 25% ethanol in PBS. After two washes in PBT [0.2% Triton X-100 in PBS] the slides were blocked in [2% Bovine Serum Albumin, 2% DMSO in PBT]. After 2 hours fresh blocking solution containing 1:10 Alexa Fluor™ 594 phalloidin (Molecular Probes) and 1:2000 dilution of Yo-Pro1 (Molecular Probes) was added to the slides. The slides were stained for 30 minutes then washed 3 times 10 minutes and finally mounted in aqueous mounting media (molecular probes).

#35: Histology (sections)

To visualise the histology, paraffin sections were stained with Eosin and Hematoxylin. The sections were rehydrated through a series of alcohol washes, 100%, 95%, 70% and then transferred into distilled water for 1 minute. The sections were then stained for Hematoxylin for 2-5 minutes, rinsed in tap water for 1 minute and transferred to a blueing agent for 30-60 seconds. After two washes in tap water the slides were stained with Eosin and finally was three times in alcohol.

6.6 Bone Staining

#36: Bonestain

The protocol used for bone staining is modified from Kessel and Gruss, 1991. Embryos aged between E15.5 and E18.5 was dissected out and fixed in 100% ethanol. The length of the ethanol step varied, in periods ranging from 3 days to several months. The embryos were then transferred to 100% acetone for 3 days and stained for 10 days in staining solution [1 volume of 0.3% alcian blue (Sigma) in 70% ethanol, 1 volume of 0.1% alizarin red S (Sigma) in 95% ethanol, 1 volume of 100% acetic acid and 17 volumes of 100% ethanol]. After rinsing the embryos were kept in 1% aqueous KOH until the skeleton became visible 12-48 hours. To clear the

tissue the embryos were taken into 1 volume of glycerol and 4 volumes of 1% KOH at 37°C overnight. For storage the specimens were transferred into 50%, 80% and finally 100% glycerol.

6.7 Multiplex PCR

#37: Isolation of mRNA

The desired tissue was dissected out and frozen immediately in liquid nitrogen. When ready for use the tissue was homogenised in RNazol and the mRNA was isolated according to manufacturers description. Extreme care was taken not to contaminate the samples with RNases.

#38: Preparation of cDNA

The isolated RNA (#37) was diluted to 0.2 µg/µl, denatured at 85°C for 10 minutes and allowed to cool for 10 minutes on ice. 5µl RNA was mixed with 20µl RT mastermix [5.0µl 5x RT-buffer, 1.0µl dNTPs (25mM), 1.0 µl Random primers, 2.5µl DDT (0.1mM), 1.0µl RNAsin, 7.5µl DEPC water and 1.0 µl M-MLV Reverse transcriptase] and left on ice for 10 minutes to facilitate proper priming. The RT reaction was carried out at 37°C for 1 hour and finally the cDNA was diluted in 50 µl DEPC water.

#39: MPX-PCR

The volumes used for one 25µl MPX-PCR reaction was 0.75µl 50µM MgCl₂, 2.5µl 10xPCR buffer, 0.125µl dNTP [8mM dA, dG, DTTP and 4mM dCTP]. 0.25µl of each primer 20µM, 0.25µl Taq Polymerase (2u/µl), 0.125µl αP³²-dCTP, 3µl cDNA (#38) and H₂O up to 25µl. The reaction was covered by 25µl mineral oil and run under the following condition: denaturing 96°C for 30 seconds, annealing at 55°C for 30 seconds and extending at 73°C for 30 seconds. This program was repeated for 22 cycles. The primers used for the MPX-PCR have been designed by researchers at the Hagedorn Research Institute and can be obtained on request to Dr. Palle Serup.

6.8 Mouse Stocks

#40: Mouse strains

The *Dh* mutation is kept on the C57/BL6 inbred mouse strain, but due to genetic variation, the severity of the *Dh* phenotype increases progressively when kept on this background. Unfortunately one of the phenotypic traits that becomes more pronounced is genital abnormalities which results in reduced fertility. On several occasions this led to a shortage of homozygous embryos and to prevent the colony from being lost the mutation occasionally underwent rounds of out-breeding to BalbC mice. However, as a result the *Dh* phenotype changed in severity during the project so all comparisons of phenotypic differences between wild type and mutant are based on littermates.

#41: Obtaining mutant embryos

The morning, on which the vaginal plug was detected, was considered as embryonic day 0.5 (E0.5) of development. When the embryos had reached the desired stage of development, the pregnant female was sacrificed and the uterus was removed. The embryos were dissected out in DEPC treated PBS (dPBS). For embryos <E10.5 this procedure was carried out under a dissecting microscope. To insure proper genotyping, each embryo and its membranes was treated and stored individually until the genotype had been determined. The embryos were fixed overnight at 4°C in 2ml dPBS containing 4% paraformaldehyde. The following day the embryos were dehydrated through a methanol series and stored in 100% methanol at -20°C.

#42: Preparation of DNA from mutant embryos

The extra-embryonic membranes from each embryo were digested separately overnight at 55°C in 0.5ml "tail tip" buffer [1% SDS, 0.3M Na-acetate, 10mM TRIS (pH 7.9) and 1mM EDTA] containing 10mg/ml proteinase K. Once the membranes were completely digested, the DNA was precipitated with 0.5 ml isopropanol. After centrifugation and removal of the supernatant the genomic DNA was resuspended in 0.25ml of H₂O and stored at 4°C.

#43: Genotyping mutant embryos

For genotyping of individual embryos, DNA isolated from extra embryonic membranes was used as template in PCR reactions (#6). Since the gene affected by

the *Dh* mutation is unknown, polymorphic markers mapping close to the *Dh* mutation, have been identified. This polymorphism, a CA repeat mapping 10 kb from *Inh β b*, has been shown to be non-recombinant with the *Dh* mutation in a backcross of 869 mice (Maurene et al., unpublished data) and they are reliably used for genotyping of *Dh* embryos. For genotyping of *Bapx1* the DNA of each embryo was purified using phenol/chloroform extraction (#10). Additionally, because of the high GC content 10% DMSO was added to the PCR reactions.

After completion of PCR program, 10 μ l of each sample was loaded on an agarose gel. The primers and conditions used to genotype *Dh*, *Bapx1* and *pHEXc10* transgenic embryos are listed in appendix IV (table A4.1).

References

- Afzelius, B. A.** (1976). A human syndrome caused by immotile cilia. *Science* **193**, 317-9.
- Afzelius, B. A.** (1995). Situs inversus and ciliary abnormalities. What is the connection? *Int J Dev Biol* **39**, 839-44.
- Ahlgren, U., Jonsson, J. and Edlund, H.** (1996). The morphogenesis of the pancreatic mesenchyme is uncoupled from that of the pancreatic epithelium in IPF1/PDX1-deficient mice. *Development* **122**, 1409-16.
- Ahlgren, U., Pfaff, S. L., Jessell, T. M., Edlund, T. and Edlund, H.** (1997). Independent requirement for ISL1 in formation of pancreatic mesenchyme and islet cells. *Nature* **385**, 257-60.
- Akasaka, T., van Lohuizen, M., van Der Lugt, N., Mizutani-Koseki, Y., Kanno, M., Taniguchi, M., Vidal, M., Alkema, M., Berns, A. and Koseki, H.** (2001). Mice doubly deficient for the Polycomb Group genes *Mel18* and *Bmi1* reveal synergy and requirement for maintenance but not initiation of Hox gene expression. *Development* **128**, 1587-97.
- Akazawa, H., Komuro, I., Sugitani, Y., Yazaki, Y., Nagai, R. and Noda, T.** (2000). Targeted disruption of the homeobox transcription factor *Bapx1* results in lethal skeletal dysplasia with asplenia and gastroduodenal malformation. *Genes Cells* **5**, 499-513.
- Alkema, M. J., van der Lugt, N. M., Bobeldijk, R. C., Berns, A. and van Lohuizen, M.** (1995). Transformation of axial skeleton due to overexpression of *bmi-1* in transgenic mice. *Nature* **374**, 724-7.
- Ang, S. L., Wierda, A., Wong, D., Stevens, K. A., Cascio, S., Rossant, J. and Zaret, K. S.** (1993). The formation and maintenance of the definitive endoderm lineage in the mouse: involvement of HNF3/forkhead proteins. *Development* **119**, 1301-15.
- Apelqvist, A., Ahlgren, U. and Edlund, H.** (1997). Sonic hedgehog directs specialised mesoderm differentiation in the intestine and pancreas. *Curr Biol* **7**, 801-4.
- Armstrong, J. F., Pritchard-Jones, K., Bickmore, W. A., Hastie, N. D. and Bard, J. B.** (1993). The expression of the Wilms' tumour gene, *WT1*, in the developing mammalian embryo. *Mech Dev* **40**, 85-97.
- Aubin, J., Lemieux, M., Tremblay, M., Berard, J. and Jeannotte, L.** (1997). Early postnatal lethality in *Hoxa-5* mutant mice is attributable to respiratory tract defects. *Dev Biol* **192**, 432-45.
- Aza-Blanc, P., Lin, H. Y., Ruiz i Altaba, A. and Kornberg, T. B.** (2000). Expression of the vertebrate Gli proteins in *Drosophila* reveals a distribution of activator and repressor activities. *Development* **127**, 4293-301.
- Baldock, R. A., Verbeek, F. J. and Vonesch, J. L.** (1997). 3-D Reconstructions for graphical databases of gene expression. *Seminars in Cell and Developmental Biology* **8**, 499-507.

- Beck, F., Erler, T., Russell, A. and James, R.** (1995). Expression of Cdx-2 in the mouse embryo and placenta: possible role in patterning of the extra-embryonic membranes. *Dev Dyn* **204**, 219-27.
- Bellusci, S., Grindley, J., Emoto, H., Itoh, N. and Hogan, B. L.** (1997). Fibroblast growth factor 10 (Fgf10) and branching morphogenesis in the embryonic mouse lung. *Development* **124**, 4867-78.
- Bisgrove, B. W., Essner, J. J. and Yost, H. J.** (1999). Regulation of midline development by antagonism of lefty and nodal signaling. *Development* **126**, 3253-62.
- Bitgood, M. J. and McMahon, A. P.** (1995). Hedgehog and Bmp genes are coexpressed at many diverse sites of cell-cell interaction in the mouse embryo. *Dev Biol* **172**, 126-38.
- Boettger, T., Wittler, L. and Kessel, M.** (1999). Fgf8 functions in the specification of the right body side of the chick. *Curr Biol* **9**, 277-80.
- Boulet, A. M. and Capecchi, M. R.** (1996). Targeted disruption of *hoxc-4* causes esophageal defects and vertebral transformations. *Dev Biol* **177**, 232-49.
- Bowers, P. N., Brueckner, M. and Yost, H. J.** (1996). The genetics of left-right development and heterotaxia. *Semin Perinatol* **20**, 577-88.
- Brooke, N. M., Garcia-Fernandez, J. and Holland, P. W.** (1998). The *ParaHox* gene cluster is an evolutionary sister of the *Hox* gene cluster. *Nature* **392**, 920-2.
- Brown, C. W., Houston-Hawkins, D. E., Woodruff, T. K. and Matzuk, M. M.** (2000). Insertion of *Inhbb* into the *Inhba* locus rescues the *Inhba*-null phenotype and reveals new activin functions. *Nat Genet* **25**, 453-7.
- Burke, A. C., Nelson, C. E., Morgan, B. A. and Tabin, C.** (1995). *Hox* genes and the evolution of vertebrate axial morphology. *Development* **121**, 333-46.
- Burke, A. C. and Tabin, C. J.** (1996). Virally mediated misexpression of *Hoxc-6* in the cervical mesoderm results in spinal nerve truncations. *Dev Biol* **178**, 192-7.
- Campione, M., Steinbeisser, H., Schweickert, A., Deissler, K., van Bebber, F., Lowe, L. A., Nowotschin, S., Viebahn, C., Haffter, P., Kuehn, M. R. et al.** (1999). The homeobox gene *Pitx2*: mediator of asymmetric left-right signaling in vertebrate heart and gut looping. *Development* **126**, 1225-34.
- Capdevila, I. and Belmonte, J. C.** (2000). Knowing left from right: the molecular basis of laterality defects. *Mol Med Today* **6**, 112-8.
- Capdevila, J., Vogan, K. J., Tabin, C. J. and Izpisua Belmonte, J. C.** (2000). Mechanisms of left-right determination in vertebrates. *Cell* **101**, 9-21.
- Carpenter, E. M., Goddard, J. M., Davis, A. P., Nguyen, T. P. and Capecchi, M. R.** (1997). Targeted disruption of *Hoxd-10* affects mouse hindlimb development. *Development* **124**, 4505-14.
- Chang, D. T., Lopez, A., von Kessler, D. P., Chiang, C., Simandl, B. K., Zhao, R., Seldin, M. F., Fallon, J. F. and Beachy, P. A.** (1994). Products, genetic linkage and limb patterning activity of a murine hedgehog gene. *Development* **120**, 3339-53.
- Charite, J., de Graaff, W., Consten, D., Reijnen, M. J., Korving, J. and Deschamps, J.** (1998). Transducing positional information to the *Hox* genes: critical interaction of

cdx gene products with position-sensitive regulatory elements. *Development* **125**, 4349-58.

- Charite, J., de Graaff, W., Shen, S. and Deschamps, J.** (1994). Ectopic expression of Hoxb-8 causes duplication of the ZPA in the forelimb and homeotic transformation of axial structures. *Cell* **78**, 589-601.
- Chawengsaksophak, K., James, R., Hammond, V. E., Kontgen, F. and Beck, F.** (1997). Homeosis and intestinal tumours in Cdx2 mutant mice. *Nature* **386**, 84-7.
- Chen, F. and Capecchi, M. R.** (1997). Targeted mutations in hoxa-9 and hoxb-9 reveal synergistic interactions. *Dev Biol* **181**, 186-96.
- Cheng, A. M., Thisse, B., Thisse, C. and Wright, C. V.** (2000). The lefty-related factor Xatv acts as a feedback inhibitor of nodal signaling in mesoderm induction and L-R axis development in xenopus. *Development* **127**, 1049-61.
- Cohn, M. J., Izpisua-Belmonte, J. C., Abud, H., Heath, J. K. and Tickle, C.** (1995). Fibroblast growth factors induce additional limb development from the flank of chick embryos. *Cell* **80**, 739-46.
- Cohn, M. J., Patel, K., Krumlauf, R., Wilkinson, D. G., Clarke, J. D. and Tickle, C.** (1997). Hox9 genes and vertebrate limb specification. *Nature* **387**, 97-101.
- Cohn, M. J. and Tickle, C.** (1996). Limbs: a model for pattern formation within the vertebrate body plan. *Trends Genet* **12**, 253-7.
- Collignon, J., Varlet, I. and Robertson, E. J.** (1996). Relationship between asymmetric nodal expression and the direction of embryonic turning. *Nature* **381**, 155-8.
- Crossley, P. H. and Martin, G. R.** (1995). The mouse Fgf8 gene encodes a family of polypeptides and is expressed in regions that direct outgrowth and patterning in the developing embryo. *Development* **121**, 439-51.
- Crossley, P. H., Minowada, G., MacArthur, C. A. and Martin, G. R.** (1996). Roles for Fgf8 in the induction, initiation, and maintenance of chick limb development. *Cell* **84**, 127-36.
- Davies, J.** (1994). Control of calbindin-D28K expression in developing mouse kidney. *Dev Dyn* **199**, 45-51.
- de la Cruz, C. C., Der-Avakian, A., Spyropoulos, D. D., Tieu, D. D. and Carpenter, E. M.** (1999). Targeted disruption of Hoxd9 and Hoxd10 alters locomotor behavior, vertebral identity, and peripheral nervous system development. *Dev Biol* **216**, 595-610.
- Dear, T. N., Colledge, W. H., Carlton, M. B., Lavenir, I., Larson, T., Smith, A. J., Warren, A. J., Evans, M. J., Sofroniew, M. V. and Rabbitts, T. H.** (1995). The Hox11 gene is essential for cell survival during spleen development. *Development* **121**, 2909-15.
- Ding, Q., Motoyama, J., Gasca, S., Mo, R., Sasaki, H., Rossant, J. and Hui, C. C.** (1998). Diminished Sonic hedgehog signaling and lack of floor plate differentiation in Gli2 mutant mice. *Development* **125**, 2533-43.

- Dolle, P., Izpisua-Belmonte, J. C., Falkenstein, H., Renucci, A. and Duboule, D.** (1989). Coordinate expression of the murine Hox-5 complex homeobox-containing genes during limb pattern formation. *Nature* **342**, 767-72.
- Dominguez, M., Brunner, M., Hafen, E. and Basler, K.** (1996). Sending and receiving the hedgehog signal: control by the Drosophila Gli protein Cubitus interruptus. *Science* **272**, 1621-5.
- Dong, Z., Brennan, A., Liu, N., Yarden, Y., Lefkowitz, G., Mirsky, R. and Jessen, K. R.** (1995). Neu differentiation factor is a neuron-glia signal and regulates survival, proliferation, and maturation of rat Schwann cell precursors. *Neuron* **15**, 585-96.
- Donovan, M. J., Natoli, T. A., Sainio, K., Amstutz, A., Jaenisch, R., Sariola, H. and Kreidberg, J. A.** (1999). Initial differentiation of the metanephric mesenchyme is independent of WT1 and the ureteric bud. *Dev Genet* **24**, 252-62.
- Duprez, D. M., Kostakopoulou, K., Francis-West, P. H., Tickle, C. and Brickell, P. M.** (1996). Activation of Fgf-4 and HoxD gene expression by Bmp-2 expressing cells in the developing chick limb. *Development* **122**, 1821-8.
- Edlund, H.** (1998). Transcribing pancreas. *Diabetes* **47**, 1817-23.
- Edlund, H.** (1999). Pancreas: how to get there from the gut? *Curr Opin Cell Biol* **11**, 663-8.
- Eklom, M., Klein, G., Mugrauer, G., Fecker, L., Deutzmann, R., Timpl, R. and Eklom, P.** (1990). Transient and locally restricted expression of laminin A chain mRNA by developing epithelial cells during kidney organogenesis. *Cell* **60**, 337-46.
- Ericson, J., Muhr, J., Jessell, T. M. and Edlund, T.** (1995). Sonic hedgehog: a common signal for ventral patterning along the rostrocaudal axis of the neural tube. *Int J Dev Biol* **39**, 809-16.
- Essner, J. J., Branford, W. W., Zhang, J. and Yost, H. J.** (2000). Mesendoderm and left-right brain, heart and gut development are differentially regulated by pitx2 isoforms. *Development* **127**, 1081-93.
- Evans, J. A., Vitez, M. and Czeizel, A.** (1992). Patterns of acrorenal malformation associations. *Am J Med Genet* **44**, 413-9.
- Feijen, A., Goumans, M. J. and van den Eijnden-van Raaij, A. J.** (1994). Expression of activin subunits, activin receptors and follistatin in postimplantation mouse embryos suggests specific developmental functions for different activins. *Development* **120**, 3621-37.
- Feng, Z. M., Wu, A. Z., Zhang, Z. and Chen, C. L.** (2000). GATA-1 and GATA-4 transactivate inhibin/activin beta-B-subunit gene transcription in testicular cells. *Mol Endocrinol* **14**, 1820-35.
- Fernandez-Teran, M., Piedra, M. E., Simandl, B. K., Fallon, J. F. and Ros, M. A.** (1997). Limb initiation and development is normal in the absence of the mesonephros. *Dev Biol* **189**, 246-55.
- Fletcher, M. P., Ikeda, R. M. and Gershwin, M. E.** (1977). Splenic influence of T cell function: the immunobiology of the inbred hereditarily asplenic mouse. *J Immunol* **119**, 110-7.

- Francis, P. H., Richardson, M. K., Brickell, P. M. and Tickle, C.** (1994). Bone morphogenetic proteins and a signalling pathway that controls patterning in the developing chick limb. *Development* **120**, 209-18.
- Frank, E. and Sanes, J. R.** (1991). Lineage of neurons and glia in chick dorsal root ganglia: analysis in vivo with a recombinant retrovirus. *Development* **111**, 895-908.
- Fromental-Ramain, C., Warot, X., Lakkaraju, S., Favier, B., Haack, H., Birling, C., Dierich, A., Doll e, P. and Chambon, P.** (1996). Specific and redundant functions of the paralogous Hoxa-9 and Hoxd-9 genes in forelimb and axial skeleton patterning. *Development* **122**, 461-72.
- Gage, P. J., Suh, H. and Camper, S. A.** (1999). Dosage requirement of Pitx2 for development of multiple organs. *Development* **126**, 4643-51.
- Gamer, L. W. and Wright, C. V.** (1993). Murine Cdx-4 bears striking similarities to the Drosophila caudal gene in its homeodomain sequence and early expression pattern. *Mech Dev* **43**, 71-81.
- Gaunt, S. J., Dean, W., Sang, H. and Burton, R. D.** (1999). Evidence that Hoxa expression domains are evolutionarily transposed in spinal ganglia, and are established by forward spreading in paraxial mesoderm. *Mech Dev* **82**, 109-18.
- Geduspan, J. S. and Solursh, M.** (1992). A growth-promoting influence from the mesonephros during limb outgrowth. *Dev Biol* **151**, 242-50.
- Gerard, M., Zakany, J. and Duboule, D.** (1997). Interspecies exchange of a Hoxd enhancer in vivo induces premature transcription and anterior shift of the sacrum. *Dev Biol* **190**, 32-40.
- Gibson-Brown, J. J., Agulnik, S. I., Silver, L. M., Niswander, L. and Papaioannou, V. E.** (1998). Involvement of T-box genes Tbx2-Tbx5 in vertebrate limb specification and development. *Development* **125**, 2499-509.
- Golosow, N. and Grobstein, C.** (1962). Epitheliomesenchymal interaction in pancreatic morphogenesis. *Dev Biol* **4**, 242-255.
- Goodrich, L. V., Johnson, R. L., Milenkovic, L., McMahon, J. A. and Scott, M. P.** (1996). Conservation of the hedgehog/patched signaling pathway from flies to mice: induction of a mouse patched gene by Hedgehog. *Genes Dev* **10**, 301-12.
- Grapin-Botton, A. and Melton, D. A.** (2000). Endoderm development: from patterning to organogenesis. *Trends Genet* **16**, 124-30.
- Green, M. C.** (1967). A defect of the splanchnic mesoderm caused by the mutant gene dominant hemimelia in the mouse. *Dev Biol* **15**, 62-89.
- Gruss, P. and Kessel, M.** (1991). Axial specification in higher vertebrates. *Curr Opin Genet Dev* **1**, 204-10.
- Harrison, K. A., Thaler, J., Pfaff, S. L., Gu, H. and Kehrl, J. H.** (1999). Pancreas dorsal lobe agenesis and abnormal islets of Langerhans in Hlxb9-deficient mice. *Nat Genet* **23**, 71-5.
- Harvey, R. P.** (1998). Links in the left/right axial pathway. *Cell* **94**, 273-6.

- Hebrok, M., Kim, S. K. and Melton, D. A.** (1998). Notochord repression of endodermal Sonic hedgehog permits pancreas development. *Genes Dev* **12**, 1705-13.
- Hebrok, M., Kim, S. K., St Jacques, B., McMahon, A. P. and Melton, D. A.** (2000). Regulation of pancreas development by hedgehog signaling. *Development* **127**, 4905-13.
- Hecksher-Sørensen, J.** (1998). Molecular Characterisation of Abnormal Limb Development in Four Non-allelic Polydactylous Mouse Mutants: dominant hemimelia (Dh), luxate (lx), extra toes (Xt) and sasquatch (Ssq). In *MRC Human Genetic Unit*, (ed. Edinburgh: Aarhus University).
- Hecksher-Sørensen, J., Hill, R. E. and Lettice, L.** (1998). Double labeling for whole-mount in situ hybridization in mouse. *Biotechniques* **24**, 914-6, 918.
- Hecksher-Sørensen, J. and Sharpe, J.** (2001). 3D confocal reconstruction of gene expression in mouse. *Mech Dev* **100**, 59-63.
- Hemmati-Brivanlou, A., Kelly, O. G. and Melton, D. A.** (1994). Follistatin, an antagonist of activin, is expressed in the Spemann organizer and displays direct neuralizing activity. *Cell* **77**, 283-95.
- Hemmati-Brivanlou, A. and Melton, D. A.** (1992). A truncated activin receptor inhibits mesoderm induction and formation of axial structures in *Xenopus* embryos. *Nature* **359**, 609-14.
- Hemmati-Brivanlou, A. and Melton, D. A.** (1994). Inhibition of activin receptor signaling promotes neuralization in *Xenopus*. *Cell* **77**, 273-81.
- Herzer, U., Crocoll, A., Barton, D., Howells, N. and Englert, C.** (1999). The Wilms tumor suppressor gene *wilms1* is required for development of the spleen. *Curr Biol* **9**, 837-40.
- Higgins, M., Hill, R. E. and West, J. D.** (1992). Dominant hemimelia and *En-1* on mouse chromosome 1 are not allelic. *Genet Res* **60**, 53-60.
- Hogan, B. L.** (1996). Bone morphogenetic proteins: multifunctional regulators of vertebrate development. *Genes Dev* **10**, 1580-94.
- Holmes, L. B.** (1986). Identification of Dh/+ and Dh/Dh embryos through close linkage of Dh and peptidase-3. *Teratology* **34**, 353-7.
- Holmes, L. B. and Barton, R. E.** (1993). The pattern of skeletal malformations in Dh/+ and Dh/Dh day 18 fetuses. *Prog Clin Biol Res*, 163-9.
- Hostikka, S. L. and Capecchi, M. R.** (1998). The mouse *Hoxc11* gene: genomic structure and expression pattern. *Mech Dev* **70**, 133-45.
- Houle, M., Prinos, P., Iulianella, A., Bouchard, N. and Lohnes, D.** (2000). Retinoic acid regulation of *Cdx1*: an indirect mechanism for retinoids and vertebral specification. *Mol Cell Biol* **20**, 6579-86.
- Hsu, D. R., Economides, A. N., Wang, X., Eimon, P. M. and Harland, R. M.** (1998). The *Xenopus* dorsalizing factor Gremlin identifies a novel family of secreted proteins that antagonize Bmp activities. *Mol Cell* **1**, 673-83.
- Hughes, D. C., Allen, J., Morley, G., Sutherland, K., Ahmed, W., Prosser, J., Lettice, L., Allan, G., Mattei, M. G., Farrall, M. et al.** (1997). Cloning and sequencing of the

mouse Gli2 gene: localization to the Dominant hemimelia critical region. *Genomics* **39**, 205-15.

Hui, C. C. and Joyner, A. L. (1993). A mouse model of greig cephalopolysyndactyly syndrome: the extra-toesJ mutation contains an intragenic deletion of the Gli3 gene. *Nat Genet* **3**, 241-6.

Isaac, A., Rodriguez-Esteban, C., Ryan, A., Altabef, M., Tsukui, T., Patel, K., Tickle, C. and Izpisua-Belmonte, J. C. (1998). Tbx genes and limb identity in chick embryo development. *Development* **125**, 1867-75.

Iten, L. E. (1982). Pattern specification and pattern regulation in the embryonic chick limb bud. *Am Zool* **28**, 117-129.

Izpisua-Belmonte, J. C. and Duboule, D. (1992). Homeobox genes and pattern formation in the vertebrate limb. *Dev Biol* **152**, 26-36.

Izpisua-Belmonte, J. C., Tickle, C., Dolle, P., Wolpert, L. and Duboule, D. (1991). Expression of the homeobox Hox-4 genes and the specification of position in chick wing development. *Nature* **350**, 585-9.

Jessen, K. R., Brennan, A., Morgan, L., Mirsky, R., Kent, A., Hashimoto, Y. and Gavrilovic, J. (1994). The Schwann cell precursor and its fate: a study of cell death and differentiation during gliogenesis in rat embryonic nerves. *Neuron* **12**, 509-27.

Johnson, R. L. and Tabin, C. J. (1997). Molecular models for vertebrate limb development. *Cell* **90**, 979-90.

Jones, C. M., Lyons, K. M. and Hogan, B. L. (1991). Involvement of Bone Morphogenetic Protein-4 (Bmp-4) and Vgr-1 in morphogenesis and neurogenesis in the mouse. *Development* **111**, 531-42.

Jonsson, J., Carlsson, L., Edlund, T. and Edlund, H. (1994). Insulin-promoter-factor 1 is required for pancreas development in mice. *Nature* **371**, 606-9.

Karlsson, O., Thor, S., Norberg, T., Ohlsson, H. and Edlund, T. (1990). Insulin gene enhancer binding protein Isl-1 is a member of a novel class of proteins containing both a homeo- and a Cys-His domain. *Nature* **344**, 879-82.

Kawakami, Y., Capdevila, J., Buscher, D., Itoh, T., Esteban, C. R. and Belmonte, J. C. (2001). WNT Signals Control Fgf-Dependent Limb Initiation and AER Induction in the Chick Embryo. *Cell* **104**, 891-900.

Kessel, M. and Gruss, P. (1991). Homeotic transformations of murine vertebrae and concomitant alteration of Hox codes induced by retinoic acid. *Cell* **67**, 89-104.

Kim, S. K., Hebrok, M., Li, E., Oh, S. P., Schrewe, H., Harmon, E. B., Lee, J. S. and Melton, D. A. (2000). Activin receptor patterning of foregut organogenesis. *Genes Dev* **14**, 1866-71.

Kim, S. K., Hebrok, M. and Melton, D. A. (1997). Notochord to endoderm signaling is required for pancreas development. *Development* **124**, 4243-52.

Kim, S. K. and Melton, D. A. (1998). Pancreas development is promoted by cyclopamine, a hedgehog signaling inhibitor. *Proc Natl Acad Sci U S A* **95**, 13036-41.

- Kingsley, D. M.** (1994). The TGF-beta superfamily: new members, new receptors, and new genetic tests of function in different organisms. *Genes Dev* **8**, 133-46.
- Kitamura, K., Miura, H., Miyagawa-Tomita, S., Yanazawa, M., Katoh-Fukui, Y., Suzuki, R., Ohuchi, H., Suehiro, A., Motegi, Y., Nakahara, Y. et al.** (1999). Mouse Pitx2 deficiency leads to anomalies of the ventral body wall, heart, extra- and periocular mesoderm and right pulmonary isomerism. *Development* **126**, 5749-58.
- Knezevic, V., De Santo, R., Schughart, K., Huffstadt, U., Chiang, C., Mahon, K. A. and Mackem, S.** (1997). Hoxd-12 differentially affects preaxial and postaxial chondrogenic branches in the limb and regulates Sonic hedgehog in a positive feedback loop. *Development* **124**, 4523-36.
- Koehler, K., Franz, T. and Dear, T. N.** (2000). Hox11 is required to maintain normal Wt1 mRNA levels in the developing spleen. *Dev Dyn* **218**, 201-6.
- Krapp, A., Knofler, M., Ledermann, B., Burki, K., Berney, C., Zoerkler, N., Hagenbuchle, O. and Wellauer, P. K.** (1998). The bHLH protein PTF1-p48 is essential for the formation of the exocrine and the correct spatial organization of the endocrine pancreas. *Genes Dev* **12**, 3752-63.
- Kreidberg, J. A., Sariola, H., Loring, J. M., Maeda, M., Pelletier, J., Housman, D. and Jaenisch, R.** (1993). WT-1 is required for early kidney development. *Cell* **74**, 679-91.
- Krumlauf, R.** (1994). Hox genes in vertebrate development. *Cell* **78**, 191-201.
- Lander, E. S. Linton, L. M. Birren, B. Nusbaum, C. Zody, M. C. Baldwin, J. Devon, K. Dewar, K. Doyle, M. FitzHugh, W. et al.** (2001). Initial sequencing and analysis of the human genome. *Nature* **409**, 860-921.
- Laufer, E., Nelson, C. E., Johnson, R. L., Morgan, B. A. and Tabin, C.** (1994). Sonic hedgehog and Fgf-4 act through a signaling cascade and feedback loop to integrate growth and patterning of the developing limb bud. *Cell* **79**, 993-1003.
- Lettice, L., Hecksher-Sørensen, J. and Hill, R. E.** (1999a). The dominant hemimelia mutation uncouples epithelial-mesenchymal interactions and disrupts anterior mesenchyme formation in mouse hindlimbs. *Development* **126**, 4729-36.
- Lettice, L. A., Purdie, L. A., Carlson, G. J., Kilanowski, F., Dorin, J. and Hill, R. E.** (1999b). The mouse bagpipe gene controls development of axial skeleton, skull, and spleen. *Proc Natl Acad Sci U S A* **96**, 9695-700.
- Levin, M., Johnson, R. L., Stern, C. D., Kuehn, M. and Tabin, C.** (1995). A molecular pathway determining left-right asymmetry in chick embryogenesis. *Cell* **82**, 803-14.
- Levin, M., Pagan, S., Roberts, D. J., Cooke, J., Kuehn, M. R. and Tabin, C. J.** (1997). Left/right patterning signals and the independent regulation of different aspects of situs in the chick embryo. *Dev Biol* **189**, 57-67.
- Lewandoski, M., Sun, X. and Martin, G. R.** (2000). Fgf8 signalling from the AER is essential for normal limb development. *Nat Genet* **26**, 460-3.
- Li, H., Arber, S., Jessell, T. M. and Edlund, H.** (1999). Selective agenesis of the dorsal pancreas in mice lacking homeobox gene Hlxb9. *Nat Genet* **23**, 67-70.

- Lin, C. R., Kioussi, C., O'Connell, S., Briata, P., Szeto, D., Liu, F., Izpisua-Belmonte, J. C. and Rosenfeld, M. G.** (1999). Pitx2 regulates lung asymmetry, cardiac positioning and pituitary and tooth morphogenesis. *Nature* **401**, 279-82.
- Logan, M., Pagan-Westphal, S. M., Smith, D. M., Paganessi, L. and Tabin, C. J.** (1998). The transcription factor Pitx2 mediates situs-specific morphogenesis in response to left-right asymmetric signals. *Cell* **94**, 307-17.
- Lohnes, D., Kastner, P., Dierich, A., Mark, M., LeMeur, M. and Chambon, P.** (1993). Function of retinoic acid receptor gamma in the mouse. *Cell* **73**, 643-58.
- Lohr, J. L., Danos, M. C. and Yost, H. J.** (1997). Left-right asymmetry of a nodal-related gene is regulated by dorsoanterior midline structures during *Xenopus* development. *Development* **124**, 1465-72.
- Louie, A. Y., Huber, M. M., Ahrens, E. T., Rothbacher, U., Moats, R., Jacobs, R. E., Fraser, S. E. and Meade, T. J.** (2000). In vivo visualization of gene expression using magnetic resonance imaging. *Nat Biotechnol* **18**, 321-5.
- Lowe, L. A., Supp, D. M., Sampath, K., Yokoyama, T., Wright, C. V., Potter, S. S., Overbeek, P. and Kuehn, M. R.** (1996). Conserved left-right asymmetry of nodal expression and alterations in murine situs inversus. *Nature* **381**, 158-61.
- Lu, H. C., Revelli, J. P., Goering, L., Thaller, C. and Eichele, G.** (1997). Retinoid signaling is required for the establishment of a ZPA and for the expression of Hoxb-8, a mediator of ZPA formation. *Development* **124**, 1643-51.
- Lu, J., Chang, P., Richardson, J. A., Gan, L., Weiler, H. and Olson, E. N.** (2000). The basic helix-loop-helix transcription factor capsulin controls spleen organogenesis. *Proc Natl Acad Sci U S A* **97**, 9525-30.
- Lu, M. F., Pressman, C., Dyer, R., Johnson, R. L. and Martin, J. F.** (1999). Function of Rieger syndrome gene in left-right asymmetry and craniofacial development. *Nature* **401**, 276-8.
- Lyons, K. M., Hogan, B. L. and Robertson, E. J.** (1995). Colocalization of Bmp 7 and Bmp 2 RNAs suggests that these factors cooperatively mediate tissue interactions during murine development. *Mech Dev* **50**, 71-83.
- Lyons, K. M., Pelton, R. W. and Hogan, B. L.** (1990). Organogenesis and pattern formation in the mouse: RNA distribution patterns suggest a role for bone morphogenetic protein-2A (Bmp-2A). *Development* **109**, 833-44.
- Machado, E. A. and Lozzio, B. B.** (1976). Animal model of human disease: hyposplenia, asplenia, and immunodeficiency. *Am J Pathol* **85**, 515-8.
- MacKenzie, A., Purdie, L., Davidson, D., Collinson, M. and Hill, R. E.** (1997). Two enhancer domains control early aspects of the complex expression pattern of Msx1. *Mech Dev* **62**, 29-40.
- Mahmood, R., Bresnick, J., Hornbruch, A., Mahony, C., Morton, N., Colquhoun, K., Martin, P., Lumsden, A., Dickson, C. and Mason, I.** (1995). A role for Fgf-8 in the initiation and maintenance of vertebrate limb bud outgrowth. *Curr Biol* **5**, 797-806.
- Manley, N. R. and Capecchi, M. R.** (1995). The role of Hoxa-3 in mouse thymus and thyroid development. *Development* **121**, 1989-2003.

- Manning, M. J. and Horton, J. D.** (1969). Histogenesis of lymphoid organs in larvae of the South African clawed toad, *Xenopus laevis* (Daudin). *J Embryol Exp Morphol* **22**, 265-77.
- Marszalek, J. R., Ruiz-Lozano, P., Roberts, E., Chien, K. R. and Goldstein, L. S.** (1999). Situs inversus and embryonic ciliary morphogenesis defects in mouse mutants lacking the KIF3A subunit of kinesin-II. *Proc Natl Acad Sci U S A* **96**, 5043-8.
- Martin, G. R., Richman, M., Reinsch, S., Nadeau, J. H. and Joyner, A.** (1990). Mapping of the two mouse engrailed-like genes: close linkage of En-1 to dominant hemimelia (Dh) on chromosome 1 and of En-2 to hemimelic extra- toes (Hx) on chromosome 5. *Genomics* **6**, 302-8.
- Massague, J. and Chen, Y. G.** (2000). Controlling TGF-beta signaling. *Genes Dev* **14**, 627-44.
- Masuya, H., Sagai, T., Moriwaki, K. and Shiroishi, T.** (1997). Multigenic control of the localization of the zone of polarizing activity in limb morphogenesis in the mouse. *Dev Biol* **182**, 42-51.
- Masuya, H., Sagai, T., Wakana, S., Moriwaki, K. and Shiroishi, T.** (1995). A duplicated zone of polarizing activity in polydactylous mouse mutants. *Genes Dev* **9**, 1645-53.
- Mathews, L. S. and Vale, W. W.** (1991). Expression cloning of an activin receptor, a predicted transmembrane serine kinase. *Cell* **65**, 973-82.
- Mathews, L. S., Vale, W. W. and Kintner, C. R.** (1992). Cloning of a second type of activin receptor and functional characterization in *Xenopus* embryos. *Science* **255**, 1702-5.
- Matzuk, M. M., Kumar, T. R. and Bradley, A.** (1995a). Different phenotypes for mice deficient in either activins or activin receptor type II. *Nature* **374**, 356-60.
- Matzuk, M. M., Kumar, T. R., Vassalli, A., Bickenbach, J. R., Roop, D. R., Jaenisch, R. and Bradley, A.** (1995b). Functional analysis of activins during mammalian development. *Nature* **374**, 354-6.
- Matzuk, M. M., Lu, N., Vogel, H., Sellheyer, K., Roop, D. R. and Bradley, A.** (1995c). Multiple defects and perinatal death in mice deficient in follistatin. *Nature* **374**, 360-3.
- McPherron, A. C., Lawler, A. M. and Lee, S. J.** (1999). Regulation of anterior/posterior patterning of the axial skeleton by growth/differentiation factor 11. *Nat Genet* **22**, 260-4.
- Medina-Martinez, O., Bradley, A. and Ramirez-Solis, R.** (2000). A large targeted deletion of Hoxb1-Hoxb9 produces a series of single- segment anterior homeotic transformations. *Dev Biol* **222**, 71-83.
- Meno, C., Gritsman, K., Ohishi, S., Ohfuji, Y., Heckscher, E., Mochida, K., Shimono, A., Kondoh, H., Talbot, W. S., Robertson, E. J. et al.** (1999). Mouse Lefty2 and zebrafish antivin are feedback inhibitors of nodal signaling during vertebrate gastrulation. *Mol Cell* **4**, 287-98.
- Meno, C., Ito, Y., Saijoh, Y., Matsuda, Y., Tashiro, K., Kuhara, S. and Hamada, H.** (1997). Two closely-related left-right asymmetrically expressed genes, lefty-1 and lefty-2: their distinct expression domains, chromosomal linkage and direct neuralizing activity in *Xenopus* embryos. *Genes Cells* **2**, 513-24.

- Meno, C., Saijoh, Y., Fujii, H., Ikeda, M., Yokoyama, T., Yokoyama, M., Toyoda, Y. and Hamada, H.** (1996). Left-right asymmetric expression of the TGF beta-family member *lefty* in mouse embryos. *Nature* **381**, 151-5.
- Meno, C., Shimonono, A., Saijoh, Y., Yashiro, K., Mochida, K., Ohishi, S., Noji, S., Kondoh, H. and Hamada, H.** (1998). *lefty-1* is required for left-right determination as a regulator of *lefty-2* and *nodal*. *Cell* **94**, 287-97.
- Methot, N. and Basler, K.** (1999). Hedgehog controls limb development by regulating the activities of distinct transcriptional activator and repressor forms of *Cubitus interruptus*. *Cell* **96**, 819-31.
- Methot, N. and Basler, K.** (2001). An absolute requirement for *Cubitus interruptus* in Hedgehog signaling. *Development* **128**, 733-42.
- Meyer, B. I. and Gruss, P.** (1993). Mouse *Cdx-1* expression during gastrulation. *Development* **117**, 191-203.
- Meyers, E. N. and Martin, G. R.** (1999). Differences in left-right axis pathways in mouse and chick: functions of *Fgf8* and *Shh*. *Science* **285**, 403-6.
- Min, H., Danilenko, D. M., Scully, S. A., Bolon, B., Ring, B. D., Tarpley, J. E., DeRose, M. and Simonet, W. S.** (1998). *Fgf-10* is required for both limb and lung development and exhibits striking functional similarity to *Drosophila* *branchless*. *Genes Dev* **12**, 3156-61.
- Mochizuki, T., Saijoh, Y., Tsuchiya, K., Shirayoshi, Y., Takai, S., Taya, C., Yonekawa, H., Yamada, K., Nihei, H., Nakatsuji, N. et al.** (1998). Cloning of *inv*, a gene that controls left/right asymmetry and kidney development. *Nature* **395**, 177-81.
- Mohun, T. J., Leong, L. M., Weninger, W. J. and Sparrow, D. B.** (2000). The morphology of heart development in *Xenopus laevis*. *Dev Biol* **218**, 74-88.
- Moon, A. M., Boulet, A. M. and Capecchi, M. R.** (2000). Normal limb development in conditional mutants of *Fgf4*. *Development* **127**, 989-96.
- Moon, A. M. and Capecchi, M. R.** (2000). *Fgf8* is required for outgrowth and patterning of the limbs. *Nat Genet* **26**, 455-9.
- Morgan, D., Turnpenny, L., Goodship, J., Dai, W., Majumder, K., Matthews, L., Gardner, A., Schuster, G., Vien, L., Harrison, W. et al.** (1998). *Inversin*, a novel gene in the vertebrate left-right axis pathway, is partially deleted in the *inv* mouse. *Nat Genet* **20**, 149-56.
- Morin, B. J., Owen, M. H., Ramamurthy, G. V. and Holmes, L. B.** (1999). Pattern of skeletal malformations produced by Dominant hemimelia (*Dh*). *Teratology* **60**, 348-55.
- Murphy, P., Topilko, P., Schneider-Maunoury, S., Seitanidou, T., Baron-Van Evercooren, A. and Charnay, P.** (1996). The regulation of *Krox-20* expression reveals important steps in the control of peripheral glial cell development. *Development* **122**, 2847-57.
- Nelson, C. E., Morgan, B. A., Burke, A. C., Laufer, E., DiMambro, E., Murtaugh, L. C., Gonzales, E., Tessarollo, L., Parada, L. F. and Tabin, C.** (1996). Analysis of *Hox* gene expression in the chick limb bud. *Development* **122**, 1449-66.

- Nielsen, C., Murtaugh, L. C., Chyung, J. C., Lassar, A. and Roberts, D. J.** (2001). Gizzard Formation and the Role of Bapx1. *Dev Biol* **231**, 164-174.
- Niswander, L. and Martin, G. R.** (1992). Fgf-4 expression during gastrulation, myogenesis, limb and tooth development in the mouse. *Development* **114**, 755-68.
- Niswander, L., Tickle, C., Vogel, A., Booth, I. and Martin, G. R.** (1993). Fgf-4 replaces the apical ectodermal ridge and directs outgrowth and patterning of the limb. *Cell* **75**, 579-87.
- Nohno, T., Noji, S., Koyama, E., Ohyama, K., Myokai, F., Kuroiwa, A., Saito, T. and Taniguchi, S.** (1991). Involvement of the Chox-4 chicken homeobox genes in determination of anteroposterior axial polarity during limb development. *Cell* **64**, 1197-205.
- Nonaka, S., Tanaka, Y., Okada, Y., Takeda, S., Harada, A., Kanai, Y., Kido, M. and Hirokawa, N.** (1998). Randomization of left-right asymmetry due to loss of nodal cilia generating leftward flow of extraembryonic fluid in mice lacking KIF3B motor protein. *Cell* **95**, 829-37.
- Nowicki, J. L. and Burke, A. C.** (2000). Hox genes and morphological identity: axial versus lateral patterning in the vertebrate mesoderm. *Development* **127**, 4265-75.
- Offield, M. F., Jetton, T. L., Labosky, P. A., Ray, M., Stein, R. W., Magnuson, M. A., Hogan, B. L. and Wright, C. V.** (1996). PDX-1 is required for pancreatic outgrowth and differentiation of the rostral duodenum. *Development* **122**, 983-95.
- Oh, S. P. and Li, E.** (1997). The signaling pathway mediated by the type IIB activin receptor controls axial patterning and lateral asymmetry in the mouse. *Genes Dev* **11**, 1812-26.
- Ohlsson, H., Karlsson, K. and Edlund, T.** (1993). IPF1, a homeodomain-containing transactivator of the insulin gene. *Embo J* **12**, 4251-9.
- Ohuchi, H., Nakagawa, T., Yamamoto, A., Araga, A., Ohata, T., Ishimaru, Y., Yoshioka, H., Kuwana, T., Nohno, T., Yamasaki, M. et al.** (1997). The mesenchymal factor, Fgf10, initiates and maintains the outgrowth of the chick limb bud through interaction with Fgf8, an apical ectodermal factor. *Development* **124**, 2235-44.
- Ohuchi, H., Nakagawa, T., Yamauchi, M., Ohata, T., Yoshioka, H., Kuwana, T., Mima, T., Mikawa, T., Nohno, T. and Noji, S.** (1995). An additional limb can be induced from the flank of the chick embryo by Fgf4. *Biochem Biophys Res Commun* **209**, 809-16.
- Ohuchi, H. and Noji, S.** (1999). Fibroblast-growth-factor-induced additional limbs in the study of initiation of limb formation, limb identity, myogenesis, and innervation. *Cell Tissue Res* **296**, 45-56.
- Ohuchi, H., Takeuchi, J., Yoshioka, H., Ishimaru, Y., Ogura, K., Takahashi, N., Ogura, T. and Noji, S.** (1998). Correlation of wing-leg identity in ectopic Fgf-induced chimeric limbs with the differential expression of chick Tbx5 and Tbx4. *Development* **125**, 51-60.

- Ohuchi, H., Yoshioka, H., Tanaka, A., Kawakami, Y., Nohno, T. and Noji, S.** (1994). Involvement of androgen-induced growth factor (Fgf-8) gene in mouse embryogenesis and morphogenesis. *Biochem Biophys Res Commun* **204**, 882-8.
- Okada, Y., Nonaka, S., Tanaka, Y., Saijoh, Y., Hamada, H. and Hirokawa, N.** (1999). Abnormal nodal flow precedes situs inversus in iv and inv mice. *Mol Cell* **4**, 459-68.
- Onichtchouk, D., Chen, Y. G., Dosch, R., Gawantka, V., Delius, H., Massague, J. and Niehrs, C.** (1999). Silencing of TGF-beta signalling by the pseudoreceptor BAMBI. *Nature* **401**, 480-5.
- Orlando, V. and Paro, R.** (1995). Chromatin multiprotein complexes involved in the maintenance of transcription patterns. *Curr Opin Genet Dev* **5**, 174-9.
- Pabst, O., Zweigerdt, R. and Arnold, H. H.** (1999). Targeted disruption of the homeobox transcription factor Nkx2-3 in mice results in postnatal lethality and abnormal development of small intestine and spleen. *Development* **126**, 2215-25.
- Pagan-Westphal, S. M. and Tabin, C. J.** (1998). The transfer of left-right positional information during chick embryogenesis. *Cell* **93**, 25-35.
- Patterson, K. D., Drysdale, T. A. and Krieg, P. A.** (2000). Embryonic origins of spleen asymmetry. *Development* **127**, 167-75.
- Piedra, M. E., Icardo, J. M., Albajar, M., Rodriguez-Rey, J. C. and Ros, M. A.** (1998). Pitx2 participates in the late phase of the pathway controlling left-right asymmetry. *Cell* **94**, 319-24.
- Qu, S., Niswender, K. D., Ji, Q., van der Meer, R., Keeney, D., Magnuson, M. A. and Wisdom, R.** (1997). Polydactyly and ectopic ZPA formation in Alx-4 mutant mice. *Development* **124**, 3999-4008.
- Qu, S., Tucker, S. C., Ehrlich, J. S., Levorse, J. M., Flaherty, L. A., Wisdom, R. and Vogt, T. F.** (1998). Mutations in mouse Aristaless-like4 cause Strong's luxoid polydactyly. *Development* **125**, 2711-21.
- Rancourt, D. E., Tsuzuki, T. and Capecchi, M. R.** (1995). Genetic interaction between hoxb-5 and hoxb-6 is revealed by nonallelic noncomplementation. *Genes Dev* **9**, 108-22.
- Rebagliati, M. R., Toyama, R., Fricke, C., Haffter, P. and Dawid, I. B.** (1998). Zebrafish nodal-related genes are implicated in axial patterning and establishing left-right asymmetry. *Dev Biol* **199**, 261-72.
- Reuter, R., Panganiban, G. E., Hoffmann, F. M. and Scott, M. P.** (1990). Homeotic genes regulate the spatial expression of putative growth factors in the visceral mesoderm of Drosophila embryos. *Development* **110**, 1031-40.
- Riddle, R. D., Johnson, R. L., Laufer, E. and Tabin, C.** (1993). Sonic hedgehog mediates the polarizing activity of the ZPA. *Cell* **75**, 1401-16.
- Rijli, F. M., Matyas, R., Pellegrini, M., Dierich, A., Gruss, P., Dolle, P. and Chambon, P.** (1995). Cryptorchidism and homeotic transformations of spinal nerves and vertebrae in Hoxa-10 mutant mice. *Proc Natl Acad Sci U S A* **92**, 8185-9.
- Roberts, C. W., Shutter, J. R. and Korsmeyer, S. J.** (1994). Hox11 controls the genesis of the spleen. *Nature* **368**, 747-9.

- Roberts, D. J.** (2000). Molecular mechanisms of development of the gastrointestinal tract. *Dev Dyn* **219**, 109-20.
- Roberts, D. J., Johnson, R. L., Burke, A. C., Nelson, C. E., Morgan, B. A. and Tabin, C.** (1995). Sonic hedgehog is an endodermal signal inducing Bmp-4 and Hox genes during induction and regionalization of the chick hindgut. *Development* **121**, 3163-74.
- Rodriguez Esteban, C., Capdevila, J., Economides, A. N., Pascual, J., Ortiz, A. and Izpisua Belmonte, J. C.** (1999). The novel Cer-like protein Caronte mediates the establishment of embryonic left-right asymmetry. *Nature* **401**, 243-51.
- Rodriguez-Esteban, C., Tsukui, T., Yonei, S., Magallon, J., Tamura, K. and Izpisua Belmonte, J. C.** (1999). The T-box genes Tbx4 and Tbx5 regulate limb outgrowth and identity. *Nature* **398**, 814-8.
- Roelink, H., Augsburger, A., Heemskerk, J., Korzh, V., Norlin, S., Ruiz i Altaba, A., Tanabe, Y., Placzek, M., Edlund, T., Jessell, T. M. et al.** (1994). Floor plate and motor neuron induction by vhh-1, a vertebrate homolog of hedgehog expressed by the notochord. *Cell* **76**, 761-75.
- Rooze, M. A.** (1977). The effects of the Dh gene on limb morphogenesis in the mouse. *Birth Defects Orig Artic Ser* **13**, 69-95.
- Rowe, D. A., Cairns, J. M. and Fallon, J. F.** (1982). Spatial and temporal patterns of cell death in limb bud mesoderm after apical ectodermal ridge removal. *Dev Biol* **93**, 83-91.
- Ruiz i Altaba, A.** (1999). Gli proteins and Hedgehog signaling: development and cancer. *Trends Genet* **15**, 418-25.
- Ryan, A. K., Blumberg, B., Rodriguez-Esteban, C., Yonei-Tamura, S., Tamura, K., Tsukui, T., de la Pena, J., Sabbagh, W., Greenwald, J., Choe, S. et al.** (1998). Pitx2 determines left-right asymmetry of internal organs in vertebrates. *Nature* **394**, 545-51.
- Saito, H.** (1984). The development of the spleen in the Australian lungfish, *Neoceratodus forsteri* Krefft, with special reference to its relationship to the "gastro"-enteric vasculature. *Am J Anat* **169**, 337-60.
- Sampath, K., Cheng, A. M., Frisch, A. and Wright, C. V.** (1997). Functional differences among *Xenopus* nodal-related genes in left-right axis determination. *Development* **124**, 3293-302.
- Sasaki, H., Nishizaki, Y., Hui, C., Nakafuku, M. and Kondoh, H.** (1999). Regulation of Gli2 and Gli3 activities by an amino-terminal repression domain: implication of Gli2 and Gli3 as primary mediators of Shh signaling. *Development* **126**, 3915-24.
- Sassoon, D., Lyons, G., Wright, W. E., Lin, V., Lassar, A., Weintraub, H. and Buckingham, M.** (1989). Expression of two myogenic regulatory factors myogenin and MyoD1 during mouse embryogenesis. *Nature* **341**, 303-7.
- Saunders, J. W.** (1948). The proximo-distal sequence of origin of the parts of the chicken wing and the role of the ectoderm. *J Exp Zool* **108**, 363-403.
- Saunders, J. W. and Gasseling, M. T.** (1968). Ectoderm-mesenchymal interaction in the origins of wing symmetry. In *Epithelial-Mesenchymal Interactions*, (ed. R. Fleischmaier and R. E. Billingham), pp. 78-97. Baltimore: Williams and Wilkins.

- Schier, A. F. and Shen, M. M.** (2000). Nodal signalling in vertebrate development. *Nature* **403**, 385-9.
- Schott, J. J., Benson, D. W., Basson, C. T., Pease, W., Silberbach, G. M., Moak, J. P., Maron, B. J., Seidman, C. E. and Seidman, J. G.** (1998). Congenital heart disease caused by mutations in the transcription factor NKX2-5. *Science* **281**, 108-11.
- Schrewe, H., Gendron-Maguire, M., Harbison, M. L. and Gridley, T.** (1994). Mice homozygous for a null mutation of activin beta B are viable and fertile. *Mech Dev* **47**, 43-51.
- Searle, A. G.** (1964). The genetics and morphology of two luxoid mutants in the huose mouse. *Genet Res* **5**, 171-197.
- Sekine, K., Ohuchi, H., Fujiwara, M., Yamasaki, M., Yoshizawa, T., Sato, T., Yagishita, N., Matsui, D., Koga, Y., Itoh, N. et al.** (1999). Fgf10 is essential for limb and lung formation. *Nat Genet* **21**, 138-41.
- Sharpe, J., Lettice, L., Hecksher-Sørensen, J., Fox, M., Hill, R. and Krumlauf, R.** (1999). Identification of sonic hedgehog as a candidate gene responsible for the polydactylous mouse mutant Sasquatch. *Curr Biol* **9**, 97-100.
- Slack, J. M.** (1995). Developmental biology of the pancreas. *Development* **121**, 1569-80.
- Small, K. M. and Potter, S. S.** (1993). Homeotic transformations and limb defects in Hox A11 mutant mice. *Genes Dev* **7**, 2318-28.
- Smith, D. M., Nielsen, C., Tabin, C. J. and Roberts, D. J.** (2000). Roles of Bmp signaling and Nkx2.5 in patterning at the chick midgut- foregut boundary. *Development* **127**, 3671-81.
- Smith, J. C., Price, B. M., Van Nimmen, K. and Huylebroeck, D.** (1990). Identification of a potent *Xenopus* mesoderm-inducing factor as a homologue of activin A. *Nature* **345**, 729-31.
- Stern, C. D., Yu, R. T., Kakizuka, A., Kintner, C. R., Mathews, L. S., Vale, W. W., Evans, R. M. and Umesono, K.** (1995). Activin and its receptors during gastrulation and the later phases of mesoderm development in the chick embryo. *Dev Biol* **172**, 192-205.
- Stone, D. M., Hynes, M., Armanini, M., Swanson, T. A., Gu, Q., Johnson, R. L., Scott, M. P., Pennica, D., Goddard, A., Phillips, H. et al.** (1996). The tumour-suppressor gene patched encodes a candidate receptor for Sonic hedgehog. *Nature* **384**, 129-34.
- Subramanian, V., Meyer, B. I. and Gruss, P.** (1995). Disruption of the murine homeobox gene Cdx1 affects axial skeletal identities by altering the mesodermal expression domains of Hox genes. *Cell* **83**, 641-53.
- Suemori, H. and Noguchi, S.** (2000). Hox C cluster genes are dispensable for overall body plan of mouse embryonic development. *Dev Biol* **220**, 333-42.
- Sulik, K., Dehart, D. B., Iangaki, T., Carson, J. L., Vrablic, T., Gesteland, K. and Schoenwolf, G. C.** (1994). Morphogenesis of the murine node and notochordal plate. *Dev Dyn* **201**, 260-78.

- Sun, X., Lewandoski, M., Meyers, E. N., Liu, Y. H., Maxson, R. E., Jr. and Martin, G. R.** (2000). Conditional inactivation of Fgf4 reveals complexity of signalling during limb bud development. *Nat Genet* **25**, 83-6.
- Sun, X., Meyers, E. N., Lewandoski, M. and Martin, G. R.** (1999). Targeted disruption of Fgf8 causes failure of cell migration in the gastrulating mouse embryo. *Genes Dev* **13**, 1834-46.
- Supp, D. M., Brueckner, M., Kuehn, M. R., Witte, D. P., Lowe, L. A., McGrath, J., Corrales, J. and Potter, S. S.** (1999). Targeted deletion of the ATP binding domain of left-right dynein confirms its role in specifying development of left-right asymmetries. *Development* **126**, 5495-504.
- Supp, D. M., Potter, S. S. and Brueckner, M.** (2000). Molecular motors: the driving force behind mammalian left-right development. *Trends Cell Biol* **10**, 41-5.
- Supp, D. M., Witte, D. P., Potter, S. S. and Brueckner, M.** (1997). Mutation of an axonemal dynein affects left-right asymmetry in inversus viscerum mice. *Nature* **389**, 963-6.
- Suto, J., Wakayama, T., Imamura, K., Goto, S. and Fukuta, K.** (1995). Incomplete development of the spleen and the deformity in the chimeras between asplenic mutant (Dominant hemimelia) and normal mice. *Teratology* **52**, 71-7.
- Suto, J., Wakayama, T., Imamura, K., Goto, S. and Fukuta, K.** (1996). Skeletal malformations caused by the Dh (Dominant hemimelia) gene in mice. *Exp Anim* **45**, 95-8.
- Szuts, D. and Bienz, M.** (2000). An autoregulatory function of Dfos during Drosophila endoderm induction. *Mech Dev* **98**, 71-6.
- Takahashi, M., Tamura, K., Buscher, D., Masuya, H., Yonei-Tamura, S., Matsumoto, K., Naitoh-Matsuo, M., Takeuchi, J., Ogura, K., Shiroishi, T. et al.** (1998). The role of Alx-4 in the establishment of anteroposterior polarity during vertebrate limb development. *Development* **125**, 4417-25.
- Takeda, S., Yonekawa, Y., Tanaka, Y., Okada, Y., Nonaka, S. and Hirokawa, N.** (1999). Left-right asymmetry and kinesin superfamily protein KIF3A: new insights in determination of laterality and mesoderm induction by kif3A-/- mice analysis. *J Cell Biol* **145**, 825-36.
- Tanaka, E. M. and Gann, A. F.** (1995). Limb development. The budding role of Fgf. *Curr Biol* **5**, 594-7.
- Tanaka, M., Schinke, M., Liao, H. S., Yamasaki, N. and Izumo, S.** (2001). Nkx2.5 and Nkx2.6, homologs of Drosophila tinman, are required for development of the pharynx. *Mol Cell Biol* **21**, 4391-8.
- Tanimura, A., Dan, S. and Yoshida, M.** (1998). Cloning of novel isoforms of the human Gli2 oncogene and their activities to enhance tax-dependent transcription of the human T-cell leukemia virus type 1 genome. *J Virol* **72**, 3958-64.
- Taulman, P. D., Haycraft, C. J., Balkovetz, D. F. and Yoder, B. K.** (2001). Polaris, a protein involved in left-right axis patterning, localizes to basal bodies and cilia. *Mol Cell Biol* **21**, 589-99.

- Thiel, G. A. and Downey, H.** (1921). The development of the mammalian spleen with special reference to its hematopoietic activity. *Am. J. Anat.* **28**, 279-333.
- Thisse, C. and Thisse, B.** (1999). Antivin, a novel and divergent member of the TGFbeta superfamily, negatively regulates mesoderm induction. *Development* **126**, 229-40.
- Tickle, C.** (1981). The number of polarizing region cells required to specify additional digits in the developing chick wing. *Nature* **289**, 295-8.
- Tickle, C.** (1995). Vertebrate limb development. *Curr Opin Genet Dev* **5**, 478-84.
- Tickle, C., Summerbell, D. and Wolpert, L.** (1975). Positional signalling and specification of digits in chick limb morphogenesis. *Nature* **254**, 199-202.
- Tissier-Seta, J. P., Mucchielli, M. L., Mark, M., Mattei, M. G., Goridis, C. and Brunet, J. F.** (1995). Barx1, a new mouse homeodomain transcription factor expressed in cranio- facial ectomesenchyme and the stomach. *Mech Dev* **51**, 3-15.
- Tribioli, C., Frasch, M. and Lufkin, T.** (1997). Bapx1: an evolutionary conserved homologue of the Drosophila bagpipe homeobox gene is expressed in splanchnic mesoderm and the embryonic skeleton. *Mech Dev* **65**, 145-62.
- Tribioli, C. and Lufkin, T.** (1999). The murine Bapx1 homeobox gene plays a critical role in embryonic development of the axial skeleton and spleen. *Development* **126**, 5699-711.
- Tsai, F. Y., Keller, G., Kuo, F. C., Weiss, M., Chen, J., Rosenblatt, M., Alt, F. W. and Orkin, S. H.** (1994). An early haematopoietic defect in mice lacking the transcription factor GATA-2. *Nature* **371**, 221-6.
- Tsukui, T., Capdevila, J., Tamura, K., Ruiz-Lozano, P., Rodriguez-Esteban, C., Yonei-Tamura, S., Magallon, J., Chandraratna, R. A., Chien, K., Blumberg, B. et al.** (1999). Multiple left-right asymmetry defects in Shh(-/-) mutant mice unveil a convergence of the shh and retinoic acid pathways in the control of Lefty-1. *Proc Natl Acad Sci U S A* **96**, 11376-81.
- Vassalli, A., Matzuk, M. M., Gardner, H. A., Lee, K. F. and Jaenisch, R.** (1994). Activin/inhibin beta B subunit gene disruption leads to defects in eyelid development and female reproduction. *Genes Dev* **8**, 414-27.
- Vellguth, S., von Gaudecker, B. and Muller-Hermelink, H. K.** (1985). The development of the human spleen. Ultrastructural studies in fetuses from the 14th to 24th week of gestation. *Cell Tissue Res* **242**, 579-92.
- Venter, J. C. Adams, M. D. Myers, E. W. Li, P. W. Mural, R. J. Sutton, G. G. Smith, H. O. Yandell, M. Evans, C. A. Holt, R. A. et al.** (2001). The sequence of the human genome. *Science* **291**, 1304-51.
- Vogan, K. J. and Tabin, C. J.** (1999). A new spin on handed asymmetry. *Nature* **397**, 295, 297-8.
- Vogel, A., Rodriguez, C. and Izpissua-Belmonte, J. C.** (1996). Involvement of Fgf-8 in initiation, outgrowth and patterning of the vertebrate limb. *Development* **122**, 1737-50.
- Vogel, A. and Tickle, C.** (1993). Fgf-4 maintains polarizing activity of posterior limb bud cells in vivo and in vitro. *Development* **119**, 199-206.

- Wahba, G. M., Hostikka, S. L. and Carpenter, E. M.** (2001). The paralogous Hox genes *Hoxa10* and *Hoxd10* interact to pattern the mouse hindlimb peripheral nervous system and skeleton. *Dev Biol* **231**, 87-102.
- Walmsley, M. E., Guille, M. J., Bertwistle, D., Smith, J. C., Pizzey, J. A. and Patient, R. K.** (1994). Negative control of *Xenopus* GATA-2 by activin and noggin with eventual expression in precursors of the ventral blood islands. *Development* **120**, 2519-29.
- Warot, X., Fromental-Ramain, C., Fraulob, V., Chambon, P. and Dolle, P.** (1997). Gene dosage-dependent effects of the *Hoxa-13* and *Hoxd-13* mutations on morphogenesis of the terminal parts of the digestive and urogenital tracts. *Development* **124**, 4781-91.
- Wells, J. M. and Melton, D.** (1999). Vertebrate endoderm development. *Annu. Rev. Cell Dev. Biol.* **15**, 393-410.
- Wessels, N. K. and Cohen, J. H.** (1967). Early pancreas organogenesis: morphogenesis, tissue interactions and mass effects. *Dev Biol* **15**, 237-270.
- Wlodarski, K., Morrison, K. and Michowski, D.** (1982). The effect of dominant hemimelia (*Dh*) genes on the number of mast cells in lymph nodes. *Folia Biol* **28**, 254-8.
- Wolpert, L.** (1969). Positional information and the spatial pattern of cellular differentiation. *J Theor Biol* **25**, 1-47.
- Xu, X., Weinstein, M., Li, C., Naski, M., Cohen, R. I., Ornitz, D. M., Leder, P. and Deng, C.** (1998). Fibroblast growth factor receptor 2 (*FgfR2*)-mediated reciprocal regulation loop between *Fgf8* and *Fgf10* is essential for limb induction. *Development* **125**, 753-65.
- Yang, Y., Drossopoulou, G., Chuang, P. T., Duprez, D., Marti, E., Bumcrot, D., Vargesson, N., Clarke, J., Niswander, L., McMahon, A. et al.** (1997). Relationship between dose, distance and time in Sonic Hedgehog-mediated regulation of anteroposterior polarity in the chick limb. *Development* **124**, 4393-404.
- Yassine, F., Feddecka-Bruner, B. and Dieterlen-Lievre, F.** (1989). Ontogeny of the chick embryo spleen--a cytological study. *Cell Differ Dev* **27**, 29-45.
- Yee, S. P. and Rigby, P. W.** (1993). The regulation of myogenin gene expression during the embryonic development of the mouse. *Genes Dev* **7**, 1277-89.
- Yokouchi, Y., Vogan, K. J., Pearse, R. V., 2nd and Tabin, C. J.** (1999). Antagonistic signaling by *Caronte*, a novel Cerberus-related gene, establishes left-right asymmetric gene expression. *Cell* **98**, 573-83.
- Yokoyama, T., Copeland, N. G., Jenkins, N. A., Montgomery, C. A., Elder, F. F. and Overbeek, P. A.** (1993). Reversal of left-right asymmetry: a situs inversus mutation. *Science* **260**, 679-82.
- Yoshioka, H., Meno, C., Koshiba, K., Sugihara, M., Itoh, H., Ishimaru, Y., Inoue, T., Ohuchi, H., Semina, E. V., Murray, J. C. et al.** (1998). *Pitx2*, a bicoid-type homeobox gene, is involved in a lefty-signaling pathway in determination of left-right asymmetry. *Cell* **94**, 299-305.
- Yost, H. J.** (1998). The genetics of midline and cardiac laterality defects. *Curr Opin Cardiol* **13**, 185-9.

- Yost, H. J.** (1999). Diverse initiation in a conserved left-right pathway? *Curr Opin Genet Dev* **9**, 422-6.
- Yu, B. D., Hess, J. L., Horning, S. E., Brown, G. A. and Korsmeyer, S. J.** (1995). Altered Hox expression and segmental identity in Mll-mutant mice. *Nature* **378**, 505-8.
- Zakany, J., Gerard, M., Favier, B. and Duboule, D.** (1997). Deletion of a HoxD enhancer induces transcriptional heterochrony leading to transposition of the sacrum. *Embo J* **16**, 4393-402.
- Zakany, J., Gerard, M., Favier, B., Potter, S. S. and Duboule, D.** (1996). Functional equivalence and rescue among group 11 Hox gene products in vertebral patterning. *Dev Biol* **176**, 325-8.
- Zhou, Y., Lim, K. C., Onodera, K., Takahashi, S., Ohta, J., Minegishi, N., Tsai, F. Y., Orkin, S. H., Yamamoto, M. and Engel, J. D.** (1998). Rescue of the embryonic lethal hematopoietic defect reveals a critical role for GATA-2 in urogenital development. *Embo J* **17**, 6689-700.
- Zhu, L., Marvin, M. J., Gardiner, A., Lassar, A. B., Mercola, M., Stern, C. D. and Levin, M.** (1999). Cerberus regulates left-right asymmetry of the embryonic head and heart. *Curr Biol* **9**, 931-8.

Appendix

Appendix I: Sequencing of the pHEX construct

Table A1.1: Nucleotide sequence alignment of the pHEX construct

Appendix II: MPX-PCR - annotated gels

Heck01: Annotated Gel
Heck02: Annotated Gel
Heck03: Annotated Gel
Heck04: Annotated Gel
Heck05: Annotated Gel
Heck06: Annotated Gel
Heck07: Annotated Gel
Heck08: Annotated Gel
Heck09: Annotated Gel
Heck10: Annotated Gel
Heck11: Annotated Gel
Heck12: Annotated Gel
Heck13: Annotated Gel
Heck14: Annotated Gel

Appendix III: Degenerate PCR's

Table A3.1: Sequence alignment of the inhibinb family

Table A3.2: Sequence alignment of the Bmp family

Appendix IV: Primer sequences

Table A4.1: Primer sequences used for cloning and genotyping

Table A4.2: Oligo sequences used for sequencing

Table A4.3: Oligo sequences used for cloning of the pHEX construct

Table A4.4: Primer sequences used for making *in situ* probes

Table A4.5: Enzymes used for verification of pPAX plasmids

Appendix V: Data sheets for *In situ* probes and Antibodies

Table A5.1: Data Sheet for *in situ* probes

Table A5.2: Data sheet for primary and secondary antibodies

Appendix VI: Confocal Paper

Hecksher-Sørensen, J. and Sharpe, J. (2001). 3D confocal reconstruction of gene expression in mouse. *Mech Dev* **100**, 59-63.

Appendix VII: *Bapx1* Paper

Lettice, L., Hecksher-Sørensen, J. and Hill, R. (2001). The role of *Bapx1* (*Nkx3.2*) in the development and evolution of the axial skeleton. *J. Anat.* **199**, 181-187

Appendix I: Sequencing of the pHEX construct

Table A1.1: Nucleotide sequence alignment of the *pHEX* construct

Table A1.1: Nucleotide sequence alignment of the *pHEXc10* construct (forward from intron)

Primer	Sequence
PHEXc10	TAGCCTCGAGAATTCACGGTGTCTCCGCTGTAGTATTGCTCCTTAAAAACCCCTCTCTCTGAAAATGACATGCCCTCGCAATGTAAC
F1	TAGCCTCGAGAATTCACGGTGTCTCCGCTGTAGTATTGCTCCTTAAAAACCCCTCTCTCTGAAAATGACATGCCCTCGCAATGTAAC
F2	-----
F3	-----
F4	-----
Alignment	TAGCCTCGAGAATTCACGGTGTCTCCGCTGTAGTATTGCTCCTTAAAAACCCCTCTCTCTGAAAATGACATGCCCTCGCAATGTAAC
PHEXc10	TCCGAACTCGTACGGGAGCCCTTGGCTGCGCCGGGAGGAGGAGCGCTATAACCGTAACGCAAGATGTATGCAATCTGGGAGTGA
F1	TCCGAACTCGTACGGGAGCCCTTGGCTGCGCCGGGAGGAGGAGCGCTATAACCGTAACGCAAGATGTATGCAATCTGGGAGTGA
F2	-----
F3	-----
F4	-----
Alignment	TCCGAACTCGTACGGGAGCCCTTGGCTGCGCCGGGAGGAGGAGCGCTATAACCGTAACGCAAGATGTATGCAATCTGGGAGTGA
PHEXc10	CTTCAACTGCGGGGTGATGAGGGGTGCGGGCTCGCGCCCTCTCTCTCCAAGAGGGACGAGGGAGGCAGCCAAACCTAGCCCTCAACAC
F1	CTTCAACTGCGGGGTGATGAGGGGTGCGGGCTCGCGCCCTCTCTCTCCAAGAGGGACGAGGGAGGCAGCCAAACCTAGCCCTCAACAC
F2	-----
F3	-----
F4	-----
Alignment	CTTCAACTGCGGGGTGATGAGGGGTGCGGGCTCGCGCCCTCTCTCTCCAAGAGGGACGAGGGAGGCAGCCAAACCTAGCCCTCAACAC
PHEXc10	CTACCCGCTCCTACCTCTCGCAGCTGGACTCTGGGGGACCCCAAAGCCGCTACCCTGGAACAACCTGTTGGCAGCCCTGTCTCTC
F1	CTACCCGCTCCTACCTCTCGCAGCTGGACTCTGGGGGACCCCAAAGCCGCTACCCTGGAACAACCTGTTGGCAGCCCTGTCTCTC
F2	-----
F3	-----
F4	-----
Alignment	CTACCCGCTCCTACCTCTCGCAGCTGGACTCTGGGGGACCCCAAAGCCGCTACCCTGGAACAACCTGTTGGCAGCCCTGTCTCTC
PHEXc10	CTGTTCTACCCACCTAGTGTCAAGGAGGAGAAATGTCTGCTGATGTACAGTGCAGAGAAGCGGGCGAAAAGTGGCCCTGAGGCAGCTCT
F1	CTGTTCTACCCACCTAGTGTCAAGGAGGAGAAATGTCTGCTGATGTACAGTGCAGAGAAGCGGGCGAAAAGTGGCCCTGAGGCAGCTCT
F2	-----
F3	-----
F4	-----
Alignment	CTGTTCTACCCACCTAGTGTCAAGGAGGAGAAATGTCTGCTGATGTACAGTGCAGAGAAGCGGGCGAAAAGTGGCCCTGAGGCAGCTCT
PHEXc10	CTACTCCACCCCTGCGGGAGTCTTGCCTTGGGGAGCAGGAGTACCTGTACCAGCTACTACCAGCCAGCCC--GAGCTACTCCGGCC
F1	CTACTCCACCCCTGCGGGAGTCTTGCCTTGGGGAGCAGGAGTACCTGTACCAGCTACTACCAGCCAGCCC--GAGCTACTCCGGCC
F2	-----
F3	-----
F4	-----
Alignment	CTACTCCACCCCTGCGGGAGTCTTGCCTTGGGGAGCAGGAGTACCTGTACCAGCTACTACCAGCCAGCCC--GAGCTACTCCGGCC
PHEXc10	TGGACAAAACGCCCCACTGTGCTGGGGCAACGAGTTCGAAGCCCTTTGAGCAGCGGGCCAGTCTCAACCCGCGCACCGAACATCTGG
F1	TGGACAAAACGCCCCACTGTGCTGGGGCAACGAGTTCGAAGCCCTTTGAGCAGCGGGCCAGTCTCAACCCGCGCACCGAACATCTGG
F2	-----
F3	-----
F4	-----
Alignment	TGGACAAAACGCCCCACTGTGCTGGGGCAACGAGTTCGAAGCCCTTTGAGCAGCGGGCCAGTCTCAACCCGCGCACCGAACATCTGG
PHEXc10	AATCGCCTCAGCTTGGGGCAAAAGTGAGTTTCTTGAGACCCCAAGTCCGACAGCCAGACCCCAAGTCCCAATGAGATCAAGACAGAGC
F1	AATCGCCTCAGCTTGGGGCAAAAGTGAGTTTCTTGAGACCCCAAGTCCGACAGCCAGACCCCAAGTCCCAATGAGATCAAGACAGAGC
F2	-----
F3	-----
F4	-----
Alignment	AATCGCCTCAGCTTGGGGCAAAAGTGAGTTTCTTGAGACCCCAAGTCCGACAGCCAGACCCCAAGTCCCAATGAGATCAAGACAGAGC
PHEXc10	AAAGCTTGGGGCCCAAAGGCCAGCCCTCGGAGAGCGAGAAGGAAAGCCGACAGCTCCAGTCCAGACACCTCGGATAACG
F1	AAAGCTTGGGGCCCAAAGGCCAGCCCTCGGAGAGCGAGAAGGAAAGCCGACAGCTCCAGTCCAGACACCTCGGATAACG
F2	-----
F3	-----
F4	-----
Alignment	AAAGCTTGGGGCCCAAAGGCCAGCCCTCGGAGAGCGAGAAGGAAAGCCGACAGCTCCAGTCCAGACACCTCGGATAACG
PHEXc10	AAGCTAAAGAGGAGATAAAGGCAGAAAACACCACAGGAAATTGGCTGACAGCAAAGAGCGGAAGGAAAGAGGTGCCCTATACTAAAC
F1	AAGCTAAAGAGGAGATAAAGGCAGAAAACACCACAGGAAATTGGCTGACAGCAAAGAGCGGAAGGAAAGAGGTGCCCTATACTAAAC
F2	-----
F3	-----
F4	-----
Alignment	AAGCTAAAGAGGAGATAAAGGCAGAAAACACCACAGGAAATTGGCTGACAGCAAAGAGCGGAAGGAAAGAGGTGCCCTATACTAAAC

Table A1.1: Continued

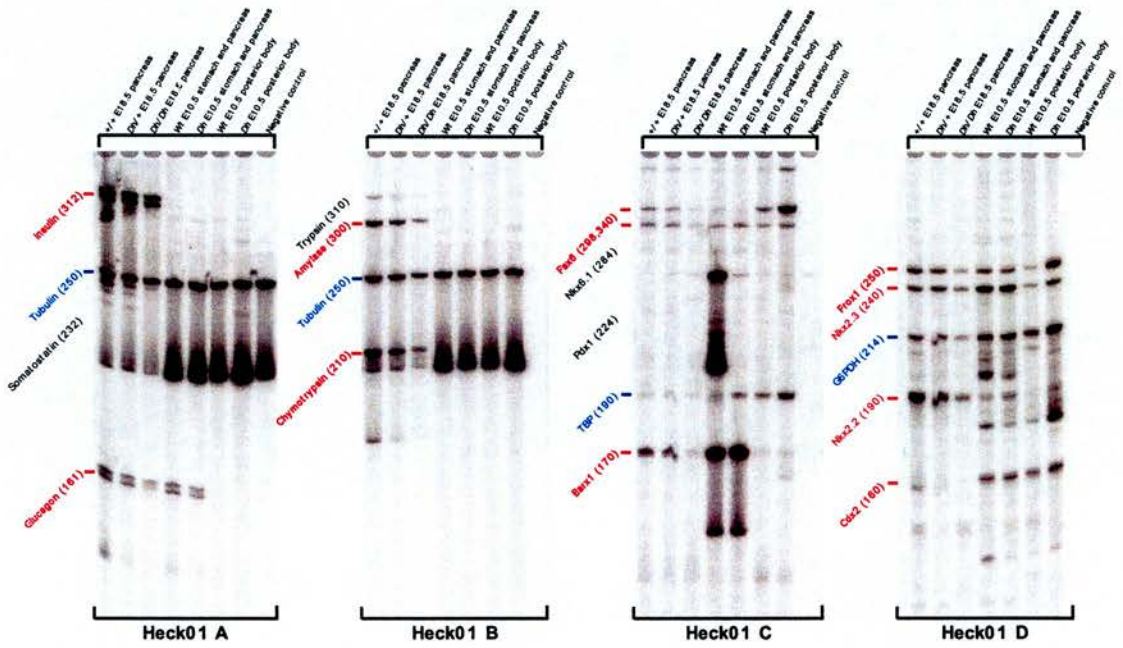
Primer	Sequence
PHExc10	ACCAGACGCTGGAAATGGAGAAAAGAAATTCGTGTTCAATATGTATTTGACGCGAGAGCGCCGCTGGAGATTAGCAAGACCATTAAACCTTA
F1	-----
F2	ACGAACGCTGGAAATGGAGAAAAGAAATTCGTGTTCAATATGTATTTGACGCGAGAGCGCCGCTGGAGATTAGCAAGACCATTAAACCTTA
F3	ACCAGACGCTGGAAATGGAGAAAAGAAATTCGTGTTCAATATGTATTTGACGCGAGAGCGCCGCTGGAGATTAGCAAGACCATTAAACCTTA
F4	-----
Alignment	ACCAGACGCTGGAAATGGAGAAAAGAAATTCGTGTTCAATATGTATTTGACGCGAGAGCGCCGCTGGAGATTAGCAAGACCATTAAACCTTA
PHExc10	CAGACAGACAAGTCAAAATCTGGTTTCAAAATCGCAGAATGAAACTCAAGAAAATGAACCGAGAGAATCGGATCCGGGAACAGACCTCCA
F1	-----
F2	CAACAGACAAATCAAAATCTGGTTTCAAAATCGCAGAATGAAACTCAAGAAAATGAACCGAGAGAATCGGATCCGGGAACAGACCTCCA
F3	CAGACAGACAAGTCAAAATCTGGTTTCAAAATCGCAGAATGAAACTCAAGAAAATGAACCGAGAGAATCGGATCCGGGAACAGACCTCCA
F4	-----
Alignment	CAGACAGACAAGTCAAAATCTGGTTTCAAAATCGCAGAATGAAACTCAAGAAAATGAACCGAGAGAATCGGATCCGGGAACAGACCTCCA
PHExc10	ATTTTAATTTACCTTGAGCCAGCGTCATCTCCTCCGCCCTCCCTTCTCCCTTTCGCCGCCCTCCTCCCTTTGTGCTTGGTGTATATTT
F1	-----
F2	ATTTTAATTTACCTTGAGCCAGCGTCATCTCCTCCGCCCTCCCTTCTCCCTTTCGCCGCCCTCCTCCCTTTGTGCTTGGTGTATATTT
F3	ATTTTAATTTACCTTGAGCCAGCGTCATCTCCTCCGCCCTCCCTTCTCCCTTTCGCCGCCCTCCTCCCTTTGTGCTTGGTGTATATTT
F4	-----
Alignment	ATTTTAATTTACCTTGAGCCAGCGTCATCTCCTCCGCCCTCCCTTCTCCCTTTCGCCGCCCTCCTCCCTTTGTGCTTGGTGTATATTT
PHExc10	TTTTTCCCTCCCTGAGTATAAATGCAACTAGCTAGTGGATCCCGGGTTCGACCATGTGGCGTCTTACCA-GTACAGCCAATATGGGCAGA
F1	-----
F2	TTTTTCCCTCCCTGAGTATAAATGCAACTAGCTAGTGGATCCCGGGTTCGACCATGTGGCGTCTTACCA-GTACAGCCAATATGGGCAGA
F3	TTTTTCCCTCCCTGAGTATAAATGCAACTAGCTAGTGGATCCCGGGTTCGACCATGTGGCGTCTTACCA-GTACAGCCAATATGGGCAGA
F4	-----
Alignment	TTTTTCCCTCCCTGAGTATAAATGCAACTAGCTAGTGGATCCCGGGTTCGACCATGTGGCGTCTTACCA-GTACAGCCAATATGGGCAGA
PHExc10	GCAAGGTGAATACCAGCACTGTACTACTGTAGAAAAGACTGTCACTGTTTATCCTCTAAAAAGGGCTTCATTGGATTGGTGGAAATAAA
F1	-----
F2	GCAAGGTGAATACCAGCACTGTACTACTGTAGAAAAGACTGTCACTGTTTATCCTCTAAAAAGGGCTTCATTGGATTGGTGGAAATAAA
F3	GCAAGGTGAATACCAGCACTGTACTACTGTAGAAAAGACTGTCACTGTTTATCCTCTAAAAAGGGCTTCATTGGATTGGTGGAAATAAA
F4	-----
Alignment	GCAAGGTGAATACCAGCACTGTACTACTGTAGAAAAGACTGTCACTGTTTATCCTCTAAAAAGGGCTTCATTGGATTGGTGGAAATAAA
PHExc10	GCAAAATATTACTTAATTTGAATTTGCTCTCAATAATGTCAGAAAGATTATTTATGTTTCATGAGACTTTGTCAAAATTTTTGCAACATACTA
F1	-----
F2	GCAAAATATTACTTAATTTGAATTTGCTCTCAATAATGTCAGAAAGATTATTTATGTTTCATGAGACTTTGTCAAAATTTTTGCAACATACTA
F3	GCAAAATATTACTTAATTTGAATTTGCTCTCAATAATGTCAGAAAGATTATTTATGTTTCATGAGACTTTGTCAAAATTTTTGCAACATACTA
F4	-----
Alignment	GCAAAATATTACTTAATTTGAATTTGCTCTCAATAATGTCAGAAAGATTATTTATGTTTCATGAGACTTTGTCAAAATTTTTGCAACATACTA
PHExc10	TGTAGTCTTAATTTATGGGAAATTTTACACAACTTTACATCATTTTAACTAAAGGACCCAAATTTGCAATTTGTTCCAAATCTA
F1	-----
F2	TGTAGTCTTAATTTATGGGAAATTTTACACAACTTTACATCATTTTAACTAAAGGACCCAAATTTGCAATTTGTTCCAAATCTA
F3	TGTAGTCTTAATTTATGGGAAATTTTACACAACTTTACATCATTTTAACTAAAGGACCCAAATTTGCAATTTGTTCCAAATCTA
F4	-----
Alignment	TGTAGTCTTAATTTATGGGAAATTTTACACAACTTTACATCATTTTAACTAAAGGACCCAAATTTGCAATTTGTTCCAAATCTA
PHExc10	TTATGATATTTTGGAAAGATGTTTCTACTTGGTTATACACTGTAAAAAGTGATTA-GTTACTTGTATAAAAAATAAATTTGAGGTAAC
F1	-----
F2	TTATGATATTTTGGAAAGATGTTTCTACTTGGTTATACACTGTAAAAAGTGATTA-GTTACTTGTATAAAAAATAAATTTGAGGTAAC
F3	TTATGATATTTTGGAAAGATGTTTCTACTTGGTTATACACTGTAAAAAGTGATTA-GTTACTTGTATAAAAAATAAATTTGAGGTAAC
F4	-----
Alignment	TTATGATATTTTGGAAAGATGTTTCTACTTGGTTATACACTGTAAAAAGTGATTA-GTTACTTGTATAAAAAATAAATTTGAGGTAAC
PHExc10	CTGTTACCTTAAAA-GTGACAAGTTGACTTTGAGTAAACCTGTTGTAACCGAGAAGCTTATTATTACTCACATAGTTCATTACCTAAA
F1	-----
F2	CTGTTACCTTAAAA-GTGACAAGTTGACTTTGAGTAAACCTGTTGTAACCGAGAAGCTTATTATTACTCACATAGTTCATTACCTAAA
F3	CTGTTACCTTAAAA-GTGACAAGTTGACTTTGAGTAAACCTGTTGTAACCGAGAAGCTTATTATTACTCACATAGTTCATTACCTAAA
F4	-----
Alignment	CTGTTACCTTAAAA-GTGACAAGTTGACTTTGAGTAAACCTGTTGTAACCGAGAAGCTTATTATTACTCACATAGTTCATTACCTAAA
PHExc10	TTTTTTTAACTCTTAAAGACCAAGGTGTTTTTTTTACATGCATTT
F1	-----
F2	TTTTTTTAACTCTTAAAGACCAAGGTGTTTTTTTTACATGCATTT
F3	TTTTTTTAACTCTTAAAGACCAAGGTGTTTTTTTTACATGCATTT
F4	-----
Alignment	TTTTTTTAACTCTTAAAGACCAAGGTGTTTTTTTTACATGCATTT

Hoxc10
zPax3-3' UTR
Minc2 discrepancy
Minc2 discrepancy

Appendix II: MPX-PCR - annotated gels

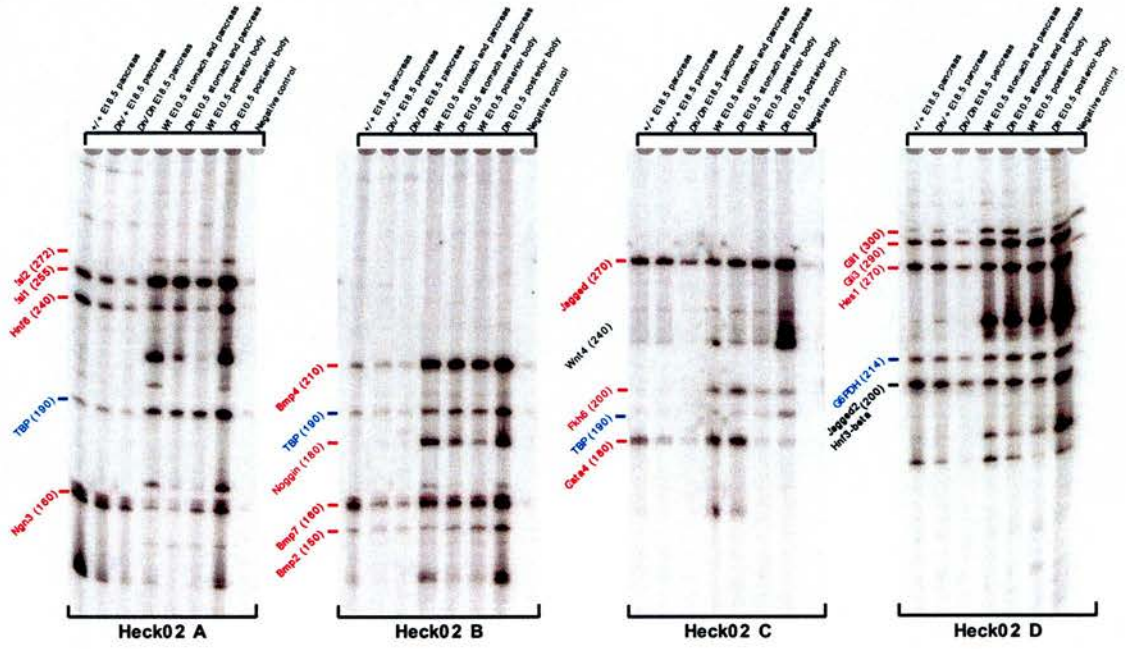
Heck01: Annotated Gel
Heck02: Annotated Gel
Heck03: Annotated Gel
Heck04: Annotated Gel
Heck05: Annotated Gel
Heck06: Annotated Gel
Heck07: Annotated Gel
Heck08: Annotated Gel
Heck09: Annotated Gel
Heck10: Annotated Gel
Heck11: Annotated Gel
Heck12: Annotated Gel
Heck13: Annotated Gel
Heck14: Annotated Gel

Heck01



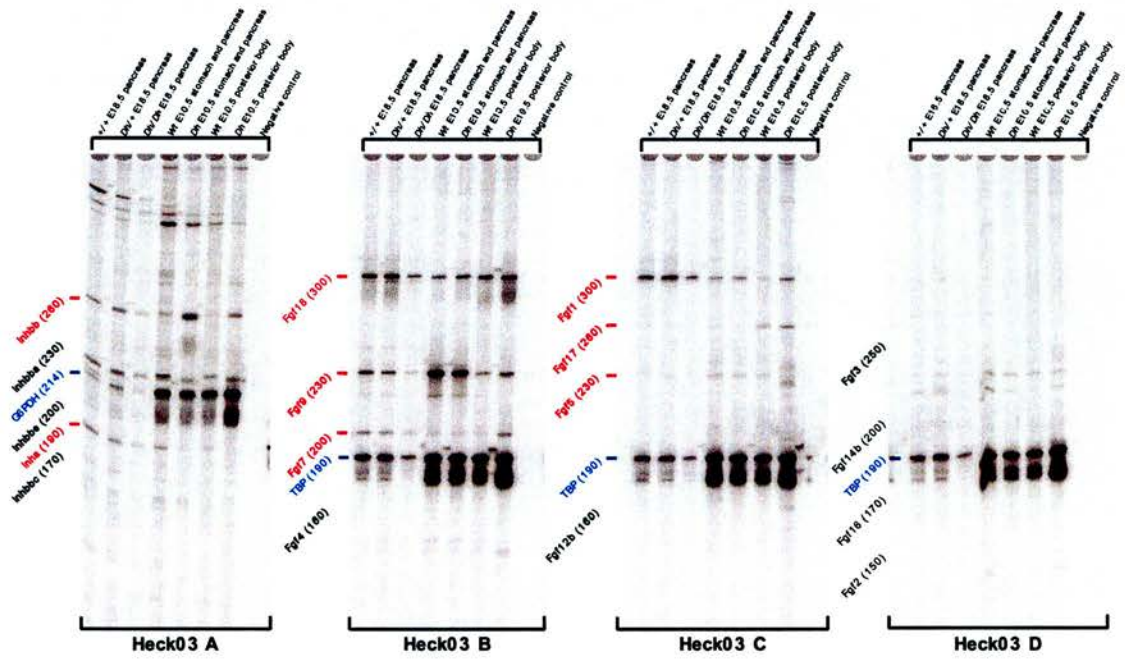
- Internal control
- No PCR product detected
- PCR product present at the correct size

Heck02



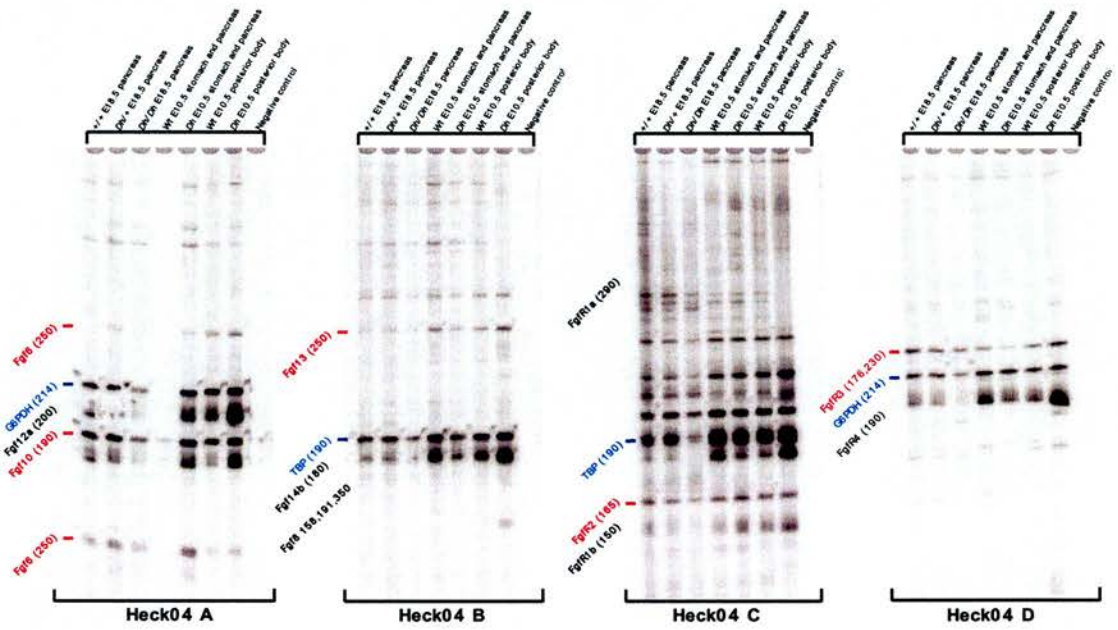
- Internal control
- No PCR product detected
- PCR product present at the correct size

Heck03



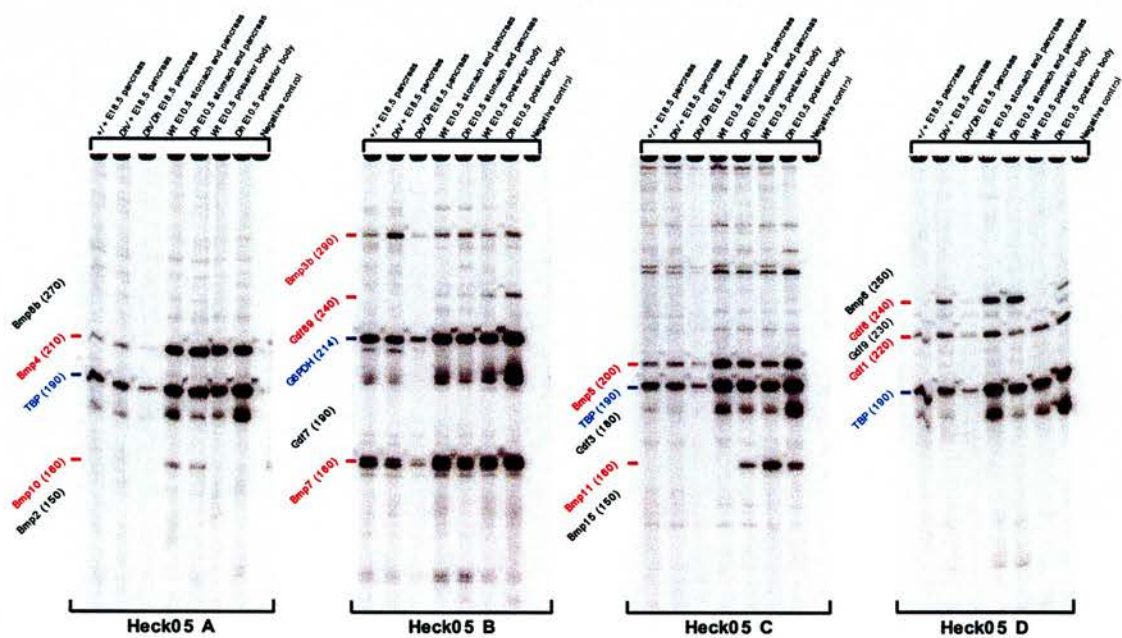
- Internal control
- No PCR product detected
- PCR product present at the correct size

Heck04



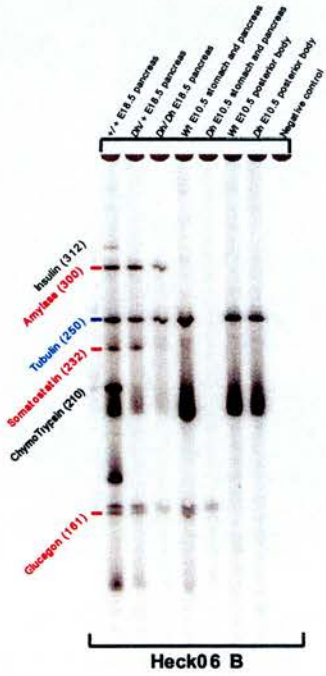
- Internal control
- No PCR product detected
- PCR product present at the correct size

Heck05



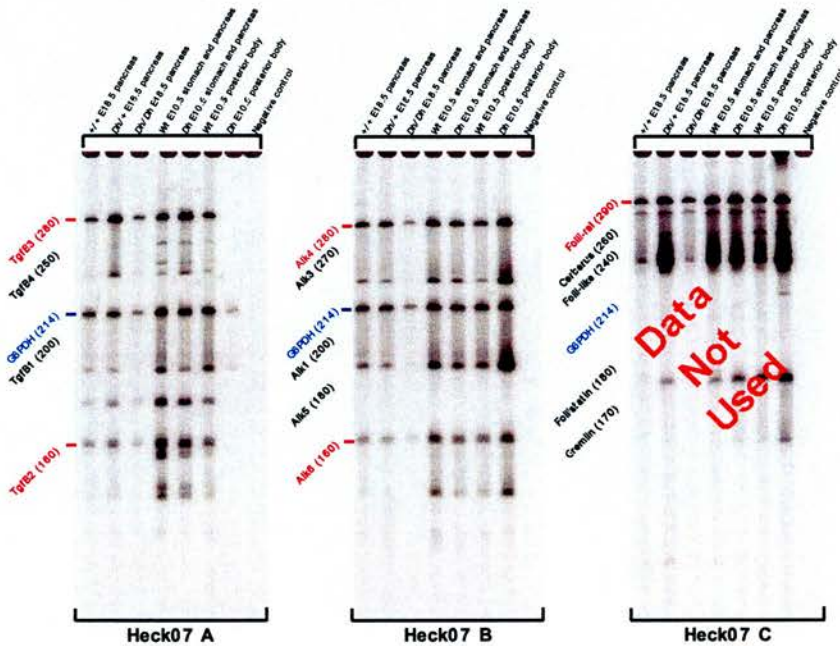
- Internal control
- No PCR product detected
- PCR product present at the correct size

Heck06



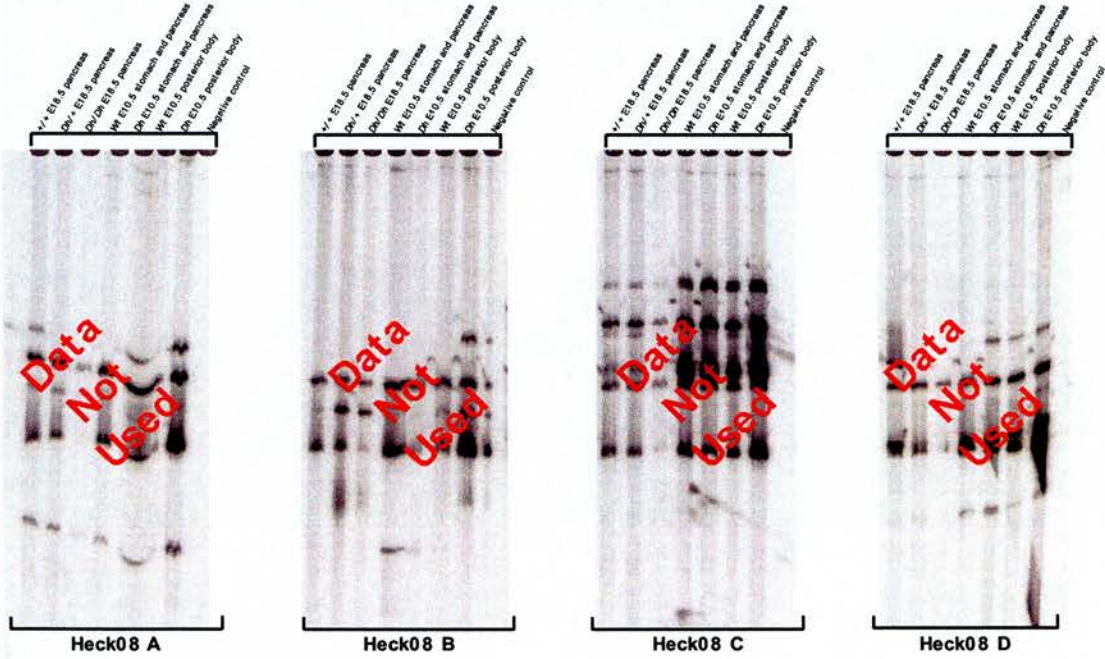
- Internal control
- No PCR product detected
- PCR product present at the correct size

Heck07

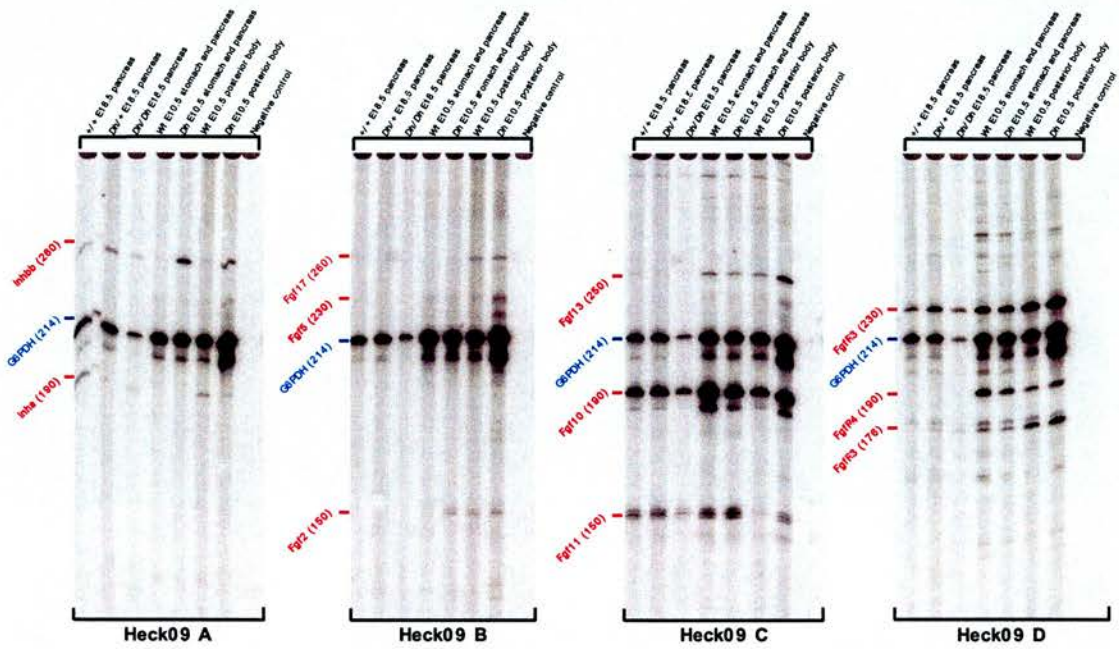


- Internal control
- No PCR product detected
- PCR product present at the correct size

Heck08

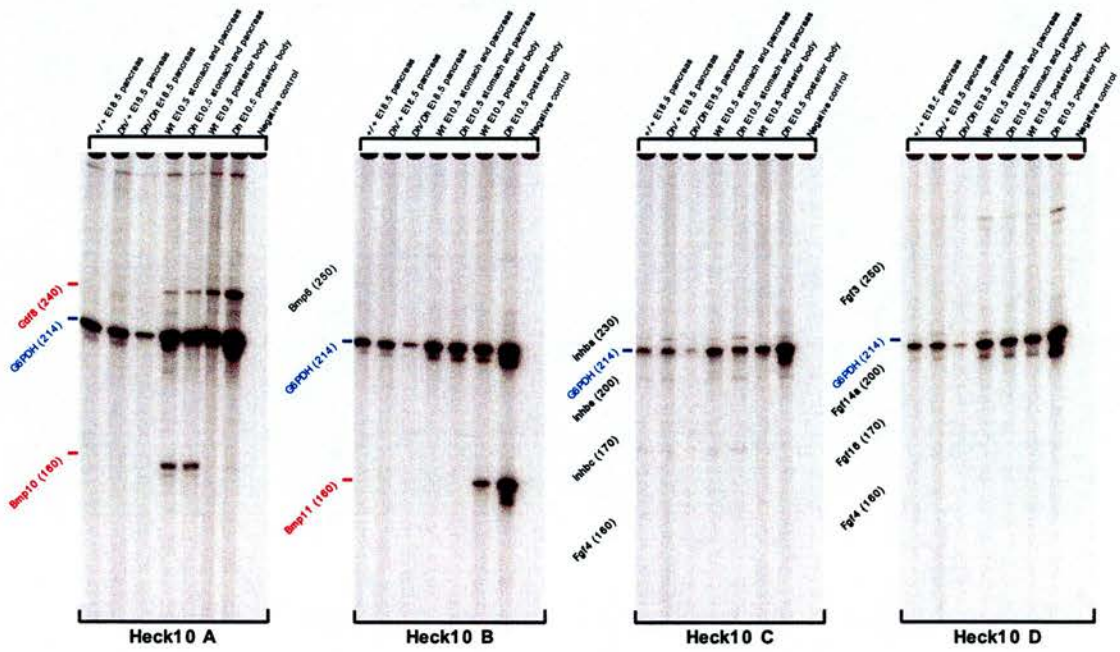


Heck09



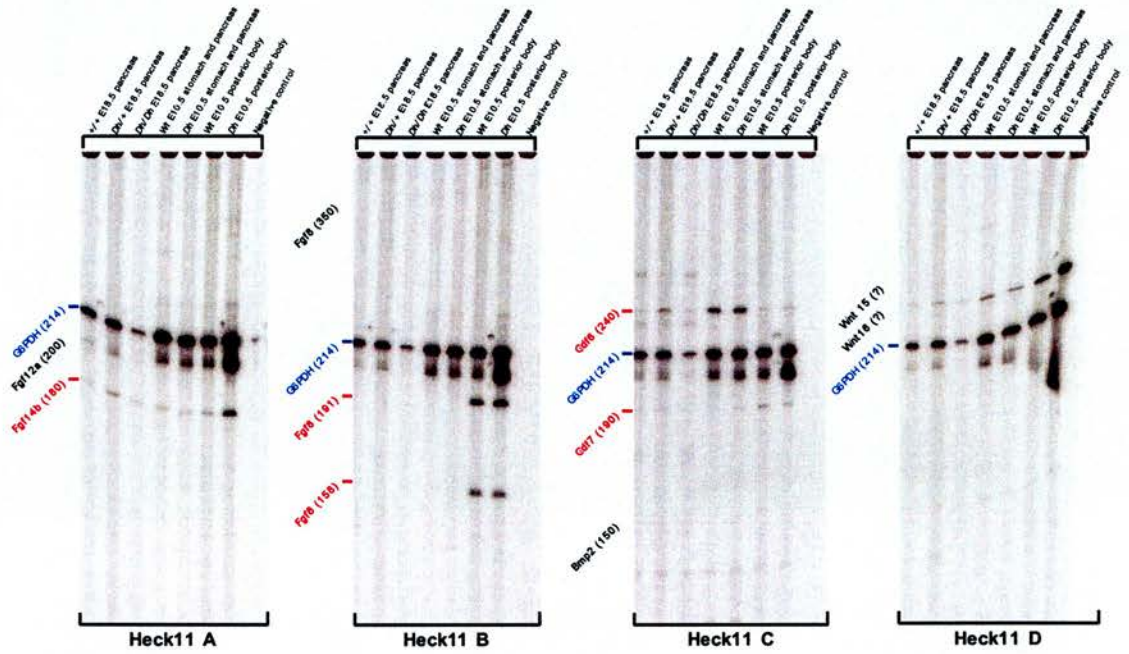
- Internal control
- No PCR product detected
- PCR product present at the correct size

Heck10



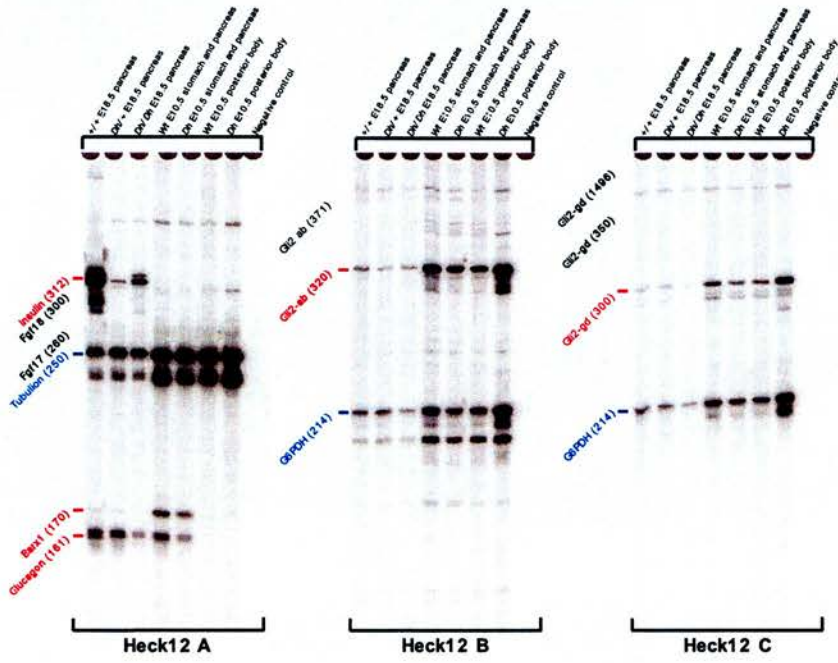
- Internal control
- No PCR product detected
- PCR product present at the correct size

Heck11

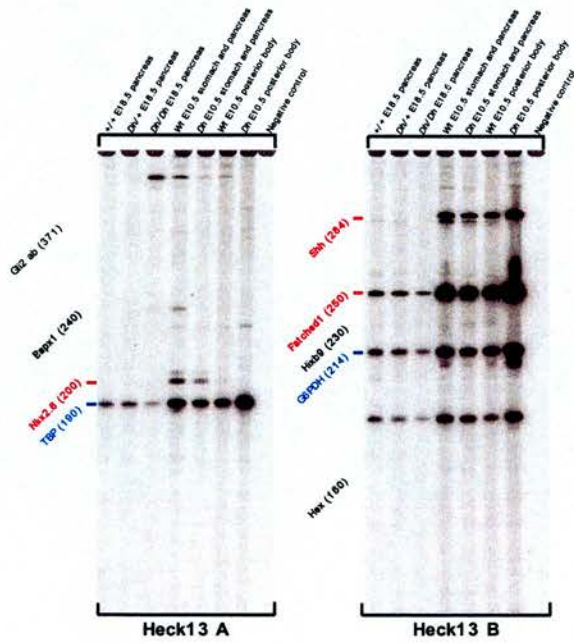


- Internal control
- No PCR product detected
- PCR product present at the correct size

Heck12

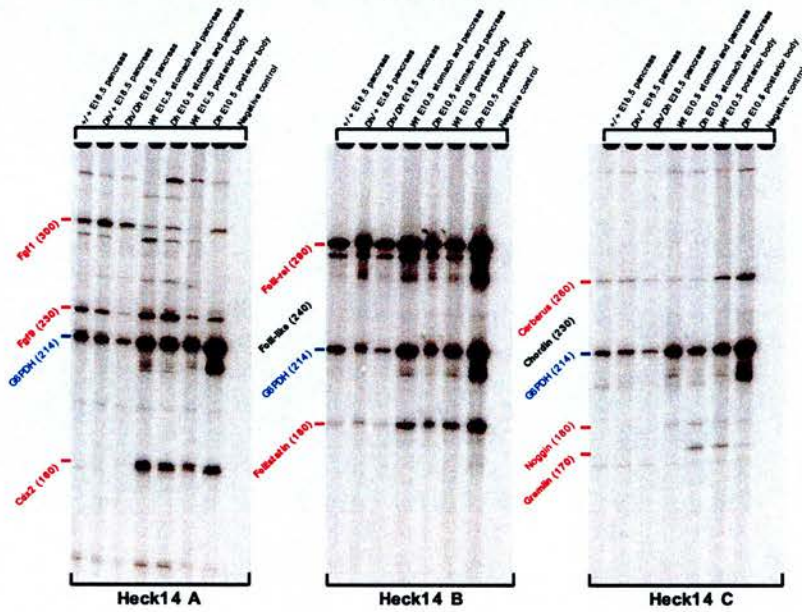


Heck13



- Internal control
- No PCR product detected
- PCR product present at the correct size

Heck14



- Internal control
- No PCR product detected
- PCR product present at the correct size

Appendix III: Degenerate PCR's

Table A3.1: Sequence alignment of the inhibin β family

Table A3.2: Sequence alignment of the BMP family

Appendix IV: Primer sequences

Table A4.1: Primer sequences used for cloning and genotyping

Table A4.2: Oligo sequences used for sequencing

Table A4.3: Oligo sequences used for cloning of the pHEX construct

Table A4.4: Primer sequences used for making *in situ* probes

Table A4.5: Enzymes used for verification of pPAX plasmids

Table A4.1: Primer sequences used for cloning and genotyping

Template		Conditions ¹			Primers	
no	PCR product	Ann. C°	Den. C°	Cycles	Direction	Primer sequence 5'→ 3'
1	Zebrafish <i>Pax3</i> 3'UTR	65	93	35	Forward	GGTACAGCGTCGACCATGTGGCG
					Reverse	TTACTATTATACGGCGGCCGCACATTTTAGCTCTGAAG
2	<i>Hoxc10</i> ²	62	93	35	Forward	CGACGCGTGCTCCTCCGCTGTAGTATTGC
					Reverse	GCACTAGTTGCATTATACTCAGGGAGGG
3	<i>Myogenin</i>	65	93	35	Forward	TGGGGCTGTCCTGATGTCCAGA
					Reverse	GACCTTGGCAGACGGCAGCTTT
4	<i>pHEX</i> (across intron)	65	93	35	Forward	TCTGCAGAAGTTGGTCGTGAGG
					Reverse	CGCAGTTGAAGTCACTCCCAGA
5	<i>Dh</i> (<i>Inhβb</i>)	57	93	35	Forward	GGAAGAGTGGTCTAGTTTCTATGG
					Reverse	AGCCTGGAGGCTTAAGTAGCAC
6	<i>Bapx1</i>	65	93	35	Forward	CCGAACCAGAACAGCCGTGG
					Reverse	CAGCCCCCTTCTGGAGAAC
7	<i>Inhβb</i> (Exon1) ³	65	93	35	Forward	CCTGCCTTCTGCTCCTGGTG
					Reverse	CCACCTGTCTCTGCAAAGCTGA
8	<i>Inhβb</i> (Exon2)	65	93	35	Forward	GGTCCGCCTGTACTTCTTCGTC
					Reverse	GCCTCTCCTGCTCCCTCAAAG
9	<i>Inhβb</i> (Intron)	65	93	10/25	Forward	TCCGAGATCATCAGCTTTCAG
					Reverse	GCCTGCACCACGAATAGGTTCT
10	<i>Inhβb</i> (degenerate)	60	93	35	Forward	GGSTGGMNRNGAITGGATCMT
					Reverse	CCRCASKCCTCNACNAYCATGT
11	<i>Bmp</i> (degenerate)	60	93	35	Forward	GAISTSGGNTGGMWKGAITGG
					Reverse	ATGGCRTGGTTRGTKGMRTTWA
12	<i>Bmp11</i>	60	93	35	Forward	CATGGAGCTTCGAGTCTAGAG
					Reverse	CAGGGATCTTGCCGTAGATAAT

¹ Elongation of DNA strands was carried out at 72°C.

² The *Hoxc10* gene was amplified using the PfuI polymerase (# 7)

³ The *Inhβb* was amplified using GC Advantage®-GC Genomic PCR (#8)

Table A4.2: Oligo sequences used for sequencing

Oligo		Conditions ¹			Sequence	
no	name	Ann. C°	Den. C°	Cycles	Direction	Primer sequence 5'→3'
1	T7	50	94	25	Forward	GTAATACGACTCACTATAGGGC
2	M13 reverse	50	94	25	Reverse	GGAACAGCTATGACCATG
3	pHEX (<i>β</i> Globin left)	50	94	25	Reverse	CGACAAGCCCAGTTTCTATTG
4	pHEX (<i>Hoxc10 a</i>)	50	94	25	Forward	TTTGCCTTTCTCTCCACAGG
5	pHEX (<i>Hoxc10 b</i>)	50	94	25	Forward	ACTCCTGGGGCGACCCCAAA
6	pHEX (<i>Hoxc10 c</i>)	50	94	25	Forward	TCCGACAGCCAGACCCCCAG
7	pHEX (<i>Hoxc10 d</i>)	50	94	25	Forward	TCGGATCCGGGAAGTACCT

¹ Elongation of DNA strands was carried out at 60°C.

Table A4.3: Sequences for oligos used for cloning of the pHEX construct

Cloning Step	Restriction sites	Oligo sequence
Constructs	comments	Primer sequence 5'→3'
pPAX3.1-pPAX3.2	<i>ΔBamHI-SfiI-SacII-ΔBamHI</i>	Oligo1: GATCAGGCCATTATGGCCGCGGT Oligo2: GATCACCGCGGCCATAATGGCCT
pPAX3.2-pPAX3.3	<i>BglII-SfiI-SacII-NgoIV-KasI-PstI</i>	Oligo1: GGCGCCGGCCGCGGCCTATTAGGCCA Oligo2: GATCTGGCCTAATAGGCCGCGGCCGGCGCCTGCA
pPAX3.3-pPAX3.4	<i>XbaI-SpeI-BamHI-SmaI-ΔSall</i>	Oligo1: CTAGACTAGTGGATCCC GGGT TCGAACCCGGGAT Oligo2: CCACTAGT
pPAX3.4-pPAX3.5	<i>NarI-EcoRV-Sall-HindIII-BclI-PstI</i>	Oligo1: GTGATCAAGCTTGTGACGATATCGG TCGCCGATA Oligo2: TCGTCGACAAGCTTGATCACTGCA
pPAX3.5-pHEX	<i>βGlobin Basal promoter</i>	Oligo1: GAAGCAAATGTAAGCAATAGATGGCTCTGCCCTGA CTTTTATGCCAGCCCGGAAGCTGATCAGCTTCC Oligo2: CGGGCTGGGCATAAAAGTCAGGGCAGAGCCATCTA TTGCTTACATTTGCTTCTGCA

Blue indicates the restriction site has been preserved
Red indicates the restriction site has been deleted

Table A4.4: Primer sequences for *in situ* probes

Template	Conditions ¹				Size	Direction	Primers
	Gene	Ann. C°	Den. C°	Cycles			
<i>*Hox11</i>	57	93	35	530bp	Forward	AGAGGAACGTGAGGCCGAGA	
					Reverse	GGATCCCAGAAGCCTCCGG	
<i>*Barx1</i>	60	93	35	376bp	Forward	AGACAATTAAGGGCCAGACAAG	
					Reverse	CCGTCTTTGTAAGAGAGGGGTA	
<i>*Pdx1</i>	56	93	35	700bp	Forward	CGAGAGACACATCAAAATCTGG	
					Reverse	CAGAAGCAGCCTCAAAGTTTTC	
<i>ActR11b</i>	65	93	35	513bp	Forward	CCCCAGGTGACTTCTGCTGCT	
					Reverse	GTAATACGACTCACTATAGGGGTGCTGAAGATTTCCCGTTCA	
<i>Bmp3b</i>	65	93	35	471bp	Forward	CACAGCCGCTTCCACTTCTAC	
					Reverse	GTAATACGACTCACTATAGGGGCTGCTCCAGGCTCAAAGTCTC	
<i>Bmp5</i>	65	93	35	478bp	Forward	CACCTTTGCCAGCCTACATGA	
					Reverse	GTAATACGACTCACTATAGGGGCTCTTCCACAAGACCAGCAG	
<i>Bmp10</i>	65	93	35	452bp	Forward	CAAAGGCATCGTCACCAAATG	
					Reverse	GTAATACGACTCACTATAGGGGGAGAGAAAGGCTCCCGGTACAT	
<i>Bmp11</i>	65	93	35	472bp	Forward	ATCCTGGATCTGCACGACTTCC	
					Reverse	GTAATACGACTCACTATAGGGCAAAGGCGTTGATCTCGATTCC	
<i>Capsulin</i>	65	93	35	468bp	Forward	GCCCAGTCAGGCTCTTCTCACTC	
					Reverse	GTAATACGACTCACTATAGGGCTTTTCTTAGTGGGCGCCTTCC	
<i>Fgf9</i>	65	93	35	466bp	Forward	TGGACAGTCCGGTGTGCTAAA	
					Reverse	GTAATACGACTCACTATAGGGCTTCTCTTGAGTCCCGTCCCT	
<i>Fgf11</i>	65	93	35	477bp	Forward	CAGAAACAGCTCCTCATCCTG	
					Reverse	GTAATACGACTCACTATAGGGCTTGGTCTTCTGACTCGGTTT	
<i>Fgf13</i>	65	93	35	478bp	Forward	CATTGATGGCACCAAGACGAG	
					Reverse	GTAATACGACTCACTATAGGGGCTCATGGATTGCTCCATTC	
<i>Fgf18</i>	65	93	35	472bp	Forward	TGGTATGTGGGCTTACCAAGA	
					Reverse	GTAATACGACTCACTATAGGGCCTCGTTCAAGTCTCTCTGG	
<i>FgfR1</i>	65	93	35	466bp	Forward	GGGAGCATCAACCACCTACC	
					Reverse	GTAATACGACTCACTATAGGGAGGCCCGGTGCAGTAGATAAT	
<i>FgfR2</i>	65	93	35	477bp	Forward	GCTTCATCTGCCTGGTCTTGGT	
					Reverse	GTAATACGACTCACTATAGGGTGGTCCAGTACGGTCTCTCTG	
<i>FgfR3</i>	65	93	35	471bp	Forward	TGGTGACCAGGACAATGTGAT	
					Reverse	GTAATACGACTCACTATAGGGCACCTGGCAGTACTGCTCAAA	
<i>FgfR4</i>	65	93	35	472bp	Forward	AGGTGGTCAGTGGGAAGTCTGG	
					Reverse	GTAATACGACTCACTATAGGGCGAGGAGCTGCTGAGTGTCTTG	
<i>Gdf6</i>	65	93	35	346bp	Forward	GCAAGCGACATGGCAAGAAGT	
					Reverse	GTAATACGACTCACTATAGGGGACTCCACCACCATGTCCCTCAT	
<i>Inhbb</i>	65	93	35	500bp	Forward	GGTCCGCTGTACTTCTTCGTC	
					Reverse	GTAATACGACTCACTATAGGGATGAGCCGAAAGTCGATGAAGAAGT	
<i>Lefty</i>	65	93	35	431bp	Forward	CCATGATTGTGAGCGTGAAGGA	
					Reverse	GTAATACGACTCACTATAGGGTGGGATTCTGCTCTTGGTTTG	
<i>Nkx2.5</i>	65	93	35	328bp	Forward	ACTTGAACACCGTGCAGAGTCC	
					Reverse	GTAATACGACTCACTATAGGGGTGTGGAATCCGTCGAAAGTGC	
<i>Nodal</i>	65	93	35	350bp	Forward	GTGAAGACCAAGCCACTGAGCA	
					Reverse	GTAATACGACTCACTATAGGGATACACCCAGCCTTTGCACAC	
<i>Pitx2</i>	65	93	35	412bp	Forward	TAGAAGGTCGTGCGCACTATGG	
					Reverse	GTAATACGACTCACTATAGGGCTTTGCTCGAAGCGAAAAATC	

¹ Elongation of the DNA strands is carried out at 72°C for all markers.

* PCR products were subsequently cloned into pCR2.1

Red indicates T7 promoter sequence

Table A4.5: Enzymes used for verification of plasmids

Construct		Conditions		Band sizes	
Step no	Plasmid	Plasmid	Restriction enzymes	Bacterial Vector	Other products
1	<i>pPAX3.1</i>	<i>pCI</i>	<i>EcoRI</i> and <i>NotI</i>	~4000bp	0bp
		<i>pPAX3.1</i>	<i>EcoRI</i> and <i>NotI</i>	~4000bp	~900bp
2	<i>pPAX3.2</i>	<i>pPAX3.1</i>	<i>BglII</i> and <i>SfiI</i>	~4900bp	0bp
		<i>pPAX3.1</i>	<i>BglII</i> and <i>SfiI</i> and <i>NheI</i>	~3800bp	1100bp
		<i>pPAX3.2</i>	<i>BglII</i> and <i>SfiI</i>	~2600bp	~2300bp
		<i>pPAX3.2</i>	<i>BglII</i> and <i>SfiI</i> and <i>NheI</i>	~2600bp	~1200bp and ~1100bp
3	<i>pPAX3.3</i>	<i>pPAX3.2</i>	<i>SfiI</i>	~4900bp	0bp
		<i>pPAX3.2</i>	<i>BglII</i> and <i>SfiI</i>	~2600bp	~2300bp
		<i>pPAX3.2</i>	<i>BglII</i> and <i>SfiI</i> and <i>NheI</i>	~2600bp	~1200bp and ~1100bp
		<i>pPAX3.3</i>	<i>SfiI</i>	~2600bp	~1500bp
		<i>pPAX3.3</i>	<i>SfiI</i> and <i>NheI</i>	~2600bp	~1200bp and ~300bp
4	<i>pPAX3.4</i>	<i>pPAX3.3</i>	<i>SfiI</i> and <i>SalI</i>	~2600bp	~1200bp and ~300bp
		<i>pPAX3.3</i>	<i>SfiI</i> and <i>SpeI</i>	~2600bp	~1500bp
		<i>pPAX3.4</i>	<i>SfiI</i> and <i>SalI</i>	~2600bp	~1500bp
		<i>pPAX3.4</i>	<i>SfiI</i> and <i>SpeI</i>	~2600bp	~1200bp and ~300bp
5	<i>pPAX3.5</i>	<i>pPAX3.4</i>	<i>NotI</i> and <i>SalI</i>	~4200bp	0bp
		<i>pPAX3.4</i>	<i>NotI</i> and <i>PstI</i>	~3000bp	~1200bp
		<i>pPAX3.5</i>	<i>NotI</i> and <i>SalI</i>	~3000bp	~1200bp
		<i>pPAX3.5</i>	<i>NotI</i> and <i>PstI</i>	~3000bp	~1200bp
6	<i>pHEX</i>	<i>pPAX3.5</i>	<i>HinDIII</i> and <i>BamHI</i>	~3900bp	~300bp
		<i>pPAX3.5</i>	<i>SmaI</i>	~4200bp	0bp
		<i>pHEX</i>	<i>HinDIII</i> and <i>BamHI</i>	~3900bp	~400bp
		<i>pHEX</i>	<i>SmaI</i>	~4000bp	~300bp
7	<i>pHEX-IE</i>	<i>pHEX</i>	<i>HinDIII</i> and <i>SalI</i>	~4300bp	0bp
		<i>pHEX-IE</i>	<i>HinDIII</i> and <i>SalI</i>	~4300bp	~2900bp
8	<i>pHEX-NE</i>	<i>pHEX</i>	<i>HinDIII</i>	~4300bp	0bp
		<i>pHEX-IE</i>	<i>HinDIII</i>	~4300bp	~1900bp
9	<i>pHEXc10-IE</i>	<i>pHEX-IE</i>	<i>MluI</i> and <i>SpeI</i>	~7200bp	0bp
		<i>pHEXc10-IE</i>	<i>MluI</i> and <i>SpeI</i>	~7200bp	~1200bp
10	<i>pHEXc10-NE</i>	<i>pHEX-NE</i>	<i>MluI</i> and <i>SpeI</i>	~6200bp	0bp
		<i>pHEXc10-NE</i>	<i>MluI</i> and <i>SpeI</i>	~6200bp	~1200bp

After *Hoxc10* had been cloned into *pHEX-NE* to give *pHEXc10-NE* the construct was sequenced.

Appendix V: Data sheets for *In situ* probes and Antibodies

Table A5.1: Data Sheet for *in situ* probes

Table A5.2: Data sheet for primary and secondary antibodies

Table A5.1: Data sheet of *in situ* probes

Gene	Antisense		Comments		
	<i>In situ</i> probe	Restriction enzyme	RNA polymerase	Template	Source
<i>ActR11b</i>	-		T7	PCR product	Hecksher-Sørensen, J.
<i>Alx4</i>	Sall		T3	Plasmid	-
<i>Bapx1</i>	HinDIII		T7	Plasmid	Lettice, L.
<i>Barx1</i>	BamHI		T7	Plasmid	Hecksher-Sørensen, J.
<i>Bmp2</i>	XbaI		T3	Plasmid	-
<i>Bmp3b</i>	-		T7	PCR product	Hecksher-Sørensen, J.
<i>Bmp4</i>	AccI		T7	Plasmid	Hogan, B.
<i>Bmp5</i>	-		T7	PCR product	Hecksher-Sørensen, J.
<i>Bmp7</i>	Sall		Sp6	Plasmid	-
<i>Bmp10</i>	-		T7	PCR product	Hecksher-Sørensen, J.
<i>Bmp11</i>	-		T7	PCR product	Hecksher-Sørensen, J.
<i>Capsulin</i>	-		T7	PCR product	Hecksher-Sørensen, J.
<i>α-Collagen</i>	EcoRI		T3	Plasmid	-
<i>Dhh</i>	EcoRI		T7	Plasmid	McMahon, A.
<i>En1</i>	Clal		T7	Plasmid	-
<i>Fgf4</i>	EcoRI		T3	Plasmid	Lettice, L.
<i>Fgf8</i>	HinDIII		T3	Plasmid	Mahmood, R.
<i>Fgf9</i>	-		T7	PCR product	Hecksher-Sørensen, J.
<i>Fgf10</i>	BamHI		T3	Plasmid	-
<i>Fgf11</i>	-		T7	PCR product	Hecksher-Sørensen, J.
<i>Fgf13</i>	-		T7	PCR product	Hecksher-Sørensen, J.
<i>Fgf18</i>	-		T7	PCR product	Hecksher-Sørensen, J.
<i>FgfR1</i>	-		T7	PCR product	Hecksher-Sørensen, J.
<i>FgfR2</i>	-		T7	PCR product	Hecksher-Sørensen, J.
<i>FgfR3</i>	-		T7	PCR product	Hecksher-Sørensen, J.
<i>FgfR4</i>	-		T7	PCR product	Hecksher-Sørensen, J.
<i>Formin</i>	NsiI		T7	Plasmid	-
<i>Follistatin</i>	EcoRI		T7	Plasmid	Dickman, D.
<i>Gdf6</i>	-		T7	PCR product	Hecksher-Sørensen, J.
<i>Gli2</i>	KpnI		T3	Plasmid	Lettice, L.
<i>Gremlin</i>	PstI		T3	Plasmid	-
<i>Hox11</i>	HinDIII		T7	Plasmid	Hecksher-Sørensen, J.
<i>Hoxa9</i>	HinDIII		T7	Plasmid	Capecchi, M.
<i>Hoxa10</i>	XhoI		T7	Plasmid	Capecchi, M.
<i>Hoxa11</i>	Asp718		T7	Plasmid	Capecchi, M.
<i>Hoxb8</i>	EcoRI		T7	Plasmid	Krumlauf, R.
<i>Hoxb9</i>	EcoRI		T7	Plasmid	Krumlauf, R.
<i>Hoxc9</i>	EcoRI		T3	Plasmid	Capecchi, M.
<i>Hoxc10</i>	XhoI		T7	Plasmid	Capecchi, M.
<i>Hoxc11</i>	XbaI		T3	Plasmid	Capecchi, M.
<i>Hoxd9</i>	BamHI		T7	Plasmid	Duboule, D.
<i>Hoxd10</i>	EcoRI		T7	Plasmid	Duboule, D.
<i>Hoxd11</i>	EcoRI		T7	Plasmid	Duboule, D.
<i>Hoxd12</i>	BamHI		T7	Plasmid	Duboule, D.
<i>Hoxd13</i>	PvuII		T7	Plasmid	Duboule, D.
<i>lhh</i>	XbaI		T7	Plasmid	McMahon, A.
<i>Inh1b</i>	-		T7	PCR product	Hecksher-Sørensen, J.
<i>Krox20</i>	BamHI		T3	Plasmid	-
<i>Lefty1</i>	-		T7	PCR product	Hecksher-Sørensen, J.
<i>Msx1</i>	BssHII		T7	Plasmid	Hill, R. E.
<i>Myogenin</i>	EcoRI		T7	Plasmid	-
<i>Nkx2.5</i>	-		T7	PCR product	Hecksher-Sørensen, J.
<i>Nkx3.1</i>	EcoRV		T7	Plasmid	-
<i>Nodal</i>	-		T7	PCR product	Hecksher-Sørensen, J.
<i>Patched</i>	BamHI		T3	Plasmid	-
<i>Pax1</i>	HinDIII		T7	Plasmid	-
<i>Pax3</i>	HinDIII		T7	Plasmid	-
<i>Pax9</i>	BamHI		T3	Plasmid	-
<i>Pitx2</i>	-		T7	PCR product	Hecksher-Sørensen, J.
<i>Pdx1</i>	Apal		T3	Plasmid	Hecksher-Sørensen, J.
<i>RdR1</i>	Sall		T3	Plasmid	-
<i>Scleraxis</i>	Apal		Sp6	Plasmid	-
<i>Shh</i>	HinDIII		T3	Plasmid	McMahon, A.
<i>Sox9</i>	XhoI		T3	Plasmid	Koopman, P.
<i>Tbx4</i>	EcoRV		T7	Plasmid	-
<i>Tbx5</i>	EcoRV		T7	Plasmid	-
<i>Wnt7a</i>	BamHI		T7	Plasmid	-
<i>Wnt5a</i>	EcoRI		SP6	Plasmid	-
<i>Wnt7b</i>	HinDIII		T7	Plasmid	-

Table A5.2: Data sheet of primary and secondary antibodies

Antibody data sheet						
1 st Antibody	Dilution	Raised in	Cell type	Company	Catalogue no	Prize
α -Insulin	1:10C	Guinea Pig	Pancreas/ β -cells	Dako	A0564	£82.66 (0.2ml)
α -Glucagon	1:100C	Mouse	Pancreas/ α -cells	Sigma	G2654	£57.70 (0.2ml)
α -Somastatin	1:30C	Rabbit	Pancreas/ δ -cells	Dako	A0566	£79.33 (0.2ml)
α -PP	1:10C	Rabbit	Pancreas/ γ -cells	Dako	A0619	£116.66 (0.2ml)
α -Pdx1	1:80C	Rabbit	Pancreatic Endoderm	Hagedorn	-	Gift
α -Isl1	1:25	Mouse	Dorsal Mesenchyme	P. Rashbash	-	Gift
α -Hnf3 β	1:50C	Rabbit	Endoderm	B. Hogan	-	Gift
α -E-cadherin	1:25	Mouse	Epithelial cells	Santa Cruz	Sc-8426	£150.00 (200 μ g)
α -Calbindin	1:10C	Mouse	Collecting tubules	Chemicon	AB1778	-
α -Laminin	1:10C	Rabbit	Epithelia	Sigma	L9393	-
α -BrdU	1:20C	Mouse	BrdU	-	-	-
α -NF160	1:80C	Mouse	Neurofilament	Sigma	N5264	£65.80 (0.2ml)
2 nd Antibody	Dilution	Raised in	Label	Company	Catalogue	Prize
α -Mouse IgG	1:20C	Goat	Alexa 488 (green)	Mol. Probes	A-11001	£79.62 (0.5 ml)
α -Rabbit IgG	1:20C	Goat	Alexa 594 (red)	Mol. Probes	A-11012	£101.52 (0.5 ml)
α -Rabbit IgG	1:20C	Goat	Alexa 488 (green)	Mol. Probes	A-11008	£79.62 (0.5 ml)
α -Guinea Pig IgG	1:20C	Goat	Alexa 594 (red)	Mol. Probes	A-11076	£101.52 (0.5 ml)

Appendix VI: Confocal Paper

Hecksher-Sørensen, J. and Sharpe, J. (2001). 3D confocal reconstruction of gene expression in mouse. *Mech Dev* **100**, 59-63.

Short communication

3D confocal reconstruction of gene expression in mouse

Jacob Hecksher-Sørensen, James Sharpe*

Department of Comparative and Developmental Genetics, MRC Human Genetics Unit, Western General Hospital, Crewe Road, EH4 2XU, UK

Received 4 September 2000; received in revised form 9 October 2000; accepted 10 October 2000

Abstract

Three-dimensional computer reconstructions of gene expression data will become a valuable tool in biomedical research in the near future. However, at present the process of converting in situ expression data into 3D models is a highly specialized and time-consuming procedure. Here we present a method which allows rapid reconstruction of whole-mount in situ data from mouse embryos. Mid-gestation embryos were stained with the alkaline phosphatase substrate Fast Red, which can be detected using confocal laser scanning microscopy (CLSM), and cut into 70 μm sections. Each section was then scanned and digitally reconstructed. Using this method it took two days to section, digitize and reconstruct the full expression pattern of *Shh* in an E9.5 embryo (a 3D model of this embryo can be seen at genex.hgu.mrc.ac.uk). Additionally we demonstrate that this technique allows gene expression to be studied at the single cell level in intact tissue. © 2001 Elsevier Science Ireland Ltd. All rights reserved.

Keywords: Mouse; Development; Gene expression; In situ hybridization; Confocal microscopy; Reconstruction; 3D

1. Results

1.1. Single-cell resolution

Whole-mount in situ hybridization was performed on mouse embryos using Fast Red (Roche) as the final substrate, and these were then embedded in 5% LMP agarose and cut into 70–100 μm sections using a vibratome. Using a confocal microscope to visualize fluorescence from the Fast Red precipitate we were able to detect a signal resolution which makes it possible to identify the expression pattern of a specific gene at the single cell level.

We first examined the expression of *Shh*, *Gli2* and *Patched*. Although *Shh* and *Patched* are strongly expressed genes which are easy to visualize with in situ techniques, *Gli2* is weakly expressed and therefore a good test of the sensitivity of the assay. All three genes could be well visualized (Fig. 1a–c) and corresponded to their previously described domains of expression (Echelard et al., 1993; Ding et al., 1998; Goodrich et al., 1996).

In another experiment we examined *Pax6* expression in the developing eye of an E10.5 mouse embryo and explored the use of a counter-stain to visualize all the nuclei of the tissue. In addition to the Fast Red staining, the tissue was

stained with the nuclear dye YoPro-1 iodide (Fig. 1d,d'). The results show *Pax6* expression in lens, the tips of the optic cup and in the overlying epithelium (Walther and Gruss, 1991; Grindley et al., 1995).

The high resolution offered by this technique provides an ideal tool for studying gene interactions between neighbouring cells. To test this possibility we carried out an experiment looking at the expression of *Shh* and *Patched* in combination with an antibody staining of the homeobox protein PDX1 in the developing gut (Fig. 1e,f). During the development of the pancreas *Shh* expression is excluded from the pancreatic buds, while *Pdx1* is expressed exclusively in this tissue. *Patched* is expressed in the mesenchyme adjacent to the *Shh* expressing endoderm but not in the mesenchyme adjacent to the *Pdx1* expressing endoderm. Our results agree with these observations and clearly demonstrate that this technique can be used to analyze gene interaction at the single cell level in intact tissue.

1.2. 3D data collection

The ability to scan the expression pattern as a fluorescent signal to a significant depth means that complete 3D blocks of high-resolution data can be captured in a single process, as is often done for antibody staining (Mohun et al., 2000). An E10.0 embryo was stained for *Shh* and cut into 70 μm sections. Seventy micrometers is the maximum depth at which good cellular resolution can be obtained (data not

* Corresponding author. Tel.: +44-131-332-2471; fax: +44-131-343-2620.

E-mail address: jsharpe@hgu.mrc.ac.uk (J. Sharpe).

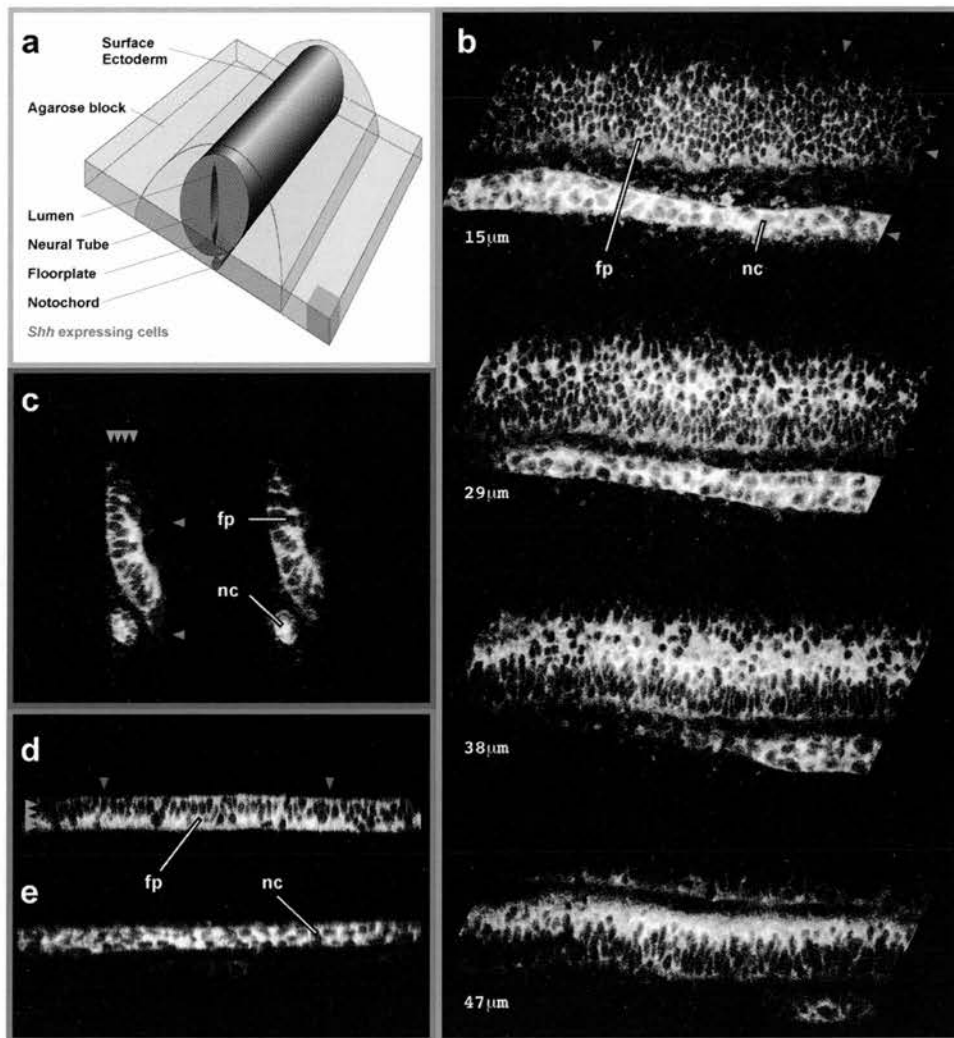


Fig. 2. 3D scanning of *Shh* expression data. (a) Illustration showing *Shh* expression in the neural tube and floorplate. The agarose block represents the thick section described in this figure. (b) Confocal images at various depths of the section (15, 29, 38 and 47 μm). The green outline refers to the coloured box in a, and represents the two dimensions of these sections in relation to the 3 dimensions of the whole block. The blue and red arrows show the positions of the virtual sections in (c–e). (c) Virtual sections cutting transversely through the neural tube. (d,e) Virtual sections cutting along the neural tube and notochord, respectively. In all sections *Shh* mRNA is strongly localized to the cytoplasm. The cell nuclei can be seen as dark spots. fp, floorplate; nc, notochord.

along the body of the embryo: the floorplate of the neural tube extending into the brain, and the embryonic gut including the stomach. At this stage of development *Shh* is expressed at low levels in the limb buds and weak staining was detected in the ZPA of the left forelimb (not visible in this figure). The visible streak of fluorescence in the right forelimb (blue arrowheads) is presumably caused by Fast Red crystals stuck to the surface ectoderm. Towards the posterior end of the floorplate, there appears to be a gap in expression (red arrowhead). This is due to one of the sections being distorted (a potential drawback for any technique that relies on multiple-section reconstruction). The resulting 3D embryo can be viewed from any angle (panel g); a movie of the embryo rotating can be seen at genex.hgu.mrc.ac.uk

Fig. 3c shows an image of one of the original optical sections (which has been patched together from 8 overlapping images). The morphology of most tissues (neural tube, somites, heart) can clearly be seen from the background fluorescence, and give enough information to select anatomical 'landmarks' for the alignment process. Fig. 3d–f show 'virtual' sections equivalent to a frontal view of the embryo (orthogonal to the original section in Fig. 3b), which demonstrate how well the thick sections align with each other. As with all expression analyses, distinguishing between the background and the ISH signal must be performed by selecting an appropriate threshold value. In this case we have made the threshold value (which differentiates between background and signal) more explicit, by artificially colouring everything above the threshold yellow (corresponding to the *Shh* signal).

goat anti-rabbit [1:200 (Molecular Probes)]. Residual antibodies were removed by washing 5 times 1 h in TNT containing 0.1% BSA. The in situ signal was then developed as described above.

3.3. Embedding, cutting and counterstaining

After fixing the embryos were embedded in 5% LMP agarose in PBS. When the agarose was set the embryos were cut into 70–100 μm sections on a vibratome, and each section was lifted from the vibratome waterbath onto a slide. If counter-staining was performed, the sections were incubated in a 5000-fold dilution of 1 mM Yo-Pro-1 (Molecular Probes, Y-3603). The section was then covered by a thin coverslip, was which glued to the slide at either end – a slight pressure being applied at each end, to ensure that the section lies flat. In order protect the morphology of the tissue the lifting and mounting should be performed very carefully. The mounted sections were stored in PBS to prevent them from drying out.

3.4. Confocal microscopy

We used an MRC-600 confocal with an Argon ion laser (488/514 nm) and the standard A1, A2 filter set (514 nm excitation filter, 540 nm green channel, >600 nm red channel). Image intensity was controlled by turning the gain up to maximum and keeping the pinhole to the minimal size that still provides a bright image. All scanning was performed at the slowest speed (3 s per frame). Low resolution images (i.e. the whole-embryo *Shh* expression pattern) were scanned using the 10 \times objective, while the cellular resolution images were captured using the 25 \times objective. As 3D scans progressed from the upper surface of the specimen downwards into the tissue, adjustments were sometimes needed to compensate for the weaker signal captured at lower depths. This was performed either manually, by gradually opening the pinhole during the scan, or automatically using a computer setting in which scanning continues to accumulate data from the same depth, each time improving the image, until a given intensity is reached.

3.5. Computer manipulation

Reconstructing the data from the confocal into 3D images was performed using either software from the Mouse Atlas Project or scripts written for IPLab which can perform the same functions. IPLab is a widely available image-processing program (Scanalytics, Inc.), and the scripts can be obtained from the authors at genex.hgu.mrc.ac.uk. The 3D data was visualized using the software package VTK (Visualization Toolkit, Kitware Inc.), however many other

commercial programs exist which can provide similar visualization functions.

Acknowledgements

We would like to acknowledge Paul Perry for help with confocal microscopy and computer imaging. Also people involved in the Mouse Atlas Project who have developed the software programmes used for the reconstructions and warping, especially Richard Baldock and Bill Hill whose technical assistance has been very helpful. Robert E. Hill, Duncan Davidson and Laura Lettice for reading the manuscript. Jacob Hecksher-Sørensen is funded by the Danish Research Academy and James Sharpe by a MRC Training Fellowship.

References

- Baldock, R.A., Verbeek, F.J., Vonesch, J.L., 1997. 3-D Reconstructions for graphical databases of gene expression. *Semin. Cell. Dev. Biol.* 8, 499–507.
- Ding, Q., Motoyama, J., Gasca, S., Mo, R., Sasaki, H., Rossant, J., Hui, C.C., 1998. Diminished Sonic hedgehog signaling and lack of floor plate differentiation in *Gli2* mutant mice. *Development* 125, 2533–2543.
- Echelard, Y., Epstein, D.J., St-Jacques, B., Shen, L., Mohler, J., McMahon, J.A., McMahon, A.P., 1993. Sonic hedgehog, a member of a family of putative signaling molecules, is implicated in the regulation of CNS polarity. *Cell* 75, 1417–1430.
- Goodrich, L.V., Johnson, R.L., Milenkovic, L., McMahon, J.A., Scott, M.P., 1996. Conservation of the hedgehog/patched signaling pathway from flies to mice: induction of a mouse *Patched* gene by Hedgehog. *Genes Dev.* 10, 301–312.
- Grindley, J.C., Davidson, D.R., Hill, R.E., 1995. The role of Pax-6 in eye and nasal development. *Development* 121, 1433–1442.
- Hammond, K.L., Hanson, I.M., Brown, A.G., Lettice, L.A., Hill, R.E., 1998. Mammalian and *Drosophila* dachshund genes are related to the *Ski* proto-oncogene and are expressed in eye and limb. *Mech. Dev.* 74, 121–131.
- Louie, A.Y., Huber, M.M., Ahrens, E.T., Rothbacher, U., Moats, R., Jacobs, R.E., Fraser, S.E., Meade, T.J., 2000. In vivo visualization of gene expression using magnetic resonance imaging. *Nat. Biotechnol.* 18, 321–325.
- Mohun, T.J., Leong, L.M., Weninger, W.J., Sparrow, D.B., 2000. The morphology of heart development in *Xenopus laevis*. *Dev. Biol.* 218, 74–88.
- Palmes-Saloma, C., Saloma, C., 2000. Long-depth imaging of specific gene expressions in whole-mount mouse embryos with single-photon excitation confocal fluorescence microscopy and FISH. *J. Struct. Biol.* 131, 56–66.
- Streicher, J., Donat, M.A., Strauss, B., Sporle, R., Schughart, K., Muller, G.B., 2000. Computer-based three-dimensional visualization of developmental gene expression. *Nat. Genet.* 25, 147–152.
- Walther, C., Gruss, P., 1991. Pax-6, a murine paired box gene, is expressed in the developing CNS. *Development* 113, 1435–1449.

Appendix VII: *Bapx1* Paper

Lettice, L., Hecksher-Sørensen, J. and Hill, R. (2001). The role of *Bapx1* (*Nkx3.2*) in the development and evolution of the axial skeleton. *J. Anat.* **199**, 181-187

The role of *Bapx1* (*Nkx3.2*) in the development and evolution of the axial skeleton

LAURA LETTICE, JACOB HECKSHER-SØRENSEN AND ROBERT HILL

MRC-Human Genetics Unit, Western General Hospital, Edinburgh, UK

(Accepted 6 April 2001)

ABSTRACT

The bagpipe-related homeobox-containing genes are members of the NK family. *bagpipe* (*bap*) was first identified in *Drosophila* and there are three different bagpipe-related genes in vertebrates. Only two of these are found in mammals, the *Nkx3.1* and the *Bapx1* (*Nkx3.2*) gene. The targeted mutation in the mouse *Bapx1* gene shows a vertebral phenotype in which the ventromedial elements are lacking; these are the centra and the intervertebral discs. In addition, a region of gastric mesenchyme is abnormal. This mesenchyme surrounds the posterior region of the presumptive stomach and duodenum, and in the mutant fails to support normal development of the spleen. In *Drosophila*, *bagpipe* has a role in gut mesoderm and the mutant embryos have no midgut musculature. Thus *bap* related genes in mouse and *Drosophila* have roles in patterning gut mesoderm; however, neither of the mammalian genes has a discernible role in the gut musculature. In contrast, both mammalian genes have roles in developmental processes that have appeared recently in evolution. The *Bapx1* gene found in fish, amphibians, birds and mammals appears to have derived vertebrate specific functions sometime after the split between the jawless fish and gnathostomes.

Key words: *Bapx1*; axial skeleton; *Nkx3.1*; development; evolution.

INTRODUCTION

The mammalian *Bapx1* gene (Triboli & Luifkin, 1997; Triboli et al. 1997) (also referred to as *Nkx3.2*) contains a homeobox and belongs to the NK family of developmental genes first identified in *Drosophila* (Kim & Nirenberg, 1989). This gene family was initially described as being comprised of 3 closely related members: the NK2, 3 and 4 genes responsible for the *ventral nervous system defective* (*vnd*), *bagpipe* (*bap*) and the *tinman* (*tin*) phenotypes respectively (reviewed in Harvey, 1996). The *bap* and *tin* genes are now known to comprise a cluster of related homeobox containing genes (referred to as the 93DE cluster) which includes *slouch* (*slou*), *ladybird* (*lbe* and *lbl*) and *C15* (for review see Jagla et al. 2001). *Bapx1* is most similar to the *Drosophila bap* (*Nkx3*) gene and along with closely related vertebrate genes in chick (Schneider et al. 1999), amphibian (both *Xenopus* [Newman et al. 1997] and urodele [Nicolas et al. 1999]) and fish (C. Kimmel, this volume), appear to form a distinct subgroup within the NK family.

In *Drosophila*, *bap* is required for the specification of the visceral mesoderm during midgut musculature formation (Azpiazu & Frasch, 1993). Genetic lesions within the *Drosophila bap* gene show a reduction or deletion in the visceral musculature. The role of *bap* in gut musculature and the expression of *Bapx1* in splanchnic mesoderm surrounding the gut led to the suggestion that the *Drosophila* and mouse genes may have similar roles during gut development (Triboli et al. 1997). Analysis of *Bapx1* mutant mice does not support a similar role and in contrast, suggests that *Bapx1* has acquired novel functions during vertebrate evolution.

RESULTS AND DISCUSSION

Nkx3 genes in vertebrates

To determine the number of *Nkx3*-like genes in mouse, we did a large genomic screen using the *Bapx1* homeobox region as probe. In addition a conserved

A.

Dm <i>Bap</i>	KRSRAAFSHAQVFELERRFAQORYLSGPERSEMAKSLRLTETQVKIWFQNRRYKTKRKQ		
Mm <i>Bapx1</i>	-----NH-----ADL-A--K-----R-	87%	} <i>Nkx3.2</i>
Hs <i>BAPX1</i>	-----NH-----ADL-A--K-----R-	87%	
Gg <i>Nkx3.2</i>	-----NH-----ADL A--K-----R-	87%	
Xl <i>Xbap</i>	-----NH-----ADL-A--K-----R-	87%	
Pw <i>Nkx3.2</i>	-----NH-----ADL-A--K-----R-	87%	
Mm <i>Nkx3.1</i>	-----T--I--K-SH-K--A--AHL--N-K-----	78%	} <i>Nkx3.1</i>
Hs <i>NKX3.1</i>	-----T--I--K-SH-K--A--AHL--N-K-----	78%	
Xl <i>Koza</i>	-----S--I--K-SS-K--A--AQL--K-----	82%	
Pw <i>Nkx3.3</i>	-----Y-----SL-----AAL-A--K-----	86%	} <i>Nkx3.3</i>
Xl <i>Zax</i>	-----Y-----SL-----ADL-A--K-----L	85%	

B.

	N-terminal	C-terminal
<i>Nkx3.2</i>		
Mm <i>Bapx1</i>	LTPFSIQAIL NKKEER	KVAVKVLVRDDQRQLYLPGEVLRPPSLLPLQPSY.YYPY.YC.LPGW
Hs <i>BAPX1</i>	LTSFSIQAIL NKKEER	KVAVKVLVRDDQRQYLPGEVLRPPSLLPLQPSY.YYPY.YC.LPGW
Gg <i>Nkx3.2</i>	LTPFSIQAIL NKKEER	KVAVKVLVRDDQRQYLPGEVLRPPSLLALQPSY.YYPY.YC.LPGW
Xl <i>Xbap</i>	LTPFSIQAIL NKKEER	KVAVKVLVRDDQRQYHPGEVLH.PSLLPLQAPY.FYPY.YCALPGW
Pw <i>Nkx3.2</i>	LTPFSIQAIL NKREDE	KVAVKVLVRDDQRQYLPGEILR.PSLLPLQAPY.FYPY.YCALPGW
<i>Nkx3.1</i>		
Mm <i>Nkx3.1</i>	LTSFLIQDIL.RDRAER	SLVSVYTSYPYPYLYC.LGSW
Hs <i>Nkx3.1</i>	LTSFLIQDIL.RDGAQR	SLVSVYNSYPYPYLYC.VGSW
Xl <i>Koza</i>	LTSFLIQDILARTGGNR	SLLSFYQNYQRYPYLYY.LAGW
<i>Nkx3.3</i>		
Xl <i>Zax</i>	LRSFLIQDILSHMGPGS	KVAVKVLVKDDQRQYCPEDMLS.PSLLSLYHAYQYYPMYC.LPAW
Pw <i>Nkx3.3</i>	ITSFRIQDILSRGSEGD	RVAIRVLRDDQLQSGPEEAPR.PSPLSLYQACHYYPMYC.LPGW

Fig. 1. Comparison of the amino acid sequences of the vertebrate *Nkx3* genes shows 3 sequences subgroups. (A) Lineup of the homeodomains of the vertebrate *Nkx3* genes in comparison to the *Drosophila bagpipe* (Dm *bap*) homeobox (top line). Clustering of the sequences into three subgroups is evident. The subgroups are *Nkx3.2* (at the top), *Nkx3.1* and *Nkx3.3*. The percentage identity with *bap* is shown to the right hand side of each sequence. Dm, *Drosophila melanogaster*; Mm, *Mus musculus*; Hs, human; Gg, *Gallus gallus*; Xl, *Xenopus laevis*; Pw, *Pleurodeles waltl* (a urodele amphibian). (B) Regions of additional sequence similarity in the *Nkx3* genes. The N-terminal box and C-terminal box are located to their respective sides of the homeodomain. The identical amino acids among all three subgroups are denoted by shading in black. Grey shading represents amino acids conserved within subgroups. The similarities with the N- and C-terminal boxes further support the classification of the subgroups. *Nkx3.1* genes do not show any appreciable similarity to *Nkx3.1* and *Nkx3.3* in the 5' half of the C-terminal box.

region 3' of the homeobox (shown in Fig. 1C) was also used. Only the *Bapx1* and *Nkx3.1* genes were isolated. Several non *bap* *Nkx2*-like genes were selected using the homeobox region as probe due to cross-similarities within these subgroups. In addition, screening the Human Genome Database, the mouse genome (HTGS), and EST databases (dbEST), only *Bapx1* and *Nkx3.1* genes were found. Thus the data supports only 2 *bagpipe*-related genes in mouse and man. This is further supported by a recent study by Pollard & Holland (2000). They conclude that the *Nkx1*, 3, and 4 genes occupy distinct locations within a large primordial chromosomal cluster containing a number of homeobox-containing genes, termed the NKL cluster. In both mouse and human, 2 clusters are

predicted which contain *Nkx3* related genes; the clusters are a result of chromosomal duplications events that occurred during vertebrate evolution. The *bap*-related genes that reside in these syntenic linkage groups are *Bapx1* and *Nkx3.1*.

Nkx3 related genes have been isolated from a number of vertebrates, and we have grouped these by overall sequence similarity (Fig. 1). Analysis of the homeobox sequence, the most highly conserved domain within the NK gene family, shows that the *Nkx3* genes cluster into three subgroups (Fig. 1A). The *Nkx3.2* subgroup of genes displays marginally higher sequence similarity to *Drosophila bagpipe*. Outside the homeodomain, the subgroups are divergent suggesting derivation from ancient gene duplication

events from a common ancestral gene. Even within the subgroups there has been a high degree of divergence. For example, discounting similarity in the homeodomain, the 2 mammalian *Nkx3.1* proteins show 40% amino acid nonidentity. Multiple sequence alignments (pileup in the GCG suite of programs) reveal two other conserved domains in the remainder of the proteins that distinguish the vertebrate *Nkx3* genes. These are an N-terminal box, encompassing the TN domain (Harvey, 1996) found in other NK genes, and a longer C-terminal box encompassing part of the NK2-SD domain. These are distinctly different from other vertebrate NK genes and further distinguish the subgroups of *Nkx3* genes (Fig. 1 B).

Interestingly, homologues of *Nkx3.3* have not been reported in birds and were not found in mammals. *Xenopus laevis* contains a number of novel genes due to a tetraploidy event in the recent ancestry of that species. *Nkx3.3* did not arise from such an event, since the gene appears in the urodele *Pleurodeles waltl* (Nicolas et al. 1999). Thus *Nkx3.3* either arose as a unique amphibian member to the *Nkx3* class or was lost later in the evolutionary lineage to mammals. The *Nkx3.3* gene in *Xenopus* called *zampogna* (*Zax*) (an Italian bagpipe; Newman & Kreig, 1999) is expressed in the muscle layer of the forming midgut and in the pharyngeal endoderm. It is interesting to speculate that the *Nkx3.3* gene provides the primordial function related to the role of *Drosophila bap* in specification of gut musculature.

Expression of *Bapx1* in development

Bapx1 expression in the mouse (Tribioli et al. 1997) is detected initially at E8.5 in the splanchnic mesoderm adjacent to the prospective gut endoderm and in the sclerotomal portion of the somites. At E10.5 *Bapx1* is detected in limb mesenchyme and the first branchial arch that becomes restricted to the precursor of Meckel's cartilage. At the time that *Pax1* is first seen in the sclerotome *Bapx1* expression turns on. By E9.5 *Bapx1* is evident in the sclerotome (Fig. 2 A), and (by E10.5) *Bapx1* is expressed in migrating sclerotome that moves toward and surrounds the notochord (Fig. 2 B).

Early lateral plate *Bapx1* expression has been reported to show left-right asymmetry (Schneider et al. 1999). In chick, expression is highest in the left lateral plate mesoderm and is responsive to left-sided signals such as Nodal, Lefty2 and Shh. In contrast, mouse (E8.5) expression is higher in the right lateral mesodermal plate. Organ asymmetry is reversed in the

inv/inv mutant mouse and *Bapx1* expression follows, now found higher on the left side. However, by E9.5 this reported asymmetry of expression is lost (Fig. 2 A), as seen in the splanchnic mesoderm surrounding the gut. At E10.5, expression of *Bapx1* is seen broadly in the region of the pancreatic mesenchyme, the mesenchyme dorsal to the pancreas bud associated with spleen development (Fig. 2 B, dashed line in C). It is not clear what role this early asymmetric expression plays.

Role of *Bapx1* in axial skeletal development

To determine the function of the *Bapx1* gene, we (Lettice et al. 1999) and others (Tribioli & Lufkin, 1999; Akazawa et al. 2000) targeted mutations into that locus by homologous recombination into mouse ES cells. The mutation is neonatal homozygous lethal, and no mutant newborns survive past the first few hours. The heterozygotes on the whole appear normal except that ~50% display tail kinks. At E18.5 the homozygous mutant fetuses appear shorter and squatter (Fig. 3 A, B). Further observations, which explain the outward stubby appearance, revealed that the axial skeleton is defective, the ventromedial aspects of each vertebra (the centra and the intervertebral discs) being absent (Fig. 3 C, D). The number of sclerotomal cells surrounding the notochord are markedly reduced, whereas those populating the lateral aspects of the vertebrae appear normal. The lateral prechondrogenic condensations appear normal and the timing of appearance of the multiple ossification centres in all aspects of the vertebra except the ventromedial component is unaffected (Fig. 3 C, D). Thus a deficiency of *Bapx1* results in specific loss of the midline components of each vertebra.

We examined a number of DNA markers by *in situ* hybridisation to define the developmental processes disrupted by the *Bapx1* mutation (Table). Several other mutations in mouse are known which affect the developing intervertebral bodies of the vertebra. In particular the *Pax1* (Wilm et al. 1998) (originally the undulated [*un*] mutation) and the *Gli2* (Mo et al. 1997) mutations show loss of the intervertebral bodies. Analysis of expression of *Pax1* and *Gli2* in *Bapx1*^{-/-} embryos (E13.5) showed no appreciable affect on the levels (Lettice et al. 1999; Tribioli & Lufkin, 1999). Since the notochord is a source for *Shh* production, we examined the expression of a number of genes responsive to Shh signaling (Table). No abnormal expression was found. Other expression patterns, *Mfh1*, *Mox1*, and *scleraxis*, representing early sclerotomal developmental events were analysed.

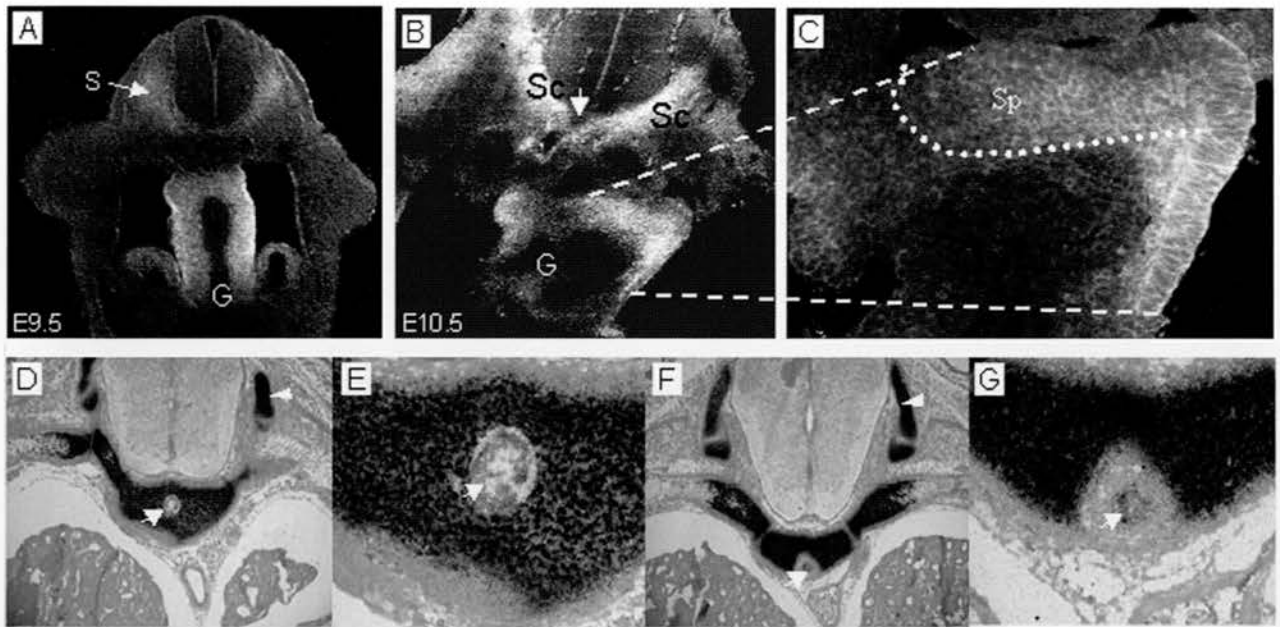


Fig. 2. Gene expression patterns in the developing mouse. (A–C) Expression of *Bapx1* in E9.5 (A) and E10.5 (B, C) wildtype mouse embryos. In (A), *Bapx1* expression is detected in the sclerotome component of the somite (arrow) and splanchnic mesenchyme surrounding the gut. In (B), the sclerotomal cells which are migrating toward the notochord (arrow) express *Bapx1*. Also the gastric mesenchyme expresses *Bapx1* which is shown at a higher magnification in (C). The portion of the mesenchyme that will give rise to the spleen is outlined by a dotted line and expresses *Bapx1*. (D–E) Transverse sections through E12.5 embryos expressing $\alpha 1$ (II) collagen; wildtype, compared with *Bapx1*^{-/-} mutant embryos (F, G). Expression of $\alpha 1$ (II) collagen is shown in the lateral elements (arrowheads, D and F) of both wildtype and mutant animals. Lack of expression specifically around the notochord (arrows, E and G) appears as a halo of cells. G, gut; S, somite; Sc, sclerotome; Sp, spleen.

Mfh1 is of particular interest, since its role is associated with sclerotomal cell proliferation (Winnier et al. 1997). No appreciable differences were seen for the expression of any of these genes. Thus initial patterning of sclerotome occurs normally in the mutants and there appears to be no defect in cell proliferation. Cell proliferation was analysed more directly by BrdU labelling experiments in the *Bapx1* mutants (Tribioli & Lufkin, 1999) and confirmed the above data.

Analysis of differentiation markers, however, showed a contrasting account. Alpha1 (II) collagen (Fig. 3D–G) is expressed during chondrogenesis in a similar vertebral pattern. In the *Bapx1* mutants the expression of alpha1 (II) collagen in the ventromedial elements of each vertebra is missing, whereas expression throughout the remainder of the developing vertebrae are normal. Recently Tribioli & Lufkin (1999) have shown that the migration of sclerotomal cells toward the notochord is unaffected by the *Bapx1* mutation, however there is a high degree of cell death in the cells associated with the notochord. Therefore *Bapx1* is required for directing a subset of sclerotomal cells toward a chondroblastic pathway. In the absence of the gene, the cells migrate but do not survive resulting in the reduction in the cell number of ventromedial cells.

Table. Analysis of gene expression in *Bapx1*^{-/-}

Genes with similar vertebral phenotypes
<i>Pax1</i>
<i>Gli2</i>
Genes in the <i>Shh</i> pathway
<i>Gli2</i>
<i>Shh</i>
<i>Ptc</i>
Early sclerotomal markers
<i>Mox1</i>
<i>Mfh1</i>
<i>Scleraxis</i>
<i>BMP7</i>
Cellular proliferation marker
<i>Mfh1</i>
Differentiation markers
<i>Sox9</i>
<i>al</i> (II)-collagen

Evolution of *Bapx1* function

The whole of each vertebra undergoes the process of chondrogenesis. The question, therefore, arises as to why a gene essential to this process only affects a subset of sclerotomal cells, i.e. those that will give rise to each of the centra. First of all, it is apparent that different parts of each vertebra require different signals for their normal development. Both *Pax1* and *Bapx1* participate in production of the intervertebral bodies and are responsive to *Shh* in the notochord

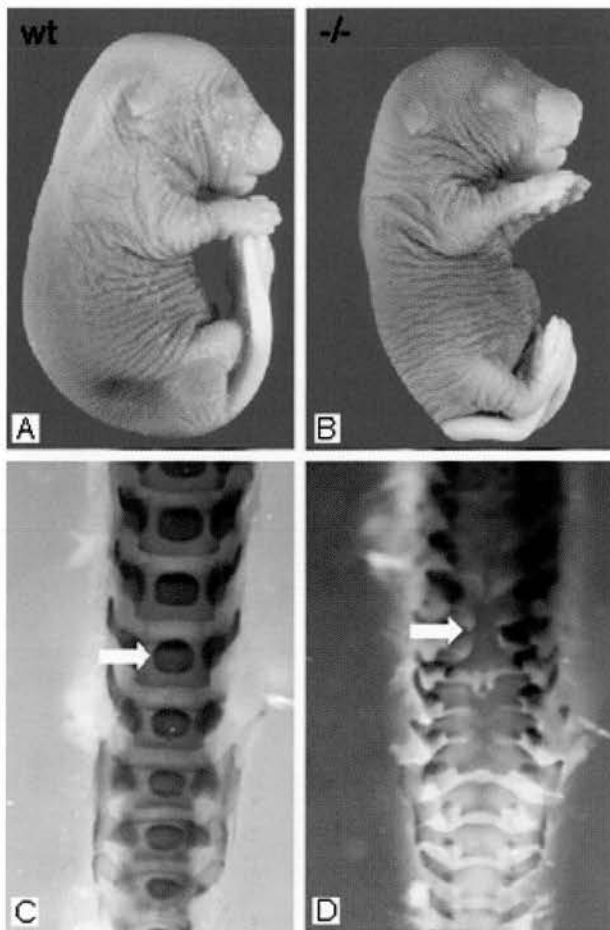


Fig. 3. The phenotypic characteristics of the *Bapx1* mutant fetuses. Top panels compare the outward phenotype of wildtype (A) and mutant (B) E18.5 embryos. Note that the mutant embryo is squatter and does not show the rounded rump region of the wildtype, and the tail is shorter and bent. The bottom panel shows a ventral view of the vertebral column in E18.5 wildtype (C) and mutant (D) fetuses. The white arrow in (C) indicates the ossification center that will give rise to one of the centra in the wildtype animal. These are missing in the mutant mouse (D).

(Fan & Tessier-Lavigne, 1994; Wallin et al. 1994). In the absence of *Shh* (in the *Shh* mutant mouse), sclerotomal cells appear and initially express *Pax1* at a low level. However, *Pax1* expression never reaches wildtype levels and is lost. Furthermore both *Pax1* and *Bapx1* are induced by SHH in somite culture experiments (Fan & Tessier-Lavigne, 1994, and personal communication). Other genes affecting more lateral aspects of each vertebra are not under the influence of notochordal signals. For example, expression of *Uncx4.1* is not dependent on notochordal signaling but rather requires the Notch/Delta signaling pathway. Deletion of *Uncx4.1*, a paired-like homeobox-containing gene, causes loss of lateral elements such as pedicles, transverse processes and proximal ribs (Leites et al. 2000; Mansouri et al.

2000). We suggest that sclerotomal cells respond to signals differently depending on their gene expression profile and form vertebral elements adjacent to the signalling source. These discriminating processes specify the individual vertebral components which make up an individual vertebra.

So how did this assemblage of genes and signalling pathways required to form a vertebra come about? The evolutionary history of the early vertebrates suggests that vertebrae evolved in a progression of steps. Individual elements of the vertebra arose at different times in evolution (reviewed in Brand-Saberi & Christ, 2000). In the agnathans such as lamprey and primitive cartilaginous fishes such as the chimera (see Fig. 4), the major support along the anterior posterior axis is the notochord and the fibrous sheath in which it is encased. However, in these primitive fishes there are dorsal cartilaginous elements that protrude from this fibrous sheath that surround the neural tube (reviewed in Brand-Saberi & Christ, 2000). In the selachians (sharks and rays) and the bony fishes the notochord for the first time is surrounded by cartilaginous (in sharks) or bony centra. The dorsal elements presumably gave rise to the neural arches in these fishes. Thus an evolutionary progression is evident in the appearance of elements that compose the vertebrae; the addition of the ventromedial located centra occurred later at a distinct stage in vertebrate evolution. We predict that genes such as *Bapx1* and *Pax1* acquired sclerotomal functions sometime after the split with the agnathans within the lineage of gnathostomes coincident with the appearance of the centra (Fig. 4). A chromosomal duplication event (tetraploidisation) is predicted to have occurred during this evolutionary period (Holland et al. 1994). It seems likely that *Bapx1* function arose during this period as a result of the duplication.

Do the genes acquire additional expression domains in this acquisition of novel function? An indirect argument focuses around the *Pax9* gene. *Pax9* is closely related to *Pax1* and is expressed in sclerotomal cells (and other embryonic regions) overlapping those that express *Pax1*. In mouse, deletion of the *Pax9* gene in combination with *Pax1* $-/-$ shows severe ventromedial defects in the vertebrae (Peters et al. 1999). Therefore *Pax9* is a marker of sclerotomal cells and operates in skeletal development acting in conjunction with *Pax1*. In the agnathan *Lampetra japonica* *Pax9* is not expressed in the sclerotomal compartment (Ogasawara et al. 2000); however, in teleost *Pax9* marks the sclerotome (Nornes et al. 1996). *Pax9* and presumably *Pax1* and *Bapx1* are recruited from other developmental compartments or

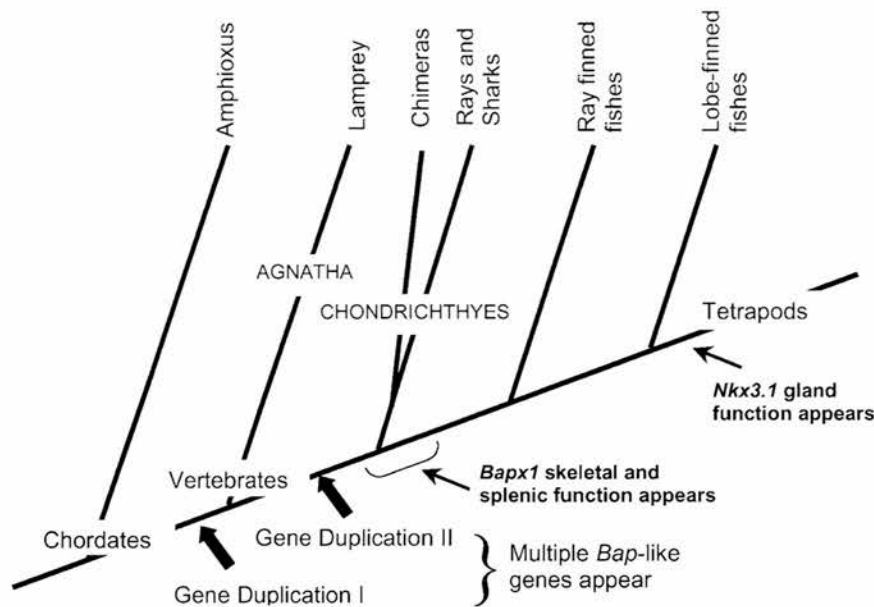


Fig. 4. Predicted evolutionary history of the *Bapx1* and *Nkx3.1* gene functions. The extant species representative of each class is shown at the top of the diagram. The bottom timeline goes from the chordate amphioxus to the appearance of the tetrapods and predicts the points at which gene duplications have been suggested to occur. We predict based on *Bapx1* and *Nkx3.1* functions in mouse at what point *Bapx1* and *Nkx3.1* acquired their functions.

newly appear (as may be the case for *Bapx1*) to participate in this novel developmental function.

The second developmental function for *Bapx1* is the formation of the spleen. *Bapx1* is expressed in spleen mesenchyme (Fig. 2C), and in the absence of *Bapx1* the spleen does not appear. This is an early developmental effect; expression of the spleen specific marker *Hox11* (*Tlx1*) is not detected in the mutant embryos (Lettice et al. 1999). The advent of the spleen in vertebrate evolution is not clear. Hildebrand (1988) suggests that cords of spleen tissue exist in lamprey; however, these are associated with the gut submucosa. In selachians, ray-finned fish and all tetrapods the spleen develops external to the gut residing in surrounding dorsal mesentery. We suggest that the *Bapx1* spleen function has arisen as part of genetic network required for reorganisation of the spleen to the periphery of the gut. A crucial stage in spleen evolution may be the repositioning to a location independent of the gut in the gastric mesentery.

Evolution of other members of the *Nkx3* group

Targeted deletions of *Nkx3.1* in mouse have recently demonstrated the functions of this NK family member (Bhatia-Gaur et al. 1999; Schneider et al. 2000; Tanaka et al. 2000). The mutant phenotype suggests roles in the proliferation of glandular epithelium and in the formation of ducts in the prostate gland and in a minor set of salivary glands called the palatine. The prostate is mammalian specific and salivary glands

arose in vertebrates as a requirement once tetrapods became true land-based feeders. Hence, this gene has apparently acquired vertebrate specific functions quite late in vertebrate evolution.

Thus it appears that the *bagpipe*-related genes have undergone a continual acquisition of functions throughout vertebrate evolution. A source for genetic diversity is the process of chromosomal tetraploidisation that is predicted to have occurred twice in vertebrate evolution (Holland et al. 1994) (Fig. 4). These events play an important role in vertebrate evolution particularly for the appearance of vertebrate specific organ systems. Both *Bapx1* and *Nkx3.1* genes were probably generated during these early duplication events (Pollard & Holland, 2000). *Bapx1* may have acquired roles in both spleen and vertebral development at the time of one of these duplication events. *Nkx3.1*, on the other hand, was co-opted later for roles in glandular epithelial development.

Remnants of four NKL clusters (discussed above) are present in the mouse and human genomes; however, only two *Nkx3*-like genes remain suggesting that two were lost. We speculate that the *Nkx3.3* gene identified in amphibian was one of the genes lost in the lineage to mammals.

ACKNOWLEDGEMENTS

We would like to thank Liz Graham and Vince Ranaldi for their expert technical assistance. J.H.S. was funded by the Danish Research Academy.

REFERENCES

- AKAZAWA H, KOMURO I, SUGITANI Y, YAZAKI Y, NAGAI R, NODA T (2000) Targeted disruption of the homeobox transcription factor *Bapx1* results in lethal skeletal dysplasia with asplenia and gastroduodenal malformation. *Genes and Cells* **5**, 499–513.
- AZPIAZU N, FRASCH M (1993) *tinman* and *bagpipe*: two homeobox genes that determine cell fates in the dorsal mesoderm of *Drosophila*. *Genes and Development* **7**, 1325–1340.
- BHATIA-GAUR R, DONJACOUR AA, SCIAVOLINO PJ, KIM M, DESAI N, YOUNG P et al. (1999) Roles for *Nkx3.1* in prostate development and cancer. *Genes and Development* **13**, 966–977.
- BRAND-SABERI B, CHRIST B (2000) Evolution and development of distinct cell lineages derived from somites. *Current Topics Developmental Biology* **48**, 1–42.
- FAN CM, TESSIER-LAVIGNE M (1994) Patterning of mammalian somites by surface ectoderm and notochord: evidence for sclerotome induction by a hedgehog homolog. *Cell* **79**, 1175–1186.
- HARVEY RP (1996) NK-2 homeobox genes and heart development. *Developmental Biology* **178**, 203–216.
- HILDEBRAND M (1988) *Analysis of Vertebrate Structure*, pp. 272–275. Chichester: John Wiley and Sons.
- HOLLAND PW, GARCIA-FERNANDEZ J, WILLIAMS NA, SIDOW A (1994) Gene duplications and the origins of vertebrate development. *Development (Suppl.)*, 125–133.
- JAGLA K, BELLARD M, FRASCH M (2001) A cluster of *Drosophila* homeobox genes involved in mesoderm differentiation programs. *BioEssays* **23**, 125–133.
- KIM Y, NIRENBERG M (1989) *Drosophila* NK-homeobox genes. *Proceedings of the National Academy of Sciences of the USA* **86**, 7716–7720.
- LEITGES M, NEIDHARDT L, HAENIG B, HERRMANN BG, KISPERT A (2000) The paired homeobox gene *Uncx4.1* specifies pedicles, transverse processes and proximal ribs of the vertebral column. *Development* **127**, 2259–2267.
- LETTICE LA, PURDIE LA, CARLSON GJ, KILANOWSKI F, DORIN J, HILL RE (1999) The mouse *bagpipe* gene controls development of axial skeleton, skull, and spleen. *Proceedings of the National Academy of Sciences of the USA* **96**, 9695–9700.
- MANSOURI A, VOSS AK, THOMAS T, YOKOTA Y, GRUSS P (2000) *Uncx4.1* is required for the formation of the pedicles and proximal ribs and acts upstream of *Pax9*. *Development* **127**, 2251–2258.
- MO R, FREER AM, ZINYK DL, CRACKOWER MA, MICHAUD J, HENG HH et al. (1997) Specific and redundant functions of *Gli2* and *Gli3* zinc finger genes in skeletal patterning and development. *Development* **124**, 113–123.
- NEWMAN CS, GROW MW, CLEAVER O, CHIA F, KRIEG P (1997) *Xbap*, a vertebrate gene related to *bagpipe*, is expressed in developing craniofacial structures and in anterior gut muscle. *Developmental Biology* **181**, 223–233.
- NEWMAN CS, KREIG PA (1999) The *Xenopus bagpipe*-related homeobox gene *zampogna* is expressed in the pharyngeal endoderm and the visceral musculature of the midgut. *Development, Genes and Evolution* **209**, 132–134.
- NICOLAS S, CAUBIT X, MASSACRIER A, CAU P, LE PARCO Y (1999) Two *Nkx-3*-related genes are expressed in the adult and regenerating central nervous system of the urodele *Pleurodeles waltl*. *Developmental Genetics* **24**, 319–328.
- NORNES S, MIKKOLA I, KRAUSS S, DELGHANDI M, PERANDER M, JOHANSEN T (1996) Zebrafish *Pax9* encodes two proteins with distinct C-terminal transactivating domains of different potency negatively regulated by adjacent N-terminal sequences. *Journal of Biological Chemistry* **271**, 26914–26923.
- OGASAWARA M, SHIGETANI Y, HIRANO S, SATOH N, KURATANI S (2000) *Pax1/Pax9*-related genes in an agnathan vertebrate, *Lampetra japonica*: expression pattern of *LjPax9* implies sequential evolutionary events toward the gnathostome plan. *Developmental Biology* **223**, 399–410.
- PETERS H, WILM B, SAKAI N, IMAI K, MAAS R, BALLING R (1999) *Pax1* and *Pax9* synergistically regulate vertebral column development. *Development* **126**, 5399–5408.
- POLLARD S, HOLLAND PWH (2000) Evidence for 14 homeobox gene clusters in human genome ancestry. *Current Biology* **10**, 1059–1062.
- SCHNEIDER A, MIJALSKI T, SCHLANGE T, DAI W, OVERBEEK P, ARNOLD HH et al. (1999) The homeobox gene *NKX3.2* is a target of left-right signalling and is expressed on opposite sides in chick and mouse embryos. *Current Biology* **9**, 911–914.
- SCHNEIDER A, BRAND T, ZWEIGERDT R, ARNOLD H (2000) Targeted disruption of the *nkx3.1* gene in mice results in morphogenetic defects of minor salivary glands: parallels to glandular duct morphogenesis in prostate. *Mechanisms of Development* **95**, 163–174.
- TANAKA M, KOMURO I, INAGAKI H, JENKINS NA, COPELAND NG, IZUMO S (2000) *Nkx3.1*, a murine homolog of *Drosophila bagpipe*, regulates epithelial ductal branching and proliferation of the prostate and palatine glands. *Developmental Dynamics* **219**, 248–260.
- TRIBIOLI C, LUFKIN T (1997) Molecular cloning, chromosomal mapping and developmental expression of *BAPX1*, a novel human homeobox-containing gene homologous to *Drosophila bagpipe*. *Gene* **203**, 225–233.
- TRIBIOLI C, LUFKIN T (1999) The murine *Bapx1* homeobox gene plays a critical role in embryonic development of the axial skeleton and spleen. *Development* **126**, 5699–5711.
- TRIBIOLI C, FRASCH M, LUFKIN T (1997) *Bapx1*: an evolutionary conserved homologue of the *Drosophila bagpipe* homeobox gene is expressed in splanchnic mesoderm and the embryonic skeleton. *Mechanisms of Development* **65**, 145–162.
- WALLIN J, WILTING J, KOSEKI H, FRITSCH R, CHRIST B, BALLING R (1994) The role of *Pax-1* in axial skeleton development. *Development* **120**, 1109–1121.
- WILM B, DAHL E, PETERS H, BALLING R, IMAI K (1998) Targeted disruption of *Pax1* defines its null phenotype and proves haploinsufficiency. *Proceedings of the National Academy of Sciences of the USA* **95**, 8692–8697.
- WINNIER GE, HARGETT L, HOGAN BL (1997) The winged helix transcription factor *MFH1* is required for proliferation and patterning of paraxial mesoderm in the mouse embryo. *Genes and Development* **11**, 926–940.